

Inferring Body Mass in Extinct Terrestrial Vertebrates and the Evolution of Body Size in a Model-Clade of Dinosaurs (Ornithopoda)

by

Nicolás Ernesto José Campione Ruben

A thesis submitted in conformity with the requirements
for the degree of Doctor of Philosophy

Ecology and Evolutionary Biology
University of Toronto

© Copyright by Nicolás Ernesto José Campione Ruben 2013

Inferring body mass in extinct terrestrial vertebrates and the evolution of body size in a model-clade of dinosaurs (Ornithopoda)

Nicolás E. J. Campione Ruben

Doctor of Philosophy

Ecology and Evolutionary Biology
University of Toronto

2013

Abstract

Organismal body size correlates with almost all aspects of ecology and physiology. As a result, the ability to infer body size in the fossil record offers an opportunity to interpret extinct species within a biological, rather than simply a systematic, context. Various methods have been proposed by which to estimate body mass (the standard measure of body size) that center on two main approaches: volumetric reconstructions and extant scaling. The latter are particularly contentious when applied to extinct terrestrial vertebrates, particularly stem-based taxa for which living relatives are difficult to constrain, such as non-avian dinosaurs and non-therapsid synapsids, resulting in the use of volumetric models that are highly influenced by researcher bias. However, criticisms of scaling models have not been tested within a comprehensive extant dataset. Based on limb measurements of 200 mammals and 47 reptiles, linear models were generated between limb measurements (length and circumference) and body mass to test the hypotheses that phylogenetic history, limb posture, and gait drive the relationship between stylopodial circumference and body mass as critics suggest. Results reject these and instead

recover a highly conserved relationship that provides a robust method to estimate body mass in extinct quadrupedal tetrapods. The constrained model is then used to derive a mathematical correction that permits the body mass of bipedal taxa to be estimated from the quadrupedal-based equation. These equations thus form the empirical baseline dataset with which to assess the accuracy of mass estimates derived from volumetric reconstructions, which, although subjective, are crucial for interpreting biomechanical and physiological attributes in extinct forms. The models developed through this research provide accurate and consistent estimates of body size in terrestrial vertebrates, with important implications for generating large datasets aimed at reconstructing macroevolutionary patterns of body size in association with changing Earth systems.

I dedicate this thesis to my greatest contribution, Dominic, whom I can't wait to run through a dinosaur gallery with; to my wife Michelle for always being by my side and emotionally supporting me over the past 5 years of this work; to Sofía and Alejandro for being the greatest sister and brother; and lastly, to my parents José Campione and Martha Ruben for encouraging my love for science from a young age, and in particular for taking me to *la Isla de las Ardillas* (a.k.a., Victoria Island, on the Ottawa River) about 25 years ago, where I found my first fossil (an Ordovician cephalopod).

Acknowledgments

When I began my journey to complete a PhD in September 2008, I could not have imagined the plethora of people that would be integral to its completion. Over the past five years I have had the pleasure of meeting and discussing my research with some of the best palaeobiologists and evolutionary biologists in the world and through their experiences and knowledge I have learned an amazing range of both theoretical and methodological concepts that have made me the scientist I am today.

First and foremost I need to thank my supervisor David Evans. I am David's first PhD student and I could not be more certain that I made the right choice five years ago when I joined the then young Evans lab. David has provided me with all the necessary tools and guidance that I needed not only to complete this PhD but also prepare me for an academic career. Dave, I will forever cherish our numerous travels around the world. Second, I must thank Robert Reisz, my co-supervisor. Robert supported my desire to pursue graduate school, supporting me through my M.Sc., and being a great resource with whom to discuss results and implications. Two world-class biologists round out my supervisory committee: Matthew Carrano has been pivotal in discussing and suggesting methods critical to this project, as well as sharing personal data and greatly improving the quality of my PhD; and Daniel Brooks has been central in getting me to think a bit broader about the significance of my work. My appraisal examination committee has been critical for expanding my horizons and directing me along the right research path. For this I thank Jason Head and Deborah MacLennan.

I am indebted to the members of the Evans and Reisz labs. Without you guys, I would not have been able to keep my sanity over the last five years. You have not only helped me academically (putting up with my ill-prepared talks and manuscripts) and in pursuing new avenues of research (a.k.a, side projects) but also emotionally over beers or coffee. Thank you Kirstin Brink, Caleb Brown, Kentaro Chiba, Daniel Dufault, Derek Larson, Aaron Leblanc, David Mazierski, Christopher McGarrity, Lorna O'brien (Honorary Member), Collin VanBuren, Ryan Schott, Diane Scott, and Matthew Vavrek. In particular, I need to thank Matthew Vavrek for his amazing help with R; if I know anything about R now, it's because of you. Caleb, thank you for your help with deriving the correction factor (a.k.a., the Brown Constant) and for showing me the secrets to good figure making. Kirstin, thank you for making everyday Friday!

Along the way, I have had the honour of discussing my doctoral research with several awe-inspiring researchers that have taken the time to share their thoughts; all of whom have helped me arrive to this point in my life: John Alroy, Jason Anderson, Jessica Arbour, Paul Barrett, Stephen Brusatte, Richard Butler, Per Christiansen, Philip Currie, Robin Cuthbertson, Alexander Dececchi, Jerry De Iulius, Peter Dodson, Richard Fariña, Denver Fowler, Jörg Fröbisch, Nadia Fröbisch, Stephen Gatsey, Donald Henderson, John Horner, Grant Hurlburt, John Hutchinson, Donald Jackson, Matthew Lamanna, Hans Larsson, Michel Laurin, Hernan Lopez-Fernandez, Hillary Maddin, Susannah Maidment, Jordan Mallon, Philip Manning, Albert Prieto-Márquez, Michael Ryan, Natalia Rybczynski, Rowan Sage, Martin Sanders, John Scannella, Mary Silcox, Corwin Sullivan, Matthew Wedel, and David Weishampel.

Numerous individuals have helped on specific aspects of my research; in particular Roger Benson has been an invaluable resource for discussing and understanding methods for reconstructing evolutionary patterns of body size; Lars Schmitt helped with conducting

independent contrasts analyses; Roland Sookias, provided R-code and help in reproducing some of his previous research on my dataset; David Warton aided in understanding linear model-fitting techniques in R; and both Graham Slater and David Bapst (through the R-sig-phylo List) helped understand errors when running model-fitting analyses on phylogenetic trees.

My doctoral research relied on numerous collections and museum staff in order to reach completion. In particular, I am indebted to the efforts of Kevin Seymour, Suzan Woodward, Mark Peck, and Ross MacCulloch at the ROM, without whom the extant datasets presented in this thesis would not have been possible. They have amassed one of the most useful collections in world in which skeletonized specimens are directly associated with body mass data. For their help with accessing and handling specimens I thank Kevin Seymour, Ian Morrison, and Bian Iwama (ROM); Kieran Shephard, Margaret Currie, Alan MacDonald, and Clayton Kennedy (CMN); Brendan Strilisky (TMP); Mogen Andersen (ZMUC); Paul Barrett (NHM); Pascal Godefroit, Pascaline Lauters, and Annelise Folie (IRSNB); Corwin Sullivan and Xu Xing (IVPP), Carl Mehling and Mark Norell (AMNH), Amy Henrici (CM); Peter Larson (BHI); Chinzorig Tsogtbaatar and Khishigjav Tsogtbaatar (MPC); John Horner (MOR); and Michael Brett-Surman (USNM).

Finally, but definitely not least I thank my family: my wife Michelle Campione van Zetten and my baby boy Dominic, thank you for following me in this crazy dream of mine; my parents José Campione and Martha Ruben for always believing in me; my sister Sofia Campione and brother Alejandro Campione for their love and always being around to talk; to my niece Anya Campione for always being keenly aware that I like dinosaurs; to my in-laws Debbie and John van Zetten; and finally to my large family in Uruguay. You've all supported me

emotionally (and sometimes financially) and I cannot imagine being here today without you,
los quiero mucho!

Table of Contents

ACKNOWLEDGMENTS	V
TABLE OF CONTENTS	IX
LIST OF TABLES	XIII
LIST OF FIGURES	XV
LIST OF APPENDICES	XVIII
LIST OF INSTITUTIONAL ABBREVIATIONS	XIX
BACKGROUND AND CONTEXT	1
CHAPTER 1 A UNIVERSAL SCALING RELATIONSHIP BETWEEN BODY MASS AND PROXIMAL LIMB BONE DIMENSIONS IN QUADRUPEDAL TERRESTRIAL TETRAPODS	4
1.1 ABSTRACT	4
1.2 INTRODUCTION	5
1.3 MATERIALS AND METHODS	10
<i>1.3.1 Database Construction</i>	<i>10</i>
<i>1.3.2 Statistical Analyses</i>	<i>13</i>
<i>1.3.3 Phylogenetic Independent Contrasts</i>	<i>16</i>
1.4 RESULTS	19
<i>1.4.1 Raw Data Results</i>	<i>19</i>
<i>1.4.2 Independent Contrast Results</i>	<i>22</i>
1.5 DISCUSSION	23

1.5.1	<i>Stylopodial Scaling as a Predictor of Body Mass.....</i>	26
1.5.2	<i>Implications for Body Mass Estimation.....</i>	31
1.6	CONCLUDING REMARKS	34
1.7	TABLES	35
1.8	FIGURES.....	50

CHAPTER 2 A MATHEMATICAL CORRECTION FACTOR FOR ESTIMATING BODY MASS IN TERRESTRIAL BIPEDAL TETRAPODS58

2.1	ABSTRACT	58
2.2	INTRODUCTION	59
2.3	MATHEMATICAL DERIVATION	62
2.3.1	<i>Methodological Assumptions.....</i>	64
2.3.2	<i>Empirical Tests</i>	66
2.4	DISCUSSION	69
2.4.1	<i>Body Mass of Non-Avian Bipedal Dinosaurs</i>	71
2.4.2	<i>Inferring Body Size in the Fossil Record.....</i>	73
2.5	R-PACKAGE: MASSTIMATE v1.0	76
2.5.1	<i>Source Code.....</i>	77
2.6	TABLES	79
2.7	FIGURES.....	85

CHAPTER 3 INFERRING BODY MASS IN THE FOSSIL RECORD: A *POST HOC* MODEL FOR CONSTRAINING VOLUMETRIC DENSITY MASS ESTIMATES OF NON-AVIAN DINOSAURS.....91

3.1	ABSTRACT	91
-----	----------------	----

3.2	INTRODUCTION	92
3.3	BODY MASS INFERENCE IN THE FOSSIL RECORD	95
3.3.1	<i>Volumetric-Density Approach</i>	95
3.3.2	<i>Extant Scaling Approach</i>	104
3.3.3	<i>Advantages and Limitations of VD and ES Approaches</i>	109
3.4	A <i>POST HOC</i> ASSESSMENT OF VD-APPROACHES	111
3.4.1	<i>Methods</i>	114
3.4.2	<i>Results</i>	117
3.5	DISCUSSION	120
3.6	CONCLUSIONS.....	126
3.7	TABLES	128
3.8	FIGURES.....	129

**CHAPTER 4 THE EVOLUTION OF BODY SIZE IN ORNITHOPOD DINOSAURS:
TESTING COPE'S RULE, INSULAR DWARFISM, AND UPPER BODY SIZE LIMITS
IN NON-AVIAN DINOSAURS**

4.1	ABSTRACT	159
4.2	INTRODUCTION	160
4.2.1	<i>Body Size Evolution in Dinosauria</i>	161
4.2.2	<i>Body Size Evolution in Ornithopoda</i>	164
4.2.3	<i>Cope's Rule</i>	166
4.3	METHODOLOGY	170
4.3.1	<i>Dataset Construction</i>	170
4.3.2	<i>Phylogenetic Context</i>	176
4.3.3	<i>Analyses</i>	179

4.4 RESULTS	183
4.4.1 <i>Missing Data Estimation</i>	183
4.4.2 <i>Trend Analyses</i>	184
4.4.3 <i>Ancestor-Descendent Contrasts</i>	187
4.4.4 <i>Testing Upper Size Limits</i>	188
4.5 DISCUSSION	189
4.5.1 <i>Insular Dwarfism in Ornithopoda</i>	189
4.5.2 <i>Upper Size Limits in Ornithopoda</i>	195
4.5.3 <i>Cope's Rule in Ornithopoda</i>	198
4.6 ORNITHOPOD SIZE EVOLUTION: AN ADAPTIVE RADIATION?	202
4.7 CONCLUDING REMARKS	208
4.7.1 <i>Branch Lengths</i>	210
4.7.2 <i>Model-Fitting at Nodes</i>	211
4.7.3 <i>Model-Fitting and Sample Size</i>	212
4.8 TABLES	214
4.9 FIGURES.....	224
REFERENCES.....	248
APPENDICES	284
COPYRIGHT ACKNOWLEDGEMENTS.....	313

List of Tables

TABLE 1-1. STYLOPODIAL SCALING IN MAMMALS AND NON-AVIAN REPTILES.	35
TABLE 1-2. SLOPE AND INTERCEPT COMPARISONS OF STYLOPODIAL SCALING PATTERNS IN MAMMALIAN CLADES.....	37
TABLE 1-3. SLOPE AND INTERCEPT COMPARISONS OF STYLOPODIAL SCALING PATTERNS IN MAMMALS AND NON-AVIAN REPTILES.....	39
TABLE 1-4. RAW AND PIC STYLOPODIAL SCALING IN A SUBSET OF THE MAMMALIAN DATASET AND NON-AVIAN REPTILES.....	40
TABLE 1-5. STYLOPODIAL SCALING IN MAMMALS FOR DIFFERENT SIZES.	42
TABLE 1-6. SLOPE AND INTERCEPT COMPARISONS OF STYLOPODIAL SCALING PATTERNS IN DIFFERENT MAMMALIAN SIZE CLASSES.	44
TABLE 1-7. PHYLOGENETICALLY CORRECTED STYLOPODIAL SCALING IN MAMMALS AND NON- AVIAN REPTILES.	45
TABLE 1-8. RAW AND PIC STYLOPODIAL SCALING IN ARTIODACTYLA AND BOVIDAE.....	47
TABLE 1-9. PREDICTIVE POWER OF VARIOUS BODY MASS ESTIMATION EQUATIONS.	48
TABLE 1-10. BODY MASS ESTIMATES OF COMMONLY CITED NON-AVIAN QUADRUPEDAL DINOSAURS.	49
TABLE 2-1. SCALING RESULTS BETWEEN VARIOUS LIMB MEASUREMENTS AND BODY MASS IN EXTANT AVIANS.	79
TABLE 2-2. SUMMARY RESULTS OF REGRESSIONS SHOWN IN FIGURE 2-2 WITH MEAN PERCENT PREDICTION ERROR (PPE) OF VARIOUS ESTIMATION EQUATIONS.	79

TABLE 2-3. MEAN PROPORTIONAL DIFFERENCES BETWEEN THE CIRCUMFERENCE OF THE HUMERUS AND FEMUR IN A SAMPLE ON EXTANT TERRESTRIAL TETRAPODS.....	80
TABLE 2-4. BODY MASS ESTIMATES (IN KG) OF WELL-KNOWN NON-AVIAN BIPEDAL DINOSAURS COMPARED TO THOSE OBTAINED USING VOLUMETRIC RECONSTRUCTIONS.....	81
TABLE 2-5. BODY MASS ESTIMATES (IN KG) OF WELL-KNOWN NON-AVIAN BIPEDAL DINOSAURS COMPARED TO THOSE BASED ON OTHER SCALING REGRESSIONS.....	83
TABLE 2-6. BODY MASS (IN KG) ESTIMATES OF <i>TYRANNOSAURUS REX</i>	84
TABLE 3-1. MEAN RESIDUAL AND ABSOLUTE PPE OF VARIOUS VOLUMETRIC-DENSITY MASS ESTIMATES.....	128
TABLE 4-1. STATISTICAL SUMMARY OF ANCESTOR-DESCENDENT CONTRASTS IN ORNITHOPODS.	214
TABLE 4-2. RESULTS OF PHYLOGENETIC MODEL-FITTING ANALYSES FOR ORNITHOPODA AND CERTAIN CLADES THEREIN.....	216
TABLE 4-3. ANCESTOR-DESCENDENT BODY MASS (IN \log_{10} G) CONTRASTS BASED ON THE ‘MBL’ ORNITHOPOD TREE.....	218
TABLE 4-4. SUMMARY OF ANALYSES SUPPORTING A TREND IN BODY SIZE EVOLUTION IN ORNITHOPODS (I.E., COPE’S RULE).....	222
TABLE 4-5. PRELIMINARY RESULTS MODELING THE EVOLUTION OF UPPER BODY SIZE LIMITS WITHIN THE CONTEXT OF EXTRINSIC FACTORS.....	223

List of Figures

FIGURE 1-1. LIMB SCALING PATTERNS IN MAMMALIAN CLADES.	50
FIGURE 1-2. LIMB SCALING PATTERNS IN QUADRUPEDAL TERRESTRIAL TETRAPODS.	52
FIGURE 1-3. LIMB SCALING PATTERNS IN DIFFERENT MAMMALIAN SIZE CLASSES.....	54
FIGURE 1-4. RAW OLS REGRESSION FOR BODY MASS ESTIMATION AND PERCENT PREDICTION ERROR OF BODY MASS PROXIES.	56
FIGURE 2-1. MATHEMATICAL RELATIONSHIP BETWEEN THE CIRCUMFERENCE AND AREA OF A CIRCLE.	85
FIGURE 2-2. PLOT OF FEMORAL CIRCUMFERENCE TO BODY MASS IN A SAMPLE OF 70 EXTANT BIRDS.	87
FIGURE 2-3. COMPARISON OF BODY MASS ESTIMATE OF FOUR COMMONLY CITED SPECIMENS OF <i>TYRANNOSAURUS REX</i>	89
FIGURE 3-1. PLASTER RECONSTRUCTIONS USED BY COLBERT (1962).	129
FIGURE 3-2. EXPERIMENTAL DESIGN OF ALEXANDER (1985).	131
FIGURE 3-3. EXAMPLE OF GRAPHIC DOUBLE INTEGRATION AS APPLIED TO THE NON-THERAPSID SYNAPSID <i>EDAPHOSAURUS BOANERGES</i>	133
FIGURE 3-4. METHODOLOGICAL BASIS FOR THE ‘POLYNOMIAL’ TECHNIQUE DEVELOPED BY SEEBACHER (2001).	135
FIGURE 3-5. METHODOLOGICAL BASIS OF THE PHOTOGRAMMETRIC TECHNIQUE AS APPLIED TO NON-AVIAN DINOSAURS.	137
FIGURE 3-6. MATHEMATICAL SLICING TECHNIQUE OF HENDERSON (1999).	139
FIGURE 3-7. MINIMUM CONVEX HULL TECHNIQUE INTRODUCED BY SELLERS <i>ET AL.</i> (2012).	141

FIGURE 3-8. REGRESSION OF ANDERSON <i>ET AL.</i> (1985) BASED ON A SAMPLE OF 33 EXTANT MAMMALS.....	143
FIGURE 3-9. PLOT OF STYLOPODIAL CIRCUMFERENCES AGAINST VD MASS ESTIMATES OR RESIDUALS GROUPED BY MAJOR TAXONOMIC DESIGNATIONS.	145
FIGURE 3-10. BOXPLOTS OF RESIDUALS AND ABSOLUTE PERCENT PREDICTIONS ERRORS GROUPED BY MAJOR TAXONOMIC DESIGNATIONS.	147
FIGURE 3-11. PLOT OF STYLOPODIAL CIRCUMFERENCES AGAINST VD MASS ESTIMATES OR RESIDUALS GROUPED BY METHODOLOGY USED TO IMPLEMENT THE MODEL.	149
FIGURE 3-12. BOXPLOTS OF RESIDUALS AND ABSOLUTE PERCENT PREDICTION ERRORS GROUPED BY METHODOLOGY USED TO MEASURE THE VOLUME OF A MODEL.....	151
FIGURE 3-13. RELATIONSHIP BETWEEN SIZE (FEMORAL CIRCUMFERENCE) AND THE ERROR BETWEEN VD MASS ESTIMATES AND THOSE DERIVED FROM STYLOPODIAL CIRCUMFERENCE SCALING.....	153
FIGURE 3-14. RELATIONSHIP BETWEEN YEAR OF MODEL PUBLICATION AND ABSOLUTE PPE.....	155
FIGURE 3-15. <i>POST HOC</i> VALIDATION TEST OF PHYSICAL VD MODELS PRESENTED IN CHRISTIANSEN AND FARIÑA (2004) AND MAZZETTA <i>ET AL.</i> (2004).	157
FIGURE 4-1. PHYLOGENETIC TREE OF ORNITHOPODA.	224
FIGURE 4-2. PHYLOGENY OF HADROSAURIDAE SHOWING THE EFFECTS OF DIFFERENT SCALING METHODS ON RECONSTRUCTED BRANCH LENGTHS.....	226
FIGURE 4-3. BIVARIATE PLOTS OF HUMERAL AND FEMORAL LENGTH AND CIRCUMFERENCE INCLUDING BOTH ORIGINAL DATA AND ESTIMATED MISSING DATA VIA THE BPCA METHOD OF OBA <i>ET AL.</i> (2003).....	228

FIGURE 4-4. BIVARIATE PLOTS OF HUMERAL AND FEMORAL LENGTH AND CIRCUMFERENCE INCLUDING BOTH ORIGINAL DATA AND ESTIMATED MISSING DATA VIA THE BEST-FIT REGRESSION METHOD OF BROWN ET AL. (2012A)	230
FIGURE 4-5. DISTRIBUTION OF ANCESTOR-DESCENDENT CONTRASTS IN ORNITHOPODS.....	232
FIGURE 4-6. RELATIONSHIP BETWEEN AGE/CLADE-RANK AND BODY MASS IN ORNITHOPODS.....	234
FIGURE 4-7. BOXPLOTS OF ANCESTOR-DESCENDENT CONTRASTS BASED ON FOUR BRANCH LENGTH ESTIMATION METHODS.....	236
FIGURE 4-8. UPPER BODY SIZE LIMITS IN ORNITHOPODS RELATIVE TO TIME.....	238
FIGURE 4-9. UPPER BODY SIZE LIMITS IN ORNITHOPODS WITHIN THE CONTEXT OF SAUROPODOMORPH DIVERSITY DYNAMICS.....	240
FIGURE 4-10. SEQUENTIAL MODEL-FITTING TO THE MBL ORNITHOPOD TREE.....	242
FIGURE 4-11. SEQUENTIAL MODEL-FITTING OF SUBSAMPLED DATA BASED ON THE MBL ORNITHOPOD TREE.....	244
FIGURE 4-12. BODY MASS VARIANCE AND EVOLUTIONARY RATES BASED ON THE MBL ORNITHOPOD TREE.....	246

List of Appendices

APPENDIX 1. LIMB MEASUREMENT AND BODY MASS DATA IN EXTANT MAMMALS AND REPTILES.	284
APPENDIX 2. PHYLOGENETIC TREE OF MAMMALIAN AND REPTILIAN TAXA INCLUDED IN CHAPTER 1 (CAMPIONE AND EVANS, 2012).	290
APPENDIX 3. LIMB MEASUREMENT AND BODY MASS DATA IN EXTANT BIRDS.	293
APPENDIX 4. DATASET OF BODY MASS ESTIMATES OF NON-AVIAN DINOSAURS DERIVED FROM VOLUMETRIC-DENSITY MODELS.	295
APPENDIX 5. LIMB MEASUREMENTS OF ORNITHOPOD DINOSAURS USED TO DERIVE BODY MASS ESTIMATES.	302
APPENDIX 6. AGES AND BODY MASS ESTIMATES OF ORNITHOPOD DINOSAURS.	306
APPENDIX 7. NODE-AGE RECONSTRUCTIONS FOR VARIOUS TIME-SCALED VERSIONS OF THE ORNITHOPOD TREE.	308
APPENDIX 8. MAXIMAL BODY SIZE DATA IN ORNITHOPODS AT THREE DIFFERENT BIN SIZES.	311

List of Institutional Abbreviations

AENM	Amur Natural History Museum of the Far Eastern Institute of Mineral Resources, FEB RAS, Blagoveschensk, Russia
AMNH	American Museum of Natural History, New York, U.S.A.
ANSP	Academy of Natural Sciences, Philadelphia, U.S.A.
BHI	Black Hills Institute, Hill City, U.S.A.
BMNH	The Natural History Museum, London, U.K.
BP	Bernard Price Institute for Palaeontological Research, University of Witwaaterstrand, Johannesburg, South Africa
BSP	Bayerische Staatssammlung für Paläontologie und Geologie, Munich, Germany
BYU	Brigham Young University, Provo, U.S.A.
CEUM	College of Eastern Utah, Prehistoric Museum, Price, U.S.A.
CM	Carnegie Museum, Pittsburgh, U.S.A.
CMN	Canadian Museum of Nature, Ottawa, Canada
DMNH	Denver Museum of Natural History, Denver, U.S.A.
FMNH	Field Museum of Natural History, Chicago, U.S.A.
FWMSH	Fort Worth Museum of Science and History, Fort Worth, U.S.A.
GCC	Museum of the Chengdu University of Technology, Chengdu, China
GI	Geological Institute, Section of Palaeontology and Stratigraphy, Academy of Sciences of the Mongolian People's Republic, Ulaanbaatar, Mongolia
GMH	Geological Museum of Heilongjiang, Harbin, China
GMNH	Gunma Museum of Natural History, Gunma, Japan
GPIT	Institut und Museum für Geologie und Paläontologie, Universitat Tübingen, Tübingen
GSGM	Gansu Geological Museum, Lanzhou, China
HMN	Museum für Naturkunde der Humboldt, Berlin, Germany
IGM	Geological Institute, Mongolian Academy of Sciences, Ulaanbaatar, Mongolia
IMM	Inner Mongolian Museum, Hohhot, China
IPS	Instituto de Paleontología de Sabadella, Sabadell, Spain
IRSNB	Institut Royal des Sciences Naturelles de Belgique, Brussels, Belgium
IVPP	Institute of Vertebrate Paleontology and Paleoanthropology, Beijing, China
JLUM	Jilin University Museum, Changchun, China
KDRC	Korea Dinosaur Research Center, Gwangju, Republic of Korea

LACM	Los Angeles County Museum, Los Angeles, U.S.A.
LH	Long Hao Geologic and Palaeontological Research, Center, China
MACN-CH	Museo Argentino de Ciencias Naturales, Chubut, Argentina
MACN-N	Museo Argentino de Cicencis Naturales, Coleccion Rio Negro, Argentina
MAFI	Magyar Állami Földtani Intézet, Budapest, Hungary
MBR	Museums für Naturkunde der Humboldt, Berlin, Germany
MCF-PVPH	Museo Carmen Funes, Vertebrate Paleontology of Plaza Huincul, Plaza Huincul, Argentina
MCZ	Museum of Comparative Zoology, Cambridge, U.S.A.
ML	Musée de Lectoure, Lectoure, France
MNHN	Muséum National d'Histoire Naturelle, Paris, France
MNN	Musée National du Niger, Niger
MOR	Museum of the Rockies, Bozeman, U.S.A.
MPC	Palaeontological Center, Mongolian Academy of Sciences, Ulaanbaatar, Mongolia
MPCA	Museo Provincial Carlos Ameghino, Cipolletti, Argentina
MPEF	Muso Palaeontologico Egidio Fergulio, Trelew, Argentina
MPG	Museo Paleontológico de Galve, Galve, Spain
MPM	Museo Padre Molina, Río Gallegos, Santa Cruz, Argentina
MPZ	Museo Paleontológico de la Universidad de Zaragoza, Zaragoza, Spain
MTM	Magyar Termeszettudományi Múzeum, Budapest, Hungary
MUCPv	Museo de la Universidad Nacional del Comahue, Vertebrate Palaeontology, Neuquen, Argentina
NCSM	North Carolina State Museum, Raleigh, U.S.A.
NHMG	Natural History Museum of Guangxi, Guangxi, China
NSM	National Science Museum, Tokyo, Japan
OMNH	Sam Noble Oklahoma Museum of Natural History, Norman, U.S.A.
OUM	Oxford University Museum, Oxford, U.K.
OXFUM	Oxford University Museum of Natural History, Oxford, U.K.
PIN	Palaeontological Institute, Russian Academy of Sciences, Moscow, Russia
PIUW	Paläontologisches Institut, University of Vienna, Vienna, Austria
PMNH	Beijing (Peking) Museum of Natural History, Beijing, China
PMU	Paleontological Museum of Uppsala, Sweden
PVL	Palaeontologia de Vertebrados Lillo, Universidad Nacional de Tucuman, Tucman, Argentina

PVSJ	Museo de Ciencias Naturales, Universidad Nacional de San Juan, San Juan, Argentinia
QG	Queen Victoria Museum, Salsbury, U.K.
ROM	Royal Ontario Museum, Toronto, Canada
RSM	Royal Saskatchewan Museum, Eastend, Canada
SAM	Iziko South African Museum, Cape Town, South Africa
SC	Italian State collections
SGM	Ministère de l'Énergie et des Mines, Rabat, Morocco
SM	Senckenberg Museum, Frankfurt, Germany
SMA	Sauriermuseum, Aathal, Switzerland
SMU	Southern Methodist University, Dallas, Texas
TMM	Texas Memorial Museum, Austin, U.S.A.
TMP	Royal Tyrrell Museum of Paleontology, Drumheller, Canada
UALVP	University of Alberta, Laboratory for Vertebrate Palaeontology, Edmonton, Canada
UC OBA	University of Chicago, Department of Organismal Biology an Anatomy, Chicago, U.S.A.
UCMP	University of California Museum of Paleontology, Berkeley, U.S.A.
UMNH	Utah Museum of Natural History, Salt Lake City, U.S.A.
UNPSJB-Pv	Universidad Nacional de la Patagonia San Juan Bosco, Vertebrate Paleontology, Trelew, Argentina
USNM	United States National Museum, Smithsonian Institute, Washington D.C., U.S.A
YHZ	Yizhou Fossil Museum, Yixian City, China
YPM	Yale Peabody Museum, New Haven, U.S.A.
ZDM	Zigong Dinosaur Museum, Dashanpu, Zigong, China
ZJZ	Zhoucheng, China
ZMH	Zhejiang Museum of Natural History, Hangzhou, China
ZMUC	Zoological Museum, Copenhagen, Denmark
ZPAL	Zoological Institute of Paleobiology, Polish Academy of Sciences, Warsaw, Poland

Background and Context

In extant communities, body size is recognized among the most important biological properties because it strongly correlates with both physiological and ecological factors, such as metabolic rates (Kleiber, 1947; Hemmingsen, 1960; Gillooly *et al.*, 2001), growth rates (Peters, 1983; Gillooly *et al.*, 2002), fecundity (Brown *et al.*, 1993), diversity (McClain and Boyer, 2009), population density (Damuth, 1981; Calder, 1984), as well as home range and land area (Brown *et al.*, 1993; Gaston and Blackburn, 1996; Burness *et al.*, 2001), which are related to the productivity of the host environment (Capellini and Gosling, 2007). As a result, estimates of body mass (the standard measure of body size) are essential for inferring the palaeobiology of extinct taxa, and investigating large-scale evolutionary and ecological patterns in the history of life.

Due to the biological implications of body size, it is not surprising that numerous palaeontological studies have used size to construct and interpret a wide range of patterns in the fossil record including body size evolution (Laurin, 2004; Carrano, 2005; Hone *et al.*, 2005; Carrano, 2006; Finarelli and Flynn, 2006; Therrien and Henderson, 2007; Turner *et al.*, 2007; Butler and Goswami, 2008; Finarelli, 2008; Hone *et al.*, 2008; Sookias *et al.*, 2012a; Sookias *et al.*, 2012b; Dececchi and Larsson, in press), brain-size allometry and evolution (Jerison, 1969, 1973; Hopson, 1977, 1979), evolution of reproduction (Janis and Carrano, 1992; Varricchio *et al.*, 1997; Varricchio *et al.*, 2008), growth rates (Erickson *et al.*, 2001; Erickson, 2005), postural allometry and locomotion (Carrano, 1998; Christiansen, 1999c; Carrano, 2005), metabolism (Bakker, 1972; Gillooly *et al.*, 2006; Pontzer *et al.*, 2009), palaeotemperature (Head *et al.*, 2009), visceral organ size (Franz *et al.*, 2009), and community and trophic structures (Farlow, 1976;

Peczkis, 1994; Burness *et al.*, 2001; Codron *et al.*, 2012b; O’Gorman and Hone, 2012; Brown *et al.*, 2013b). In order to infer biological properties such as those outlined above, palaeontological studies require an estimate, or proxy, of body size, the value of which can have a large effect on the final interpretation.

Due to the biological utility of body size for interpreting biological patterns in the fossil record, it is important to understand, and if possible control for the set of assumptions/errors incurred by estimation methods. The dissertation presented here will focus on the methods currently used to estimate body mass in fossil record, and in particular as it pertains to non-avian dinosaurs. The main goal will be to quantitatively and empirically test previously proposed methodologies and discuss their various drawbacks and merits.

Body mass estimation of extinct members of crown clades (e.g., Mammalia and Aves) rely on the use of scaling relationships derived from extant members (Damuth and MacFadden, 1990; Gingerich, 1990; Campbell Jr and Marcus, 1992; Fortelius and Kappelman, 1993; De Esteban-Trivigno *et al.*, 2008; Millien and Bovy, 2010; De Esteban-Trivigno and Köhler, 2011) because it is the most objective and efficient method. However, the utility of scaling relationships for estimating body mass in distantly related, and morphologically disparate taxa, such as non-avian dinosaurs has been criticized in various studies (e.g., Casinos, 1996; Carrano, 2001; Hutchinson *et al.*, 2011). Therefore, the first chapter will address the utility of scaling relationships to estimating the body mass of taxa and empirically test the criticisms forwarded against a universal scaling relationship for estimating body mass. Given the dataset used in the first chapter (mammals and non-avian reptiles), the results only pertain to terrestrial quadrupeds. As a result, in my second chapter I will discuss the methods available for estimating body mass in extinct bipeds (e.g., non-avian theropods) and present a new equation mathematically derived

from the quadrupedal dataset for estimating body mass in bipeds. The third chapter will review the various methodological formulations proposed to create volumetric reconstructions in order to estimate body size, and, using the results of chapter 1 (Campione and Evans, 2012) and chapter 2 as a baseline dataset, test these formulations within an empirical context, thereby indirectly testing the unavoidable assumption associated with reconstructions.

The final chapter (Chapter 4) will apply the results obtained in this dissertation to reconstructing the macroevolutionary patterns of body size in a model clade of non-avian dinosaurs, Ornithopoda. This clade is an ideal group with which to assess patterns of body size evolution because it represents a diverse group (approximately 90 species) with a fossil record that spans over 100 million years (from the early/middle Jurassic to the end of the Mesozoic). In addition, ornithopods exhibit a possible four orders of magnitude range in body size, [hypsilophodontids (~5 kg) to iguanodontians (>10,000 kg) (Paul, 1997; Seebacher, 2001)], making them a model clade with which to test three patterns often cited for non-avian dinosaurs:

1. Dinosaurs exhibit a trend towards increasing body size throughout their evolutionary history (Hone *et al.*, 2005; Carrano, 2006), a pattern predicted by Cope's Rule.
2. Upper body size limits in dinosaurs are driven by intrinsic physiological factors, not environmental factors (Sanders *et al.*, 2010; Sookias *et al.*, 2012a).
3. Several ornithopod species are hypothesized to represent examples of insular dwarfism (Weishampel *et al.*, 1993; Dalla Vecchia, 2009; Benton *et al.*, 2010) based on their putative size and reconstructed palaeoenvironment.

Chapter 1

A Universal Scaling Relationship Between Body Mass and Proximal Limb Bone Dimensions in Quadrupedal Terrestrial Tetrapods

1.1 Abstract

Body size is intimately related to the physiology and ecology of an organism. Therefore, accurate and consistent body mass estimates are essential for inferring numerous aspects of palaeobiology in extinct taxa, and investigating large-scale evolutionary and ecological patterns in the history of life. Scaling relationships between skeletal measurements and body mass in birds and mammals are commonly used to predict body mass in extinct members of these crown clades, but the applicability of these models for predicting mass in more distantly related stem taxa, such as non-avian dinosaurs and non-mammalian synapsids, have been criticized on biomechanical grounds. Here we test the major criticisms of scaling methods for estimating body mass using an extensive dataset of mammalian and non-avian reptilian species derived from individual skeletons with live weights. Significant differences in the limb scaling of mammals and reptiles are noted in comparisons of limb proportions and limb length to body mass. Remarkably, however, the relationship between proximal (stylopodial) limb bone circumference and body mass is highly conserved in extant terrestrial mammals and reptiles, in spite of their disparate limb postures, gaits, and phylogenetic histories. As a result, we are able to conclusively reject the

main criticisms of scaling methods that question the applicability of a universal scaling equation for estimating body mass in distantly related taxa. The conserved nature of the relationship between stylopodial circumference and body mass suggests that the minimum diaphyseal size of the individual major weight-bearing bones is only weakly influenced by the varied forces exerted on the limbs (i.e., compression or torsion) and most strongly related to the mass of the animal. Our results therefore provide a much-needed, robust, phylogenetically corrected framework for accurate and consistent estimation of body mass in extinct terrestrial quadrupeds, which is important for a wide range of palaeobiological studies (including growth rates, metabolism, and energetics) and meta-analyses of body size evolution.

1.2 Introduction

In extant taxa, body size is recognized as one of the most important biological properties because it strongly correlates with numerous physiological and ecological factors, such as metabolic rates (Kleiber, 1947; Hemmingsen, 1960; Gillooly *et al.*, 2001), growth rates (Peters, 1983; Gillooly *et al.*, 2002), fecundity (Brown *et al.*, 1993), diversity (McClain and Boyer, 2009), population density (Damuth, 1981; Calder, 1984), as well as home range and land area (Brown *et al.*, 1993; Gaston and Blackburn, 1996; Burness *et al.*, 2001), which are related to the productivity of the host environment (Capellini and Gosling, 2007). Due to these relationships, estimates of body mass (the standard measure of body size) are essential for inferring the palaeobiology of extinct taxa, and investigating large-scale evolutionary and ecological patterns in the history of life.

Due to the biological implications of body size, it is not surprising that numerous palaeontological studies have used body mass estimates to construct and interpret patterns of

body size evolution (Laurin, 2004; Carrano, 2005; Hone *et al.*, 2005; Carrano, 2006; Finarelli and Flynn, 2006; Therrien and Henderson, 2007; Turner *et al.*, 2007; Butler and Goswami, 2008; Finarelli, 2008; Hone *et al.*, 2008), brain-size allometry and evolution (Jerison, 1969, 1973; Hopson, 1977, 1979), evolution of reproduction (Janis and Carrano, 1992; Varricchio *et al.*, 1997; Varricchio *et al.*, 2008), growth rates (Erickson *et al.*, 2001; Erickson, 2005), postural allometry and locomotion (Carrano, 1998; Christiansen, 1999c; Carrano, 2005), metabolism (Bakker, 1972; Gillooly *et al.*, 2006; Pontzer *et al.*, 2009), palaeotemperature (Head *et al.*, 2009), visceral organ size (Franz *et al.*, 2009), and community and trophic structures (Farlow, 1976; Peczkis, 1994; Burness *et al.*, 2001). In order to infer the biological properties outlined above, these studies require the use of an estimate or proxy of body size, which can have a large effect on the final interpretation. As a result, it is important to understand the set of assumptions/errors incurred by body size estimates and proxies.

Currently, there are two types of methods used to estimate body mass in extinct animals: volumetric reconstructions, and skeletal scaling relationships. The latter method is commonly used to predict body mass in extinct members of relatively recent crown clades (i.e., of Mesozoic origin) such as Mammalia and Aves (Damuth and MacFadden, 1990; Gingerich, 1990; Campbell Jr and Marcus, 1992; Finarelli and Flynn, 2006; De Esteban-Trivigno *et al.*, 2008; Millien and Bovy, 2010). However, in extinct stem groups (e.g., non-avian dinosaurs and non-mammalian synapsids), estimations are often based on volumetric reconstructions, which involve either physical three-dimensional scale models (Gregory, 1905; Colbert, 1962; Alexander, 1985; Christiansen and Fariña, 2004), graphic double integration of two-dimensional reconstructions (Gunga *et al.*, 1999; Hurlburt, 1999; Seebacher, 2001), or computer-generated life reconstructions (Henderson, 1999; Motani, 2001; Gunga *et al.*, 2007; Gunga *et al.*, 2008; Bates *et al.*, 2009a; Hutchinson *et al.*, 2011). Such estimates are widely used in the literature (e.g.,

Bakker, 1972; Franz *et al.*, 2009) despite the fact that they are prone to a considerable amount of error. In a typical example, body mass estimates for a single mounted skeleton of *Brachiosaurus brancai* recently published by the same research group have resulted in estimates of 38 tonnes and 74.4 tonnes (Gunga *et al.*, 2002; Gunga *et al.*, 2008). This is the result of different interpretations of a multitude of factors associated with the mass and proportion of an organism's tissues and organs (Grand, 1990), or the effects of air sacs and lungs, which will likely have a large effect on specific gravity (i.e., density of the animal in relation to water), needed to estimate mass from a volume. Within non-avian reptiles specific gravity has been noted to range from 0.8 to 1.2 (Colbert, 1962; Hurlburt, 1999); however, given the varying levels of bone pneumaticity observed in saurischian dinosaurs (Wedel, 2003; Benson *et al.*, 2011), and the fact that birds typically exhibit lower densities than mammals and other reptiles (Hazlehurst and Rayner, 1992), it is almost certain that the specific gravity of extinct animals also varied (Wedel, 2003). As a result, assumptions based on a set density parameter will considerably affect a mass estimate (Gunga *et al.*, 2002; Gunga *et al.*, 2008). Perhaps more importantly, the numerous assumptions about soft tissue properties and body shape (e.g., muscle sizes) in many of the models make it difficult to control for sources of error and to determine the confidence associated with a given mass estimate, although recent computational modelling advances attempt to outline maximum and minimum body mass bounds (e.g., Gunga *et al.*, 2008; Bates *et al.*, 2009b; Hutchinson *et al.*, 2011). Despite the complications associated with life reconstructions of extinct taxa, models are important for testing numerous biomechanical hypotheses (Henderson, 2004; Henderson, 2006; Henderson, 2010; Hohn, 2011; Hutchinson *et al.*, 2011; Mallison, 2011a, c). Therefore, it is important that models be constrained by data derived from extant taxa, such as those obtained from scaling relationships.

An alternative method to reconstructions, and one that can be used to test scale and computational models (e.g., Motani, 2001), is the use of scaling relationships between body mass and skeletal dimensions derived from extant taxa. A skeletal measure, if strongly related to body mass, will provide an estimate that controls for the sources of error associated with making a reconstruction, such as determination of tissue volume and specific gravity, which are virtually impossible to constrain in life-reconstructions. Furthermore, skeletal measurements are generally easier to obtain than full body scale reconstructions, especially for taxa that are only partially preserved, and are therefore more practical estimators in large-scale evolutionary and ecological studies (e.g., Laurin, 2004; Hone *et al.*, 2005; Carrano, 2006; Hone *et al.*, 2008). Finally, the variation in the extant dataset can be used to quantify the degree of confidence in the estimated parameter, and can thus provide a range in which a particular body mass is likely to fall, thereby providing a constraint for estimates produced by reconstructed models. Scaling methods are almost universally accepted as a means to estimate body mass accurately for extinct taxa of crown groups, such as mammals and birds (e.g., Hone *et al.*, 2008; Millien and Bovy, 2010), but have been extensively criticized when applied to more distantly related stem taxa that fall outside the body size range observable in extant representatives, such as *Indricotherium* (Fortelius and Kappelman, 1993), xenarthrans (De Esteban-Trivigno *et al.*, 2008), and non-avian dinosaurs (Alexander, 1989; Paul, 1997; Carrano, 2001; Hutchinson *et al.*, 2011). For the first two groups, studies have since shown that scaling relationships still provide the most reliable mass estimates (Fortelius and Kappelman, 1993; De Esteban-Trivigno *et al.*, 2008).

Dinosaurian body masses are still generally estimated using reconstructions, with the exception of two studies (Anderson *et al.*, 1985; Campbell Jr and Marcus, 1992). The pioneering work completed by Anderson *et al.* (1985), herein referred to as the Anderson method, suggested that the body mass of dinosaurs could be estimated using the measured scaling relationship

between live mass and total circumference of the stylopodia (humerus + femur) derived from a sample of 33 species of extant terrestrial mammals. Although the Anderson method provides a more objective way to estimate body mass in extinct taxa, it has been criticized by numerous authors (e.g., Casinos, 1996; Paul, 1997; Carrano, 2001; Seebacher, 2001; Gunga *et al.*, 2002; Hutchinson *et al.*, 2007; Lehman and Woodward, 2008; Hutchinson *et al.*, 2011). Here we use an extensive dataset of extant mammals and non-avian reptiles compiled from individual skeletons of live-weighed animals, in order to directly test the three main criticisms made towards the use of a universal limb scaling relationship to estimate body mass in extinct terrestrial amniotes:

1. The widely cited Anderson method, especially among non-avian dinosaur researchers, is criticised based on its use of a taxonomically biased sample towards ungulates (e.g., (Carrano, 2001)). Studies examining limb-scaling patterns in mammals have noted that the limb proportions of ungulates differ from that of other mammals (Alexander *et al.*, 1979; Bertram and Biewener, 1990; Carrano, 2001). However, whether ungulates differ from other groups of mammals in their scaling patterns of limb circumference to body mass has never been tested.
2. Differences in gait and limb posture impart different stress regimes on the limbs (Rubin and Lanyon, 1984; Blob and Biewener, 1999). These differences may affect limb morphology, thereby negating the applicability of a single equation to estimate body mass in a variety of extinct vertebrates. Given different stress regimes, we test for differential limb scaling between animals of various gaits and limb posture by comparing differently size sub-samples of mammals, and parasagittal mammals to sprawling reptiles.
3. Residual outliers (i.e., large residual values) and extreme outliers (i.e., values at the upper and lower extremes of the dataset) can have a large effect on regression coefficients

(Sokal and Rohlf, 1969). The problem of residual outliers in the large-bodied mammal sample of Anderson *et al.* (1985) was discussed by Packard *et al.* (2009). We have expanded the sample size of the large-bodied dataset and will address the effect that potential residual outliers have on the circumference to body mass relationship. The effect of extreme outliers on limb scaling is, in part, mediated by logarithmic transformation of the data, but will also be assessed through size class comparisons. Although the issue of body mass extrapolation to giant extinct taxa (e.g., Sauropoda; (Alexander, 1989; Gunga *et al.*, 1999)) will always exist, the vast majority of extinct animals, including most non-avian dinosaurs, fall within the body mass range of extant taxa.

All three of these criticisms are tested for the first time, within the context of 200 mammal and 47 non-avian reptile species (Additional file 1, Dataset). Based on our results we develop a universal scaling equation between the total circumference of the stylopodia and body mass that is applicable to all terrestrial quadrupeds, and permits estimation of body mass in extinct taxa along with an error factor that can constrain estimates for use in future palaeobiological studies.

1.3 Materials and Methods

1.3.1 Database Construction

In order to test the hypotheses outlined above, we amassed an extensive dataset of limb bone measurements of 200 mammal and 47 non-avian reptile species from individuals that were

weighed on a scale either prior to death or skeletonization; no extant body masses were estimated (Appendix 1). For the most part, the dataset was built with newly measured specimens; however, it was augmented with published measurements from Christiansen and Harris (2005) and Anderson *et al.* (1985). Measurements were taken from stylopodial elements, including maximum lengths and minimum circumference. Length measurements less than 150 mm were taken with digital callipers, longer dial callipers were used for measurements between 300 - 150 mm, and fibreglass measuring tape for those greater than 300 mm. Following Anderson *et al.* (1985), we use minimum circumference (thinnest region along the diaphysis) as a proxy for limb robusticity. In addition to reproducing the analysis presented by Anderson *et al.* (1985), minimum circumference should provide a proxy of the minimum cross-sectional area of the bone and therefore be related to the overall compressive strength of the limb. Cross-sectional area was not used due to the cost of collecting this data. Moreover, circumference can be more easily measured on both extant and fossil samples, providing a larger extant dataset and a more inclusive framework for future predictive studies. Circumference measurements were taken with thin paper measuring tapes of different widths, depending on the size of the specimen being measured, and the minimum circumference was determined by taking various measurements along the diaphysis and opting for the thinnest measurement. All measurements were taken from both sides of the specimen, where possible, and averaged. Specimens measured are of adult body size. For most of the mammalian sample, the ontogenetic status of the specimen was determined based on the level of epiphyseal fusion. For the non-avian reptile sample, as well as some of the largest mammals, maturity was established by verifying that the body mass of the measured specimen is similar to published reports of average body masses for that species (e.g., Andrews and Pough, 1985; Woodward *et al.*, 1995; Blob, 2000; Jones *et al.*, 2009). In general, only a single specimen of each species could be obtained; however, in instances where more than one

adult individual was available, the largest individual was used in this study. In these cases, none of these exemplars used seem unusually large compared to reported adult body mass in that species. Finally, this study compares taxa with different growth strategies [mammals have determinate growth whereas growth in reptiles is generally considered indeterminate, but asymptotic (Andrews, 1982)] that may result in differences in size structuring within and between populations of taxa with these different strategies. If, and/or how, these differences affect limb to body mass scaling analyses is unknown at this time. However, the masses of the reptiles used here fall within the range of what is considered typical for an adult of each species, and, given our large sample and the nature of our results (see below), we expect that these effects will be minimal, yet may warrant future consideration.

1.3.1.1 Taxon Sampling

Taxa were chosen based on three criteria: 1) The dataset must include a large range in body mass, so that size-related postural differences can be assessed (Jenkins, 1971; Carrano, 1999). We significantly expand upon the dataset of Anderson *et al.* (1985), especially for large bodied mammalian species, to more completely represent the range of variation in limb proportions at large sizes and address the contention that certain large taxa are residual outliers (Packard *et al.*, 2009). Due to the limitations of measuring limb bone circumference at very small size, taxa below 50 g were not included in this study. 2) The sample must encompass a wide phylogenetic scope, so that most major mammalian and reptilian clades are sampled. 3) The sample must include taxa from a broad spectrum of lifestyles. Our study focuses on terrestrial taxa; however, we have also included mammalian or reptilian taxa with specialized lifestyles that have the potential to affect limb proportions and their relationship with body size. These include saltators (e.g., Macropodidae), brachiators (e.g., *Hylobates lar*, and *Pongo pygmaeus*), burrowers (e.g.,

Talpidae), and amphibious taxa (e.g., Hippopotamidae and Crocodylia). The former three categories are associated with salient morphological features that allow these lifestyles to be recognized in the fossil record; however, the amphibious nature of several extinct taxa remains uncertain, and may affect how limb measurements scale with body mass due to the effects of buoyancy.

Avian taxa were not included in the current study because they are bipedal. The forces exerted by body mass in a biped are transmitted through two limbs compared to four in a quadruped, and therefore direct comparisons of limb to body mass scaling between birds and quadrupedal tetrapods are difficult to interpret. A small sample of lissamphibians (one caudatan and seven anurans) for which live body mass is known was examined in this study. Unfortunately, the current sample size does not provide enough power to make meaningful slope and intercept comparisons, and lissamphibians are not included in the main comparisons presented in the results section.

1.3.2 Statistical Analyses

The distribution of the variables used in this study are all positively skewed and, therefore, highly different from a normal distribution; as such all variables were logarithmically transformed (at base 10) to better approximate a log-normal distribution. In addition to normality, log transforming reduces the level of heteroscedasticity in the data set, minimizes the effect of extreme outliers, and allows for the visualization of data in a linear fashion, which simplifies the visual comparisons of slopes (Zar, 1968; Sokal and Rohlf, 1969). The benefits and complications regarding the application of log transformation in predictive scaling relationships was recently debated by Packard *et al.* (2009) and Cawley and Janacek (2009). We agree with the latter study, which demonstrated that log-transformed data are preferred for this type of

analysis as it assigns an equal weight to all data points in a regression, rather than upper extreme values (Cawley and Janacek, 2009).

1.3.2.1 Interspecific limb scaling

All measurements were incorporated into a variety of bivariate plots and analyzed using the Standardized Major Axis line-fitting method (SMA; also known as Reduced Major Axis) (Warton *et al.*, 2006). The analyses compare a variety of measurements, including: 1) limb proportions, such as femur length to humerus length and humerus/femur length to circumference; and 2) limb measurements to body mass, such as humerus/femur length vs. body mass and humerus/femur circumference vs. body mass. All SMA analyses were conducted using the open-source software R (R Development Core Team, 2012) and the package ‘smatr’ (Warton *et al.*, 2006; Warton *et al.*, 2011).

To address the criticisms raised against the Anderson method, subgroups within the data were compared. These include comparisons between mammalian groups for which a sample size greater than ten could be obtained, such as Ungulata, Carnivora, Marsupialia, Euarchonta, and Glires. In addition, comparisons were made between different size classes. Size class comparisons were based on three body mass thresholds: 20 kg, which was previously used by Economos (1983) to show differential scaling in mammals, and it is also thought to represent the lower size limit for migratory mammals and hence may affect limb scaling patterns (Peters, 1983); 50 kg, a threshold at which mammalian limb scaling has been previously noted to vary (Christiansen, 1999b); and 100 kg, previously used by Bertram and Biewener (1990), and which allows better representation of the large-bodied portion of the dataset.

Fitted lines of different subsamples were compared based on the 95% confidence intervals of the slope and intercept, and differences were considered to be significant when intervals did not overlap. However, given that statistical significance can still be obtained even though confidence intervals overlap (Sokal and Rohlf, 1969), we conducted a series of pairwise comparisons of the slopes and intercepts using a likelihood ratio test and a t-test, respectively. These tests have the added benefit that they can be corrected for errors associated with multiple comparisons using the False Discovery Rate (FDR), an approach that, as far as we are aware, cannot be applied to confidence intervals (Benjamini and Hochberg, 1995; Curran-Everett, 2000). The likelihood ratio was implemented with the ‘smatr’ package (Warton *et al.*, 2006; Warton *et al.*, 2011). Conventional methods for comparing intercepts (e.g., ANCOVA, Wald statistic, and traditional t-tests) alter the original intercepts by forcing a common slope to each group being analyzed (Zar, 1968; Warton *et al.*, 2006). Although this may make statistical sense (Warton *et al.*, 2006), it involves permuting the best fit-line away from the original biological data. As a result, here we compare intercepts using a two-tailed t-test based on equation 18.25 of Zar (1968):

$$t = (b_1 - b_2) / \text{SE}_{\text{SMA}}$$

where b_1 and b_2 represent the pair of intercepts being compared, and SE_{SMA} is the standard error of the difference in SMA intercepts, calculated as per equation 18.26 of Zar (1968). Comparing intercepts using this method has the added benefit of allowing comparisons of y-values along the true SMA lines at x-values other than 0. This is advisable when comparing biological scaling lines because first, the intercept at $x=0$ is an extrapolation of the line beyond the range of the data (Zar, 1968), but perhaps more importantly given the type of data used here, a value of $x=0$ is biologically meaningless. As a result, in addition to presenting the results of the t-test at the true

intercept, we compare y-values at the minimum value along the x-axis using the same t-test method. The results of the two intercept comparison methods described above are presented, and all p-values are corrected using the FDR (Benjamini and Hochberg, 1995; Curran-Everett, 2000), implemented with the ‘*p.adjust*’ function in R. In total, 14 pairwise comparisons are made for each analysis.

In addition to comparing limb scaling patterns between different groups, scaling coefficients were used to test theoretical scaling models, such as geometric (GS), elastic (ES), and static (SS) similarity (McMahon, 1973; McMahon, 1975b). The models predict that under GS: circumference \propto length; mass \propto length³; mass \propto circumference³, under ES: circumference \propto length^{1.5}; mass \propto length⁴; mass \propto circumference^{8/3}, and finally under SS: circumference \propto length²; mass \propto length⁵; mass \propto circumference^{2.5}. These models were tested against the empirical slopes obtained in this study using the method described by Warton *et al.* (2006).

1.3.3 Phylogenetic Independent Contrasts

In addition to plotting the raw data, as was done by Anderson *et al.* (1985), we calculated the phylogenetic independent contrasts (PIC) for the entire dataset in order to correct for non-independence of the raw data as a result of common ancestry (Felsenstein, 1985). We compared the scaling coefficients from the raw and phylogenetically corrected data to test if non-independence significantly alters the scaling patterns obtained from the raw data. The phylogenetic tree (Appendix 2) was constructed in Mesquite (Maddison and Maddison, 2010), based on recent phylogenetic analyses obtained for extant Mammalia (Bininda-Emonds *et al.*, 2007), and non-avian reptiles (Gaffney and Meylan, 1988; Ast, 2001; Engstrom *et al.*, 2004; Townsend *et al.*, 2004; Vidal and Hedges, 2005; Le *et al.*, 2006; Spinks and Shaffer, 2009).

Branch lengths are measured in millions of years. For the mammalian portion of the phylogeny we used the branch lengths of Bininda-Emonds *et al.* (2007). Branch lengths in the reptile portion of the tree were largely calculated using molecular estimates of divergence times (Amer and Kumazawa, 2005; Near *et al.*, 2005; Wiens *et al.*, 2006; Roos *et al.*, 2007; Naro-Maciel *et al.*, 2008; Albert *et al.*, 2009; Okajima and Kumazawa, 2009; Okajima and Kumazawa, 2010). However, species-level divergence times of some taxa, such as turtles, are poorly constrained, and as a result, we estimated the branch lengths based on the oldest known fossil occurrence for the species or genus obtained from the Palaeobiology Database (<http://palaeodb.org/>).

Both theoretical and empirical studies of PIC state that in order for contrasts to receive equal weighting and thereby conform to assumptions stipulated by parametric analyses and statistics, branch lengths must be adjusted so that contrasts are standardized, and therefore have a non-significant relationship with their standard deviation (Garland *et al.*, 1992). The criterion was not met by the raw branch lengths, but was obtained by transforming the branch lengths by their natural log. Branch lengths were assigned and transformed in Mesquite and the tree file was imported into R, where contrasts were calculated using the ‘APE’ package (Paradis *et al.*, 2004). A best fit line was calculated for the contrasts using a SMA in the package ‘smatr’ (Warton *et al.*, 2006), which allows for the line to pass through the origin, as stipulated by Garland *et al.* (1992). The PIC slopes for the entire dataset and subsets (as described above) were compared to slopes obtained from the raw data using the 95% confidence intervals.

1.3.3.1 Body Mass Estimation

In order to provide the best estimation parameter for body mass, a Model I (Ordinary Least Squares, OLS) regression analysis is preferred. It is the most appropriate model for estimating a value of y based on x , as it accounts for the complete error of the y variable that can be explained

by the x variable (Sokal and Rohlf, 1969; Hansen and Bartoszek, 2012). The analysis was performed on the entire dataset ($N = 247$) between body mass and a variety of limb measurements in order to test for the best predictor. The ‘goodness of fit’ of a predictor was examined based on the commonly used coefficient of determination (R^2); however, this value is considered a poor representation of the strength of a regression, due largely to its strong association with sample size (Smith, 1984). Therefore, given the large dataset presented here, we provide three additional metrics, including the standard error of the estimate (SEE), the mean percent prediction error (PPE), and the Akaike Criterion (AIC). The mean PPE is perhaps the best metric of regression strength for these types of analyses as it deals with the predictive strength of the relationship in relation to the non-logged data. In addition, the PPE has the added benefit of allowing for calculation of confidence intervals around the mean PPE, and therefore facilitates comparison between the mean PPE of different models.

In addition to the OLS bivariate regression outlined above, we included all limb measurements into a suite of multiple regression analyses and, given that this technique is highly recommended (Smith, 2002; Christiansen and Fariña, 2004; De Esteban-Trivigno *et al.*, 2008), tested if they are significantly better predictors of body mass than bivariate regressions. The predictive accuracy of each analysis was compared using SEE, PPE, and AIC. Finally, because none of the bivariate or multiple regressions account for correlation and covariance of morphology between taxa as a result of phylogenetic history, we re-analyzed the data using a phylogenetic generalized least squares approach (Martins and Hansen, 1997), a method recently applied to estimate body mass in extinct bovids (De Esteban-Trivigno and Köhler, 2011). Application of this method is based on the same phylogenetic tree, branch lengths, and a Brownian motion model of evolution (Appendix 2). This approach was implemented using the ‘APE’ and ‘nlme’ packages in R.

1.4 Results

1.4.1 Raw Data Results

Results from the SMA analyses comparing clades based on the raw non-phylogenetically corrected data are provided in Figure 1-1 and Figure 1-2, and Table 1-1; comparisons are summarized in Table 1-2 and Table 1-3. Size class comparisons are presented in Figure 1-3, Table 1-5, and Table 1-6. All analyses show strong correlations with each other, and to body mass (i.e., size) as indicated by a mean coefficient of determination of 0.9446 ± 0.0093 for the clade comparisons, and 0.914 ± 0.014 for comparisons between size classes.

In total, 80 pairwise comparisons are made between mammalian clades (Table 1-2). Of these comparisons, the 95% confidence intervals indicate 12 significant differences between scaling coefficients and 13 significant differences between intercepts. In comparison, the likelihood ratio test, the results of which are adjusted for multiple comparisons using FDR, reveals 14 significant differences between slopes, and a t-test of the true intercepts indicate ten significant differences, however, when the intercept is corrected and compared at a more biologically meaningful value, the minimum value along the x-axis, the t-test indicates that there are no significant differences in intercept.

Regardless of the comparison method used, the most significant variation is noted in the scaling of stylopodial proportions (length to circumference) of the humerus and femur, as well as in the scaling of humeral and femoral lengths with body mass (Figure 1-1; Table 1-1 and Table 1-2). This is especially true for ungulates, which possess stylopodial proportions and lengths that

scale significantly different from all other groups examined here. No significant differences in scaling coefficients were recovered in the scaling of either the humeral or femoral circumference to body mass using the likelihood ratio test, and only two differences were recovered by the 95% confidence interval comparisons in the scaling of humerus circumference to body mass (Marsupialia scales significantly higher than Ungulata and Carnivora).

In total, ten and 13 significant differences were noted in comparisons between intercepts using confidence intervals and a t-test, respectively, including a significant difference in the intercept of Carnivora and Glires using 95% confidence intervals. However, visual inspection reveals major overlap between the data points at the minimum values along the x-axis (Figure 1-1) suggesting that significant differences may be due to extrapolation of the SMA line to a value of $x = 0$. This is likely a valid interpretation as an adjusted t-test comparing the intercepts at the minimum values along the x-axis (Table 1-2) indicate that intercepts are not significantly different between mammalian groups in all of the comparisons made here.

Mammalian and reptilian scaling patterns show similar scaling coefficients, overall. Of the eight comparisons, two scaling coefficients showed significant differences using both the 95% confidence intervals and the likelihood ratio test. More specifically, the humeral proportions and humeral length to body mass in reptiles scale above that observed for mammals (Figure 1-2; Table 1-1 and Table 1-3). Comparison of the confidence intervals revealed significant differences in the intercepts of mammals and reptiles in the relationship between femur circumference and body mass, as well as humerus length to body mass. However, these differences were not recovered by either t-test. When the circumference of the humerus and femur is combined, all tests indicate that the total stylopodial (humerus + femur) circumference to body mass relationship of reptiles is statistically indifferentiable from that of mammals.

Finally, in order to assure that the results obtained for mammals and reptiles are not influenced by differences in body size range in the two samples, we re-ran the analyses using a subset of the mammalian dataset ($N = 174$), which corresponds to all mammals equal to, or below, the mass of the *Alligator mississippiensis* specimen (168 kg), the largest reptile measured in this study. In general, results of this pruned analysis were similar to those obtained with the entire mammalian dataset (Table 1-3 and Table 1-4). In particular, comparisons of slopes based on the likelihood ratio test are identical. Differences between the two analyses were noted in comparisons using the 95% confidence intervals, which revealed an additional difference in the scaling of femoral length and circumference between mammals and reptiles, but failed to recover a significant difference between the intercepts in the analysis of femoral circumference against body mass. The t-test on the pruned data also revealed a significant difference between the intercepts of mammals and reptiles in the relationship of humeral length to body mass as well as femoral to humeral length. Despite differences in the scaling of stylopodial length, no significant differences were noted in the scaling of stylopodial circumference to body mass between mammals and reptiles.

Size class comparisons, based on the mammalian dataset ($N = 200$), at three different thresholds reveal greater variation in scaling patterns between subsamples at lower body size thresholds (Table 1-5 and Table 1-6), although this may be due to the smaller sample size of the large body size class at the 100 kg threshold ($N = 36$). In particular, the limb proportions of the humerus scaled differently in animals smaller than 20 kg compared to those larger than 20 kg, a pattern also noted at the 50 kg threshold. A significant difference in the proportional scaling of femur is also noted at 50 kg. Significant differences were noted in the scaling of humeral length to body mass between individuals at the 20 kg and 50 kg threshold. As in the mammalian and

reptilian comparisons, the combined circumferences showed no significant differences between scaling coefficients of different size classes (Figure 1-3; Table 1-6).

1.4.2 Independent Contrast Results

Overall, phylogenetically corrected scaling relationships reveal lower coefficients of determination than the raw data. The mean R^2 (0.9126 ± 0.0105) for the corrected data are significantly lower than that obtained from the raw data (two tailed t-test: $t = -4.4721$; $p << 0.0001$). As a result, fewer significant differences were noted between mammalian clades and between mammals and reptiles (Table 1-7). Of the 80 mammalian comparisons made, two showed significant differences recovered by both the 95% confidence intervals and the likelihood ratio test. The differences include a significantly lower scaling coefficient of Carnivora compared to Glires and Ungulata, in the scaling of femur length to humerus length. Confidence intervals indicate two other differences in which the humeral length of reptiles scales significantly higher than that of mammals when compared to body mass and the humeral circumference in ungulates scales higher than that of carnivorans when compared to body mass.

Most importantly, however, based on the confidence intervals, comparisons between scaling coefficients obtained from the raw data (Table 1-1) and the phylogenetically corrected data (Table 1-7) reveal only a single significant difference for the scaling of humeral proportions in Glires. Other than that comparison, the lack of significant differences between the raw data and phylogenetically corrected data suggest that phylogeny does not play a significant role in dictating the scaling patterns tested here with regards to the major weight-bearing bones in terrestrial tetrapods. For this reason, and for ease of comparison with previous limb scaling studies, further discussion will be based on results obtained from the raw data.

1.5 Discussion

Skeletal limb morphology in vertebrates is considered to reflect a trade-off between the energetic requirements imposed by movement and the functional requirements imposed by loadings on the bone from behavioural qualities and/or body size (Rubin and Lanyon, 1982; Bertram and Biewener, 1990; Carrano, 1999; Christiansen, 1999a; Blob, 2000; Garcia and da Silva, 2006; Clemente *et al.*, 2011). Biomechanical studies using in-vivo strain gauges and force platforms in mammals and birds have concluded that peak functional strains [i.e., safety factors (strain at which yield or failure occur/peak functional strain)] placed on a limb bone during locomotion are consistent among taxa of different size and different lifestyles (i.e., terrestrial, aquatic, and aerial; (Rubin and Lanyon, 1984)). However, in non-avian reptiles, safety factors are higher compared to mammals suggesting that functional strains are lower in the former (Blob and Biewener, 1999, 2001; Butcher *et al.*, 2008). Nevertheless, in order to mitigate decreases in safety factors associated with increases in body size, the architecture of the skeletal limb, such as limb robustness, cortical thickness, and/or curvature, are expected to vary (Rubin and Lanyon, 1982, 1984; Biewener, 1989; Clemente *et al.*, 2011).

Interspecific limb scaling patterns are often used to test theoretical biomechanical models, such as geometric, elastic, and static similarity, which predict scaling patterns based on biomechanical observations and/or assumptions (Alexander *et al.*, 1979; Biewener, 1983; Economos, 1983; Bertram and Biewener, 1990; Christiansen, 1999b, a; Blob, 2000; Carrano, 2001). These theoretical models were formally presented by McMahon (1973; 1975b), who provided empirical support for elastic scaling in terrestrial vertebrates (using ungulates as a

proxy), as opposed to a strict geometric (isometric) scaling. These models were subsequently revisited by other authors who present empirical evidence that elastic similarity is restricted to ungulates with other mammals following either a geometric trend (Alexander *et al.*, 1979) or not clearly conforming to either the elastic or geometric theoretical models (Economos, 1983; Christiansen, 1999b, a). In general, empirical scaling studies of terrestrial mammals have found relatively minor support for elastic similarity [see (Garcia and da Silva, 2006), for full review]. In reptiles, however, Blob (2000) recovered significant support for elastic similarity in several regressions comparing limb diameters to body mass in varanids and iguanians.

The results obtained here suggest that limb scaling in mammalian and reptilian clades exhibits a great deal of variation with respect to elastic and geometric similarity, and as suggested by Christiansen (1999b, a), depending on the variables being compared, clades and subgroups appear to follow a variety of scaling models, and no theoretical scaling model can be used to describe all terrestrial vertebrates. However, this study suggests that elastic similarity is more prevalent than previously suggested, especially in the scaling of humeral circumference with body mass. Of the eight clades examined (Table 1-1), only a single group, Marsupialia, did not follow a significant allometric trend (i.e., significantly different than geometric similarity), and six of the clades follow the model predicted by elastic or static similarity. In contrast, the scaling of humeral length to body mass is more closely associated with geometric similarity, as no clade follows elastic similarity, two clades follow geometric similarity, and four are negatively allometric (and therefore are below any theoretical model). Only two groups (Reptilia and Ungulata) are significantly above geometric similarity and therefore exhibit an allometric pattern whereby the length of the humerus gets shorter as body size increases, approaching a more elastic pattern. A similar pattern is present in the scaling of femoral measurements with body mass. These patterns suggest that circumference measurements tend towards allometric

models suggested by McMahon (1973; 1975b), whereas length measurements follow a pattern that cannot be differentiated from isometry when compared to body mass.

The results presented here reveal that the general scaling patterns of limb circumference in numerous different terrestrial vertebrates, though not always strictly elastic (as defined by McMahon), follow consistent allometric trajectories. Such allometric relationships indicate that, interspecifically, as animals get larger their limbs increase in robusticity at a higher rate compared to body mass. These changes in the architecture of the limb in relation to size support the dynamic similarity hypothesis proposed by Rubin and Lanyon (1984), which predicts changes in limb structure in order to maintain safety factors (Rubin and Lanyon, 1982). The morphological changes in limb skeletal structure, as suggested by Rubin and Lanyon (1984), are not the only shifts to occur with size, and likely work in concert with other shifts, such as postural and behavioural (Rubin and Lanyon, 1982, 1984; Blob, 2000; Clemente *et al.*, 2011), to mitigate the response of safety factors to changes in body size. It is important to note in this respect that this study only examines the external dimensions of the bones, and that factors such as posture may influence aspects of cross-sectional bone shape and internal bone distribution that are not captured here. Nevertheless, the highly conserved relationship between total humeral and femoral circumference and body mass suggests that in terrestrial quadrupeds external circumference measurements of the stylopodia are largely independent of posture and gait, and are most strongly associated with size, allowing us to forward the hypothesis that stylopodial circumference is more closely associated with the body mass than with the type of force (i.e., compression or torsion) acting on the limb. Our results therefore present regressions that are most suitable for body mass estimation of extinct terrestrial quadrupedal vertebrates, regardless of the group under consideration.

1.5.1 Stylopodial Scaling as a Predictor of Body Mass

As body mass is correlated with numerous physiological and ecological properties, (e.g., Peters, 1983; Marquet *et al.*, 2005), consistent and accurate estimation of body mass in extinct taxa is important when attempting to reconstruct the dynamics of palaeoecosystems and the life history of extinct taxa. The use of skeletal scaling to estimate body mass is common in extinct mammals and birds (e.g., Damuth and MacFadden, 1990; Campbell Jr and Marcus, 1992; Hone *et al.*, 2008; Boyer and Jetz, 2010; Millien and Bovy, 2010); however, it is less common in extinct non-avian archosaurs and non-mammalian synapsids [(Anderson *et al.*, 1985; Hurlburt, 1999; Young *et al.*, 2011) being notable exceptions]. Scaling methods are often criticized when models are extended to more distantly related stem taxa, based on arguments such as uneven taxon sampling (ungulate bias), its applicability to animals of different gaits and limb postures, as well as its susceptibility to residual and extreme outliers (Alexander, 1989; Henderson, 1999; Carrano, 2001; Packard *et al.*, 2009). Our dataset allows us to address these major criticisms with empirical data.

1.5.1.1 Ungulate uniqueness and bias

Ungulates, and in particular artiodactyls or bovids, are considered to exhibit scaling patterns distinct from those seen in other mammals. In particular, their limbs are considered to follow an elastic trend (McMahon, 1975b; McMahon, 1975a; Alexander *et al.*, 1979; Bertram and Biewener, 1990; Christiansen, 1999b; Carrano, 2001). In addition to finding elastic trends in other mammalian clades and in reptiles, we reject previous interpretations that limb scaling in ungulates is strictly elastic. In the sample of 41 ungulates examined here (including 34 artiodactyls of which 20 are bovids), elastic similarity was recovered only in humeral

circumference compared to body mass, a pattern also noted in most other clades (Table 1-1).

Scaling of other limb measurements in ungulates either cannot be differentiated from geometric similarity, or follows allometric patterns significantly different from either theoretical model (Table 1, Sim=0). These patterns are robust even when assessed at more exclusive levels (artiodactyls or bovids; Table 1-8). As a result, a strict relationship between stylopodial scaling patterns and a cursorial lifestyle does not characterize ungulates to the exclusion of other mammalian clades. As such, cursorial adaptations in the limbs of ungulates may be limited to other stylopodial measurements (e.g., diameter) or more distal limb bones (Carrano, 1999; Christiansen, 1999b).

The different patterns of limb scaling observed in ungulates compared to mammals (Alexander *et al.*, 1979; Bertram and Biewener, 1990; Carrano, 2001) are often used to cast doubt on the use of the Anderson method to estimate body mass in extinct taxa. New data confirms some differences in limb scaling between ungulates and other mammalian clades, but only in comparisons of limb proportions (length to circumference) and length to body mass (Figure 1-1; Table 1-2).

Circumference to body mass relationships reveal very high coefficients of determination and recovered no significant differences between ungulates and other groups of mammals. The combined circumference of the stylopodia revealed the strongest relationship to body mass (Figure 1-4A) and shows that a bias towards ungulates does not significantly alter the relationship; ungulates follow the same scaling relationships of this variable to body mass as other mammals, as well as non-avian reptiles.

1.5.1.2 Limb Scaling Patterns at Different Gaits and Limb Postures

Extant terrestrial vertebrates have a variety of gaits and limb postures (Rubin and Lanyon, 1984; Blob and Biewener, 1999). In vivo strain studies have also shown that in mammals limbs of taxa

of smaller body size are primarily loaded in torsion, whereas compression predominates in larger taxa, resulting from postural differences with size (also related to the dynamic similarity hypothesis). Such differences are also noted in reptiles compared to mammals, in which the former hold their limbs in a sprawling fashion and hence their stylopodia are generally loaded under torsion (Blob and Biewener, 1999). Given these postural differences, it was hypothesized that the scaling pattern of limb robusticity with body mass should vary in response to differences in limb loading (Christiansen, 1999a; Blob, 2000). Comparisons made here between differently sized mammals, as well as between mammals and reptiles, reveals significant differences in limb proportions, as well as in the relationships between length and body mass (Figure 1-2 and Figure 1-3; Table 1-2 and Table 1-6), and support previous studies (Economos, 1983; Bertram and Biewener, 1990; Christiansen, 1999a). Surprisingly, however, the relationships between limb circumference and body mass is conserved between these different groups, and no significant differences in circumferential scaling between differently sized animals and between mammals and reptiles were observed. Furthermore, we find limited evidence for geometric similarity of limb robusticity in both small and large size class samples. Instead, circumference measurements follow a general negatively allometric pattern indicating a consistent relative increase in circumference compared to body size in both small and large mammals. The total stylopodial circumference (Figure 1-4A) provides the strongest relationship ($R^2 = 0.9861$) and suggests that this variable is a strong predictor of body size for both parasagittal and sprawling taxa alike, and that combined limb circumference is not strongly correlated with gait. These results concur with other studies on non-avian reptiles (Blob, 2000) and birds (Farke and Alicea, 2009) that have shown remarkable morphological similarities of limb circumference (or diameter) between taxa with highly variable limb posture.

1.5.1.3 Outliers

The final criticism made towards the use of skeletal scaling methods such as the Anderson method to estimate body mass is related to the effects outliers have on the final predictive equation, especially at large body size where the sample size is low (Packard *et al.*, 2009). In the relationship between combined humeral and femoral circumference and body mass, a residual outlier test reveals that none of the largest animals in our greatly expanded dataset are residual outliers, including the buffalo, hippopotamus, and elephant (Figure 1-4A). The only outliers identified here appear to be related to unique ecologies, such as suspension locomotion (*Choloepus didactylus*) and burrowing (*Priodontes maximus*, *Condylura cristata*, *Parascalops breweri*), which can generally be inferred from skeletal anatomy as a potential confounding factor to mass estimation based on their highly derived limb morphologies (Bou *et al.*, 1987). Both representatives of Soricomorpha, *C. cristata* and *P. breweri*, are the farthest residual outliers, and, due to their especially apomorphic anatomy, will be removed from the body mass equation. Only one residual outlier, the turtle *Trachemys scripta* is difficult to explain, but its relatively high weight may be a factor of captivity or measurement error when the live weight was taken.

A recent study by Packard *et al.* (2009) suggested that because of its amphibious lifestyle, *Hippopotamus amphibius* may have a high body mass compared to its limb circumference measurement. As a result, it may represent a residual outlier, which justifies the removal of *H. amphibius* from the analysis. This assertion is based on the observation that if the raw data (non-log) of Anderson *et al.* (1985) is regressed using non-linear least-squares regression methods, the hippopotamus, the bison, and the elephant are all outliers. The statistical merits and flaws of logarithmically transforming data have been heavily debated (e.g., Sokal and Rohlf, 1969; Smith,

1984; Cawley and Janacek, 2009; Packard *et al.*, 2009)) and will not be discussed further here. However, based on the suggestions of Packard *et al.* (2009) we regressed our non-log transformed expanded dataset using a non-linear least squares regression, implemented with the ‘nls’ function in R, and tested for potential outliers in the residual variance. The results indicate that 40 species are outliers in the non-log residual data. In order to test for potential significant effects, we removed the 40 outliers and re-ran the log-log OLS regression, which resulted in a slope of 2.802 ± 0.055 and is statistically indistinguishable from that obtained when using the complete dataset. This suggests that these data points are not significantly affecting the final result. More importantly, examination of the mean percent prediction error (PPE) indicates that despite the need for back-transformation, the log-transformed linear regression is a significantly better model for predicting body mass than a non-linear model (log PPE = $25\% \pm 3\%$; non-log PPE = $43\% \pm 3\%$; Figure 1-4B; two-tailed t-test: $t = -8.3245$, $p << 0.0001$).

Extreme outliers, those at the upper and lower extremes of the dataset, also have the potential to significantly affect regression results. In the current dataset, there are no extreme outliers when the data are log transformed. However, as is generally the case with size data, there are several positive extreme outliers in the non-log dataset. Thirty-three extreme outliers are observed in the body mass and combined humeral and femoral circumference data. When these taxa are removed and the log-log analysis is re-run ($m = 2.745 \pm 0.057$, $b = -1.099 \pm 0.09$), the regression is virtually identical to that obtained with the total dataset. The observation that extreme positive values do not affect the log-log OLS regression is further supported by the non-significant variation in scaling coefficients between different mammalian size classes (Figure 1-3).

The empirical data presented here falsifies the main criticisms against skeletal-body mass regression models for predicting body mass in extinct taxa, and given the highly conserved nature of the relationship between stylopodial circumference and body mass in extant terrestrial mammals and reptiles, suggests that circumference measurements represent robust proxies of body mass that can be applied to extinct, phylogenetically disparate quadrupedal amniotes. The examination of eight terrestrial lissamphibian species (one caudatan and seven anurans; not included in the final analysis; see Appendix 1) reveals that, based on their total stylopodial circumference and body mass, they plot within the range of variation present in the mammalian and reptilian dataset (Figure 1-2). Although at this time their small sample and range preclude any meaningful statistical comparisons between the limb scaling patterns of lissamphibians and other tetrapods, these preliminary results suggest that the conserved relationship between body mass and proximal limb bone circumference could be extended to encompass the majority of quadrupedal terrestrial tetrapods.

1.5.2 Implications for Body Mass Estimation

In extinct taxa, skeletal measurement proxies of body size are often preferred to actual body mass estimates. Of the limb measurements taken here, results suggest that the regression between the total circumference of the humerus and femur to body mass exhibits the strongest relationship, with the highest R^2 values, and the lowest PPE, SEE, and AIC of all bivariate regression models (Figure 1-4B; Table 1-9). Among commonly cited proxies of size is femur length (e.g., (Carrano, 2006)). However, our analyses indicate that length measurements are generally poor indicators of size, especially compared to circumference (Figure 1-4B). Femur length exhibits an especially high amount of error, with a 70% mean PPE in living mammals and reptiles, compared to the 25% for the combined humeral and femoral circumference. Caution

should therefore be taken when using limb length as size proxies, especially when examining taxa that encompass a wide phylogenetically bracket.

Based on our results, we propose the following scaling equation as a robust predictor of body mass in quadrupedal tetrapods:

$$\log\text{BM} = 2.749 \cdot \log\text{C}_{\text{H+F}} - 1.104 \quad \text{EQ 1.1}$$

where $\text{C}_{\text{H+F}}$ is the sum of humeral and femoral circumferences needed to estimate body mass. This regression exhibits a very high coefficient of determination ($R^2 = 0.988$), and a mean PPE of 25.6%. When adjusted for phylogenetic correlation/covariance between observations (i.e., species) using a phylogenetic generalized least squares model, the equation is:

$$\log\text{BM} = 2.754 \cdot \log\text{C}_{\text{H+F}} - 1.097 \quad \text{EQ 1.2}$$

which has an almost identical mean PPE (25%) than equation 1 (Figure 1-4B).

In addition to examining bivariate estimates of body mass, we tested the predictive power of a variety of estimations based on multiple regressions by comparing their PPE, SEE, and AIC with those obtained from the bivariate regression of total circumference with body mass. Analyses including all proximal limb bone measurements also reveal low statistic values for both the raw data:

$$\log\text{BM} = 0.375 \cdot \log\text{L}_\text{H} + 1.544 \cdot \log\text{C}_\text{H} - 0.136 \cdot \log\text{L}_\text{F} + 0.954 \cdot \log\text{C}_\text{F} - 0.351 \quad \text{EQ 1.3}$$

and the phylogenetically corrected data:

$$\log\text{BM} = 0.212 \cdot \log\text{L}_\text{H} + 1.347 \cdot \log\text{C}_\text{H} - 0.533 \cdot \log\text{L}_\text{F} + 0.749 \cdot \log\text{C}_\text{F} - 0.76 \quad \text{EQ 1.4}$$

Equally low regression statistics were obtained for the multiple regression including only the circumference measurements, raw data:

$$\log BM = 1.78 \cdot \log C_H + 0.939 \cdot \log C_F - 0.215 \quad \text{EQ 1.5}$$

phylogenetically corrected data:

$$\log BM = 1.54 \cdot \log C_H + 1.195 \cdot \log C_F - 0.234 \quad \text{EQ 1.6}$$

None of the equations presented above are significantly better at predicting body mass than the combined humeral and femoral circumference (**EQ 1.1** and **EQ 1.2**); therefore, any of these equations are likely to provide robust estimates of body mass (Figure 1-4B). However, given that equations 2, 4, and 6 account for phylogenetic non-independence, they are likely to better represent the statistical error in the data than the non-phylogenetically corrected data.

Not surprisingly, the masses estimated for several commonly cited non-avian dinosaurs provided by **EQ 1.2** are more consistent with estimates generated from Anderson *et al.* (1985) than volumetric model-based estimates for the same taxa (Table 1-10). This technique is also important in that it is specimen-based, and therefore explicit and repeatable, and allows uncertainty to be expressed in the estimate. These predicted masses and prediction error ranges, when compared to previous estimates based on volumetric reconstructions (Paul, 1997; Henderson, 1999; Seebacher, 2001), show that many reconstructed models underestimate body mass, sometimes significantly below that predicted by the mean percent prediction error (Table 1-10). Given that life-reconstructions of extinct taxa remain important for addressing several biological questions, including locomotion and weight distribution, our results provide the first objective framework with which to constrain these models and test whether their assumptions conform to the patterns seen in extant terrestrial tetrapods.

1.6 Concluding Remarks

Body size is an important biological descriptor, and as a result, is critical to understanding the palaeobiology of extinct organisms and ecosystems. This study presents an extensive dataset of extant quadrupedal terrestrial amniotes, which allows testing of the main criticisms that have been put forth against the use of scaling relationships to estimate body mass in extinct taxa. Our results demonstrate a highly conserved relationship between body mass and stylopodial circumference with minimal variation between clades and groups of different gait and size, compared over a large phylogenetic scope. This general relationship allows estimation of body mass in extinct groups, and is particularly important for a wide range of palaeobiological studies, including growth rates (Erickson *et al.*, 2001), metabolism (Gillooly *et al.*, 2006), and energetics (Finnegan and Droser, 2008), as well as for quantifying body size changes across major evolutionary transitions that are accompanied by major changes in gait, including shifts in the early evolutionary history of archosaurs (Hutchinson, 2006), and in the evolution of mammals from reptile-like basal synapsids (Blob, 2001; Fröbisch, 2006).

1.7 Tables

Table 1-1. Stylopodial scaling in mammals and non-avian reptiles.

Analysis (x vs. y)	Sample	N	m	m 95% CI	b	b 95% CI	R ²	Sim.
L _F vs. L _C	All	234	1.0301	1.0616 to 0.9996	-0.6020	-0.542 to -0.6619	0.9459	G
	Mammalia	188	1.0332	1.0677 to 0.9999	-0.6148	-0.5469 to -0.6827	0.9484	G
	Reptilia	46	1.1751	1.3184 to 1.0474	-0.8115	-0.5884 to -1.0347	0.8560	>G,<E
	Ungulata	32	1.2014	1.3338 to 1.0821	-0.9810	-0.6676 to -1.2943	0.9211	>G,<E
	Carnivora	46	0.9840	1.0888 to 0.8893	-0.5409	-0.3317 to -0.75	0.8887	G
	Marsupialia	14	1.0774	1.1467 to 1.0123	-0.7317	-0.6057 to -0.8577	0.9902	>G,<E
	Euarchonta	14	1.0251	1.2141 to 0.8656	-0.7382	-0.3835 to -1.0929	0.9269	G
	Glires	66	0.9542	1.0334 to 0.8811	-0.4716	-0.3454 to -0.5979	0.8978	G
L _H vs. C _H	All	234	1.0644	1.0971 to 1.0326	-0.6229	-0.5626 to -0.6831	0.9452	>G,<E
	Mammalia	187	1.0603	1.0967 to 1.0252	-0.6199	-0.5511 to -0.6887	0.9459	>G,<E
	Reptilia	47	1.2190	1.3355 to 1.1126	-0.8536	-0.6724 to -1.0348	0.9072	>G,<E
	Ungulata	32	1.3083	1.4325 to 1.1949	-1.1391	-0.8529 to -1.4254	0.9407	>G,<E
	Carnivora	46	1.0814	1.1777 to 0.9929	-0.7101	-0.5193 to -0.9009	0.9209	G
	Marsupialia	14	1.0472	1.187 to 0.9238	-0.6059	-0.3774 to -0.8343	0.9601	G
	Euarchonta	14	0.9175	1.0816 to 0.7782	-0.4785	-0.1826 to -0.7744	0.9309	G
	Glires	66	0.9296	0.9931 to 0.8702	-0.4116	-0.3166 to -0.5066	0.9300	G
L _F vs. BM	All	234	2.9307	3.0323 to 2.8325	-2.1677	-1.9744 to -2.3611	0.9306	G
	Mammalia	188	2.9930	3.0974 to 2.8922	-2.3410	-2.1359 to -2.5461	0.9439	G
	Reptilia	46	3.2500	3.7486 to 2.8177	-2.4800	-1.7132 to -3.2468	0.7778	G
	Ungulata	32	3.4979	3.8785 to 3.1545	-3.4591	-2.5578 to -4.3603	0.9230	>G,<E
	Carnivora	46	2.7472	3.0791 to 2.451	-1.8012	-1.1427 to -2.4597	0.8584	G
	Marsupialia	14	2.9980	3.4286 to 2.6215	-2.4690	-1.7121 to -3.2258	0.9542	G
	Euarchonta	14	3.0622	3.7695 to 2.4877	-2.9486	-1.6443 to -4.253	0.8893	G
	Glires	66	2.7702	2.9779 to 2.5769	-1.9621	-1.6297 to -2.2944	0.9160	0
L _C vs. BM	All	247	2.8479	2.8997 to 2.7969	-0.4587	-0.3845 to -0.5328	0.9794	<G,>E
	Mammalia	200	2.8977	2.9504 to 2.8459	-0.5615	-0.4829 to -0.64	0.9834	<G,>E
	Reptilia	47	2.7943	2.9801 to 2.6201	-0.2653	-0.057 to -0.4736	0.9540	E
	Ungulata	41	2.9204	3.1192 to 2.7344	-0.6173	-0.232 to -1.0027	0.9586	G
	Carnivora	48	2.7893	2.9182 to 2.6661	-0.2895	-0.0946 to -0.4844	0.9768	E
	Marsupialia	14	2.7827	3.1222 to 2.4801	-0.4328	-0.0138 to -0.8518	0.9664	G,E,S
	Euarchonta	15	2.9728	3.1874 to 2.7727	-0.7271	-0.4393 to -1.0149	0.9864	G
	Glires	66	2.9031	3.084 to 2.7328	-0.5929	-0.3965 to -0.7893	0.9413	G
L _H vs. BM	All	234	2.8653	2.9489 to 2.7841	-1.8284	-1.6745 to -1.9823	0.9506	0
	Mammalia	187	2.8626	2.9522 to 2.7756	-1.8476	-1.6778 to -2.0175	0.9548	0
	Reptilia	47	3.3718	3.704 to 3.0694	-2.5472	-2.0315 to -3.0629	0.9018	>G,<E
	Ungulata	32	3.4092	3.8036 to 3.0558	-2.9639	-2.0630 to -3.8648	0.9135	>G,<E
	Carnivora	46	2.8202	3.0641 to 2.5957	-1.8667	-1.3831 to -2.3503	0.9253	G
	Marsupialia	14	3.1988	3.6508 to 2.8027	-2.3972	-1.6611 to -3.1333	0.9556	G
	Euarchonta	14	2.5359	2.9736 to 2.1627	-1.6484	-0.8577 to -2.4391	0.9354	0
	Glires	66	2.6071	2.766 to 2.4573	-1.3946	-1.1559 to -1.6332	0.9438	0
C _H vs. BM	All	247	2.6861	2.7322 to 2.6406	-0.1438	-0.0788 to -0.2087	0.9816	E
	Mammalia	200	2.6938	2.7445 to 2.6439	-0.1655	-0.0913 to -0.2398	0.9823	E
	Reptilia	47	2.7661	2.9296 to 2.6117	-0.1862	-0.0049 to -0.3675	0.9634	E

	Ungulata	41	2.5273	2.7222 to 2.3464	0.1672	0.544 to -0.2097	0.9473	E
	Carnivora	48	2.5959	2.7027 to 2.4933	-0.0012	0.1613 to -0.1637	0.9815	E,S
	Marsupialia	14	3.0547	3.4219 to 2.7269	-0.5465	-0.1208 to -0.9721	0.9673	G
	Euarchonta	15	2.7558	2.9725 to 2.5548	-0.3168	-0.0345 to -0.5992	0.9840	E
	Glires	66	2.8045	2.9447 to 2.671	-0.2403	-0.0986 to -0.3819	0.9618	<G,>E
L _F vs. L _H	All	233	1.0246	1.0469 to 1.0027	-0.1206	-0.0778 to -0.1634	0.9723	-
	Mammalia	187	1.0450	1.0682 to 1.0223	-0.1707	-0.1248 to -0.2166	0.9771	-
	Reptilia	46	0.9644	1.0644 to 0.8739	0.0190	0.176 to -0.1379	0.8943	-
	Ungulata	32	1.0260	1.107 to 0.9509	-0.1452	0.0491 to -0.3395	0.9584	-
	Carnivora	46	0.9741	1.0283 to 0.9227	0.0232	0.1338 to -0.0874	0.9682	-
	Marsupialia	14	0.9372	1.1182 to 0.7856	-0.0224	0.2894 to -0.3344	0.9204	-
	Euarchonta	14	1.2075	1.4238 to 1.0241	-0.5127	-0.106 to -0.9195	0.9307	-
	Glires	66	1.0625	1.1019 to 1.0246	-0.2177	-0.1536 to -0.2818	0.9788	-
C _{H+F} vs. BM	All	247	2.7779	2.8191 to 2.7374	-1.1564	-1.086 to -1.2267	0.9863	-
	Mammalia	200	2.8071	2.8495 to 2.7654	-1.2289	-1.1541 to -1.3037	0.9886	-
	Reptilia	47	2.7933	2.9496 to 2.6452	-1.0833	-0.8636 to -1.3031	0.9671	-
	Ungulata	41	2.7319	2.8959 to 2.5773	-1.0660	-0.6989 to -1.4331	0.9676	-
	Carnivora	48	2.6921	2.7969 to 2.5911	-0.9568	-0.7669 to -1.1466	0.9834	-
	Marsupialia	14	2.9125	3.1855 to 2.6628	-1.3738	-0.9658 to -1.7817	0.9797	-
	Euarchonta	15	2.8692	3.0561 to 2.6937	-1.3928	-1.0911 to -1.6946	0.9889	-
	Glires	66	2.8850	3.0113 to 2.764	-1.3260	-1.1561 to -1.4960	0.9705	-

Standardized Major Axis equation shown in the format $y = mx + b$. The particular theoretical scaling model (Sim.) followed by the regression is presented by G, geometric similarity, E, elastic similarity, or S, static similarity. Scaling patterns that fall between models are presented by > or <, and those that do not follow any pattern (i.e., above or below all predicted models) are represented by a 0. BM - body mass; L_F - femoral length; C_F - femoral circumference; L_H - humeral length; C_H - humeral circumference; C_{H+F} - total humeral and femoral circumference.

Table 1-2. Slope and intercept comparisons of stylopodial scaling patterns in mammalian clades.

	Ungulata			-			-			-			-			-
	Euarchonta			-	-		-	-		-	-		-	-		-
	Glires		-	-	-		-	-	-	-	-		-	-	-	-

Standardized major axis equation shown in the format $y = mx + b$. Symbols: (^o) represents differences at 90–95% ($0.1 < p > 0.05$); (*) at 95–99% ($0.05 < p > 0.01$); and (**) at greater than 95% ($p < 0.01$). Otherwise, p-values are > 0.1 . All p-values are adjusted for multiple comparisons using FDR. Hyphens (-) represent duplicate comparisons. Significant differences using 95% CI are assessed on whether the intervals overlap or not; non-overlapping comparisons are indicated with an asterisk (*). b' - intercept adjusted to correspond to the minimum value along the x-axis. 95% CI - comparisons based on 95% confidence intervals; LRT - comparisons based on a likelihood ratio test (slope only); t-test - comparisons based on a two-tailed t-test (intercept only); BM - body mass; LF - femoral length; CF - femoral circumference; LH - humeral length; CH - humeral circumference; CH+F - total humeral and femoral circumference.

Table 1-3. Slope and intercept comparisons of stylopodial scaling patterns in mammals and non-avian reptiles.

	All Data					Mammals <168 kg†				
	mCI	mP	bCI	bP	b'P	mCI	mP	bCI	bP	b'P
L _F vs C _F		°				*	°			
L _H vs C _H	*	*				*	**		°	
L _F vs BM										
C _F vs BM			*							
L _H vs BM	*	**	*	°		*	**		*	
C _H vs BM										
L _F vs L _H				°					*	
C _{H+F} vs BM										

Standardized major axis equation shown in the format $y = mx + b$. Symbols: (°) represents differences at 90–95% ($0.1 < p > 0.05$); (*) at 95–99% ($0.05 < p > 0.01$); and (**) at greater than 95% ($p < 0.01$). Otherwise, p-values are > 0.1 . All p-values are adjusted for multiple comparisons using FDR. Hyphens (-) represent duplicate comparisons. Significant differences using 95% CI are assessed on whether the intervals overlap or not; non-overlapping comparisons are indicated with an asterisk (*). † - comparisons based on a subset of the mammalian dataset that has the same body mass range as the total reptilian dataset (see Additional file 2, Table S1). mCI - slope comparisons based on 95% confidence intervals; mP - slope comparisons based on likelihood ratio test; bCI - intercept comparisons based 95% confidence intervals; bP - intercept comparisons based on two-tailed t-test; b'P - t-test comparison of adjusted intercepts to the minimum value along the x-axis; BM - body mass; LF - femoral length; CF - femoral circumference; LH - humeral length; CH - humeral circumference; CH+F - total humeral and femoral circumference.

Table 1-4. Raw and PIC stylopodial scaling in a subset of the mammalian dataset and non-avian reptiles.

		Raw Data SMA Results						
Groups	Analysis	N	<i>m</i>	<i>m</i> 95% CI	<i>b</i>	<i>b</i> 95% CI	R ²	Sim.
L _F vs. C _F	Mammalia	167	0.9878	1.0302 to 0.9471	-0.5366	-0.4575 to -0.6156	0.9251	G
	Reptilia	46	1.1751	1.3183 to 1.0473	-0.8115	-0.5883 to -1.0346	0.8560	>G,<E
L _H vs. C _H	Mammalia	166	0.9988	1.0414 to 0.9578	-0.5200	-0.4437 to -0.5962	0.9264	G
	Reptilia	47	1.2190	1.3355 to 1.1125	-0.8536	-0.6723 to -1.0347	0.9072	>G,<E
L _F vs. BM	Mammalia	167	2.8627	2.9915 to 2.7393	-2.1177	-1.8776 to -2.3576	0.9178	0
	Reptilia	46	3.2500	3.7486 to 2.8177	-2.4800	-1.7131 to -3.2468	0.7778	G
C _F vs. BM	Mammalia	174	2.8986	2.9708 to 2.828	-0.5634	-0.4651 to -0.6616	0.9732	<G,>E
	Reptilia	47	2.7943	2.9801 to 2.62	-0.2653	-0.057 to -0.4735	0.9540	E
L _H vs. BM	Mammalia	166	2.7029	2.8061 to 2.6034	-1.5895	-1.4045 to -1.7743	0.9409	0
	Reptilia	47	3.3718	3.7039 to 3.0694	-2.5472	-2.0315 to -3.0629	0.9018	>G,<E
C _H vs. BM	Mammalia	174	2.7044	2.7749 to 2.6356	-0.1780	-0.0848 to -0.2711	0.9707	E
	Reptilia	47	2.7661	2.9296 to 2.6117	-0.1862	-0.0048 to -0.3675	0.9634	E
L _F vs. L _H	Mammalia	166	1.0585	1.0886 to 1.029	-0.1937	-0.1369 to -0.2504	0.9666	-
	Reptilia	46	0.9644	1.0644 to 0.8738	0.0190	0.1759 to -0.1378	0.8943	-
C _{H+F} vs. BM	Mammalia	174	2.8203	2.879 to 2.76265	-1.2486	-1.1526 to -1.3446	0.9812	-
	Reptilia	47	2.7933	2.9496 to 2.6452	-1.0833	-0.8635 to -1.3031	0.9671	-
PIC SMA Results								
Groups	Analysis	N	<i>m</i>	<i>m</i> 95% CI	<i>b</i>	<i>b</i> 95% CI	R ²	Sim.
L _F vs. C _F	Mammalia	45	1.1880	1.2919 to 1.0923	-	-	0.9290	>G,<E
	Reptilia	166	1.0640	1.1275 to 1.004	-	-	0.8561	>G,<E
L _H vs. C _H	Mammalia	46	1.1853	1.2789 to 1.0985	-	-	0.9388	>G,<E
	Reptilia	165	1.0613	1.1198 to 1.0058	-	-	0.8782	>G,<E
L _F vs. BM	Mammalia	45	3.5139	3.9389 to 3.1348	-	-	0.8621	>G,<E
	Reptilia	166	3.0857	3.2694 to 2.9123	-	-	0.8579	G
C _F vs. BM	Mammalia	46	2.9493	3.2232 to 2.6986	-	-	0.9123	G
	Reptilia	173	2.9032	3.0359 to 2.7762	-	-	0.9115	G
L _H vs. BM	Mammalia	46	3.4403	3.7883 to 3.1242	-	-	0.8974	>G,<E
	Reptilia	165	2.9213	3.0735 to 2.7765	-	-	0.8913	G
C _H vs. BM	Mammalia	46	2.9024	3.1359 to 2.6862	-	-	0.9341	G
	Reptilia	173	2.7313	2.8571 to 2.6109	-	-	0.9100	E
L _F vs. L _H	Mammalia	45	0.9956	1.0706 to 0.9257	-	-	0.9427	-
	Reptilia	165	1.0562	1.095 to 1.0185	-	-	0.9443	-
C _{H+F} vs. BM	Mammalia	46	2.9357	3.1813 to 2.709	-	-	0.9285	-
	Reptilia	173	2.8585	2.9714 to 2.7498	-	-	0.9334	-

Mammalian subset corresponds to all taxa <168 kg in order to match body mass range in the sample of non-avian reptiles. Standardized Major Axis equation shown in the format $y = mx + b$ ($b = 0$ in PIC). The particular theoretical scaling model (Sim.) followed by the regression is presented by G, geometric similarity, E, elastic similarity, or S, static similarity. Scaling patterns that fall between models are presented by $>$ or $<$, and those that do not follow any pattern (i.e., above or below all predicted models) are represented by a 0. † - comparisons based on a subset of the mammalian dataset that has the same body mass range as the total reptilian dataset. mCI -

slope comparisons based on 95% confidence intervals; mP - slope comparisons based on likelihood ratio test; bCI - intercept comparisons based 95% confidence intervals; bP - intercept comparisons based on two-tailed t-test; b'P - t-test comparison of adjusted intercepts to the minimum value along the x-axis; BM - body mass; LF - femoral length; CF - femoral circumference; LH - humeral length; CH - humeral circumference; CH+F - total humeral and femoral circumference.

Table 1-5. Stylopodial scaling in mammals for different sizes.

Analysis (x vs. y)	Sample	N	m	m 95% CI	b	b to 95% to CI	R ²	Sim
L _F vs. C _F	<20 kg	136	0.8868	0.9335 to 0.8424	-0.3733	-0.2921 to -0.4545	0.9095	0
	>20 kg	52	1.0000	1.1370 to 0.8795	-0.4907	-0.1714 to -0.8100	0.7945	G
	<50 kg	150	0.9486	0.9987 to 0.9009	-0.4715	-0.3819 to -0.5611	0.8993	G
	>50 kg	38	1.1331	1.2731 to 1.0084	-0.8317	-0.4935 to -1.1699	0.8806	>G,<E
	<100 kg	158	0.9659	1.0123 to 0.9216	-0.5000	-0.4155 to -0.5845	0.9119	G
	>100 kg	30	1.1059	1.2659 to 0.9661	-0.7572	-0.3679 to -1.1465	0.8774	G
L _H vs. C _H	<20 kg	135	0.8778	0.9248 to 0.8331	-0.3345	-0.2567 to -0.4124	0.9073	0
	>20 kg	52	1.1541	1.2900 to 1.0326	-0.7954	-0.4848 to -1.1060	0.8459	>G,<E
	<50 kg	149	0.9040	0.9990 to 0.9040	-0.4445	-0.3613 to -0.5277	0.9060	0
	>50 kg	38	1.1856	1.3524 to 1.0394	-0.8774	-0.4879 to -1.2668	0.8475	>G,<E
	<100 kg	157	0.9710	1.0166 to 0.9274	-0.4764	-0.3967 to -0.5560	0.9161	G
	>100 kg	30	1.1229	1.3132 to 0.9602	-0.7114	-0.2646 to -1.1582	0.8352	G
L _F vs. BM	<20 kg	136	2.6288	2.7825 to 2.4836	-1.7421	-1.4756 to -2.0086	0.8892	0
	>20 kg	52	2.8571	3.2511 to 2.5108	-1.8964	-0.9788 to -2.8141	0.7920	G
	<50 kg	150	2.7619	2.9166 to 2.6754	-1.9510	-1.6751 to -2.2270	0.8873	0
	>50 kg	38	3.1523	3.5377 to 2.8089	-2.6399	-1.7089 to -3.5709	0.8831	G
	<100 kg	158	2.8104	2.9526 to 2.6750	-2.0305	-1.7717 to -2.2893	0.9025	0
	>100 kg	30	3.0497	3.5022 to 2.6557	-2.3587	-1.2593 to -3.4582	0.8715	G
C _F vs. BM	<20 kg	138	2.9559	3.0735 to 2.8429	-0.6266	-0.4858 to -0.7675	0.9471	G
	>20 kg	62	2.8638	3.0353 to 2.7020	-0.5040	-0.1723 to -0.8358	0.9492	G
	<50 kg	153	2.9054	3.0013 to 2.8126	-0.5716	-0.4504 to -0.6928	0.9592	G
	>50 kg	47	2.7816	2.9651 to 2.6094	-0.3222	0.0436 to -0.6880	0.9546	E
	<100 kg	164	2.9117	2.9945 to 2.8312	-0.5784	-0.4698 to -0.6870	0.9674	<G,>E
	>100 kg	36	2.7946	3.0538 to 2.5575	-0.3497	0.1751 to -0.8745	0.9351	G,E
L _H vs. BM	<20 kg	135	2.4386	2.5604 to 2.3225	-1.1878	-0.9858 to -1.3898	0.9192	0
	>20 kg	52	2.9807	3.2978 to 2.6940	-2.0078	-1.2791 to -2.7365	0.8728	G
	<50 kg	149	2.5866	2.7051 to 2.4734	-1.4091	-1.2063 to -1.6120	0.9245	0
	>50 kg	38	3.0525	3.4941 to 2.6667	-2.1794	-1.1501 to -3.2088	0.8392	G
	<100 kg	157	2.6465	2.7582 to 2.5394	-1.5013	-1.3060 to -1.6966	0.9321	0
	>100 kg	30	2.9405	3.4742 to 2.4888	-1.8798	-0.6326 to -3.1269	0.8127	G
C _H vs. BM	<20 kg	138	2.7768	2.8898 to 2.6683	-0.2550	-0.1255 to -0.3845	0.9447	E
	>20 kg	62	2.5793	2.7425 to 2.4258	0.0509	0.3671 to -0.2653	0.9434	E,S
	<50 kg	153	2.7188	2.8130 to 2.6277	-0.1941	-0.0793 to -0.3088	0.9551	E
	>50 kg	47	2.5612	2.7123 to 2.4184	0.1031	0.4070 to -0.2008	0.9635	E,S
	<100 kg	164	2.7253	2.8067 to 2.6463	-0.2005	-0.0972 to -0.3038	0.9640	E
	>100 kg	36	2.6488	2.8634 to 2.4504	-0.0887	0.3518 to -0.5293	0.9500	E,S
L _F vs. L _H	<20 kg	135	1.0776	1.1143 to 1.0422	-0.2261	-0.1618 to -0.2904	0.9619	-
	>20 kg	52	0.9586	1.0632 to 0.8642	0.0374	0.2839 to -0.2092	0.8666	-
	<50 kg	149	1.0672	1.1041 to 1.0315	-0.2079	-0.1414 to -0.2744	0.9564	-
	>50 kg	38	1.0327	1.1337 to 0.9407	-0.1509	0.0956 to -0.3973	0.9236	-
	<100 kg	157	1.0613	1.0945 to 1.0291	-0.1983	-0.1374 to -0.2592	0.9624	-
	>100 kg	30	1.0371	1.1743 to 0.9160	-0.1629	0.1727 to -0.4984	0.8965	-
C _{H+F} vs. BM	<20 kg	138	2.9032	2.9989 to 2.8105	-1.3628	-1.2223 to -1.5032	0.9634	-
	>20 kg	62	2.7519	2.8828 to 2.6269	-1.1186	-0.8251 to -1.4120	0.9674	-
	<50 kg	153	2.8383	2.9165 to 2.7622	-1.2743	-1.1542 to -1.3945	0.9714	-
	>50 kg	47	2.6819	2.8173 to 2.5530	-0.9409	-0.6286 to -1.2531	0.9731	-
	<100 kg	164	2.8409	2.9084 to 2.7750	-1.2778	-1.1709 to 1.3846	0.9771	-

>100 kg		36	2.7442	2.9343 to 2.5663	-1.0954	-0.6491 to -1.5416	0.9630	-
---------	--	----	--------	------------------	---------	--------------------	--------	---

Standardized Major Axis equation shown in the format $y = mx + b$. The particular theoretical scaling model (Sim.) followed by the regression is presented by G, geometric similarity, E, elastic similarity, or S, static similarity. Scaling patterns that fall between models are presented by > or <, and those that do not follow any pattern (i.e., above or below all predicted models) are represented by a 0. BM - body mass; LF - femoral length; CF - femoral circumference; LH - humeral length; CH - humeral circumference; CH+F - total humeral and femoral circumference.

Table 1-6. Slope and intercept comparisons of stylopodial scaling patterns in different mammalian size classes.

	20 kg					50 kg					100 kg				
	mCI	mP	bCI	bP	b'P	mCI	mP	bCI	bP	b'P	mCI	mP	bCI	bP	b'P
L _F vs C _F						*	*								
L _H vs C _H	*	**	*	*		*	**								
L _F vs BM															
C _F vs BM															
L _H vs BM	*	**					*								
C _H vs BM															
L _F vs L _H				°											
C _{H+F} vs BM															

Standardized major axis equation shown in the format $y = mx + b$. Symbols: (°) represents differences at 90–95% ($0.1 < p > 0.05$); (*) at 95–99% ($0.05 < p > 0.01$); and (**) at greater than 95% ($p < 0.01$). Otherwise, p-values are > 0.1 . All p-values are adjusted for multiple comparisons using FDR. Hyphens (-) represent duplicate comparisons. Significant differences using 95% CI are assessed on whether the intervals overlap or not; non-overlapping comparisons are indicated with an asterisk (*). mCI - slope comparisons based on 95% confidence intervals. mP - slope comparisons based on likelihood ratio test; bCI - intercept comparisons based 95% confidence intervals; bP - intercept comparisons based on two-tailed t-test; b'P - t-test comparison of adjusted intercepts to the minimum value along the x-axis; BM - body mass; LF - femoral length; LC - femoral circumference; LH - humeral length; CH - humeral circumference; CH+F - total humeral and femoral circumference.

Table 1-7. Phylogenetically corrected stylopodial scaling in mammals and non-avian reptiles.

Analysis (x vs. y)	Sample	N	m	m 95% CI	R ²	Sim.
L _F vs. C _F	All	233	1.0788	1.1258 to 1.0337	0.8909	>G,<E
	Mammalia	187	1.0651	1.118 to 1.0148	0.8874	>G,<E
	Reptilia	45	1.1880	1.2919 to 1.0924	0.9290	>G,<E
	Ungulata	31	1.1560	1.297 to 1.0303	0.8979	>G,<E
	Carnivora	45	0.9350	1.0493 to 0.8332	0.8553	G
	Marsupialia	13	1.0832	1.193 to 0.9836	0.9678	G
	Euarchonta	13	1.1223	1.4793 to 0.8514	0.8083	G,E
	Glires	65	1.1363	1.2512 to 1.0318	0.8506	>G,<E
L _H vs. C _H	All	233	1.0973	1.1416 to 1.0547	0.9074	>G,<E
	Mammalia	186	1.0855	1.1355 to 1.0375	0.9037	>G,<E
	Reptilia	46	1.1853	1.2789 to 1.0985	0.9388	>G,<E
	Ungulata	31	1.2592	1.3799 to 1.1489	0.9395	>G,<E
	Carnivora	45	1.0412	1.1518 to 0.941	0.8888	G
	Marsupialia	13	1.0619	1.2379 to 0.9109	0.9282	G
	Euarchonta	13	1.0725	1.4129 to 0.814	0.8199	G
	Glires	65	1.0782	1.1536 to 1.0076	0.9267	>G,<E
L _F vs. BM	All	233	3.1327	3.2749 to 2.9965	0.8828	>G,<E
	Mammalia	187	3.0855	3.2386 to 2.9395	0.8882	G
	Reptilia	45	3.5139	3.9389 to 3.1348	0.8621	>G,<E
	Ungulata	31	3.3430	3.7769 to 2.9589	0.8852	G
	Carnivora	45	2.8681	3.2383 to 2.5401	0.8393	G
	Marsupialia	13	3.4808	4.0791 to 2.9701	0.9154	E
	Euarchonta	13	3.3664	4.6175 to 2.4542	0.7459	E
	Glires	65	3.1273	3.3921 to 2.8831	0.8980	G
C _F vs. BM	All	246	2.9115	3.0128 to 2.8136	0.9261	G
	Mammalia	199	2.9058	3.0165 to 2.799	0.9287	G
	Reptilia	46	2.9493	3.2232 to 2.6986	0.9123	E
	Ungulata	40	2.9790	3.2356 to 2.7427	0.9310	G
	Carnivora	47	3.0589	3.3484 to 2.7943	0.9068	G
	Marsupialia	13	3.2133	3.6006 to 2.8676	0.9554	G
	Euarchonta	14	2.9518	3.2729 to 2.6622	0.9701	G,E
	Glires	65	2.7522	2.9952 to 2.5288	0.8876	E
L _H vs. BM	All	233	3.0135	3.1346 to 2.8969	0.9077	G
	Mammalia	186	2.9539	3.0838 to 2.8293	0.9123	G
	Reptilia	46	3.4403	3.7883 to 3.1242	0.8974	>G,<E
	Ungulata	31	3.0640	3.4547 to 2.7174	0.8959	G
	Carnivora	45	2.9738	3.2944 to 2.6842	0.8857	G
	Marsupialia	13	3.1335	3.7171 to 2.6413	0.9016	G
	Euarchonta	13	2.9668	3.8852 to 2.2654	0.8292	G,E
	Glires	65	2.8571	3.0576 to 2.6697	0.9278	G
C _H vs. BM	All	246	2.7254	2.818 to 2.6358	0.9295	E
	Mammalia	199	2.6990	2.8012 to 2.6004	0.9295	E
	Reptilia	46	2.9024	3.1359 to 2.6862	0.9341	G
	Ungulata	40	2.4023	2.6051 to 2.2152	0.9337	S
	Carnivora	47	2.8622	3.129 to 2.6181	0.9096	G,E
	Marsupialia	13	2.9508	3.4882 to 2.4961	0.9183	G,E,S

	Euarchonta	14	2.7329	3.0467 to 2.4514	0.9670	G,E,S
	Glires	65	2.6499	2.8328 to 2.4787	0.9319	E,S
L _F vs. L _H	All	232	1.0387	1.068 to 1.0101	0.9537	-
	Mammalia	186	1.0442	1.0766 to 1.0126	0.9552	-
	Reptilia	45	0.9956	1.0706 to 0.9257	0.9427	-
	Ungulata	31	1.0911	1.1564 to 1.0293	0.9764	-
	Carnivora	45	0.9645	1.0235 to 0.9088	0.9618	-
	Marsupialia	13	1.1108	1.337 to 0.9228	0.8918	-
	Euarchonta	13	1.1347	1.3601 to 0.9466	0.9108	-
	Glires	65	1.0946	1.1499 to 1.0418	0.9615	-
C _{H+F} vs. BM	All	246	2.8463	2.932 to 2.7631	0.9444	-
	Mammalia	199	2.8325	2.9249 to 2.7429	0.9473	-
	Reptilia	46	2.9357	3.1813 to 2.709	0.9285	-
	Ungulata	40	2.6829	2.8825 to 2.497	0.9480	-
	Carnivora	47	2.9730	3.2331 to 2.7337	0.9199	-
	Marsupialia	13	3.1220	3.4650 to 2.8129	0.9629	-
	Euarchonta	14	2.8459	3.1375 to 2.5813	0.9734	-
	Glires	65	2.7539	2.9332 to 2.5855	0.9395	-

Standardized major axis equation in format $y = mx + b$. The particular scaling similarity model (Sim.) followed by the scaling coefficient is presented by G, geometric similarity, E, elastic similarity, or S, static similarity. Scaling patterns that fall between models are presented by > or <, and those that do not follow any pattern are represented by a 0. BM - body mass; L_F - femoral length; C_F - femoral circumference; L_H - humeral length; C_H - humeral circumference; C_{H+F} - total humeral and femoral circumference.

Table 1-8. Raw and PIC stylopodial scaling in Artiodactyla and Bovidae.

		Raw Data SMA Results						
Groups	Analysis	N	m	m 95% CI	b	b 95% CI	R ²	Sim.
Bovidae	L _F vs C _F	13	1.1070	1.3723 to 0.8929	-0.7480	-0.173 to -1.3229	0.8909	G
	L _H vs C _H	13	1.1678	1.3857 to 0.984	-0.8030	-0.3356 to -1.2703	0.8874	G
	L _F vs BM	13	3.2973	3.9924 to 2.7232	-2.9690	-1.4467 to -4.4912	0.9290	G
	C _F vs BM	20	3.0957	3.3733 to 2.8409	-0.9512	-0.4385 to -1.4638	0.8979	G
	L _H vs BM	13	3.3338	4.0989 to 2.7115	-2.8181	-1.2036 to -4.4325	0.8553	G,E
	C _H vs BM	20	2.5940	2.8665 to 2.3474	0.0122	0.5127 to -0.4882	0.9678	E,S
	L _F vs L _H	13	0.9891	1.1017 to 0.8878	-0.0453	0.2112 to -0.3018	0.8083	-
	C _{H+F} vs BM	20	2.8489	3.076 to 2.6385	-1.3367	-0.8494 to -1.8239	0.8506	-
Artiodactyla	L _F vs C _F	26	1.1409	1.2947 to 1.0053	-0.8399	-0.4833 to -1.1964	0.9074	>G,<E
	L _H vs C _H	26	1.2526	1.3877 to 1.1305	-1.0152	-0.7076 to -1.3226	0.9037	>G,<E
	L _F vs BM	26	3.3611	3.8167 to 2.9598	-3.1304	-2.0748 to -4.1858	0.9388	>G,<E
	C _F vs BM	34	2.9937	3.2067 to 2.7947	-0.7410	-0.336 to -1.146	0.9395	G
	L _H vs BM	26	3.1906	3.5841 to 2.8401	-2.4783	-1.5887 to -3.3677	0.8888	G
	C _H vs BM	34	2.4813	2.7106 to 2.2713	0.2501	0.6838 to -0.1836	0.9282	E,S
	L _F vs L _H	26	1.0725	1.4129 to 0.814	-0.2044	-0.0146 to -0.394	0.8199	-
	C _{H+F} vs BM	34	1.0782	1.1536 to 1.0076	-1.0639	-0.6401 to -1.4876	0.9267	-
PIC SMA Results								
Groups	Analysis	N	m	m 95% CI	b	b 95% CI	R ²	Sim.
Bovidae	L _F vs C _F	12	1.1531	1.5416 to 0.8624	-	-	0.8133	G,E
	L _H vs C _H	12	1.1513	1.434 to 0.9243	-	-	0.9081	G
	L _F vs BM	12	3.4556	4.525 to 2.6388	-	-	0.8426	G,E
	C _F vs BM	19	3.1673	3.5813 to 2.8011	-	-	0.9379	G
	L _H vs BM	12	3.2715	4.3059 to 2.4855	-	-	0.8444	G,E
	C _H vs BM	19	2.5269	2.8351 to 2.2522	-	-	0.9456	E,S
	L _F vs L _H	12	1.0563	1.1839 to 0.9424	-	-	0.9715	-
	C _{H+F} vs BM	19	2.8455	3.1446 to 2.5748	-	-	0.9590	-
Artiodactyla	L _F vs C _F	25	1.1480	1.3096 to 1.0062	-	-	0.8889	G
	L _H vs C _H	25	1.2482	1.3858 to 1.1241	-	-	0.9356	>G,<E
	L _F vs BM	25	3.2810	3.7657 to 2.8586	-	-	0.8805	G
	C _F vs BM	33	2.9651	3.2428 to 2.7111	-	-	0.9324	G
	L _H vs BM	25	3.0167	3.4531 to 2.6353	-	-	0.8932	G
	C _H vs BM	33	2.3860	2.6049 to 2.1854	-	-	0.9347	S
	L _F vs L _H	25	1.0876	1.1593 to 1.0203	-	-	0.9757	-
	C _{H+F} vs BM	33	2.6658	2.8816 to 2.4662	-	-	0.9487	-

Standardized Major Axis equation shown in the format $y = mx + b$ ($b = 0$ in PIC). The particular theoretical scaling model (Sim.) followed by the slope is represented by G, geometric similarity, E, elastic similarity, or S, static similarity. Scaling patterns that fall between models are represented by $>$ or $<$, and those that do not follow any pattern (that is, above or below all predicted models) are represented by a 0. BM - body mass; L_F - femoral length; C_F - femoral circumference; L_H - humeral length; C_H - humeral circumference; C_{H+F} - total humeral and femoral circumference.

Table 1-9. Predictive power of various body mass estimation equations.

Equation	PPE	PPE CI	SEE	R ²	AIC
OLS Regression					
1. logBM = 2.749logC _{H+F} - 1.104	25.63	28.513 to 22.748	0.134	0.988	-281.882
2. logBM = 2.818logC _F - 0.417	33.934	38.224 to 29.645	0.175	0.979	-152.014
3. logBM = 2.651logC _H - 0.089	26.922	30.117 to 23.727	0.143	0.986	-251.996
4. logBM = 2.843logL _F - 2.005	70.822	87.438 to 54.206	0.311	0.93	122.345
5. logBM = 2.802logL _H - 1.716	50.658	57.212 to 44.104	0.264	0.95	46.983
Non-linear Regression					
BM = 0.421C _{H+F} ^{2.47}	42.321	45.021 to 39.622	-	-	-
Multiple Regression					
1. logBM = 0.375logL _H + 1.544logC _H - 0.136logL _F + 0.954logC _F - 0.351	24.462	27.308 to 21.616	0.13	0.987	-275.173
2. logBM = 1.78logC _H + 0.939logC _F - 0.215	24.932	27.64 to 22.224	0.131	0.988	-293.67
3. logBM = 2.432logL _H + 0.379logL _F - 1.763	50.263	56.719 to 43.807	0.262	0.951	42.203
Phylogenetic GLS Regression					
1. logBM = 2.754logC _{H+F} - 1.097	25.03	27.711 to 22.349	0.135	-	-232
2. logBM = 0.212logL _H + 1.347logC _H - 0.533logL _F + 0.749logC _F - 0.76	26.326	29.184 to 23.467	0.146	-	-220.396
3. logBM = 1.54logC _H + 1.195logC _F - 0.234	24.624	27.221 to 22.027	0.132	-	-227.056

Bivariate and multiple regression statistics for various body mass proxies discussed here (that is, circumference and length of the humerus and femur). Statistics include the Percent Prediction Error (PPE), along with its upper and lower 95% PPE Confidence Intervals (PPE CI), the Standard Error of the Estimate (SEE), the Coefficient of Determination (R²), and the Akaike Information Criterion Score (AIC). BM - body mass; C_F - femoral circumference; C_H - humeral circumference; C_{H+F} - total humeral and femoral circumference; L_F - femoral length; L_H - humeral length.

Table 1-10. Body mass estimates of commonly cited non-avian quadrupedal dinosaurs.

Taxon	Sp #	C1962	A1985§	P1997	H1999	S2001	This study
<i>Iguanodon bernisartensis</i>	IRSNB R51	4510	7204	3200	3790	3776	8680 6510-10850
<i>Corythosaurus casuarius</i>	ROM 845	3820	3030	2800	-	3079	3620 2720-4530
<i>Protoceratops andrewsi</i>	MPC-D 100/504	177	68	164	-	23.7	79 59 - 98
<i>Styracosaurus albertensis</i>	AMNH 5372	3690	3649	1800	-	-	4370 3280-5460
<i>Triceratops horridus</i>	NSM PV 20379	8480	5310	6400	3938	4964	7400 5550-9250
<i>Stegosaurus mjosi</i>	SMA 0018‡	1780	4131	2200	2530	2611	4950 3720-6190
<i>Diplodocus longus</i>	USNM 10865*	10560	9061	11400	13421	19655	10940 8200-13670
<i>Brachiosaurus brancai</i>	HMN SII†	78260	29336	31500	25789∫	28655	35780 26840-44730

Body masses estimated in this study are based on the phylogenetically corrected total stylopodial circumference equation (**EQ 1.2**) and the error range is based on the 25% mean prediction error obtained from the equation. References: A1985, Anderson *et al.* (1985); C1962, Colbert (1962); H1999, Henderson (1999); P1997, Paul (1997); S2001, Seebacher (2001). Museum abbreviations in dataset file (Additional Files 1, Dataset). * - limb measurements based off of a cast mounted at the Senckenberg Museum, Frankfurt, Germany; † - measurements taken from Anderson *et al.* (1985); ‡ - measurements from Redelstorff and Sander (2009); § - all estimates presented under A1985 are based on the equations presented in that study, but based on the limb measurements presented in dataset S1, the only exceptions are *B. brancai* and *T. rex*, which are based on data from A1985; ∫ - estimate from Campbell and Marcus (1992); ∫ - estimate from Henderson (2004).

1.8 Figures

Figure 1-1. Limb scaling patterns in mammalian clades. Lines are fitted based on the SMA results presented in table 1. (A) Log femoral length and circumference plotted against log body mass. (B) Log humeral length and circumference against log body mass. (C) Log femoral length plotted against log humeral length. (D) The log of combined humeral and femoral circumference against log body mass.

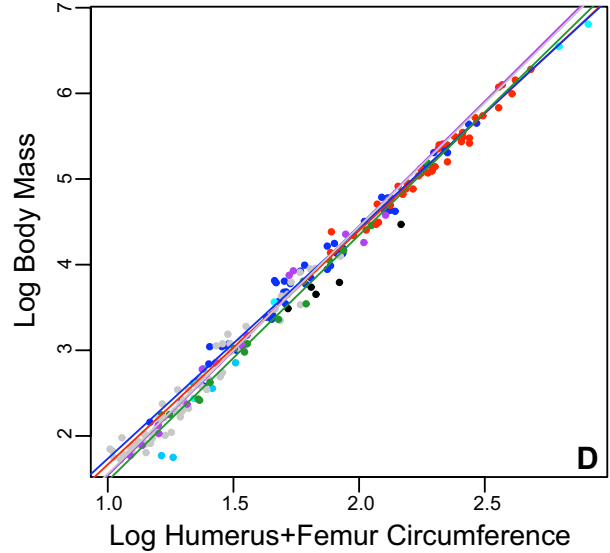
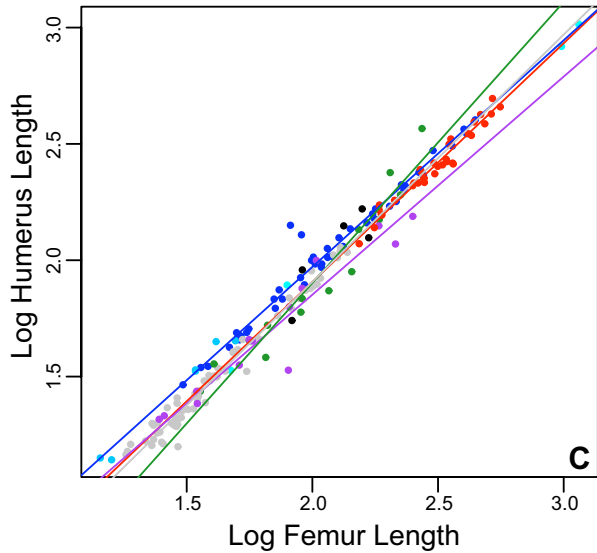
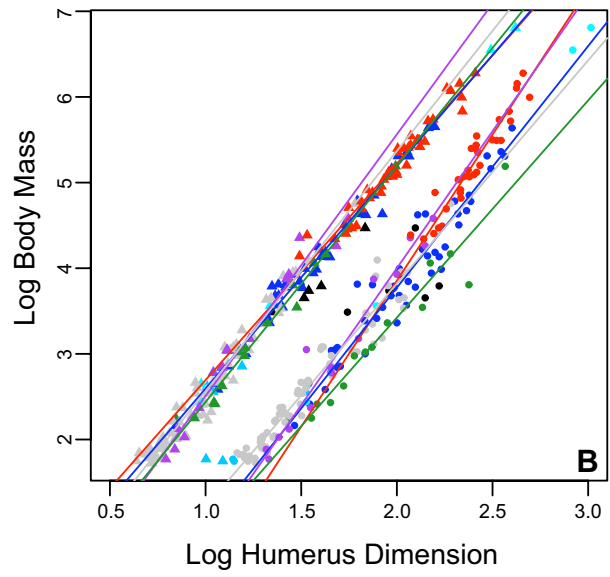
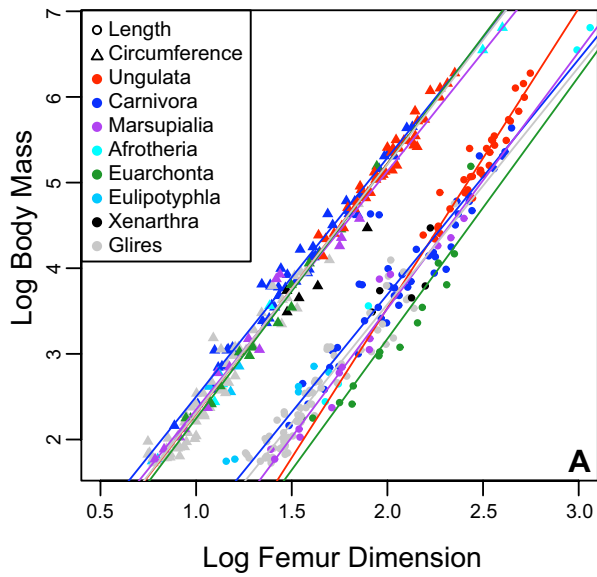


Figure 1-2. Limb scaling patterns in quadrupedal terrestrial tetrapods. Lines are fitted based on the SMA results presented in table 1. Lissamphibians are plotted (green) but no line was fitted due to its small sample size and body mass range. (A) Log femoral length and circumference plotted against log body mass. (B) Log humeral length and circumference against log body mass. (C) Log femoral length plotted against log humeral length. (D) The log combined humeral and femoral circumference against log body mass.

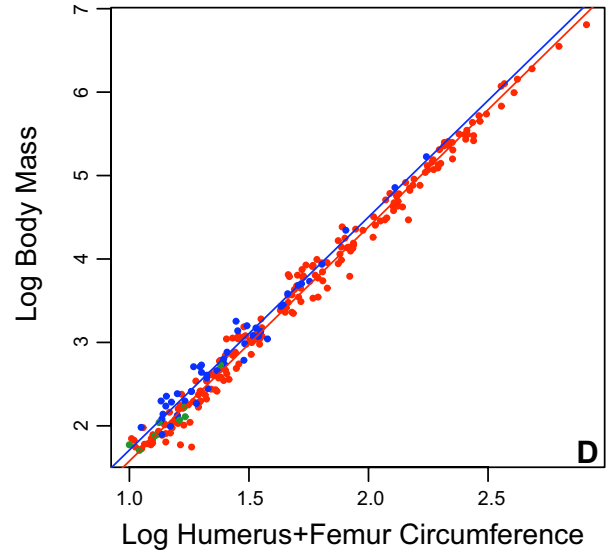
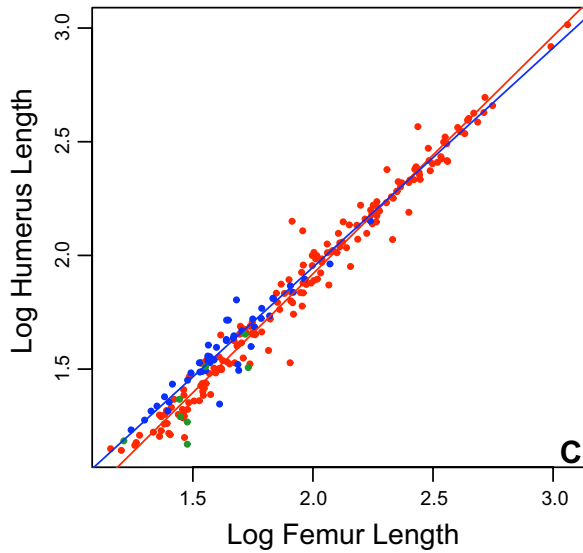
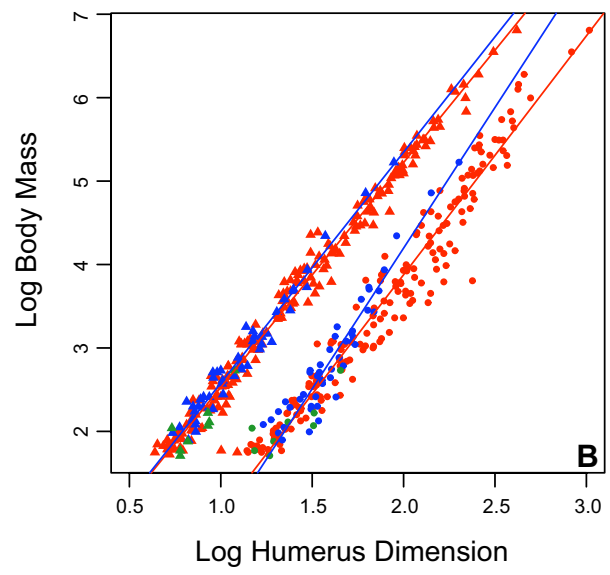
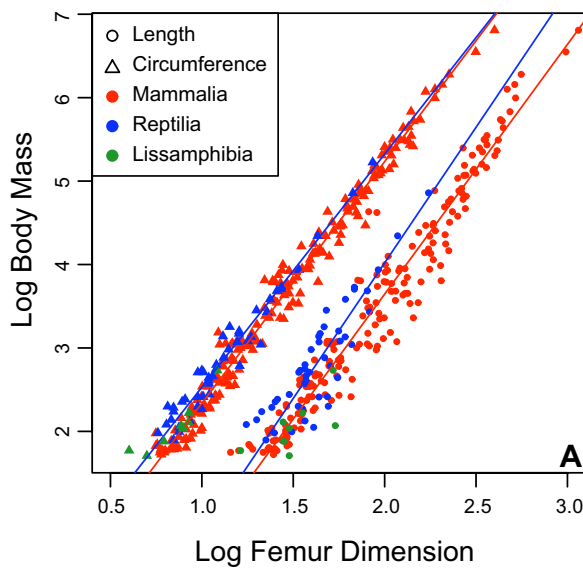


Figure 1-3. Limb scaling patterns in different mammalian size classes. Lines are fitted based on the SMA results presented in table 4. All three comparisons plot the log total stylopodial circumference against log body mass in the mammalian sample of the dataset. Size class comparisons are based on previously studied thresholds discussed in the text (Economos, 1983; Bertram and Biewener, 1990; Christiansen, 1999b). Mammals above and below 20 kg (A), 50 kg (B), and 100 kg (C).

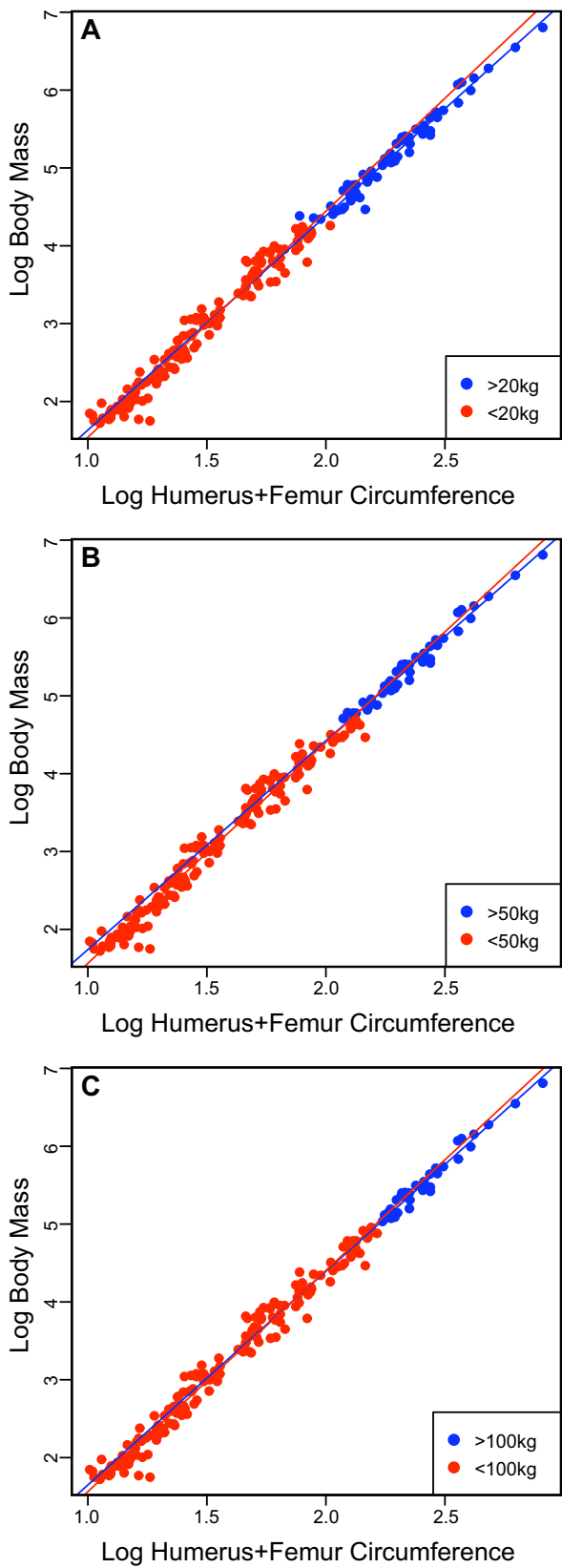
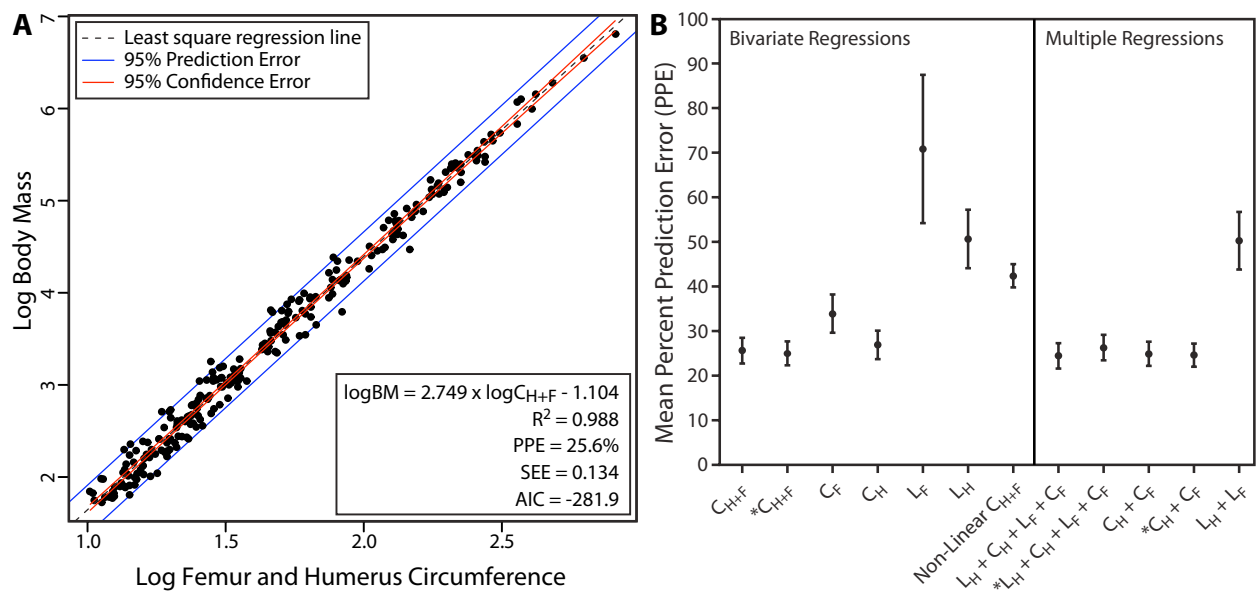


Figure 1-4. Raw OLS regression for body mass estimation and percent prediction error of body mass proxies. (A) The least-squares regression of the raw data between the log total stylopodial circumference and log body mass in a sample of 245 (talpids removed) mammals and non-avian reptiles. Regression equation shown in the format $y = mx + b$, and is presented along with its coefficient of determination (R^2), mean percent prediction error (PPE), standard error of the estimate (SEE), and Akaike Information Criterion (AIC). (B) Comparison of the predictive power of several body mass proxies based on their mean PPE. The mean PPE are represented by the black circle along with their 95% confidence error bars. The graph is divided into two sections representing the results from the bivariate and multiple regressions. Variables regressed against body mass are labelled along the x-axis. Labels marked with an * represent the analyses in which the data were phylogenetically adjusted through the use of a phylogenetic generalized least squares bivariate or multiple regression. Abbreviations: C_F , femoral circumference; C_H , humeral circumference; L_F , femoral length; L_H , humeral length.



Chapter 2

A Mathematical Correction Factor for Estimating Body Mass in Terrestrial Bipedal Tetrapods

2.1 Abstract

The scaling relationship between stylopodial circumference and body mass is highly conserved in extant terrestrial quadrupeds resulting in a robust and consistent method to estimate body mass in these taxa. Unfortunately, circumference to mass scaling patterns in quadrupeds cannot be applied directly to estimating body mass in bipeds; as a result, a new scaling equation to estimate the body mass of extinct bipeds is presented based on a mathematical correction of the quadrupedal-based model. The correction factor is derived from the systematic difference in the circumference to area scaling relationship of two circles (hypothetical quadruped) and one circle (hypothetical biped). When applied to a sample of extant birds, the correction factor reveals a mean percent prediction error that is statistically indistinguishable from that inherent to the empirical bird dataset, and is significantly better than other published bipedal body mass estimation equations. Comparisons between body masses obtained using the new correction factor to previous published methods suggest a higher consistency with estimates based on volumetric reconstructions. The equation presented here offers a straightforward and consistent method with which to estimate body mass in extinct bipeds, in particular large non-avian theropods, for investigating large-scale evolutionary patterns of body size in the fossil record of terrestrial vertebrates, such as those associated with the evolution of birds.

2.2 Introduction

Strong correlations exist between body mass and numerous physiological and ecological attributes in extant organisms (e.g., Peters, 1983; Brown *et al.*, 1993; Burness *et al.*, 2001; Gillooly *et al.*, 2001). Accurate estimates of body mass are therefore critical to understanding the palaeobiology of extinct taxa and the evolution of community structure through the history of life (e.g., Erickson *et al.*, 2001; Carrano, 2006; Gillooly *et al.*, 2006; Varricchio *et al.*, 2008). Dinosaurs exhibit the largest body size ranges in a terrestrial vertebrate clade, with several species likely approaching the upper body size limit for terrestrial vertebrates (Sookias *et al.*, 2012a). In addition, non-avian dinosaurs underwent major evolutionary shifts in limb posture and gait, including several transitions from bipedality to quadrupedality (Maidment and Barrett, 2012) that may have been associated with order of magnitude-level transitions in body size. Dinosaurs, therefore, provide a model clade for understanding body size evolution and evolutionary ecology in terrestrial vertebrates (Hone *et al.*, 2005; Carrano, 2006; Turner *et al.*, 2007; Butler *et al.*, 2009; Sookias *et al.*, 2012b). However, the capacity to reconstruct these patterns hinges on the ability to accurately and consistently estimate body size in a large sample of taxa.

In Chapter 1, I showed that, despite previous criticisms, limb scaling models [based on the relationship between total stylopodial circumference and body mass, first proposed by Anderson *et al.* (1985)], provide a robust and consistent method with which to estimate body mass in terrestrial quadrupeds, and that the relationship is independent of gait, limb posture, and phylogenetic history. Given that both limbs are involved with weight support in a quadruped, the

model's applicability to extinct quadrupeds is evident from its integration of both fore and hind limb measurements. However, this constraint does not apply to the humerus of bipeds and as a result, the quadrupedal equation from chapter 1 cannot be used to directly estimate the mass of bipeds. Despite this limitation, approximately 45% of known Mesozoic dinosaurs are theropods (based on the genus-level dataset of Barrett *et al.*, 2009; Ntotal=543, NTheropoda=247) and both sauropodomorphs and ornithischians also include bipedal taxa suggesting that over half of the known Mesozoic dinosaur diversity was bipedal. As a result, if one is to investigate the associations between major macroevolutionary events in the history of dinosaurs and changes in body size, such as the parallel evolution of quadrupedalism in sauropodomorphs, thyreophorans, marginocephalians, and ornithopods (Maidment and Barrett, 2012; Maidment *et al.*, 2012) and miniaturization across the origin of birds (Turner *et al.*, 2007), a consistent and robust method for generating large body mass datasets is needed for both quadrupedal and bipedal taxa.

Other limb scaling models, such as those based on avian taxa, have been proposed (Campbell Jr and Marcus, 1992). However, femoral circumference to body mass scaling is not as conserved in birds and exhibits overall lower coefficient of determination (Campbell Jr and Marcus, 1992; R² = 0.958) compared to that of extant quadrupeds (Chapter 1; Campione and Evans, 2012; R² = 0.988). Importantly, unlike mammals and reptiles, limb scaling patterns in birds reveal significant differences in among-clade comparisons (Campbell Jr and Marcus, 1992; Doube *et al.*, 2012). In addition, the upper body mass range of extant birds (~140 kg; Appendix 3) is much lower than extant quadrupeds (~6,000 kg; Appendix 1), and approximately 60% of non-avian bipedal dinosaurs fall above the bird range, compared to 5% above the quadrupedal range, thereby incurring an appreciable amount of extrapolation. Given the variable nature of limb circumference to body mass scaling patterns in extant avians, as well as issues with extrapolation, avian-based scaling methods cannot be adequately applied to extinct bipedal

dinosaurs. Bipedal dinosaurs are thus generally estimated using volumetric reconstructions (Henderson, 1999; Gunga *et al.*, 2007; Bates *et al.*, 2009a; Butler *et al.*, 2009; Hutchinson *et al.*, 2011). Volumetric reconstructions are critical for addressing numerous biomechanical and physiological questions in the fossil record, such as locomotion, defense, center of mass, buoyancy, and metabolism (Henderson, 1999, 2004; Henderson, 2006; Allen *et al.*, 2009; Pontzer *et al.*, 2009; Mallison, 2010, 2011c, b; Henderson, in press). However, the nature of reconstructions invokes unavoidable subjectivity, and it is therefore important that they be constrained by an external empirically based method (see Chapter 3). Finally, reconstructions are time consuming and thus impractical for generating large datasets of body sizes, and, most importantly, they rely on the presence of complete specimens, which are exceedingly rare in the fossil record.

In this chapter, I propose a new equation to estimate body mass in extinct bipeds (such as many non-avian dinosaurs) based on a mathematical correction derived from the highly conserved relationship recovered in extant terrestrial quadrupeds (Chapter 1; Campione and Evans, 2012). I test this new model within the context of a large dataset of birds, which represent the only living biped with a large sample size. Finally, this equation is applied to a sample of non-avian dinosaur bipeds revealing that it is a rapid and consistent method with which to obtain body mass. Incorporation of both this and the quadrupedal model developed in chapter 1 will have important implications for understanding the evolutionary history of Dinosauria and conducting large-scale macroevolutionary analyses of body size throughout the Mesozoic.

2.3 Mathematical Derivation

The body mass estimation equation developed in Chapter 1 (Campione and Evans, 2012) uses the combined circumference of the major weight-bearing bones (humerus and femur). Circumference is a simple measurement to obtain that provides a proxy for cross-sectional surface area, the measurement of which should be directly associated to the strength of the limb (although this still remains to be tested), and, therefore, directly related to an animal's mass (Rubin and Lanyon, 1984). As a result, given a constant body mass, the combined cross-sectional area of the humerus and femur of a quadruped should equal that of the femur of a biped. However, given equal cross-sectional area, the combined humeral and femoral circumference of a quadruped will be systematically greater than that of a biped's femur. Based on this systematic difference a purely mathematical correction factor can be developed, which would allow an extant quadrupedal equation to be used to estimate a biped's mass, without introducing outside volumetric model data (e.g., Anderson *et al.*, 1985; Seebacher, 2001; Christiansen and Fariña, 2004; O'Gorman and Hone, 2012).

In order to derive the bipdal correction factor (α) the relationship between circumference and area are needed (Figure 2-1). Here we model cross-sectional shape as a circle. The circumference (C) to area (A) relationship of one circle (i.e., a hypothetical biped) is defined by

$$A_{bip} = 0.0796 \cdot C_{bip}^2 \quad \text{EQ 2.1}$$

and the relationship between the combined circumference and the combined areas of two circles of equal size (i.e., a hypothetical quadruped) is:

$$A_{quad} = 0.0398 \cdot C_{quad}^2 \quad \text{EQ 2.2}$$

Given a constant body size, the combined cross-sectional area of a quadruped will equal that of a biped (i.e., $A_{bip} = A_{quad}$). Therefore,

$$0.0796 \cdot C_{bip}^2 = 0.0398 \cdot C_{quad}^2 \quad \text{EQ 2.3}$$

Given than the femoral circumference of a biped is systematically less than the combined circumference of the humerus and femur in a quadruped, both values will be proportional to each other so that

$$C_{bip} \propto C_{quad} \quad \text{EQ 2.4}$$

and, \therefore

$$\alpha \cdot C_{bip} = C_{quad} \quad \text{EQ 2.5}$$

where α is the bipedal correction factor of interest here. The above can be inserted into **EQ 2.3** so that,

$$0.0796 \cdot C_{bip}^2 = 0.0398 \cdot (\alpha \cdot C_{bip})^2 \quad \text{EQ 2.6}$$

and, the equation solved for α

$$\alpha = \sqrt{\frac{0.0796}{0.0398}} = \sqrt{2} \quad \text{EQ 2.7}$$

which provides a bipedal correction factor that is equal to $\sqrt{2} \approx 1.4133$.

Insertion of α into the phylogenetically corrected terrestrial quadruped equation of Chapter 1 (Campione and Evans, 2012) results in the following equation:

$$\log BM_{bip} = 2.754 \cdot \log(C_{femur} \cdot 1.4133) - 1.097 \quad \text{EQ 2.8}$$

or,

$$\log BM_{bip} = 2.754 \cdot \log C_{femur} - 0.947 \quad \text{EQ 2.9}$$

where BM_{bip} is the body mass of the biped and C_{femur} is the femoral circumference.

2.3.1 Methodological Assumptions

All techniques for estimating body mass in extinct taxa make inherent assumptions that are virtually impossible to avoid. Methods need to be explicit about their particular set of assumptions, and if possible their effect should be quantified. The correction factor (α) derived in this chapter makes two important methodological assumptions regarding: 1) the cross-sectional shape of the main weight-bearing bones, and 2) the relative proportions of the fore- and hind limbs in quadrupeds.

2.3.1.1 Cross-Sectional Shape

The circumference-area models that form the basis for deriving α assume a circular cross-sectional shape for the hypothetical humerus and femur. Most terrestrial vertebrates, especially at small size, likely meet this assumption. For instance, Carrano (2001; table 12) found that the proportional difference between mediolateral and anteroposterior diameters (i.e., eccentricity) was not significantly different from one in both mammals ($D_{ML}/D_{AP} = 1.129 \pm 0.228$) and dinosaurs ($D_{ML}/D_{AP} = 1.248 \pm 0.395$), indicating an approximate circular cross-sectional shape overall. However, the wide errors recovered around these means suggest that several taxa deviate from a circular cross-sectional shape, and at least in dinosaurs, this deviation may be associated

with body size in which larger taxa have elliptical cross-section shapes; a morphology that has been hypothesized to better accommodate increases in mediolateral forces generated at large size (Wilson and Carrano, 1999; Carrano, 2001; Maidment *et al.*, 2012). Despite these important anatomical differences, the mathematical derivation of α reveals that it is determined by square rooting the quotient calculated between the intercept values of the two circumference-area models (i.e., b in the power function bx^m ; see **EQ 2.2**, and **EQ 2.7**). Therefore, the correction factor is related to proportional differences between the models and independent of the absolute intercept values. Variation in cross-sectional shape will affect the intercept value, but not the proportional difference, and, as a result, the correction factor is independent of cross-sectional shape (i.e., eccentricity).

2.3.1.2 Fore- to Hind Limb Proportions

Since α is related to proportional differences of the modeled intercepts, the relative size of the circles will undoubtedly have an effect on the resultant corrections factor. The correction factor presupposes that the two circles that represent the humerus and femur of a quadruped are equal in circumference (i.e., $C_h/C_f = 1$). However, animals rarely have humeri and femora of the same size and it may therefore be expected that proportional differences between these bones will have a large effect on α . Indeed evidence from the empirical dataset used in chapter 1 indicate that, on average, $C_h/C_f < 1$ (Table 2-3). This is particularly evident in certain mammalian groups, such as Euarchonta (0.912 ± 0.051), Glires (0.829 ± 0.008), and Marsupialia (0.855 ± 0.085). Such differences are particularly pronounced in quadrupedal dinosaurs, in which the humerus can be almost half the size of the femur [e.g., *Edmontosaurus regalis*, $C_h/C_f = 0.517$ (Campione, in press); *Hypacrosaurus altispinus*, $C_h/C_f = 0.563$ (Evans *et al.*, 2009); *Styracosaurus albertensis*, $C_h/C_f = 0.778$; and *Apatosaurus louisae*, $C_h/C_f = 0.744$ (Anderson *et al.*, 1985)]. In order to test

the sensitivity of α to variation in proportional differences between the circumference and area of the fore- and hind limbs, I re-derived α using a modified relationship between total circumference and area of two circles, in which one of the circles is half the size of the other (i.e., $C_h/C_f = 0.5$).

$$A_{quad} = 0.0442 \cdot C_{quad}^2 \quad \text{EQ 2.10}$$

Under this criterion $\alpha \approx \sqrt{1.8} \approx 1.342$, a 0.0713 difference from that derived under the assumption of $C_h/C_f = 1$. Such a small difference suggests that proportional differences in the size of the humerus and femur will not play a major role in the final body mass estimates of bipedal taxa. However, body mass estimates can be calculated with either correction factor.

2.3.2 Empirical Tests

2.3.2.1 Methods

In order to empirically test the bipedal correction equation it was applied to a dataset of femoral circumferences collected from a sample of 70 extant avians spanning almost 3.5 orders of magnitude from 53 g (*Coccyzus melacoryphus*) to 139 kg (*Struthio camelus*). All avian taxa are based on specimens for which the live body mass is known. Data on the length of the femur and the circumference and length of the tibiotarsus were also collected. Circumference measurements were taken at the thinnest part of the limb bone (as per Chapter 1; Campione and Evans, 2012) and length measurements were taken as the maximum length of the bone.

In addition to the correction factor equation derived here (EQ 2.9), femoral circumference was used to estimate the body mass of the avian specimens using three alternative equations: 1) the extant avian regression equation of femoral circumference and body mass

presented by Campbell and Marcus (1992) based on a sample of 795 non-passerine specimens and representing 391 species:

$$\log_{10} BM_{bip} = 2.411 \cdot \log_{10} C_{femur} - 0.065 \quad \text{EQ 2.11}$$

2) the bipedal equation of Anderson *et al.* (1985), which is based on the same slope obtained from their quadrupedal regression ($m = 2.73$), and the intercept corrected based on a volumetric mass estimate of a life-size reconstruction of *Troodon formosus*:

$$BM_{bip} = 0.16 \cdot C_{femur}^{2.73} \quad \text{EQ 2.12}$$

and 3) the femoral circumference to body mass equation developed by Christiansen and Farina (2004) based on measurements of 16 non-avian theropods for which body masses were determined by calculating the volume of clay models (using water displacement methods) and an assumed body density of 0.95 g/cm³:

$$\log BM_{bip} = 2.738 \cdot \log C_{femur} - 3.607 \quad \text{EQ 2.13}$$

The mean percent prediction error (PPE) was calculated for each equation, as well as for the regression between the true body mass and femoral circumference, and all were compared using a two-tailed t-test. Percent prediction error is calculated as:

$$PPE = \left(\frac{BM_{true} - BM_{estimate}}{BM_{estimate}} \right) \times 100 \quad \text{EQ 2.14}$$

All plots and analyses were created/conducted in R (R Development Core Team, 2012).

2.3.2.2 Results

In the sample of 70 avians examined here, the relationship between femoral circumference and body mass exhibits the lowest mean PPE and the highest coefficient of determination (Table 2-1), followed by the relationship between tibiotarsal circumference and body mass, indicating that, as was the case in quadrupeds (Chapter 1; Campione and Evans, 2012), circumference measurements are more strongly related to body mass than other limb measurements, and that mass is most strongly related to the proximal, rather than distal, limb bones. However, the mean PPE calculated for the femoral circumference to body mass regression (36.7%) is significantly higher than the mean PPE obtained in the relationship between combined stylopodial circumferences and body mass in terrestrial quadrupeds (Chapter 1; Campione and Evans, 2012: 25%; $t = 2.307$; $p = 0.024$). A higher mean PPE value (and lower coefficient of determination) supports the assertion that extant avians exhibit greater variation in circumference, relative to body mass, than extant quadrupeds. Body mass estimates based on the bipedal correction factor reveal a mean PPE of 45.9% (Table 2-2), which although high is statistically indistinguishable from the true mean PPE of 36.7 ($t = -1.226$, $p = 0.222$). The equation presented by Christiansen and Fariña (2004) has a mean PPE of 38.5% and is statistically indistinguishable from either the correction factor or true mean PPE ($t = -0.954$, $p = 0.342$; $t = 0.283$, $p = 0.777$, respectively). Notably, the bipedal equation of Anderson *et al.* (1985) provides the highest PPE at 80.1%, significantly higher than that obtained from both the correction factor and true mean PPE ($t = 2.956$; $p = 0.004$; $t = 3.975$, $p << 0.01$, respectively).

Figure 2-2 provides an empirical plot between femoral circumference and body mass in the extant avian dataset. Addition of lines based on the mass estimation equations (Figure 2-2; dashed lines) reveals possible systematic differences between estimates and the empirical data.

This is also evident in that the slope and intercept coefficients of estimated lines do not fall within the 95% confidence intervals of the bird dataset (Table 2-2). Systematic error is most evident in the bipedal equation of Anderson *et al.* (1985), which also had the highest mean PPE. This equation systematically underestimates small-bodied taxa. In comparison both the corrected quadrupedal equation and the equation presented in Christiansen and Fariña (2004) appear to over estimate large-bodied birds. Not surprisingly, estimates based on the avian regression lines presented by Campbell and Marcus (1992) provide the best fit to the avians used here, and even has a slightly, though not significantly, better mean PPE compared to the true mean PPE.

2.4 Discussion

In order to investigate large-scale evolutionary patterns of body size across major evolutionary transitions, such as those associated with the evolution of flight in birds (Turner *et al.*, 2007; Dececchi and Larsson, in press) and the evolution of quadrupedality in dinosaurs (Maidment and Barrett, 2012), it is critical to have simple and consistent methods with which to generate large datasets of body mass estimates in both bipeds and quadrupeds. The correction factor derived here provides an adjustment for the difference in intercepts between bipeds and quadrupeds, and thereby permits use of the quadrupedal equation for estimating the mass of a biped, with one important caveat. This new model assumes that extinct bipeds exhibit a similar scaling coefficient (i.e., the slope) to that of the terrestrial quadruped sample. However, the femoral circumference to body mass scaling coefficient in extant birds [$m = 2.415 \pm 0.048$ (Campbell Jr and Marcus, 1992)] is significantly below that of the combined stylopodial circumference and body mass relationship in terrestrial quadrupeds [$m = 2.778 \pm 0.041$ (Table 1-1)], thereby

questioning the validity of this assumption. This is particularly important given that most extinct bipeds (i.e., non-avian theropods) represent the direct lineage that gave rise to birds. Consequently, should non-avian extinct bipeds (including non-avian theropods) be expected to follow the apomorphic scaling relationship recovered in birds, or do they retain the conserved and plesiomorphic relationship recovered in terrestrial quadrupeds (Allen *et al.*, 2013)?

In terms of limb morphology, avians exhibit numerous skeletal modifications; in particular, the majority of birds have highly pneumatic femora. Biomechanically, pneumatic bones are generally considered to be weaker than marrow-filled bones (Cubo and Casinos, 2000; Casinos and Cubo, 2001), which may explain why avian femora follow an elastic ($m=2.67$) or even static ($m=2.5$) scaling pattern in which, on average, circumference is proportionally greater for a given body mass as size increases (Table 11; McMahon, 1973; McMahon, 1975b; Campbell Jr and Marcus, 1992; Cubo and Casinos, 1998; Cubo and Casinos, 2000; Casinos and Cubo, 2001). Non-avian bipedal dinosaurs do not possess pneumatic limb bones (O'Connor, 2006) and may be therefore expected to follow plesiomorphic scaling patterns exhibited by extant terrestrial quadrupeds. Furthermore, a consistent occurrence of limb bone pneumaticity may have arisen after the common ancestor of Aves, as the limbs of *Archaeopteryx* (the putative first avian), and potentially all non-neornithine birds are also apneumatic (Casinos and Cubo, 2001; Hutchinson, 2001). Despite the conserved nature of apneumatic femora, at least among non-avian bipeds, a recent study reveals that other aspects that were presumed apomorphic of birds, such as an anteriorly positioned center of mass, may have evolved more gradually throughout the evolutionary history of theropods, in particular maniraptorans (Allen *et al.*, 2013). How directly related these gradual shifts are to changes in femoral posture, which themselves appear to be independent of cross-sectional area and shape (Farke and Alicea, 2009), remain to be tested. Finally, a plesiomorphic scaling pattern in extinct non-avian biped is also supported by

empirical observations that, based on limb scaling of femoral proportions, extinct bipedal dinosaurs (including non-avian theropods) are more similar to extant mammals than to extant avians, and that the former may represent a better model for limb scaling patterns in non-avian dinosaurs (Carrano, 1998). If one accepts the hypothesis that non-avian bipedal dinosaurs follow the plesiomorphic and highly conserved scaling patterns exhibited by extant quadrupedal tetrapods, then it strongly advocates for the use of the bipedal correction factor derived here as a robust method for estimating body mass in these taxa.

2.4.1 Body Mass of Non-Avian Bipedal Dinosaurs

Body mass estimates for certain well-known bipedal dinosaurs based on the correction factor are, in general, consistent with those estimated using volumetric reconstruction methods (Table 2-4). This is in contrast to estimates obtained using other scaling equations, which predict much lower body mass estimates at large size (greater than 100 kg; Table 2-5). Given that the correction factor is derived from an external dataset (extant terrestrial quadrupeds) to those used to generate volumetric reconstructions, the congruence between this method and the models suggests that current assumptions made during the creation of most volumetric models of bipedal taxa may be realistic. However, as I am only testing the final mass estimates provided by volumetric models and not the assumptions directly, I cannot reject that possibility that errors associated with different assumptions (e.g., soft tissue reconstruction and body density) counter-balance each other resulting in a valid mass estimate. The advantage of the correction factor, however, is that it permits rapid estimation of incomplete specimens. Here I estimate a sample of non-avian theropods, including the largest for which femoral circumference can be obtained (Table 2-4 and Table 2-5). Based on the femoral circumference, *Tyrannotitan chubutensis*, a carcharodontosaurid from South America (Novas *et al.*, 2005), is reported as the largest theropod

with an estimated body mass of over 10 tonnes. *Tyrannosaurus rex* represents the second heaviest non-avian theropod (6.7 tonnes, exemplified by CM 9380 in Table 2-4 and Table 2-5), followed by two other South American carcharodontosaurids, *Giganotosaurus carolinii* (6.4 tonnes) and *Mapusaurus roseae* (4.3 tonnes). The body mass estimate for *Fruitadens haagarum*, the putative smallest ornithischian, at 750 g is almost identical to that using a volumetric model presented by Butler *et al.* (2009) based on the method of Henderson (1999), and is very similar in mass to the smallest non-avian theropod, *Mahakala omnogovae* (2007), at 780 g.

Body mass estimates of *Tyrannosaurus rex* have been presented by virtually all mass estimation studies in dinosaurs (Colbert, 1962; Alexander, 1985; Anderson *et al.*, 1985; Campbell Jr and Marcus, 1992; Paul, 1997; Henderson, 1999; Seebacher, 2001; Christiansen and Fariña, 2004; Bates *et al.*, 2009a; Hutchinson *et al.*, 2011). As a result, *T. rex* represents a model taxon for comparing estimates between methods. Results are presented in Figure 2-3 and Table 2-6 and, in general, reveal similar patterns to that presented in Table 2-4, in which the bipedal correction factor provides estimates similar to most volumetric reconstructions, and above those predicted by other limb scaling equations (Anderson *et al.*, 1985; Campbell Jr and Marcus, 1992). Although, these results suggest a heavier mass estimate for the largest specimen of *T. rex* (FMNH PR 2081, 8.4 tonnes; Table 2-6) than traditional estimates for the species (generally around 6 tonnes), it suggests that the most recent gigantic mass estimates presented by Hutchinson *et al.* (2011; 14 tonnes) may over-estimate its body mass, which, as stipulated in that study, will have clear implications on the ecology and physiology of this species (e.g., growth rates; Erickson *et al.*, 2004).

2.4.2 Inferring Body Size in the Fossil Record

Body mass cannot be directly determined in the fossil record and therefore must be estimated.

Mass estimates can be ascertained through various methods (reviewed in Chapter 3), but in order to be validated, it is important that they be studied within the context of empirical data, generally obtained from extant taxa. Chapter 1 (Campione and Evans, 2012) showed that limb-scaling patterns in terrestrial quadrupeds reject the criticisms forwarded against the combined circumference to body mass relationship developed by Anderson *et al.* (1985) as a predictor of body mass in the fossil record of quadrupedal tetrapods. However, this methodology only applies to quadrupedal taxa, and cannot be directly applied to extinct bipeds. In this chapter, I derive a correction factor that permits the use of the terrestrial quadrupedal dataset to estimate the body mass of extinct bipeds. In order to empirically test this equation, however, it was applied to a sample of 70 avian species, which represent the only dataset large (and hence powerful) enough to make meaningful conclusions. In addition, the avian dataset was estimated using other equations between femoral circumference and body mass (Anderson *et al.*, 1985; Campbell Jr and Marcus, 1992; Christiansen and Fariña, 2004). The results indicate that all bipedal equations, except for that presented by Anderson *et al.* (1985) that underestimates most bird masses (especially at small size), are within the range of variation revealed by the empirical avian dataset Figure 2-2, indicating that, the corrected equation developed here, the total avian regression of Campbell and Marcus (1992), and the volumetric reconstruction-based regression of Christiansen and Fariña (2004) are robust predictors of body mass. This visual observation is quantitatively supported by calculation of the mean PPE (Table 2-2), in which the bipedal equation of Anderson *et al.* (1985) is significantly worse than all other equation for estimating

the mass of birds. Importantly, the error present in all other models could not be differentiated from that already inherent in the bird dataset.

The fact that the equation of Campbell and Marcus (1992) offers the lowest PPE is not surprising given that it is based on another extant avian dataset. However, as discussed above, avian taxa exhibit numerous skeletal limb apomorphies, which suggest that scaling relationships in extant avians cannot be assumed to represent those of extinct bipeds (Carrano, 1998; Cubo and Casinos, 2000; Casinos and Cubo, 2001; Hutchinson, 2001). Perhaps more importantly, based on the sample of non-avian bipedal dinosaurs in Table 2-5, approximately 60% of these exemplars are outside, and above, the size range available for avian-based mass estimation equations (e.g., Campbell Jr and Marcus, 1992), thereby necessitating extrapolation far beyond the available data. In comparison, approximately 95% of the non-avian bipedal dinosaur exemplars in Table 2-5 fall within the size range of extant quadrupeds (Appendix 1). Given this significant extrapolation, birds do not represent a strong model for estimating body masses in extinct non-avian bipeds. A second equation, proposed by Christiansen and Fariña (2004) based on the use of volumetric reconstructions of theropods, is almost identical, both in coefficients and error, to that derived using the correction factor. It provides very similar estimates (Table 2-4), it is operationally as simple, and empirical tests using the avian dataset revealed that it too was robust, and statistically indistinguishable from the error already present in the bird dataset. However, there are two advantages of the new corrected model over that of Christiansen and Fariña (2004). 1) Their model is derived from a sample of non-avian theropods that range from 58 kg to 6,300 kg. As a result, its range does not include smaller bipeds (Turner *et al.*, 2007; Butler *et al.*, 2009), which are included within the size range used to derive the correction factor. 2) The Christiansen and Fariña (2004) model is derived from volumetric reconstructions and is therefore not independent of the inherent assumptions of life reconstructions.

The observation that the error (as given by the PPE) in body mass estimates derived from the corrected equation (**EQ 2.9**) is statistically indistinguishable from error inherent to the avian dataset, in combination with the shortcomings of a purely avian model (Campbell Jr and Marcus, 1992) and disadvantages for the reconstruction-based model (Christiansen and Fariña, 2004), I propose that the correction factor derived here offers a better equation with which to estimate the body mass of extinct bipedal tetrapods, which have not undergone skeletal limb modification as those seen in birds. Furthermore, Mass estimates calculated using the bipedal correction factor in a sample of non-avian dinosaurs are consistent with estimates derived from most volumetric reconstructions, but in comparison, the correction factor is much simpler and, because it does not rely on the complete reconstruction of an individual, it can be applied to the relatively large proportion of taxa and specimens that are known from incompletely preserved skeletons (Benton, 2008; Mannion and Upchurch, 2010; Brown *et al.*, 2013b). Finally, the correction factor presents an independent model with which to constrain volumetric reconstructions of extinct bipeds that are important for testing numerous palaeobiological hypotheses (Henderson, 1999, 2004; Henderson, 2006; Hutchinson *et al.*, 2007; Henderson, 2010; Hutchinson *et al.*, 2011; Mallison, 2011a, c, b).

Body size represents a strong biological descriptor, and hence establishing this property in the fossil record is key to understanding physiological and ecological properties within a temporal and macroevolutionary context. Non-avian dinosaurs exhibit among the largest body size ranges in terrestrial vertebrates and are therefore a model group for reconstructing evolutionary patterns of body size in association with environmental changes. The bipedal correction factor presented in this chapter offers a simple, robust, and consistent method for estimating body mass in extinct bipeds. Given its simplicity, and its consistency with the majority of volumetric estimates, the correction factor has important implications for the

construction of large-scale datasets for assessing macroevolutionary patterns of body size in extinct bipedal tetrapods, in particular patterns associated with transitions from bipedality to quadrupedality in non-avian dinosaurs (Maidment and Barrett, 2012), as well as testing the upper and lower body size limits in this clade (Butler *et al.*, 2009), and hypotheses of miniaturization prior to the evolution of Aves (Turner *et al.*, 2007).

2.5 R-Package: MASSTIMATE v1.0

In an effort to make the equations derived in this chapter and in Chapter 1 (Campione and Evans, 2012) accessible to all for estimating body mass in terrestrial bipeds and quadrupeds, I have developed a software package using the statistical language R (<http://www.r-project.org/>). The package (MASSTIMATE) provides all equations based on circumference measurements under the function ‘MASSTIMATE’. In addition, various other estimation equations based on circumference measurements are included, such as the volumetric reconstruction-based femoral circumference to body mass equation for theropod dinosaurs (Christiansen and Fariña, 2004) and sauropod dinosaurs (Mazzetta *et al.*, 2004), the avian-based femoral circumference to body mass equation of Campbell and Marcus (1992), and both the quadrupedal and bipedal equations of Anderson *et al.* (1985). In the case of the ‘MASSTIMATE’ function results present both the \log_{10} and non-log results as well as the mean percent prediction error on the non-log estimates; other equations provide only the non-log mass estimate. MASSTIMATE provides the option to estimate a single specimen or a large dataset of specimens rapidly with clear utility for large-scale studies of body size evolution in the fossil record.

2.5.1 Source Code

```
MASSTIMATE<-function(HC,FC,equation,data) {
  if(equation=="quad.raw") {
    log.estimate<-2.749*log10(HC+FC)-1.104
    estimate.CE2012<-round(10^log.estimate,1)
    ppe.err<-estimate.CE2012*0.2563
    upper<-round(estimate.CE2012+ppe.err,1)
    lower<-round(estimate.CE2012-ppe.err,1)
  }
  if(equation=="quad.phylocor") {
    log.estimate<-2.754*log10(HC+FC)-1.097
    estimate.CE2012<-round(10^log.estimate,1)
    ppe.err<-estimate.CE2012*0.2503
    upper<-round(estimate.CE2012+ppe.err,1)
    lower<-round(estimate.CE2012-ppe.err,1)
  }
  if(equation=="mult.raw") {
    log.estimate<-1.78*log10(HC)+0.939*log10(FC)-0.215
    estimate.CE2012<-round(10^log.estimate,1)
    ppe.err<-estimate.CE2012*0.24932
    upper<-round(estimate.CE2012+ppe.err,1)
    lower<-round(estimate.CE2012-ppe.err,1)
  }
  if(equation=="mult.phylocor") {
    log.estimate<-1.54*log10(HC)+1.195*log10(FC)-0.234
    estimate.CE2012<-round(10^log.estimate,1)
    ppe.err<-estimate.CE2012*0.24624
    upper<-round(estimate.CE2012+ppe.err,1)
    lower<-round(estimate.CE2012-ppe.err,1)
  }
  if(equation=="bip.raw.a") {
    log.estimate<-2.749*log10(FC*sqrt(2))-1.104
    estimate.CE2012<-round(10^log.estimate,1)
    ppe.err<-estimate.CE2012*0.2563
    upper<-round(estimate.CE2012+ppe.err,1)
    lower<-round(estimate.CE2012-ppe.err,1)
  }
  if(equation=="bip.phylocor.a") {
    log.estimate<-2.754*log10(FC*sqrt(2))-1.097
    estimate.CE2012<-round(10^log.estimate,1)
    ppe.err<-estimate.CE2012*0.2503
    upper<-round(estimate.CE2012+ppe.err,1)
    lower<-round(estimate.CE2012-ppe.err,1)
  }
  if(equation=="bip.phylocor.b") {
    log.estimate<-2.754*log10(FC*sqrt(0.0796/0.0442))-1.097
    estimate.CE2012<-round(10^log.estimate,1)
```

```

ppe.err<-estimate.CE2012*0.2503
upper<-round(estimate.CE2012+ppe.err,1)
lower<-round(estimate.CE2012-ppe.err,1)
}
return(cbind(data,log.estimate,estimate.CE2012,upper,lower))
}

AHR1985<-function(HC,FC,equation,data) {
  if(equation=="quad") {
    estimate.AHR1985<-round(0.078*(HC+FC)^2.73,2)
  }
  if(equation=="bip") {
    estimate.AHR1985<-round(0.16*(FC)^2.73,2)
  }
  return(cbind(data,estimate.AHR1985))
}

CM1992<-function(FC,data) {
  log.estimate<-2.411*log10(FC)-0.065
  estimate.CM1992<-round(10^log.estimate,2)
  return(cbind(data,estimate.CM1992))
}

CF2004<-function(FC,data) {
  log.estimate<-2.738*log10(FC)-3.607
  estimate.CF2004<-round((10^log.estimate)*1000,2)
  return(cbind(data,estimate.CF2004))
}

MCF2004<-function(FC,data) {
  log.estimate<-2.955*log10(FC)-4.166
  estimate.MCF2004<-round((10^log.estimate)*1000,2)
  return(cbind(data,estimate.MCF2004))
}

```

2.6 Tables

Table 2-1. Scaling results between various limb measurements and body mass in extant avians.

	m	m 95% CI	b	b 95% CI	R²	PPE
C _f vs. BM	2.585	2.418 to 2.751	-0.401	-0.623 to -179	0.934	36.7
L _f vs. BM	2.719	2.466 to 2.971	-1.971	-2.43 to -1.512	0.875	49.5
C _t vs. BM	2.754	2.532 to 2.977	-0.458	-0.736 to -0.181	0.911	41.5
L _t vs. BM	2.242	1.912 to 2.572	-1.598	-2.27 to -0.927	0.759	67.4

C_f, femoral circumference; C_t, tibiotarsal circumference; L_f, femoral length; L_t, tibiotarsal length, PPE, mean percent prediction error. Scaling equation in format $y=mx+b$.

Table 2-2. Summary results of regressions shown in Figure 2-2 with mean percent prediction error (PPE) of various estimation equations.

Equation	m	m 95% CI	b	b 95% CI	PPE
Empirical Relationship	2.585	2.419 to 2.752	-0.402	-0.624 to -0.179	36.7
Correction Factor (α)	2.754	-	-0.682	-	45.9
Anderson <i>et al.</i> (1985)	2.73	-	-0.796	-	80.1
Campbell & Marcus (1992)	2.411	-	-0.065	-	34.8
Christiansen & Fariña (2004)	2.738	-	-0.607	-	38.5

Colours follow those used in Figure 2-2. Line equation in format $y=mx+b$.

Table 2-3. Mean proportional differences between the circumference of the humerus and femur in a sample of extant terrestrial tetrapods.

Clade	N	mean C_h/C_f	95% CI
Tetrapoda	255	0.9425**	0.9208 to 0.9642
Mammalia	200	0.9315**	0.9059 to 0.9571
Carnivora	48	1.0109	0.9729 to 1.049
Euarchonta	15	0.9121**	0.8618 to 0.9625
Glires	66	0.8293**	0.7928 to 0.8367
Marsupialia	14	0.8546**	0.7701 to 0.939
Ungulata	41	1.0081	0.9654 to 1.0509
Reptilia	47	0.9677	0.9344 to 1.001
Lissamphibia	8	1.0694	0.8778 to 1.261

** denotes a significant difference from 1 ($p < 0.05$)

N - sample size

C_h - Humeral circumference

C_f - Femoral circumference

Table 2-4. Body mass estimates (in kg) of well-known non-avian bipedal dinosaurs compared to those obtained using volumetric reconstructions.

Taxon	Sp #	C _f	P1997	H1999 ¹	S2001	C2004	This study
Ornithischia							
<i>Fruitadens haagarorum</i>	LACM 115727	19.6	-	0.74	-	0.85	0.75 (0.56–0.94)
<i>Lesothosaurus diagnosticus</i>	BMNH RUB17	43	2.4	-	-	7.3	6.6 (4.9–8.2)
<i>Jeholosaurus shangyuanensis</i>	IVPP V????	50.2	-	-	-	11.2	10 (7.5–12.5)
<i>Gasparinisaura cincosalensis</i>	MUCPv 219	55	13 ²	-	-	14.4	12.9 (6.7–16.1)
<i>Stegoceras validum</i>	UALVP 2	68	-	-	26.7	25.7	23.1 (17.4–28.9)
<i>Hyposilophodon foxi</i>	BMNH R192	70	-	-	-	27.9	25.1 (18.8–31.3)
<i>Homalocephale calathocercos</i>	MPC-D 100/1201	83	-	-	-	44.4	40.1 (30–50.1)
<i>Dryosaurus altus</i>	YPM 1876	138	103	-	104.3 ³	179	162.5 (121–203)
<i>Thescelosaurus neglectus</i>	AMNH 5891	183	-	-	-	387	353 (265–442)
Prosauropoda							
<i>Massospondylus carinatus</i>	BP/1/4934	209	-	-	-	557	510 (382–637)
<i>Plateosaurus engelhardti</i>	MBR 4398	253	-	-	-	939	862 (647–1078)
Theropoda							
<i>Mahakala omnogovae</i>	GI 100/1033	19.9	-	-	-	0.89	0.79 (0.59–0.98)
<i>Velociraptor mongoliensis</i>	MPC-D 100/25	64	11	-	-	21.8	19.6 (14.7–24.5)
<i>Ornithomimus edmontonicus</i>	ROM 851	110	111	-	-	96	87 (65.3–109)
<i>Deinonychus antirrhopus</i>	MCZ 4371	116	-	-	-	111	100 (75.5–126)
<i>Herrerasaurus ischigualastensis</i>	PVL 2566	166	124	64.33	348	294	268 (201–335)
<i>Gallimimus bullatus</i>	GI 100/11	216	438	-	586	609	558 (418–697)
<i>Majungasaurus crenatissimus</i>	FMNH ????	323	-	-	-	1833	1690 (1267–2112)
<i>Carnotaurus sastrei</i>	MACN-CH 894	325	2070	-	-	1864	1719 (1289–2149)
<i>Gigantoraptor erlianensis</i>	LH V0011	349	2000	-	-	2266	2092 (1569–2614)
<i>Albertosaurus sarcophagus</i>	ROM 807	350	2500	-	-	2284	2108 (1581–2635)
<i>Allosaurus fragilis</i>	AMNH 680	381	-	-	-	2881	2663 (1997–3329)
<i>Gorgosaurus libratus</i>	CMN 530	394	2340 ⁴	2795 ⁴	2465 ⁴	3158	2921 (2190–3651)
<i>Suchomimus tenerensis</i>	MNN GDF 500	408	2500	5207	3816	3475	3216 (2412–4020)
<i>Daspletosaurus torosus</i>	AMNH 5438	390	2400	-	-	3071	2840 (2130–3550)
<i>Acrocanthosaurus atokensis</i>	NCSM 14345	426	4400	5672	-	3911	3622 (2716–4527)
<i>Mapusaurus roseae</i>	????	455	-	-	-	4682	4342 (3265–5427)
<i>Giganotosaurus carolinii</i>	MUCPv-CH 1	525	6850	13807	6595	6931	6439 (4829–8049)
<i>Tyrannosaurus rex</i>	CM 9380	534	5700	7908	6651	7261	6748 (5061–8435)
<i>Tyrannotitan chubutensis</i>	MPEF-PV 1156	640	-	-	-	11921	11111 (8333–13888)

Ranges in brackets provide the 25% prediction error range determined in Chapter 1 (CAMPIONE AND EVANS, 2012).

¹ methodology in H1999, but estimates reported in BUTLER *ET AL.* (2009), THERRIEN AND HENDERSON (2007), and HENDERSON AND SNIVELY (2004)

² based on MUCPv-215

³ based on numerous specimens including YPM 1876

⁴ based on AMNH 5458

P1997 - Estimates from PAUL (1997)

H1999 – Estimates from Henderson (1999)

S2001 - Estimates from Seebacher (2001)

C2004 - Estimates based on the femoral circumference to body mass equation of Christiansen
and Fariña (2004)

Table 2-5. Body mass estimates (in kg) of well-known non-avian bipedal dinosaurs compared to those based on other scaling regressions.

Taxon	Sp #	C _f	A1985	C1992	This study
Ornithischia					
<i>Fruitadens haagarorum</i>	LACM 115727	19.6	0.54	1.12	0.75 (0.56–0.94)
<i>Lesothosaurus diagnosticus</i>	BMNH RUB17	43	4.6	7.5	6.6 (4.9–8.2)
<i>Jeholosaurus shangyuanensis</i>	IVPP V????	50.2	7	10.9	10 (7.5–12.5)
<i>Gasparinisaura cincosalensis</i>	MUCPv 219	55	9	13.5	12.9 (6.7–16.1)
<i>Stegoceras validum</i>	UALVP 2	68	16.1	22.6	23.1 (17.4–28.9)
<i>Hyposilophodon foxi</i>	BMNH R192	70	17.4	24.2	25.1 (18.8–31.3)
<i>Homalocephale calathocercos</i>	MPC-D 100/1201	83	27.8	36.5	40.1 (30–50.1)
<i>Dryosaurus altus</i>	YPM 1876	138	111.2	124.2	162.5 (121–203)
<i>Thescelosaurus neglectus</i>	AMNH 5891	183	240.2	245.3	353 (265–442)
Prosauropoda					
<i>Massospondylus carinatus</i>	BP/1/4934	209	345.2	338	510 (382–637)
<i>Plateosaurus engelhardti</i>	HMN MBR 4398	253	581.6	535.7	862 (647–1078)
Theropoda					
<i>Mahakala omnogovae</i>	GI 100/1033	19.9	0.56	1.17	0.79 (0.59–0.98)
<i>Velociraptor mongoliensis</i>	MPC-D 100/25	64	13.7	19.5	19.6 (14.7–24.5)
<i>Ornithomimus edmontonicus</i>	ROM 851	110	59.9	71.9	87 (65.3–109)
<i>Deinonychus antirrhopus</i>	MCZ 4371	116	69.2	81.7	100 (75.5–126)
<i>Herrerasaurus ischigualastensis</i>	PVL 2566	166	182.6	192.5	268 (201–335)
<i>Gallimimus bullatus</i>	GI 100/11	216	377.7	365.9	558 (418–697)
<i>Majungasaurus crenatissimus</i>	FMNH ????	323	1133	965.4	1690 (1267–2112)
<i>Carnotaurus sastrei</i>	MACN-CH 894	325	1152.3	979.8	1719 (1289–2149)
<i>Gigantoraptor erlianensis</i>	LH V0011	349	1400	1163	2092 (1569–2614)
<i>Albertosaurus sarcophagus</i>	ROM 807	350	1411	1172	2108 (1581–2635)
<i>Allosaurus fragilis</i>	AMNH 680	381	1778	1438	2663 (1997–3329)
<i>Gorgosaurus libratus</i>	CMN 530	394	1949	1559	2921 (2190–3651)
<i>Suchomimus tenerensis</i>	MNN GDF 500	408	2144	1696	3216 (2412–4020)
<i>Daspletosaurus torosus</i>	AMNH 5438	390	1896	1521	2840 (2130–3550)
<i>Acrocanthosaurus atokensis</i>	NCSM 14345	426	2412	1882	3622 (2716–4527)
<i>Mapusaurus roseae</i>	????	455	2887	2205	4342 (3265–5427)
<i>Giganotosaurus carolinii</i>	MUCPv-CH 1	525	4267	3114	6439 (4829–8049)
<i>Tyrannosaurus rex</i>	CMN 9380	534	4470	3244	6748 (5061–8435)
<i>Tyrannotitan chubutensis</i>	MPEF-PV 1156	640	7328	5020	11111 (8333–13888)

Ranges in brackets provide the 25% prediction error range determined in Chapter 1 (Campione and Evans, 2012).

A1985 - Estimates based on bipedal equation of Anderson *et al.* (1985)

C1992 - Estimates based on the avian regression of Campbell and Marcus (1992)

Table 2-6. Body mass (in kg) estimates of *Tyrannosaurus rex*.

Specimen	C_f (mm)	Body Mass - $\alpha=1.413$	Body Mass - $\alpha=1.342$
FMNH PR 2081	579	8432 (6324–10540)	7298 (5474–9123)
RSM P2523.8	570	8076 (6057–10095)	6990 (5243–8738)
CM 9380	534	6748 (5061–8435)	5841 (4380–7301)
MOR 555	520	6272 (4704–7840)	5429 (4071–6786)
BHI 3033	505	5786 (4340–7233)	5008 (3756–6260)

C_f - Femoral circumference

Ranges in brackets provide the 25% prediction error range determined in Chapter 1 (Campione and Evans, 2012).

2.7 Figures

Figure 2-1. Mathematical relationship between the circumference and area of a circle. Solid line represents the relationship between the circumference and area of one circle (i.e., a hypothetical biped) and the dashed line represents the relationship between the total circumference and total area of two circles (i.e., a hypothetical quadruped). Alpha (α) represents the correction factor that transforms line A into line B

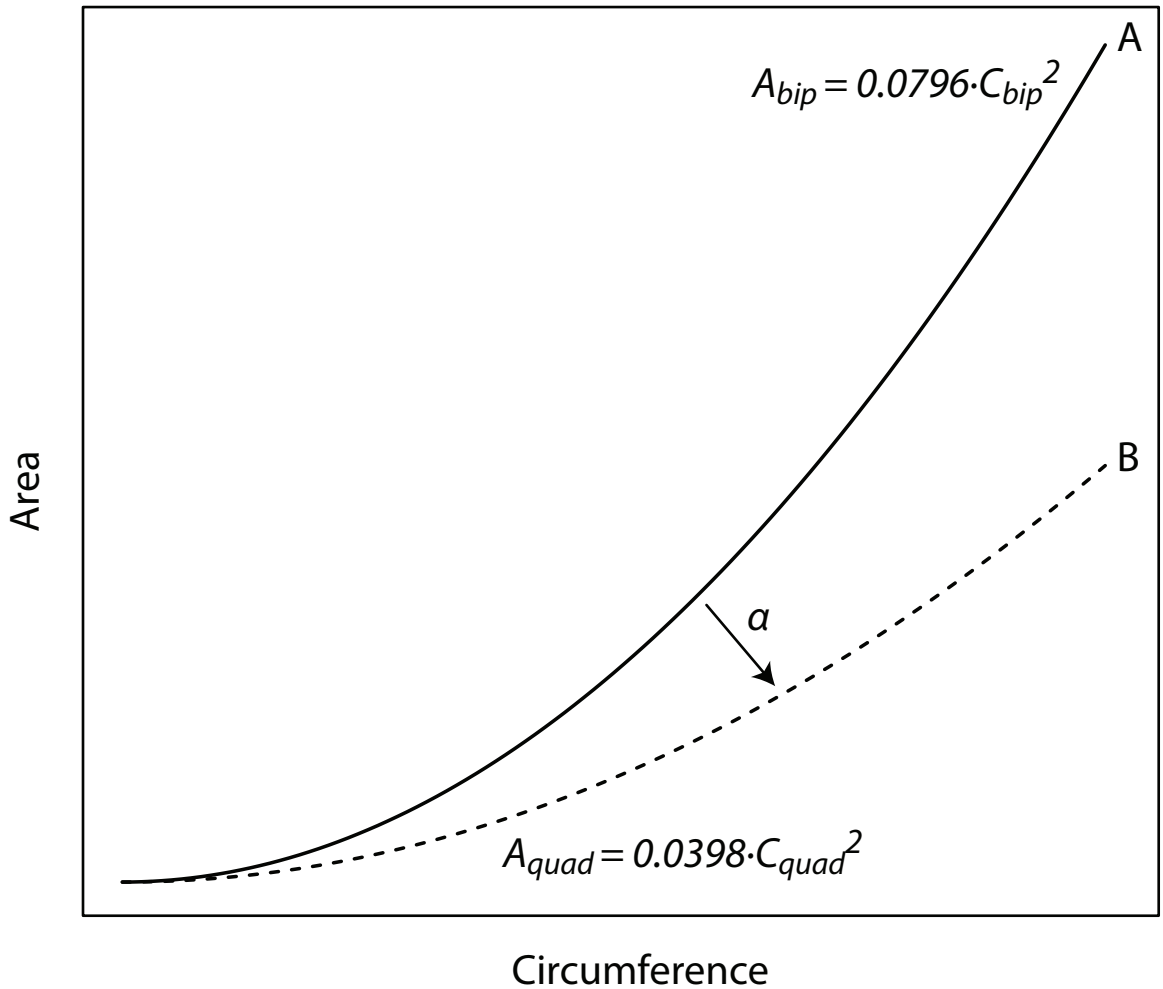


Figure 2-2. Plot of femoral circumference to body mass in a sample of 70 extant birds. Solid black line indicates the true relationship of the avian data (black points). Dashed lines represent the relationship between femoral circumference and estimated body mass based on the correction factor presented here (red) and other published bipedal mass estimation equations.

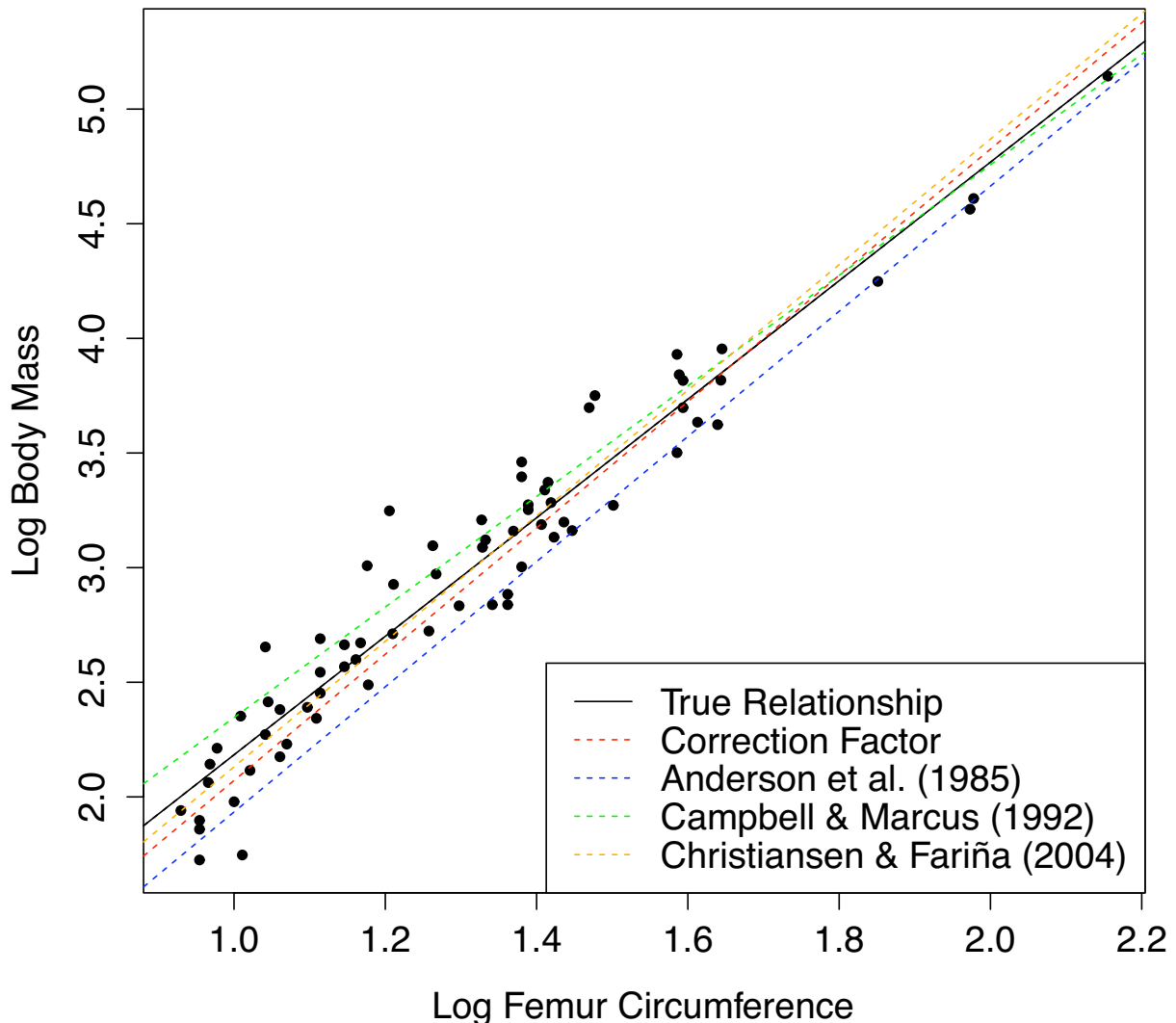
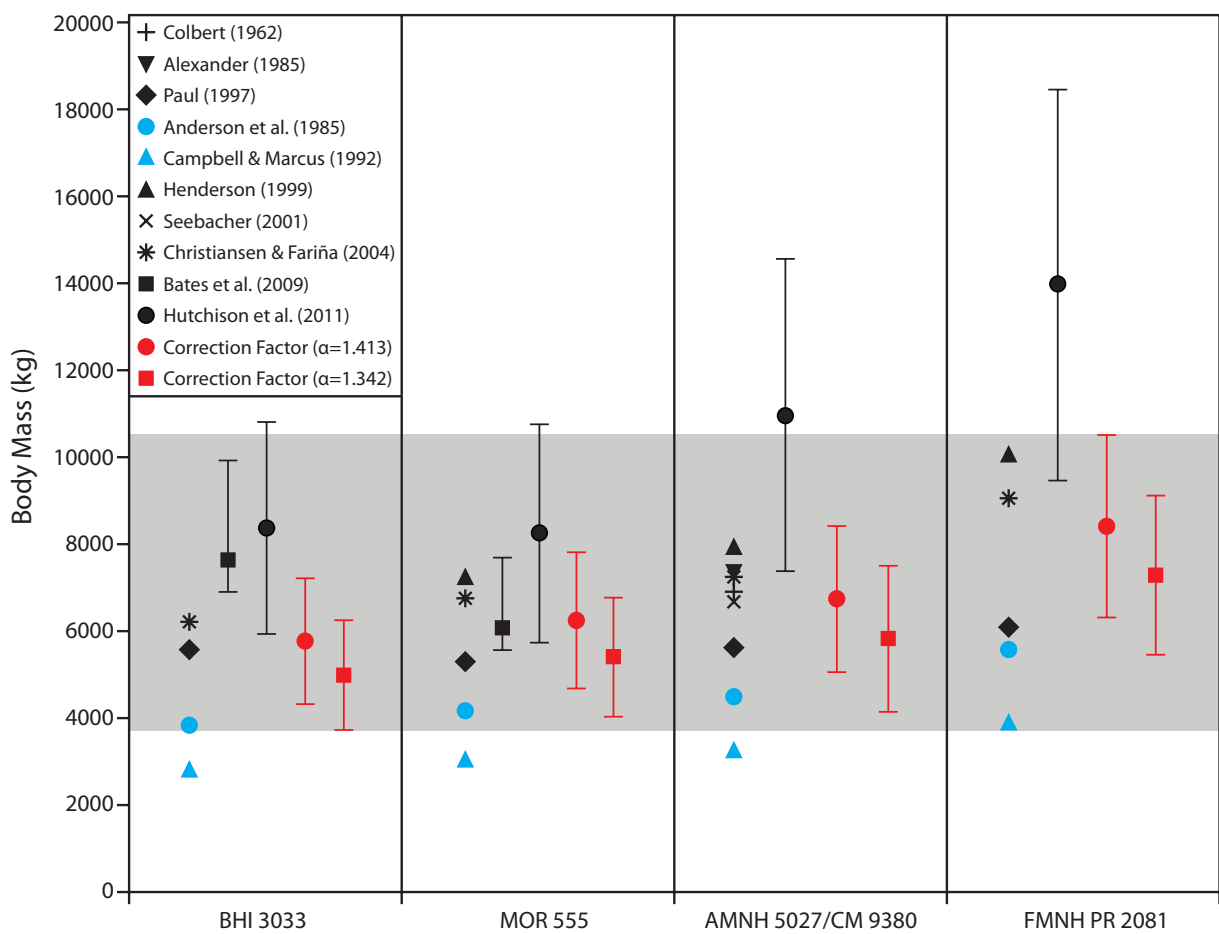


Figure 2-3. Comparison of body mass estimate of four commonly cited specimens of *Tyrannosaurus rex*. Blue symbols represents estimates based on other limb scaling relationships; black symbols represent body mass estimates based on volumetric reconstructions; and the red symbols represent estimates based on the two correction factors of the extant quadrupedal tetrapod equation. Error bars represent the ranges presented by the respective studies, and the grey area represents the total body mass range of *T. rex* based on the results obtained in this study (3756 kg–10540 kg).



Chapter 3

Inferring Body Mass in the Fossil Record: A *Post Hoc* Model for Constraining Volumetric Density Mass Estimates of Non-Avian Dinosaurs

3.1 Abstract

Inferring the body mass of fossil taxa, such as non-avian dinosaurs, provides a powerful tool for interpreting their physiology and ecology and thus the ability to study these within the context of deep time and in association with changing environments. As a result, numerous studies have advanced methods for estimating mass in dinosaurs based on two approaches: volumetric-density (VD) and extant-scaling (ES). The former has received the most attention in non-avian dinosaurs and has changed significantly over the last century; from initial physical scale models to recent 3D virtual techniques that utilize scanned data obtained from museum mounts. In comparison, the ES approach is more commonly used to estimate body masses of extinct members of crown clades, but some equations have been proposed for non-avian dinosaurs. The application of these approaches depends on the research question; biomechanical studies utilize a VD approach, whereas macroevolutionary-scale research utilizes an ES approach. This review chapter summarizes both of these approaches as they apply to non-avian dinosaurs and provides the first quantitative comparison and attempt at corroborating results obtained from both. Results indicate that, in general, mass estimates are consistent between VD and ES approaches. Inconsistencies are recovered in certain dinosaurian clades (Ornithopoda, Thyreophora, and Ceratopsia) along

with an overall tendency of VD approaches to underestimate the body mass of small-bodied taxa relative to those derived through ES. The *post hoc* model advocated here for assessing masses obtained *via* VD approaches permits identification of potential systematic biases in final estimates and will be useful for revising baseline assumptions of future models. This is particularly important given that VD approaches and resulting mass estimates are critical for addressing numerous biological questions in the fossil record, such as those related to biomechanics and physiology. Despite some notable differences between estimates derived from either approach, results indicate strong corroboration between most recent iterations of both ES and VD approaches suggesting that our current understanding of size in dinosaurs, and hence its biological correlates, has greatly improved in recent years.

3.2 Introduction

Determining the body size of extinct terrestrial vertebrates represents one of the most important and useful proxies for studying numerous biological properties in deep time (e.g., Bakker, 1972; Farlow, 1976; Erickson *et al.*, 2001; Laurin, 2004; Gillooly *et al.*, 2006; Finarelli, 2008; Pontzer *et al.*, 2009; Benson *et al.*, 2011; Sookias *et al.*, 2012a; Sookias *et al.*, 2012b). Its utility stems from decades of research in extant taxa where it became evident that body size was related to almost all aspects of organismal biology including physiology (e.g., metabolism, growth, and fecundity) and ecology (e.g., population density, land area, and extinction risk) (e.g., Kleiber, 1947; Hemmingsen, 1960; Jerison, 1969; Peters, 1983; Brown and Maurer, 1986; Brown *et al.*, 1993; Burness *et al.*, 2001; Gillooly *et al.*, 2001; Gillooly *et al.*, 2002; Capellini and Gosling, 2007; McClain and Boyer, 2009). Since body mass (the standard measure of body size) cannot

be directly measured in the fossil record, several studies have proposed methods to estimate body mass from skeletal fossil remains. These methods can be categorized into two approaches that are fundamentally different, both philosophically and methodologically. These include: 1) the Volumetric-Density (VD) approach, which attempts to include the greatest amount of information about the skeleton as possible; and 2) the Extant Scaling (ES) approach, which attempts to integrate empirical knowledge from extant analogues.

Applications of VD and ES approaches are most extensive in studies of non-avian dinosaurs (Colbert, 1962; Alexander, 1985; Anderson *et al.*, 1985; Campbell Jr and Marcus, 1992; Gunga *et al.*, 1995; Christiansen, 1997; Paul, 1997; Christiansen, 1998; Henderson, 1999; Seebacher, 2001; Christiansen and Fariña, 2004; Henderson, 2004; Henderson, 2006; Hutchinson *et al.*, 2007; Gunga *et al.*, 2008; Bates *et al.*, 2009a; Henderson, 2010; Mallison, 2010; Hutchinson *et al.*, 2011; Sellers *et al.*, 2012). Biomechanical and physiological studies interested in reconstructing properties such as locomotion, center of mass, muscle/organ volume, and metabolism most often prefer VD approaches because they integrate a more holistic interpretation of a specimen (Henderson, 2006; Hutchinson *et al.*, 2007; Pontzer *et al.*, 2009; Hutchinson *et al.*, 2011; Mallison, 2011b). In comparison, studies interested in reconstructing large-scale patterns of evolution prefer an ES approach because of its ease for assembling large datasets; however, it should be noted that there are currently no evolutionary studies in non-avian dinosaurs that utilize an extant-based ES approach, opting instead for VD-based regression equations (such as those derived by Christiansen and Fariña, 2004) or skeletal proxies (e.g., femoral length) without estimating body mass (Hone *et al.*, 2005; Carrano, 2006; Turner *et al.*, 2007; Hone *et al.*, 2008; Ősi *et al.*, 2012; Sookias *et al.*, 2012a; Sookias *et al.*, 2012b).

Given recent computational advances and innovations in 3D scanning technologies, VD approaches have received comparatively more attention than ES (but see Campione and Evans, 2012), and the specific methods have drastically shifted (e.g. Colbert, 1962; Hutchinson *et al.*, 2011). Nevertheless, the general principle behind VD approaches has remained constant. In order to estimate mass (M), the VD approach requires: 1) a life reconstruction of the fossil taxon; 2) a method with which to calculate the volume (V) of the reconstruction; and 3) an estimate of body density (D), which through the standard density equation ($D = M/V$), the body mass of an animal can be estimated ($M = D \cdot V$). In comparison, the ES approach does not require a reconstruction but rather utilizes skeletal measurements taken from living animals that are then regressed against body mass in order to derive a predictive equation. Assuming that the estimated animal follows the same scaling pattern as the extant exemplars on which the regression model is based, the resulting predictive equation can be used to estimate body mass. As is evident, both approaches can include a variety of different parameters and can be based on different datasets, both have advantages and disadvantages, both make unavoidable methodological assumptions, and, in many cases, one method may compensate for the shortcomings of the other. These differences have thus resulted in a somewhat dichotomous outlook among some research groups regarding the capacity of these approaches to accurately estimate body mass, with criticisms forwarded against both camps (Carrano, 2001; Gunga *et al.*, 2002; Hutchinson *et al.*, 2011; Campione and Evans, 2012; Sellers *et al.*, 2012). However, both can, and should, be used in tandem in order to better reconstruct the palaeobiology of extinct taxa and ecosystems within the context of deep time.

In this chapter I will: 1) review the various formulations of the VD and ES approaches; 2) discuss the assumptions that are inherent to both, as well as their advantages and disadvantages; and finally 3) in the last section of this review I compile a dataset of mass estimates derived

using VD approaches and quantitatively compare these estimates to the ES standard derived in chapter 1 in an attempt to condense and corroborate the information provided by both approaches.

3.3 Body Mass Inference in the Fossil Record

The various iterations of VD and ES approaches described below represent a compendium of the principal methods used to estimate body masses of non-avian dinosaurs. I focus on this group because, given its popularity in the general public and palaeontological community, non-avian dinosaurs have received a great deal of attention by both VS and ES approaches. However, mass estimation approaches, especially ES, have been extensively applied to extinct mammals (e.g., Romer and Price, 1940; Damuth and MacFadden, 1990; Gingerich, 1990; Fortelius and Kappelman, 1993; Fariña *et al.*, 1998; De Esteban-Trivigno *et al.*, 2008; Rinderknecht and Blanco, 2008; Millien and Bovy, 2010; De Esteban-Trivigno and Köhler, 2011), and non-therapsid synapsids (Romer and Price, 1940; Blob, 2001). The following is meant as a summary of the various methods; however, respective publications should be sought for full details and justifications.

3.3.1 Volumetric-Density Approach

3.3.1.1 Methodologies

The volumetric-density approach is the older of the two approaches. It was employed for the first time over a century ago to estimate the body mass of “*Brontosaurus*” (Gregory, 1905). Given its

long history, various permutations of the approach have been proposed over the last century.

These are summarized in the following section.

3.3.1.1.1 Physical Scale Models

The original VD approaches for estimating body mass were based on the construction of physical scale models, and were first applied by Gregory (1905), who provided the first body mass estimate for a dinosaur. Based on a reconstructed model by Charles M. Knight of *Apatosaurus excelsus* (then “*Brontosaurus*” *excelsus*), the author created plaster replicas, one of which he segmented into several pieces. Based on the Archimedes’ Principle, which states that the volume of fluid displaced by a submerged body will be equal to the volume of the body, Gregory (1905) ascertained the volume of the model by submerging the segments in water. The author initially assumed a density of water (approximately 1 g/cm³) for the body density of *A. excelsus*, and then applied a scaling factor of 16 to obtain a mass of 31 t. Finally, the author added 10% to the mass based on the assumption that *A. excelsus* was aquatic and as a result had a density greater than that of water, for a final mass estimate of 34.1 t.

The method outlined by Gregory (1905) was significantly expanded upon by Colbert (1962) who presented the first dataset of body sizes in non-avian dinosaurs, including exemplars from several parts of the dinosaurian tree (e.g., sauropods, theropods, ornithopods, ceratopsians, and thyreophorans; Figure 3-1). Colbert (1962) also used plaster reconstructions, but unlike Gregory (1905), the models were kept in one piece and submerged in sand, rather than water. The mathematical calculation to determine body mass, was the same as that presented by Gregory (1905), with the main exception that Colbert (1962) did not agree with the assumption that non-avian dinosaurs were more dense than water. Based on measurements taken from a

specimen of *Alligator* and *Heloderma*, Colbert (1962) assumed a body density of 0.9 g/cm³ for non-avian dinosaurs.

The use of Archimedes' Principle for estimating body mass from a scale model was refined by Alexander (1985) using solid, plastic, 1/40 scale models then sold at the British Museum of Natural History. Instead of measuring the volume of the fluid displaced by the scale model, the author used a scale, which at one end was hung the model within a beaker, and at the other a set of weights, which kept the scale at equilibrium (Figure 3-2). The beaker was subsequently filled with water, which decreased the weight of the model. The difference between the weight of the model in water and in air is equal to the volume of the model. This technique is less prone to measurement error as that applied by the previous authors, but still require the use of an assumed body density, which Alexander (1985) assumed to be equal to that of water (i.e., 1 g/cm³).

The most recent applications of physical reconstructions to estimate body mass were by Paul (1997), Christiansen (1997, 1998), and Mazzetta *et al.* (2004). All three created clay models based on either two-dimensional reconstructions (Paul, 1997) or measurements taken from museum mounts (Christiansen, 1998; Mazzetta *et al.*, 2004). The volumes of these models were determined using water displacement methods similar to that used by Gregory (1905), which were then multiplied by a density parameter varying from 0.85 g/cm³ to 0.95 g/cm³. A complete list of body masses obtained using the method of Paul (1997) can be found online (<http://www.gspauldino.com/data.html>).

3.3.1.1.2 Two-Dimensional Models

An alternate method for obtaining the volume of an animal is to reconstruct it in two-dimensions (i.e., an illustration), rather than a full three-dimensional sculpture. Although this method is somewhat simpler than those described in the previous section, it generally assumes a circular or oval cross-sectional shape to the body. Hurlburt (1999) presented the first formulation of this method using a method called Graphic Double Integration (GDI), originally developed by Jerison (1969) to calculate the volume of brain endocasts. This method is based on the notion that the volume of a complex 3-dimensional shape can be modeled as an elliptical cylinder. Two different reconstructed views are needed that are at a right angle to each other (e.g., lateral and dorsal). Transverse measurements are then taken at equal intervals in both views, and the mean of these measurements in each view are then used as the principal axes (a and b) of an ellipse (Figure 3-3). The length of the reconstruction is used as the height (h) of the elliptical cylinder and hence the volume of the model is calculated by using the standard equation for calculating the volume of an elliptical cylinder ($V = \pi \cdot a \cdot b \cdot h$). Jerison (1969) showed that, for his brain endocast dataset, GDI calculated volumes within 5% of that obtained using water displacement methods. Hurlburt (1999) calculated the body volume of *Edaphosaurus boanerges*, a Permian synapsid, by performing separate GDIs for the head, trunk, tail, as well as the proximal and distal portion of the fore- and hind limbs. The volume of each section was added together to obtain the total body volume, and, similar to previous studies, Hurlburt (1999) assumed a body density equal to that of water.

Seebacher (2001) developed a method known as the ‘polynomial’ technique, which, as in the case for GDI, takes length (or depth) measurements at standard intervals along the length of a two-dimensional reconstruction. Unlike GDI this is only done using a lateral view (Figure 3-4).

The depth measurements were then plotted against their position along the length of the body, and the points were fitted using an eighth order polynomial. The polynomial function is then integrated over the length of the body, which provides the volume of a circular body shape. Given that the latter is not a valid assumption in nature, Seebacher (2001) developed a correction factor based on the relationship between body depth and width. As in previous cases, a body density of 1 g/cm³ was assumed in order to convert the volume into a mass.

3.3.1.1.3 Computational/3-Dimensional Models

One of the first attempts to reconstruct a dinosaur in three-dimensions was based on the principle of photogrammetry (Gunga *et al.*, 1995; Gunga *et al.*, 1999; Gunga *et al.*, 2002), recently reviewed by Stoinski *et al.* (2011). The general principle centers around obtaining 2D photographs of museum mounts from two different angles that complement each other and hence, through the use of photogrammetric instruments, create a 3D image (Figure 3-5). Stereophotogrammetric instruments can then be used to convert the 3D depiction of a mount into a series of digital points representing particular regions of the skeleton. This technique can be applied to various portions of the skeleton (i.e., skull, neck, thorax, *etc.*). These points can be inputted into drafting software packages to create a wireframe reconstruction that, depending on the anatomical region, can be modeled as standard geometric shapes (e.g., cylinders, spherical caps, and truncated cones) from which volume can be determined using standard geometric volumetric equations. This method was applied extensively by German research groups interested in the size, and correlated physiological attributes, of *Giraffatitan* (=*Brachiosaurus brancai*, *Dicraeosaurus hansmanni*, and *Diplodocus carnegiei* (Gunga *et al.*, 1995; Gunga *et al.*, 1999; Wiedemann *et al.*, 1999; Gunga *et al.*, 2002).

An alternate method for constructing three-dimensional volumetric reconstructions from two-dimensional images of an animal was presented by Henderson (1999). The basis, with some variation, is essentially a computational translation of the two-dimensional method presented by Jerison (1969) and Seebacher (2001). Three-dimensional computational reconstructions are derived from two-dimensional reconstructions of lateral and dorsal views of an animal. These views are organized on a three-dimensional Cartesian grid (x-, y-, and z-axes). The outlines are then sliced into segments. The intersection between the slices

and the outline of the reconstruction represent a set of coordinates that can be inputted into a drafting software package. The distances between the x-y and x-z coordinates represent the main-axes of a series of ellipses along the body that correspond to the initial slices. Taken together, sets of adjacent slices form a series of three-dimensional ‘slabs’ (Figure 3-6). Using linear algebra and integration techniques [see Henderson (1999) for full details], the volume of each slab is calculated, and the total volume is therefore the sum of the slab volumes. The volume of the limbs, horns, frills, and plates, were estimated separately using the same method. Body density was assumed to be 1 g/cm³ for all dinosaurs, however, in the case of *Triceratops*, Henderson (1999) assumed a density of 1.7 g/cm³ for the horns and frill based on extant comparisons. In addition, the volume of the lungs was assumed to be 10% of the thoracic cavity.

In the last decade, with technological advances in three-dimensional scanning and 3D imaging software, computational methods need not be based on two-dimensional reconstructions, but can be obtained via complete 3D scans of museum mounts (Gunga *et al.*, 2007; Gunga *et al.*, 2008; Bates *et al.*, 2009b; Bates *et al.*, 2009a; Mallison, 2010, 2011a, b; Stoinski *et al.*, 2011; Sellers *et al.*, 2012). This methodology can rapidly (less than 24 hours) portray a full-size virtual 3D skeleton that can be imported into a drafting software package,

where the body outline can be created and volumes calculated. Scans can be obtained by various instruments [e.g., surface scanners: Mensi S25: (Gunga *et al.*, 2007; Gunga *et al.*, 2008) and RIEGL LMS-Z420i: (Bates *et al.*, 2009a; Hutchinson *et al.*, 2011), or CT Scanners: (Mallison, 2010; Hutchinson *et al.*, 2011)], but the general principle is the same (for details regarding how these scanners are used see Bates *et al.*, 2009a; Mallison, 2010; Stoinski *et al.*, 2011). Scans are taken of museum mounts from various positions around the skeleton, the number and actual position of which will depend on the complex nature of the skeleton. These scans can produce virtual images that are accurate to the sub-centimeter scale (e.g., Gunga *et al.*, 2007; Bates *et al.*, 2009a; Stoinski *et al.*, 2011). The resulting scan is in actuality a series of points in virtual 3D space that combine to create a point cloud representing the different scans taken from the skeleton. The cloud can be manipulated and condensed by various program (e.g., PolyWorks; Bates *et al.*, 2009a) where they are stitched together for form a single virtual depiction of the mounted skeleton. Once in virtual space, the scan can either be treated as a single entity or subdivided into various body segments (e.g., skull, thorax, tail, *etc.*). This segmentation technique is commonly used in VD approaches in order to reduce complex body outlines into simpler shapes, but more importantly, in order to determine the mass properties of particular anatomical regions, and their relative proportions (Gunga *et al.*, 1995; Gunga *et al.*, 1999; Henderson, 1999; Gunga *et al.*, 2002; Gunga *et al.*, 2007; Gunga *et al.*, 2008; Bates *et al.*, 2009a; Mallison, 2010; Hutchinson *et al.*, 2011). Modeling the body outline is performed by various drafting packages (e.g., AutoCad and Maya) and although original studies modeled outlines based on a series of rotational solids for distinct regions along the body (e.g., Gunga *et al.*, 2007), recent studies advocate the use of non-uniform rational B (Bézier)-splines (NURBs) (Gunga *et al.*, 2008; Bates *et al.*, 2009a; Stoinski *et al.*, 2011), which represent a mathematical model that incorporate information from two-dimensional objects (e.g., lines, circles, and arcs) to

create a three-dimensional object. These are easily manipulated by most CAD packages to create a body outline of a full-scale skeleton from which a volume can be calculated. As is the case for all VD approaches, an estimate of density is still required, which, in the studies cited above, ranges from 0.8 to 1 g/cm³.

Sellers *et al.* (2012) presented the most recent application of the VD approach, building upon original work done using LiDAR scanning techniques (Bates *et al.*, 2009b; Bates *et al.*, 2009a) described above. However, the authors provide a novel approach, which incorporates a better understanding of modeling within the context of extant taxa. The methodological foundation incorporates the original scan data obtained from a mount (i.e., the point cloud), but instead of reconstructing the body outline based on assumptions of soft-tissue, the authors separate the scan into various anatomical segments for which a three-dimensional body outline is determined by calculating minimum convex hulls (MCH) between the points in the cloud (Figure 3-7). As MCHs are derived from the skeletal data they are much more objective than traditional reconstruction techniques that attempt to reconstruct the body shape. Through the use of CAD software, the volume of the resultant MCHs is calculated and then multiplied by an assumed body density to obtain a mass estimate. It is obvious that a body mass determined via a minimum convex hull of a skeleton will always underestimate the true mass, as it will not model the full extent of muscles, and other soft-tissues. As a result, Sellers *et al.* (2012) applied this methodology to a suite of large-bodied extant mammals that ranged from approximately 90 kg to 3,000 kg, and compared masses determined via the MCH method against estimates obtained from the literature of extant exemplars. This allowed the authors to conclude that the MCH method consistently underestimated the body mass of their extant sample by approximately 20%, a figure that could be applied to MCHs derived from skeletons of extinct taxa, such as non-avian dinosaurs.

3.3.1.2 Methodological Assumptions

The various permutations of the VD approach, with the partial exception of the Sellers *et al.* (2012) MCH model, make two important assumptions: 1) they require the creation of a body outline to calculate the body volume, and 2) in order to convert a volume to a mass, they require an estimate of body density. Both assumptions are in general unavoidable but have an appreciable effect on the final mass estimate. A case example can be portrayed by body mass estimates presented by the same German research group between 1995 and 2008 for the *Giraffatitan brancai* specimen mounted at the Humboldt Museum in Berlin, Germany. Originally, Gunga *et al.* (1995) presented a body mass of 74.4 tonnes based on photogrammetric techniques, which modeled the body outlines as a series of standard shapes (e.g., truncated cones and cylinders), and an assumed body density of 1 g/cm³. In contrast, later estimates (Gunga *et al.*, 2008) incorporated lower estimates of body density (0.8 g/cm³) and a more carefully modeled the body outline based on NURBs, to obtain a final mass estimate of 38 tonnes, an almost 50% difference from the original estimate. This case study by no means reflects inaptitude on the part of earlier studies, but rather reflects changes in how palaeontologists interpret certain biological and anatomical properties in fossil taxa (e.g., skeletal pneumaticity; Wedel, 2003), as well as technological and computational improvements. That being said, recent mass estimates will be biased by current palaeobiological paradigms that will likely be modified and refined in the future. That is not to say that the VD approach should be abandoned, in fact it presently represents the most robust technique with which to test functional (e.g., locomotion and defense) and physiological (e.g., metabolism, body temperature, organ size, and circulation) hypotheses in the fossil record and hence the opportunity to study these within the context of deep time and changing Earth systems (Christiansen, 1997, 1998; Gunga *et al.*, 1999; Henderson,

2004; Henderson and Snively, 2004; Henderson, 2006; Gunga *et al.*, 2007; Hutchinson *et al.*, 2007; Gunga *et al.*, 2008; Franz *et al.*, 2009; Pontzer *et al.*, 2009; Henderson, 2010; Mallison, 2010; Hutchinson *et al.*, 2011; Mallison, 2011a, c, b; Henderson, in press). Given these implications, it is important to recognize the limitations of VD approaches and if possible constrain them *via* an external and preferentially empirical dataset.

3.3.2 Extant Scaling Approach

3.3.2.1 Methodologies

Extant scaling approaches are universally applied to estimate body mass in extinct members of crown clades, such as Mammalia and Aves (Greenewalt, 1975; Campbell Jr and Tonni, 1983; Damuth and MacFadden, 1990; Gingerich, 1990; Campbell Jr and Marcus, 1992; Finarelli and Flynn, 2006; Butler and Goswami, 2008; De Esteban-Trivigno *et al.*, 2008; Hone *et al.*, 2008; Rinderknecht and Blanco, 2008; Millien and Bovy, 2010; De Esteban-Trivigno and Köhler, 2011). These studies use various standard measurements regressed against body mass, including teeth measurements, skull length, total body length, and various appendicular measurements analyzed either within a bivariate or multivariate framework. Dental and cranial characters, however, can be highly variable, especially when considering a wide phylogenetic range, and can lead to errors in final mass estimates if interspecific scaling patterns are not properly assessed (Damuth and MacFadden, 1990; Millien, 2008; Rinderknecht and Blanco, 2008; Millien and Bovy, 2010). In contrast, limb measurements play a key role in weight-support and are therefore more often regarded to better represent mass. Among limb bones, the proximal elements are found to correlate most strongly with body mass (Damuth and MacFadden, 1990; Chapters 1 and

2). Here, I will only describe ES approaches as they relate to non-avian dinosaurs, but these methods have clear implications for estimating body mass in other extinct terrestrial vertebrates.

3.3.2.1.1 Limb Circumference to Body Mass Equations

Despite the large amount of literature on ES approaches for estimating body mass in extinct members of crown clades (see references in previous chapter), only three ES approaches have been proposed for estimating body mass in non-avian dinosaurs. The first was advanced by Anderson *et al.* (1985), who proposed a regression equation between the combined humeral and femoral circumference ($C_H + C_F$) and body mass in a sample of 33 extant mammals (ranging from 0.47 kg to 5,900 kg) as a model for predicting body mass in non-avian dinosaurs (Figure 3-8). They forwarded two equations, one intended for quadrupeds based on the raw results from the extant mammal regression:

$$BM = 0.078 \cdot C_{\text{humerus+femur}}^{2.73} \quad \text{EQ 3.1}$$

and another intended for bipeds, which assumed a constant scaling coefficient between bipeds and quadrupeds, where the intercept (or proportional constant) was adjusted based on the femoral circumference and body mass derived from a life-size reconstruction of *Troodon inequalis*. This model was estimated at 41.9 kg based on water displacement methods and an assumed density of 0.9 g/cm³.

$$BM = 0.16 \cdot C_{\text{femur}}^{2.73} \quad \text{EQ 3.2}$$

The publication by Anderson *et al.* (1985) remains one of the most highly cited papers in dinosaur biology (over 200 times according to scholar.google.com; including 12 in 2012, for an average of 14 times/annum). Despite its critics (see Chapter 1; Campione and Evans, 2012) it

remains one of the simplest and most robust methods with which to estimate body mass in a large sample of non-avian dinosaurs, and as indicated by results in Chapter 1 (Campione and Evans, 2012), **EQ 3.1** can likely be extended to all terrestrial quadrupedal tetrapods (see Chapter 2, for an empirical test of **EQ 3.2**).

In an attempt to provide an entirely empirically based equation for estimating the body mass of extinct bipeds (namely extinct birds), Campbell and Marcus (1992) published an equation based on the femoral circumference to body mass relationship in extant birds. They presented two equations, one based on an extensive specimen dataset ($N=795$):

$$\log_{10}BM = 2.411 \cdot \log_{10}C_{femur} - 0.065 \quad \text{EQ 3.3}$$

and another based on a pruned dataset in which each species was represented by one datapoint that represented its mean, weighted relative to its sample size ($N=391$):

$$\log_{10}BM = 2.414 \cdot \log_{10}C_{femur} - 0.069 \quad \text{EQ 3.4}$$

Given the low scaling coefficients exhibited in **EQ 3.3** and **EQ 3.4** these equations result in remarkably lower body mass estimates for large-bodied non-avian bipedal dinosaurs, such as for *Tyrannosaurus rex* at 3,244 kg, compared to more traditional estimates at 6,000 kg (e.g., Paul, 1997; Henderson, 1999; Seebacher, 2001; Bates *et al.*, 2009a).

Most recently, Campione and Evans (2012; Chapter 1) revisited the scaling model developed by Anderson *et al.* (1985) between combined stylopodial circumference and body mass. The authors note that, although the model has been criticized on numerous occasions, several major criticisms had yet to be tested. The criticisms were tested within the context of a large limb measurement dataset of terrestrial quadrupeds (200 mammals and 47 reptiles), the

body mass of which was measured prior to death or skeletonization. Campione and Evans (2012) found that differences between extant quadrupeds, whether due to gait, limb posture, and/or phylogenetic history, affected scaling relationships between stylopodial length and body mass or proportional scaling patterns (i.e., length vs. circumference). However, the relationship between stylopodial circumference and body mass was highly conserved, despite gait-, posture-, or phylogenetic-related differences. The relationship was particularly conserved when humeral and femoral circumferences were combined, thereby rejecting all major criticisms forwarded against Anderson *et al.*'s (1985) model. The updated equations provide a rapid, robust, and consistent method for estimating body mass in a wide range of terrestrial quadrupeds:

$$\log_{10} BM_{quad} = 2.754 \cdot \log_{10} C_{humerus+femur} - 1.097 \quad \text{EQ 3.5}$$

EQ 3.5 formed the basis for deriving the first objective, non-avian-based, equation for estimating body mass in extinct bipeds (Chapter 2):

$$\log BM_{bip} = 2.754 \cdot \log C_{femur} - 0.947 \quad \text{EQ 3.6}$$

EQ 3.6 is based on the assumption that the scaling coefficient between circumference and body mass in quadrupeds and bipeds is consistent, requiring only the intercept to be shifted to correspond the arithmetic difference between measuring both stylopodial elements in a quadruped, compared to only the femur in a biped.

3.3.2.1.2 Limb Dimension to VD Estimate Equations

Christiansen and Fariña (2004) and Mazzetta *et al.* (2004) recently attempted to reconcile the differences between VD and ES approaches by presenting a suite of regression equations derived from various hind limb measurements in a sample of 16 non-avian theropods (Christiansen and

Fariña, 2004) and 13 sauropods (Mazzetta *et al.*, 2004). Measurements in both studies include the length, circumference (or perimeter), and diameters of the femur, tibia, and fibula. These measurements were regressed against body mass estimates obtained from physical VD models (Christiansen, 1997, 1998) to generate various equations derived by both bivariate and multivariate techniques that could be used to estimate body mass in a large sample of taxa known from limited material and thus be applied to macroevolutionary-scale studies (e.g., Turner *et al.*, 2007).

3.3.2.2 Assumptions

Extant scaling approaches make one important assumption: the relationship between a skeletal measurement (e.g., femoral circumference) and body mass is assumed to be consistent between the extant taxa used to generate the model and the extinct taxa for which a body mass estimate is desired. Ideally, a proxy for body mass should be intimately related to weight-support. For this reason, limb measurements, and in particular proximal limb bone measurements (e.g., humerus/femur) are generally recognized as a better representation of size than other measurements (e.g., from teeth or crania; see Damuth and MacFadden, 1990 and chapters therein).

The assumption of scaling consistency between extant and extinct taxa can never be tested in the fossil record as true body mass cannot be determined. As a result, this presents an important limitation for the application of ES approaches to fossil taxa that are outside extant clades, and the main reason that these approaches are most prevalent for estimating body mass in extinct members of crown clades. However, a comprehensive analysis comparing particular scaling patterns among phylogenetically, morphologically, and behaviourally different extant groups can indicate whether a particular scaling pattern is robust to these differences, and

therefore applicable to a wide range of extinct morphologies, and assumed behaviours. Given the highly variable nature of the skeleton through the evolutionary history of terrestrial vertebrates it is unlikely that numerous proxies will be found that transcend these differences. However, a better understanding of interspecific scaling in the vertebrate skeleton [such as those conducted on limb scaling (Campbell Jr and Marcus, 1992; Christiansen, 1999b; Carrano, 2001; Chapter 1; Campione and Evans, 2012; Doube *et al.*, 2012)] can, at the very least, identify the strength of proxies and potential sources of error when applying ES approaches to extinct taxa outside of crown clades, such as non-avian dinosaurs.

3.3.3 Advantages and Limitations of VD and ES Approaches

Volumetric-density approaches presently represent the most robust technique with which to address biological hypotheses related to functional (e.g., locomotion and defense) and physiological (e.g., metabolism, body temperature, organ size, and circulation) properties in fossil record (Christiansen, 1997, 1998; Gunga *et al.*, 1999; Henderson, 2004; Henderson and Snively, 2004; Henderson, 2006; Gunga *et al.*, 2007; Hutchinson *et al.*, 2007; Gunga *et al.*, 2008; Franz *et al.*, 2009; Pontzer *et al.*, 2009; Henderson, 2010; Mallison, 2010; Hutchinson *et al.*, 2011; Mallison, 2011a, c, b; Henderson, in press). In terms of body mass estimation, however, the main advantage of VD approaches is that they present a more holistic approach by incorporating information about the entire skeleton, rather than particular skeletal measurements (as in ES approaches). In general, ES approaches incorporate a select few measurements that can lead to biased results, if the main assumption of ES approaches is not met (see Section 3.3.2.2); such issues have been extensively debated in the palaeomammalogy literature with regards to the advantages and disadvantages of teeth, limbs, and cranial measurements as size proxies (see also Damuth and MacFadden, 1990 and several chapters therein; Fariña *et al.*, 1998; Millien, 2008;

Rinderknecht and Blanco, 2008'; Millien and Bovy, 2010). However, a holistic approach also presents one of the biggest limitations of VD approaches and an integral advantage of ES approaches. Skeletons of non-avian dinosaurs, and likely all extinct vertebrates, are in general incomplete (Benton, 2008; Mannion and Upchurch, 2010; Brown *et al.*, 2013b), which increases the amount of subjectivity required to create a reconstruction. As a result, robust (well-defined) VD models can only be built for a select few taxa. This limitation, compounded with the time consuming nature of VD methodologies preclude its application to large-scale macroevolutionary studies. To date, only a single large-scale study of body size in the fossil record is based on estimates from VD approaches (Codron *et al.*, 2012b) and its dataset was heavily criticized for its biased taxonomic representation (Brown *et al.*, 2012b).

Nevertheless, given a complete skeletal specimen, VD approaches should provide more precise estimates of body mass, which idealistically report tighter error ranges than those provided by ES approaches. The incorporation of error ranges to mass estimates derived from VD approaches is time consuming and can be somewhat arbitrary (e.g., Gunga *et al.*, 2007; Bates *et al.*, 2009a), however, some studies have attempted to account for the sensitivity of volumetric calculations to differences in assumed lung volume (and air sacs) to better approximate error ranges associated with VD mass estimate (Henderson, 1999; Hutchinson *et al.*, 2007). Unfortunately, at present, these ranges are as wide, if not wider than those recovered from ES approaches (e.g., Figure 2-3) and therefore greatly reduce their statistical power to identify significant patterns in subsequent biological interpretations. Nevertheless, 3D scanning techniques revealed some of the lowest errors (see results) and are likely to produce some of the better mass estimate result, and given that they are constructed in virtual space represent the best method of producing a precise estimate that have the potential to take various sources of error (body volume/density) into account and test their effects on resultant estimates.

In comparison, ES approaches offer a more rapid, and generally, more consistent method with which to estimate body mass. As a result, they are more practical for reconstructing large-scale patterns in the evolution of body size (Laurin, 2004; Carrano, 2006; Finarelli and Flynn, 2006; Turner *et al.*, 2007; Hone *et al.*, 2008; Sookias *et al.*, 2012a; Sookias *et al.*, 2012b), and by extension, offer the ability to study its physiological and ecological correlates on a macroevolutionary scale and within the context of deep time and changing environments (e.g., Smith *et al.*, 2010; Sookias *et al.*, 2012a).

3.4 A Post Hoc Assessment of VD-Approaches

By definition the reconstruction of an extinct animal, which is known from taphonomically biased material, is subjective (with the partial exception of Sellers *et al.*, 2012); and although a reconstruction can be conservatively rooted by scientific data it still necessitates various assumptions to be made with regards to soft tissue reconstruction (i.e., muscle volume and organ size) and body density (i.e., lung size and relative body pneumaticity). The variation of these qualities, and how they are related to body size remains poorly understood, however, certain studies have shown that the proportions of mass appropriated by different tissues (e.g., skin, bone, and muscle) can vary significantly between mammals of constant body mass, especially for muscles linked to specific locomotor patterns (Grand, 1990). Furthermore, studies that have calculated the body density of extant taxa indicate that this property may vary wildly, especially among taxa with highly pneumatic bodies (Colbert, 1962; Hazlehurst and Rayner, 1992; Hurlburt, 1999). The relative effect of pneumaticity on overall body density is particularly important for applications of VD approaches to saurischian dinosaurs given that recent studies

conclude weak, but significant trends towards increases in pneumaticity relative to size (Benson *et al.*, 2011). Nevertheless, both body proportion and density undoubtedly varied in extinct taxa, and it cannot be presumed that these assumptions will introduce an insignificant amount of error to final VD estimates. Given the uncertainty related to building a reconstruction, it is important that volumetric reconstructions be constrained by a baseline dataset that can assess the validity of the mass estimate, and hence the “realism” of the reconstruction.

Traditionally, volumetric approaches were validated via two approaches. The most common “validation” approach is based on applying a particular reconstruction method to a suite of extant animals (Paul, 1997; Henderson, 1999; Seebacher, 2001; Gunga *et al.*, 2007; Bates *et al.*, 2009a). The derived extant mass is then compared to either actual mass (generally not available) or published averages for the particular species and if both masses approximate each other the VD technique is considered validated. As explained in section 3.3.1 all volumetric reconstruction methods comprise a three stage process comprising of the initial creation of a model (i.e., a physical sculpture or 2D/3D reconstruction), followed by the calculation of its volume, whether by traditional water displacement or modern 3D computational techniques, and finally the standard density equation ($M=D \cdot V$). When this technique is applied to an extant animal, its reconstruction is not based on assumptions of soft tissue structures and density but rather actual knowledge of these taxa. As a result, the validation process outlined by previous studies (e.g., Paul, 1997; Henderson, 1999; Seebacher, 2001; Bates *et al.*, 2009a; Stoinski *et al.*, 2011) does not validate the soft tissue and body density assumptions made for an extinct animal, but rather tests the capacity of a particular method to calculate the volume of a complex shape (sometimes including parameters related to zero volume structures, such as lungs and air sacs). In particular, when a VD approach is applied to an extant representative, its validity can only be

assumed to be true for that individual (and perhaps species) and does not constitute a true test of a model's ability to estimate body mass in extinct taxa.

The second approach is based on an *a posteriori* estimation of organ size (Gunga *et al.*, 1995; Gunga *et al.*, 2007; Gunga *et al.*, 2008; Stoinski *et al.*, 2011). The absolute sizes of organs are estimated by various body mass to organ mass regression equations derived from extant taxa and based on the VD mass estimate of the specimen. Validation is considered when organs fit “realistically” within the thoracic cavity. For example, this technique led to the tentative rejection of the “robust” model for *Plateosaurus* (Stoinski *et al.*, 2011). Although this validation technique relies on organ scaling equations for which intertaxic variation has not been well established in extant systems (Calder, 1996; Franz *et al.*, 2009), and in many cases extrapolate organ size far beyond those on which they were derived, it is perhaps a useful technique with which to test assumptions of thoracic volume. However, this methodology would be better suited *a priori* and used to build the initial body shape. Finally, this validation process applies only to the thorax, and cannot be used for other body segments (e.g., the neck and tail).

Given the nature of the fossil record, the actual proportions of soft tissue and body density will never be known, and therefore the assumptions required to create a reconstruction are virtually impossible to confirm. As a result, errors related to density and soft-tissue proportions require separate validation based on extant comparisons. For instance, these properties could be measured in a large sample of phylogenetically and morphologically distinct extant taxa (i.e., Mammalia and Reptilia) to better understand the nature and magnitude of their variation; thus permitting a better understanding of the error associated with such assumptions when applied to the fossil record. Unfortunately, the methods used to calculate such properties are time consuming and potentially invasive to extant taxa and hence operationally prohibitive

for large datasets. Alternatively, rather than attempting to constrain these assumptions, the final body mass estimates themselves could be constrained via an independent skeletal proxy.

The use of an independent proxy to test volumetric estimates was first presented by Motani (2001), who used a similar VD approach to that of Henderson (1999) to estimate the body mass of marine reptiles. In order to test his estimates the author used the measurement of fork length (measured from the tip of the snout to the middle of the fluke), which he showed to be strongly associated with body mass in extant cetaceans. Using this method, Motani (2001) was able to show that his estimates occurred within the 95% prediction intervals provided by extant cetaceans, compared to those mass estimates presented by other studies that fell outside of these intervals. Given the highly conserved relationship between combined humeral and femoral circumference and body mass in extant quadrupeds (Chapter 1; Campione and Evans, 2012) and the correction factor developed in chapter 2, I will apply a similar technique to that of Motani (2001) to test the body mass estimates obtained from volumetric reconstructions of non-avian dinosaurs (e.g., Colbert, 1962; Paul, 1997; Henderson, 1999; Seebacher, 2001; Gunga *et al.*, 2008; Bates *et al.*, 2009a; Hutchinson *et al.*, 2011). As terrestrial tetrapods, non-avian dinosaurs are expected to follow the universal combined stylopodial circumference to body mass pattern obtained in chapter 1 (Campione and Evans, 2012) and, therefore, I would predict that given a measurement of total stylopodial circumference a body mass generated by a VD approach should occur within the conservative 95% prediction intervals of the extant dataset (in log space), and on average within the 25% mean percent prediction error range (non-log space).

3.4.1 Methods

In order to test the validity of body masses generated by VD approaches I amassed a dataset of humeral and femoral circumferences for specimens that were estimated via various volumetric

reconstructions (Appendix 4). The dataset constitutes 214 entries (many based on the same specimens) from multiple studies (Gregory, 1905; Janensch, 1935; Colbert, 1962; Alexander, 1985, 1989; Christiansen, 1997; Paul, 1997; Christiansen, 1998; Paul, 1998; Christian *et al.*, 1999; Henderson, 1999; Wiedemann *et al.*, 1999; Seebacher, 2001; Gunga *et al.*, 2002; Henderson, 2003; Henderson, 2004; Mazzetta *et al.*, 2004; Henderson, 2006; Gunga *et al.*, 2007; Hutchinson *et al.*, 2007; Therrien and Henderson, 2007; Gunga *et al.*, 2008; Bates *et al.*, 2009a; Butler *et al.*, 2009; Mallison, 2010; Hutchinson *et al.*, 2011; Sellers *et al.*, 2012). This list is not meant to represent all studies that have provided mass estimates based on VD approaches but instead represents an extensive sample of the various methods reviewed in section 3.3.1. For the majority of entries the femoral and humeral circumference measurements were taken from the same specimen on which the reconstruction was based (either taken by myself or from the literature). Measurements could not be obtained for 61 of these specimens, and therefore limb measurements correspond to another specimen (of the same or closely related species) of equivalent size. For example, CM 84 is often used to generate reconstructions and mass estimates of *Diplodocus carnegii* (e.g., Christiansen, 1997; Paul, 1997; Henderson, 1999; Seebacher, 2001). Unfortunately, the humerus of that specimen is reconstructed and therefore cannot be used in the analyses outlined above. As a result, I used the limb measurements of AMNH 6341, *Barosaurus lentus*, a closely related taxon (Wilson and Upchurch, 2009) that has a femur length within 10% the length of CM 84. All analyses were run with and without the 61 models (referred to a ‘Perfect Match’) for which the exact limb measurements could not be obtained to detect if error associated with these inconsistencies affect final interpretations.

Dinosaur measurements (log transformed) were plotted against VD masses on the plot of combined humeral and femoral circumference of chapter 1 (Campione and Evans, 2012). The non-phylogenetically corrected (**EQ 1.1**) and phylogenetically corrected (**EQ 1.2**) equations

presented in chapter 1 (Campione and Evans, 2012) are very similar to each other, and given that the data from non-avian dinosaurs are not corrected within the context of EQ2, comparisons made here use the raw, non-phylogenetically corrected equation and plot (Figure 1-4A). Circumference data of quadrupedal taxa are plotted in their raw form, but in order to visualize the bipedal taxa onto the same plot, circumference measurements were modified using the correction factor derived in chapter 2. The error related to the approaches was calculated using two metrics: 1) residuals, calculated as the difference between the log-model mass derived from the VD approaches and the log predicted mass derived by **EQ 1.1**, and 2) percent prediction error (PPE), which provides a measure of error (generally in absolute terms) of the actual, rather than log transformed body mass. In this chapter PPE is calculated as:

$$PPE = \left(\frac{BM_{VD} - BM_{ES}}{BM_{ES}} \right) \times 100 \quad \text{EQ 3.7}$$

Errors were compared both at a taxonomic level, subdivided by major higher-clade groupings: Ankylosauria, Ceratopsia, Ornithopoda, Pachycephalosauria, Prosauropoda, Sauropoda, Stegosauria, and Theropoda, and a methodological level, which surmise the main applications of VD approaches: minimum convex hull (MCH), photogrammetry, physical scale models, polynomial, 3D scanning, and Slicing. In order to test for systematic errors in VD estimates, errors (both residual and PPE) were plotted against: 1) size, in this case measured as the combined stylopodial circumference for quadrupeds and femora circumference for bipeds, and 2) year of reconstruction publication to test the hypothesis that, given technological advances over the last few decades, errors in estimates of body mass based on VD approaches have decreased through time. All data were complied in Excel, and plots/analyses were completed in R (R Development Core Team, 2012).

3.4.2 Results

Comparisons between the complete sample (N=214) and the perfect-match sample (N=153) reveal little to no differences (Table 3-1), suggesting that these inconsistencies do not alter overall patterns. As a result, comparisons and interpretations are henceforth based on the complete dataset, which provides a greater level of statistical power. Inclusion of non-avian dinosaur VD mass estimates onto the plot of combined stylopodial circumference to body mass in extant quadrupedal vertebrates (Figure 1-4) reveals a general pattern of consistency between stylopodial circumference measurements and VD mass estimates (e.g., Figure 3-9). Of the 214 VD mass estimates tested here, 152 (approximately 71%) fall within the conservative 95% prediction intervals. However, the overall mean residual ($\mu_{\text{res}} \approx -0.102$) is significantly below the expected value of zero ($t = -5.565$, $p < 0.0001$; Table 3-1) indicating an overall underestimation of VD mass estimates given their stylopodial circumference. In addition, mean absolute PPE is significantly above the 25% calculated for the extant terrestrial quadrupeds (Chapter 1; Campione and Evans, 2012).

Subdivision of residuals and PPE by major taxonomic groups (Table 3-1; Taxonomy) reveals significant patterns within clades when a large enough sample was obtained. Approaches of ceratopsians, ornithopods, and sauropods on average underestimate body mass predicted by limb scaling, and theropods, although they do not differ from a mean residual of zero, have a significantly higher overall absolute PPE. Boxplots indicate that stegosaurs have been greatly underestimated by VD approaches, with most estimates falling outside the 95% prediction intervals (Figure 3-9 and Figure 3-10). The stegosaur pattern is only recovered as significant using the ‘Perfect Match’ sample, despite the lower sample size.

Subdivision of residuals and absolute PPE based on major taxonomic groupings of non-avian dinosaurs (Taxonomic) and the technique applied to reconstruction the skeleton (Method). The ‘Perfect Match’ designation represents the dataset for which the limb measurements correspond exactly to the specimen for which the VD mass estimate was based; μ_{res} - residual mean; μ_{PPE} - absolute PPE mean. Two-tailed t-tests were conducted on both the mean residual, compared against an expected value of 0, and mean PPE compared to the mean PPE obtained from the extant terrestrial quadruped dataset (i.e., ~25%; Chapter 1; Campione and Evans, 2012). Statistical tests were run at a minimum sample size of five and reported at $p<0.05^*$, $p<0.01^{**}$, and $p<0.001^{***}$.

Analyses based on the subdivision of errors by methodology indicate that both physical scale models and the polynomial technique of Seebacher (2001) significantly underestimate the body mass given by stylopodial circumferences. Polynomial estimates exhibit the highest mean PPE of any subdivision with a large sample size (53.6%; N=47) and, in particular, underestimate body mass at small size (Figure 3-11 and Figure 3-12). The latter may also be true of the slicing technique proposed by Henderson (1999), which exhibits at least one outlier (Figure 3-12) and significantly higher PPE than expected. However, the overall spread of its residuals cannot be differentiated from zero. Of the methodologies for which a meaningful sample could be compiled, those based on recent 3D scanning techniques showed the most robust results. In contrast to other VD approaches, and despite a tendency to overestimate body mass (Table 3-1; Methodology), 100% of mass estimates derived from 3D scans fall within the 95% prediction intervals, and they have the lowest overall PPE that is virtually identical to that of extant mammals and reptiles. Unfortunately, a larger sample is not available to statistically assess estimates based on photogrammetry; however, these results suggest a tendency to overestimate body mass. Finally, despite the low estimate obtained for *Giraffatitan* (23.2 tonnes compared to

34 tonnes based on **EQ 1.1**) obtained by Sellers *et al.* (2012) based on the novel minimum convex hull technique, it still falls within the conservative 95% prediction intervals suggesting that MCH may be a robust method. However, a more extensive application of this methodology is needed in order statistically assess its potential merits.

Overall patterns in the error exhibited by VD mass estimates (expressed as the difference between VD estimates and stylopodial scaling estimates) indicate a significant and negative relationship between absolute PPE and size (represented by femoral circumference; Figure 3-13). This indicates that models of small taxa exhibit a greater error relative to circumference than models of large-bodies taxa. This pattern may represent a general tendency to underestimate small-bodied forms, however, the overall relationship between residuals and femoral circumference is just outside of significance ($p = 0.062$; Figure 3-13).

In order to assess the error in VD mass estimates throughout dinosaur palaeobiology research history I plotted errors (i.e., mean absolute PPE) of models created over the past century (see complete list of references above). The time axis was initially measured as the actual year of publications; however, the majority of VD estimates (~91%) were proposed in the last two decades resulting in a highly non-normal distribution. As a result, the time axis was also measured as the \log_{10} difference (in years) between the date of model publication and the present (i.e., 2013). Regardless of this correction both analyses recovered a non-significant trend through time (Figure 3-14). The range in errors has fluctuated appreciably through time, with the largest ranges occurring in 2001, 2002, and 2007.

3.5 Discussion

Volumetric reconstructions of extinct vertebrates are necessary for addressing numerous biological questions in the fossil record. However, as discussed in previous sections, they can be somewhat subjective by nature and, consequently, result in a large variation in mass estimates over the last few decades, sometimes based on the same specimen (Alexander, 1985; Gunga *et al.*, 1995; Seebacher, 2001; Gunga *et al.*, 2008). Therefore, in order to avoid biasing subsequent biological interpretations it is important that these reconstructions be considered within the context of an external empirical dataset. This chapter reviewed the various methods utilized to estimate body mass in non-avian dinosaurs, and proposes the use of the highly conserved relationship between combined stylopodial circumference (humerus + femur) and body mass in extant terrestrial tetrapods (quadrupeds) to empirically test mass estimates obtained by the VD approach. Non-avian dinosaurs are tetrapods and thus are expected to follow this conserved pattern. Therefore, given a particular stylopodial circumference, 95% of the body masses obtained via VD reconstructions of non-avian dinosaurs should occur within the 95% prediction intervals obtained from the stylopodial circumference to body mass relationship derived from extant terrestrial quadrupeds (Chapter 1; Campione and Evans, 2012).

The results described in section 3.4.2 reveal that approximately 70% of the VD mass estimates tested here fall within the expected 95% prediction range. Although this indicates that the majority of models are consistent with predictions based on the stylopodial circumference data, the incidence of approximately 30% outliers (datapoints outside the 95% percent intervals) suggests that several reconstruction significantly miss-estimate body mass in certain non-avian dinosaurs. Indeed, the VD-derived masses exhibit an overall higher percent prediction error than that recovered from the extant dataset (Figure 3-10). Of the models recovered outside the 95%

bounds, the majority (80%) are below the 95% prediction intervals indicating an overall tendency of VD approaches to underestimate body mass, a pattern that is particularly pronounced at small size (Figure 3-13). The trend of certain VD-based models to underestimate small-bodied taxa (e.g., Seebacher, 2001), although weak, can have a profound effect on subsequent biological interpretations, including community structure (Codron *et al.*, 2012b) and metabolic rates (Seebacher, 2003; Pontzer *et al.*, 2009).

Thyreophorans (ankylosaurs and stegosaurs) exhibited the largest error with body mass estimates at the extremes of the 95% predictions bounds. This pattern is particularly evident in stegosaurians with only a single VD estimate occurring within the 95% prediction limits, one above, and four below (Figure 3-9, Figure 3-10) with masses that are half those suggested by the ES approach. Other ornithischians revealed overall lower systematic errors, with the possible exception of Ornithopoda for which half of the VD estimates occur below the 95% prediction intervals. Notable examples include small-bodied forms estimated by Seebacher (2001):

Thescelosaurus neglectus, VD-based estimate: 7.9 kg, ES-based estimate: 186 kg; *Gasparinisaura cincosalensis*, VD: 980 g, ES: 12.4 kg; and *Hypsilophodon foxii* VD: 1.4 kg, ES: 12.4 kg. In general, the ‘polynomial’ method presented by Seebacher (2001) exhibited some of the highest errors of any VD approach examined here. Large errors, such as those identified above, need to be considered when interpreting results derived via this model and indiscriminate use of its results, which in certain cases can be within an order of magnitude or more different from other models, can have a large effect on subsequent biological interpretations.

Theropoda exhibited the lowest overall error with a mean residual error that is statistically indistinguishable from zero, consistent with interpretations obtained in chapter 2 that found similar mass estimates between the bipedal correction factor and VD approaches. Despite

overall agreement, certain datapoints are significant outliers with VD mass estimates that either significantly over- or underestimate body mass (Figure 3-10; gray). Nine (of 62) theropod mass estimates were considered outliers, including five overestimations, *Avimimus portentosus* and *Deltadromeus agilis* (Seebacher, 2001), *Herrerosaurus ischigualastensis* (Henderson, 2003), *Giganotosaurus carolinii* (Therrien and Henderson, 2007), and *Ornithomimus edmontonensis* (Christiansen, 1998). The estimate for *Deltadromeus agilis* exhibited the highest PPE within the ‘Perfect Match’ sample with a VD mass estimate approximately 170% larger than that expected (1,049 kg compared to 380 kg) four underestimations, *Eoraptor lunensis* and *Ornitholestes hermanni* (Seebacher, 2001) and *Mei long* and *Sinornithoides youngi* (Therrien and Henderson, 2007).

Sauropodomorphs includes species that attained the largest body size of any terrestrial vertebrate, and attempts to infer their body mass have been more widespread than almost all other dinosaurian clades, except perhaps theropods (both have a total sample of 62 in this study). Body mass of sauropodomorphs, and in particular Sauropoda, are of particular interest because, given their large size, they are a model clade for investigating physiological and life-history attributes within the context of gigantism (see Sanders *et al.*, 2010). As a result, constraining mass estimates of these taxa is especially important as all subsequent interpretations of sauropods, especially the largest, represent significant extrapolations beyond the data available by studying extant systems. The results presented here suggest that for the most part VD approaches are consistent with the ES approach used here. Specifically, results support lower estimates (~35 tonnes) for *Giraffatitan brancai* (Anderson *et al.*, 1985; Alexander, 1989; Paul, 1997; Henderson, 1999; Seebacher, 2001; Gunga *et al.*, 2008; Sellers *et al.*, 2012) over large estimates (~70 tonnes; Colbert, 1962; Gunga *et al.*, 1995; Christian *et al.*, 1999). Similarly, *Apatosaurus louisae* (CM 3018) appears to be significantly underestimated by most studies

(between 15 and 20 tonnes; Christiansen, 1997; Paul, 1997; Henderson and Snively, 2004; Mazzetta *et al.*, 2004; Henderson, 2006), whereas circumference measurements support a higher mass (e.g.; Alexander, 1989) of approximately 40 tonnes, similar to *G. brancai*.

One of the biggest limitations to the VD approach is that in order to generate a robust reconstruction, they rely on complete, well-preserved skeletons, thereby limiting their utility for large-scaling evolutionary analyses. As a result, a few studies have proposed a series of equations generated by regressing skeletal measurements that are more readily available, such as total body length (Seebacher, 2001) and various hind limb dimensions in non-avian theropods (Christiansen and Fariña, 2004) and sauropods (Mazzetta *et al.*, 2004), against VD based mass estimates obtained in a sample of well-preserved extinct taxa. Given that these equations can be generated on a few skeletal measurements they can be applied to large-scale evolutionary studies, such as reconstructing the evolution of body size in theropods preceding the origin of birds and the evolution of flight (Turner *et al.*, 2007; Dececchi and Larsson, in press). The robusticity of these equations, however, rely on the baseline mass dataset derived from VD-based mass estimates and it is important that these estimates be properly constrained. As previously shown, the ‘polynomial’ method of Seebacher (2001) greatly underestimates small body taxa and exhibits a high amount of residual variation compared to other VD approaches. It is important that these errors be taken into account when using VD approaches to generate mass estimation equations for general use. In Chapter 2, I empirically tested the theropod femoral circumference to body mass equation of Christiansen and Fariña (2004) using an extant avian dataset. Results recovered a low mean PPE for the equation relative to other bipedal equations (e.g., Anderson *et al.*, 1985) and supported its use for estimating body masses in most theropods. A *post hoc* test of Christiansen and Fariña (2004) corroborates the results of Chapter 2 and reveals that the models made by the authors have among the lowest errors with 92% of models

occurring within the 95% predictions intervals (Figure 3-15; red). In contrast, only 57% of the models utilized by Mazzetta *et al.* (2004) occur within the expected 95% prediction intervals and the mean PPE is significantly higher than that obtained from the extant quadrupedal dataset (Figure 3-15; blue). Three models are inconsistent with stylopodial circumference measurements, including: *Amargasaurus cazaui* (MACN-N 15; estimated at 2,600 kg, compared to 9,904 kg based on stylopodial circumference), *Apatosaurus louisae* (CM 3018; 20,600 kg compared to 40,837 kg), and *Opisthocoelicaudia skarzynskii* (ZPAL MgD-I/84; 8,400 kg compared to 24,391 kg). These results recommend caution when using the modeled weight or equations presented by Mazzetta *et al.* (2004) but indicate that those of Christiansen and Fariña (2004) are likely robust when applied to theropods. This is particularly true for their equation between femoral circumference and body mass but may be extended to all bivariate and multivariate regressions presented by the authors, with the caveat that the assumptions inherent to scaling equations have been met (see Section 3.3.2.2).

Inferring the body mass of non-avian dinosaurs has been the subject of numerous studies spanning the last century (see Sections 3.1 and 3.3 for a full list of references). Interpretations of the biology, behaviour, and overall appearance of dinosaurs, however, have drastically changed over this time (Bakker, 1986; Sampson, 2009), and are assumed to have played an important role in the observed variation in body masses derived from VD approaches (Gunga *et al.*, 1995; Gunga *et al.*, 2008; Stoinski *et al.*, 2011). These paradigm shifts in dinosaurian palaeobiology are built upon new fossil discoveries that allow to putatively better reconstruct these taxa, and as a result, one would expect that errors in body mass should decrease towards the present. Results presented here (Figure 3-14) reveal no significant trend in any direction, and surprisingly, early estimates, such as those of Gregory (1905), Janensch (1935), and certain models of Colbert (1962) exhibit very low errors relative to stylopodial limb circumference and well within the

25% mean PPE. In comparison, some recent estimates (Physical: Paul, 1997; Slicing: Henderson, 1999; Polynomial: Seebacher, 2001) present VD reconstructions with some of the highest errors, although, in general, most of their estimates occur within the 95% prediction bounds. A non-significant error trend through time, does not necessarily indicate that early reconstructions were robust given our current understanding of dinosaurian biology, but rather suggests that some of the assumptions inherent to early VD approaches (i.e., amount of soft-tissue reconstructed and assumed body density, overall body proportions, *etc.*) may have been valid. In particular, it indicates that these assumptions can trade-off between each other to create a validated mass estimate. Understanding these trade-offs will be important for future studies aimed at reconstructing non-avian dinosaurs and can be best approached through the use of 3D scanning techniques, which permit manipulation of these parameters in virtual space (e.g., Hutchinson *et al.*, 2007; Bates *et al.*, 2009a; Mallison, 2010; Hutchinson *et al.*, 2011; Stoinski *et al.*, 2011). Furthermore, the method outlined by Sellers *et al.* (2012), although not derived for this purpose, may provide a more objective way to determine the amount of soft tissue needed to reconstruct extinct forms based on a ‘null’ reconstruction objectively derived from the scanned skeleton (see Section 3.3.1.1.3). Unfortunately, it presently only includes a small sample of extant mammals and future work should investigate the universality of the systematic error identified by that study and assess its variation between various vertebrate groups. Nevertheless, its estimate for *Giraffatitan brancai* falls within the 95% prediction intervals and, pending a more comprehensive application to extinct taxa, may represent a more objective method for estimating body mass compared to traditional VD approaches.

3.6 Conclusions

The ecological and physiological implications of body mass have been well studied (e.g., Kleiber, 1947; Peters, 1983; Calder, 1984; Brown *et al.*, 1993; Burness *et al.*, 2001; Capellini and Gosling, 2007; McClain and Boyer, 2009). As a result, the ability to reconstruct the mass of extinct forms such as non-avian dinosaurs offers the unique opportunity to study these animals in a biological context and in turn study the evolution of these properties in deep time (e.g., Bakker, 1972; Farlow, 1976; Christiansen, 1999c; Henderson, 2004; Erickson, 2005; Henderson, 2006; Varricchio *et al.*, 2008; Franz *et al.*, 2009; Pontzer *et al.*, 2009; Hutchinson *et al.*, 2011; Codron *et al.*, 2012b). Despite its utility, body mass cannot be directly measured in the fossil record and must be estimated. Several studies have forwarded methods for estimating body mass in the fossil record of non-avian dinosaurs (see Section 3.3) that are based on two overall approached, Volumetric-Density or Extant-Scaling. To date, no study has quantitatively compared these models and assessed potential systematic error (i.e., differences) between them.

This study reviews the various iterations of the VD and ES approaches as they apply to non-avian dinosaurs and presents the first quantitative comparison between approaches. The comparisons underscore the utility of the *post hoc* model for substantiating the information provided by both approaches and, in particular, is strongly advocated here for future VD-based reconstructions. Body mass estimates derived through VD approaches over the last century are, in general, consistent with the most recent ES model (Campione and Evans, 2012) derived from stylopodial circumference data in extant terrestrial quadrupeds. However, the *post hoc* model identified several inconsistencies, and in particular suggests that some VD models (e.g., the polynomial method) underestimate small-body taxa. This result can have important effects on subsequent biological interpretations, especially since many biological questions can only be

addressed by VD approaches (e.g., Henderson, 2004; Pontzer *et al.*, 2009; Hutchinson *et al.*, 2011). Despite these differences, results indicate that three-dimensional scanning techniques of complete skeletons, which have been advocated over the last five years (Gunga *et al.*, 2007; Hutchinson *et al.*, 2007; Gunga *et al.*, 2008; Bates *et al.*, 2009b; Bates *et al.*, 2009a; Mallison, 2010Sellers, 2012 #2133; Hutchinson *et al.*, 2011), provide the most robust VD approach for estimating body mass. Mass estimates based on this method are strongly corroborated by the limb circumference ES model (Campione and Evans, 2012) providing strong evidence that our overall understanding of the biology and appearance of non-avian dinosaurs has greatly improved over the last few years. Studies utilizing methods such as those based on 3D specimen scans will thus provide the best option for reconstructing the biology of extinct taxa and ecosystems, thereby providing the opportunity to understand both their origins and evolution throughout the Phanerozoic.

3.7 Tables

Table 3-1. Mean residual and absolute PPE of various volumetric-density mass estimates.

		Perfect Match Sample ¹			Complete Sample		
		N	μ_{res}	μ_{PPE}	N	μ_{res}	μ_{PPE}
	All	153	-0.1309***	40.99***	214	-0.1018***	39.69***
Taxonomy	Ankylosauria	2	0.1385	75.05	7	-0.0947	68.28
	Ceratopsia	7	-0.3191***	51.72***	15	-0.204***	34.51
	Ornithopoda	33	-0.2532***	40.2**	46	-0.2425***	38.55**
	Pachycephalosauria	3	0.1108	39.32	3	0.1108	39.32
	Prosauropoda	5	-0.2332*	39.3	13	-0.0369	34.94
	Sauropoda	47	-0.1611***	41.8***	62	-0.1087***	38.26***
	Stegosauria	5	-0.4127**	58.59**	6	-0.2535	90.26
	Theropoda	51	0.0148	36.49*	62	0.0243	36.12*
Methodology	MCH	1	-0.1655	31.69	1	-0.1655	31.69
	Photogrammetry	3	0.1681	54.7	5	0.2167*	72.5
	Physical	81	-0.1662***	35.98***	113	-0.1292***	33.17**
	Polynomial	31	-0.1764*	51.12**	47	-0.1549*	53.61***
	Scan	13	0.1042**	34.58	20	0.0809**	27.07
	Slicing	24	-0.1164	46.99**	28	-0.0871	46.1**

3.8 Figures

Figure 3-1. Plaster reconstructions used by Colbert (1962). The volume of these models was determined by volumetric displacement in sand (modified from Colbert, 1962).

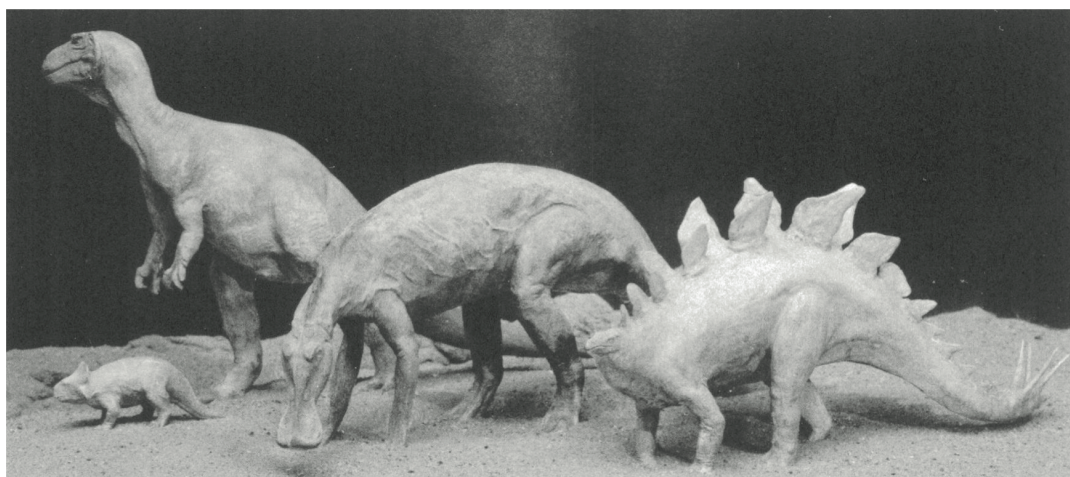


Figure 3-2. Experimental design of Alexander (1985). Model based on solid plastic reconstructions then sold at the British Museum of Natural History. Volume is calculated based on the Archimedes Principle that the difference between the weight of an object in water and in air is equal to its volume (modified from Alexander, 1985).

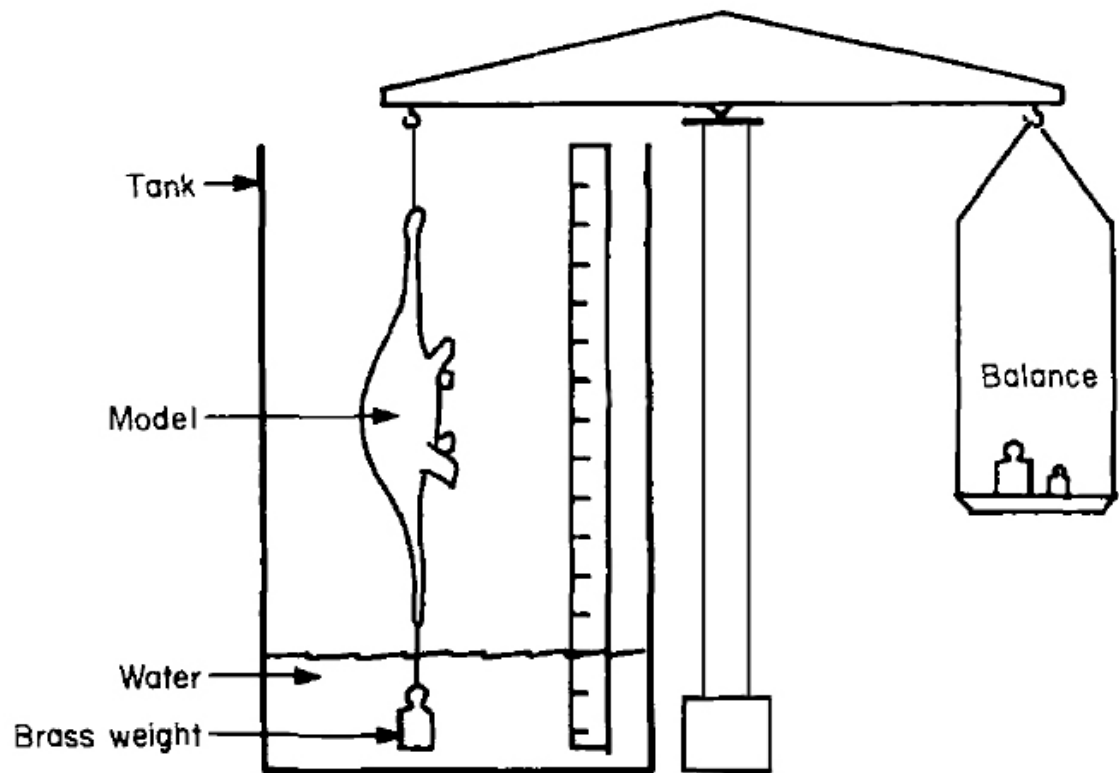


Figure 3-3. Example of Graphic Double Integration as applied to the non-therapsid synapsid *Edaphosaurus boanerges*. Dotted lines indicate the segmentation of the model and the standard measurements taken from the dorsal (top) and lateral (bottom) views (modified from Hurlburt, 1999).

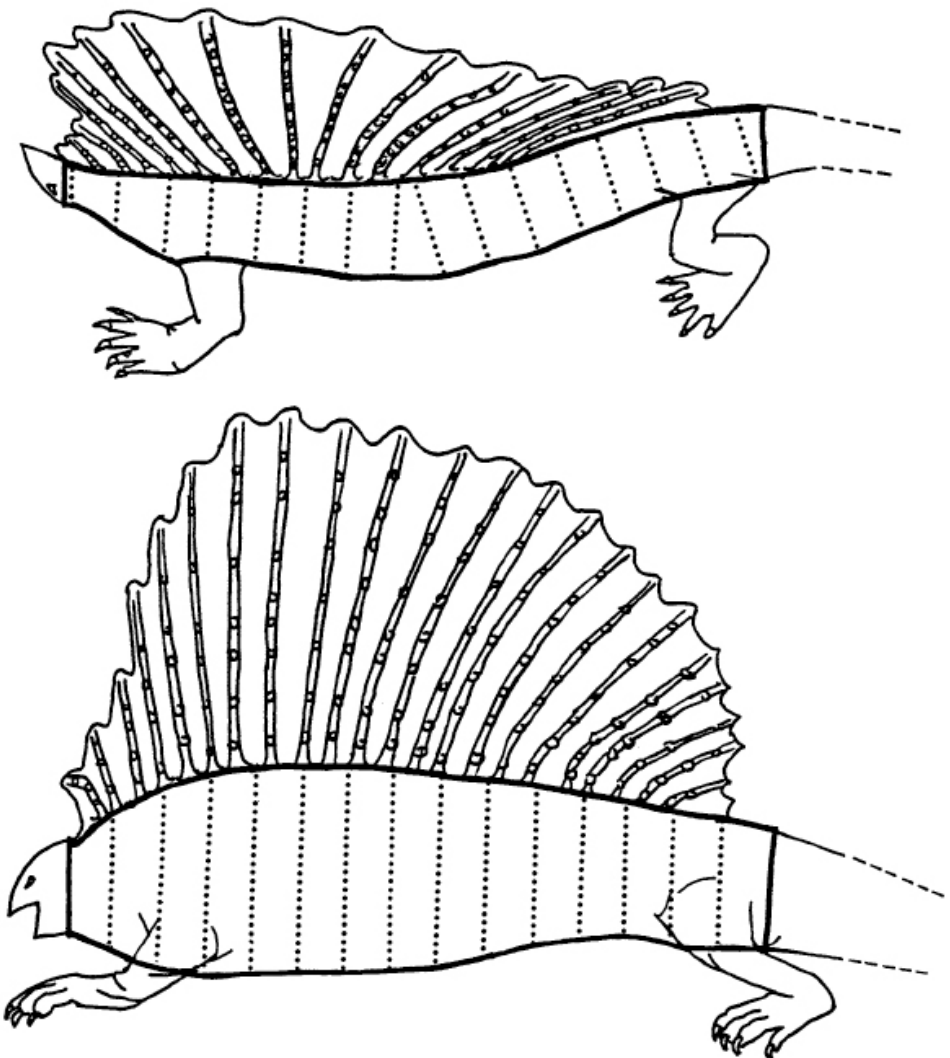


Figure 3-4. Methodological basis for the ‘polynomial’ technique developed by Seebacher (2001). Depth measurements are taken at set intervals across a lateral reconstruction of an animal (right). Depth measurements are then plotted against their relative positions along the length of the reconstruction and a line is fitted via an eighth order polynomial (left) (taken from Seebacher, 2001).

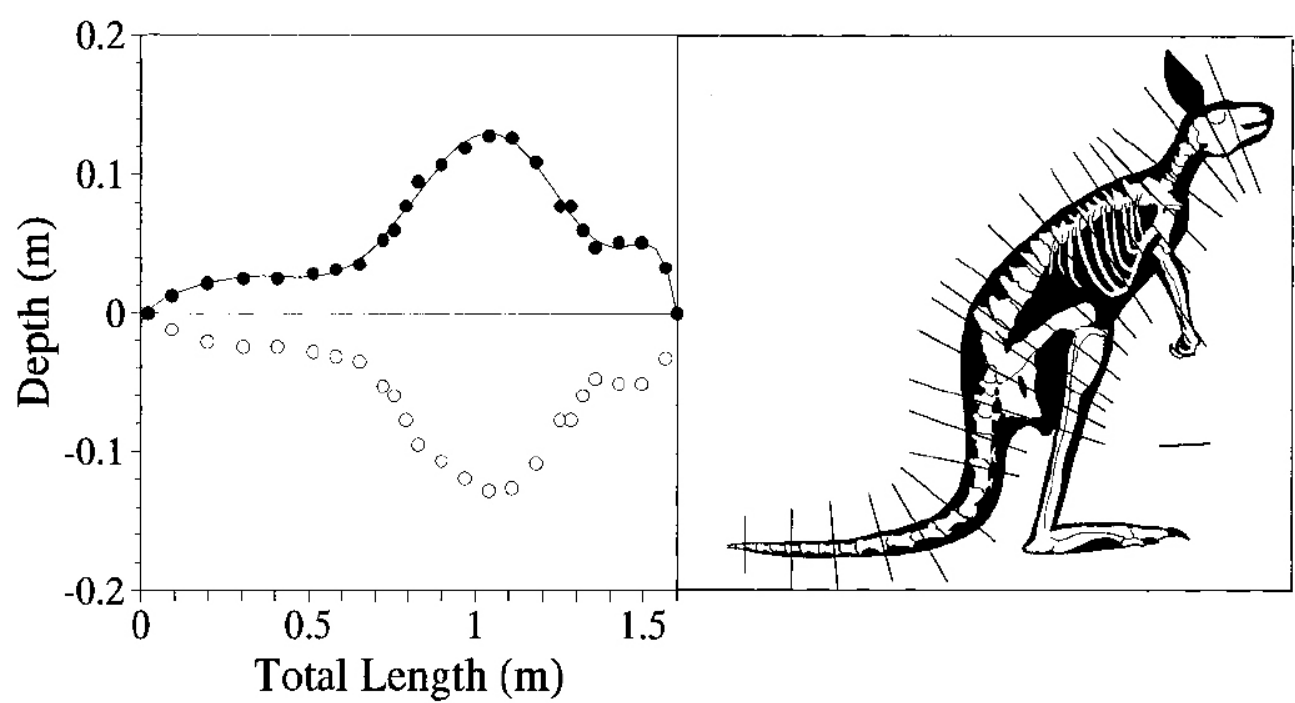


Figure 3-5. Methodological basis of the photogrammetric technique as applied to non-avian dinosaurs. The method is based on taking photographs from various positions along a skeletal mount (O' and O''; left) that stereoscopically complement each other to form a 3D image (at P). This depiction can be digitally converted and forms the basis for a reconstruction (right) that can be divided into segments (I–XI) whose volume can be calculated using various standard volumetric equations (modified from Gunga *et al.*, 1999 and Wiedmann *et al.*, 1999).

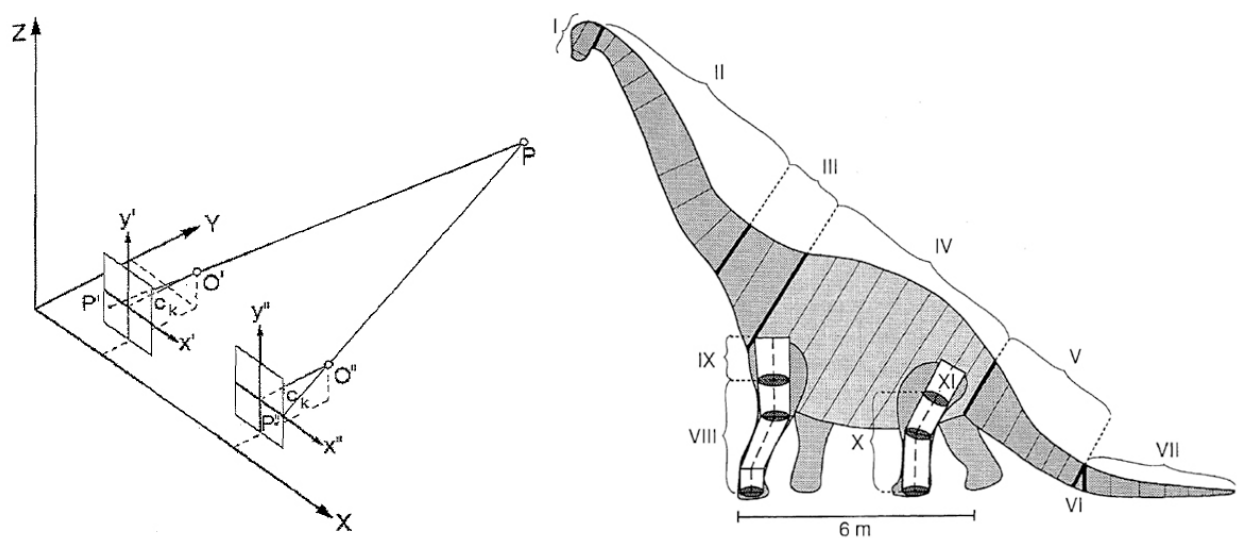


Figure 3-6. Mathematical slicing technique of Henderson (1999). This method converts two-dimensional reconstructions (left) into a three-dimensional virtual object made up of segments, or slabs (top right), which form the basis for calculating the volume of the complete reconstructions (bottom right) (modified from Henderson, 1999).

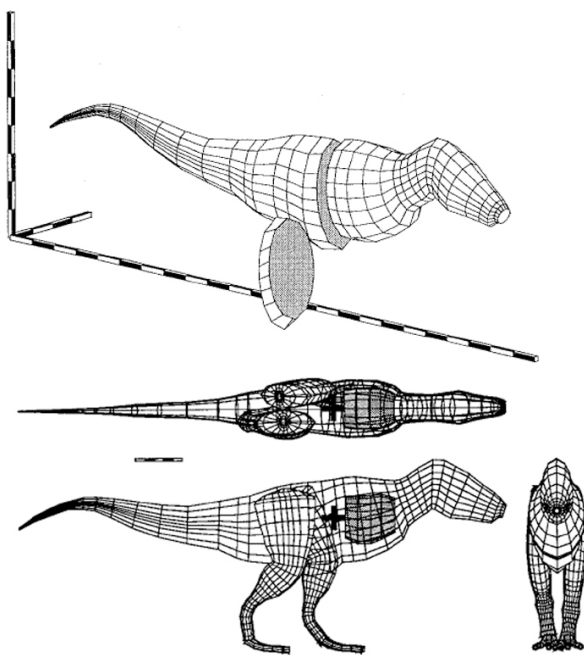
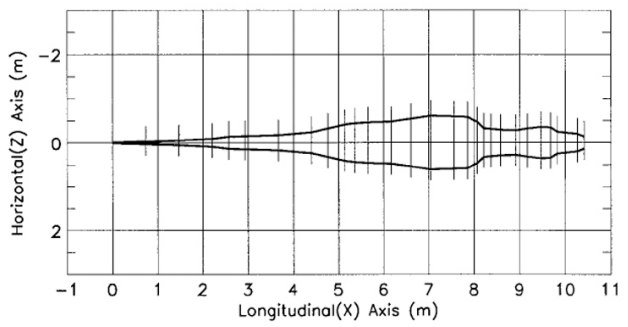
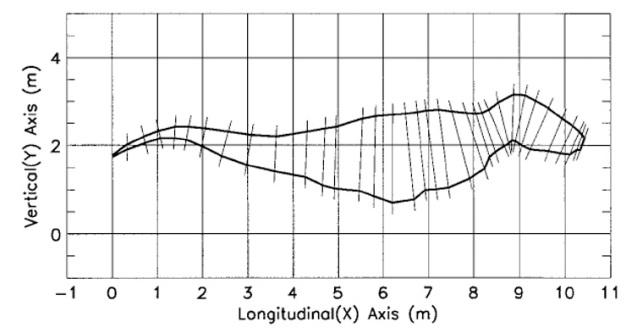


Figure 3-7. Minimum convex hull technique introduced by Sellers *et al.* (2012). This method incorporates the use of a 3-dimensional point cloud created via 3D scans of mounted skeletons (top and middle), which are segmented into various anatomical regions. A minimum convex hull is determined for each region (bottom), which forms the basis for volume calculation (taken from Sellers *et al.*, 2012).

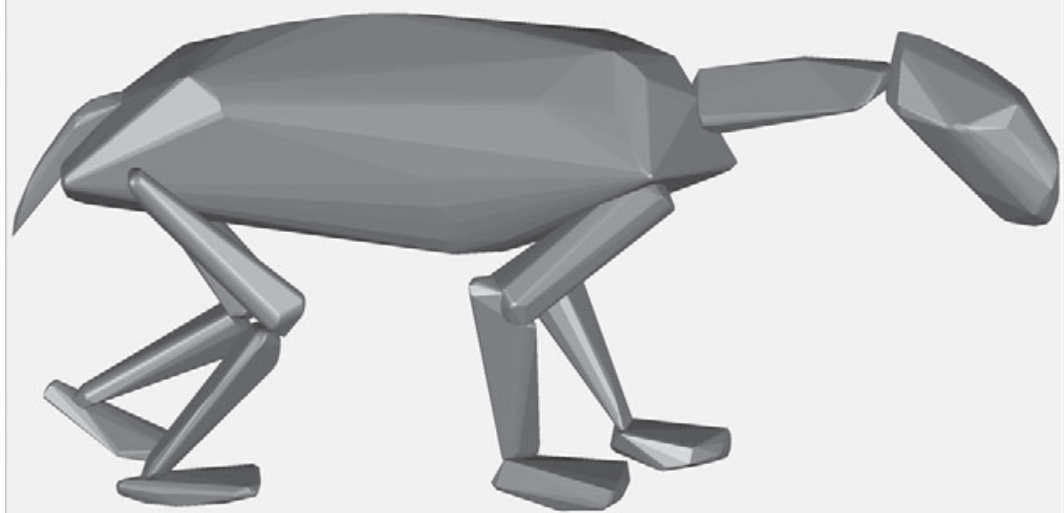
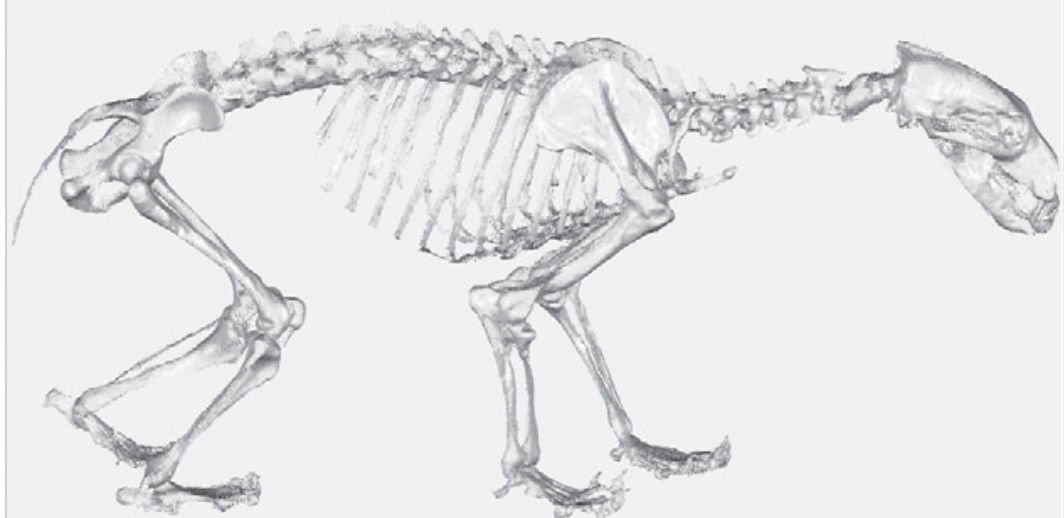


Figure 3-8. Regression of Anderson *et al.* (1985) based on a sample of 33 extant mammals. The regression plots the combined humeral and femoral circumference against body mass and serves as a model for estimating body mass in quadrupedal dinosaurs (EQ 3.1); it was adjusted to estimate body mass in non-avian bipedal dinosaurs (EQ 3.2)

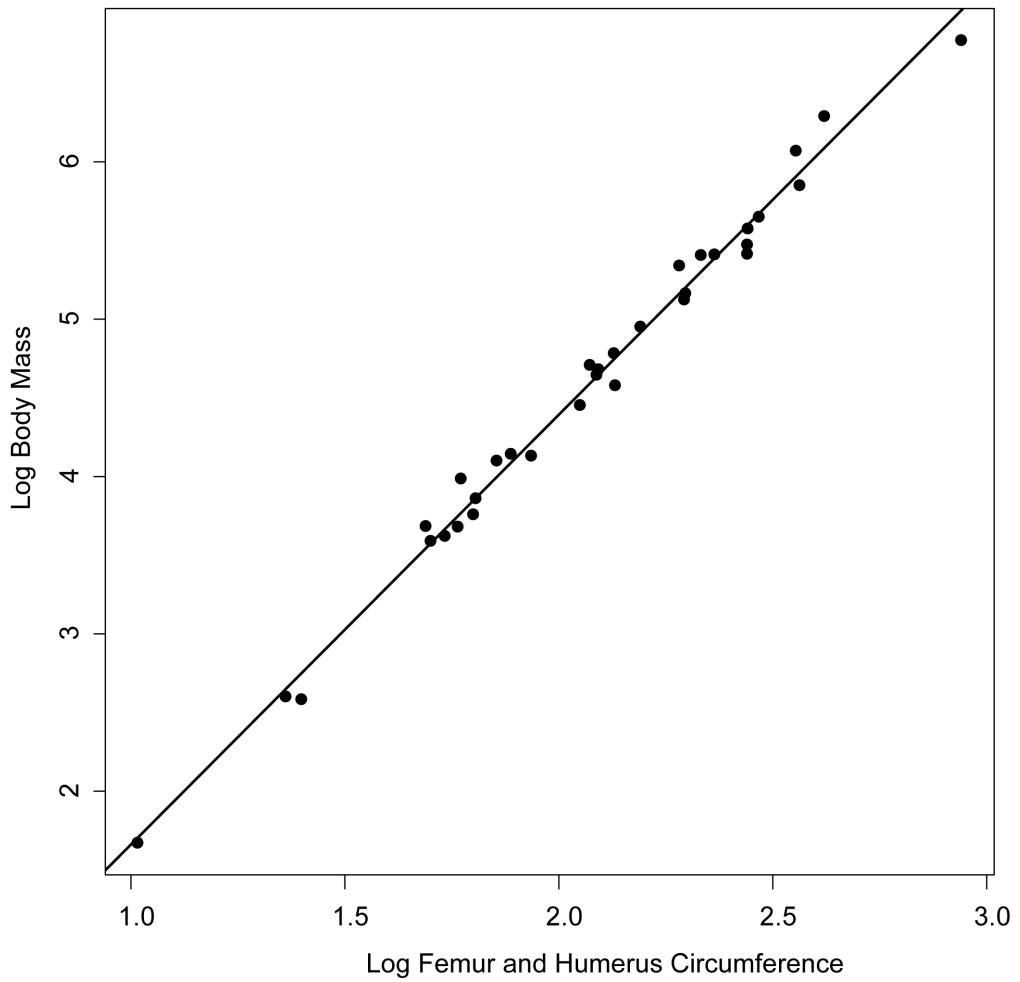


Figure 3-9. Plot of stylopodial circumferences against VD mass estimates or residuals grouped by major taxonomic designations. Stylopodial circumference refers to the combined humeral and femoral circumference for assumed quadrupeds, whereas it refers to solely the femoral circumference for assumed bipeds (See Appendix 4 for full list of gait designations).

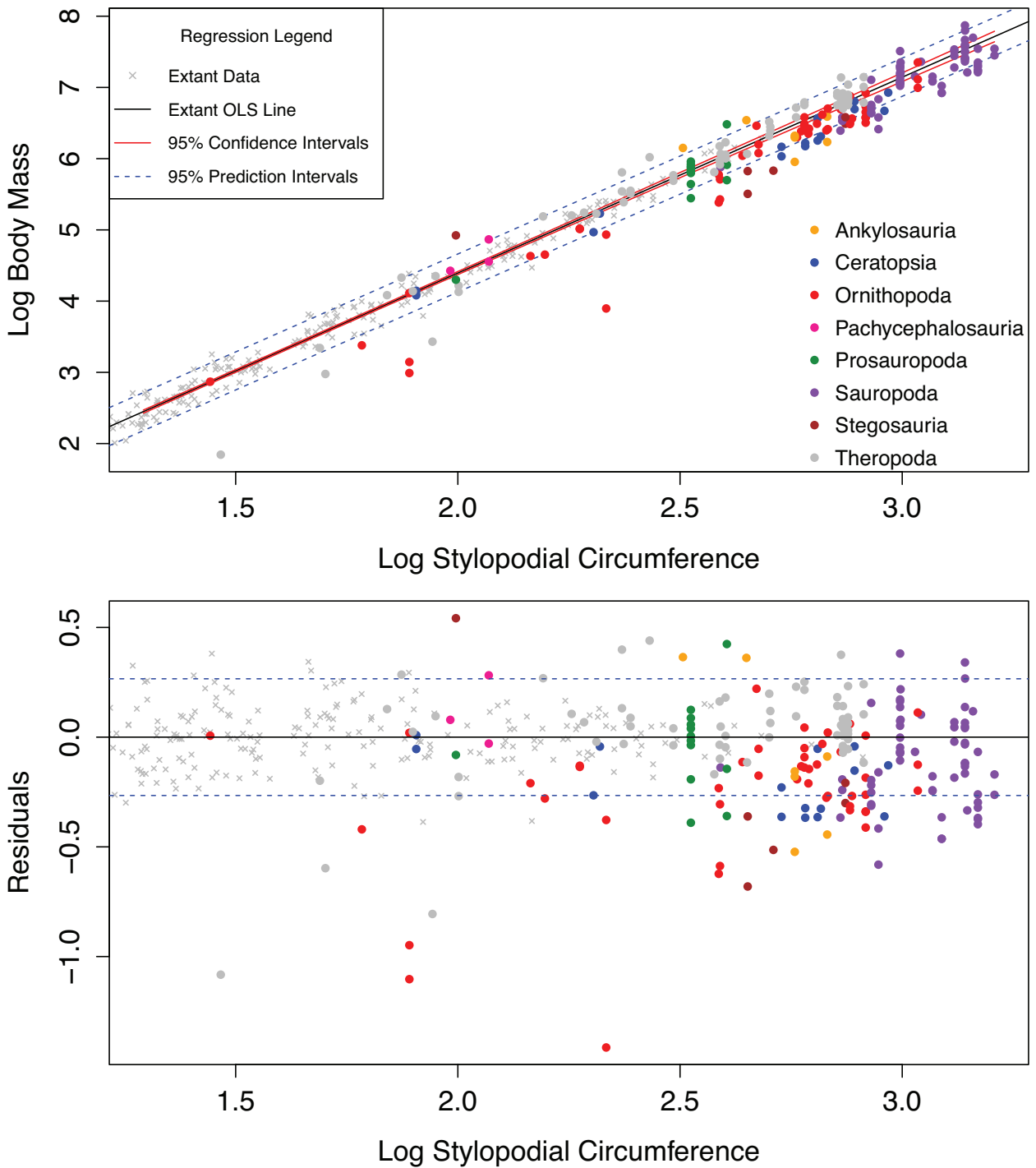


Figure 3-10. Boxplots of residuals and absolute percent predictions errors grouped by major taxonomic designations. Dashed lines represent the 95% prediction intervals (top), and the ~25% mean PPE (bottom), both recovered from the extant terrestrial quadrupedal dataset. Colours correspond of the legend in Figure 3-9.

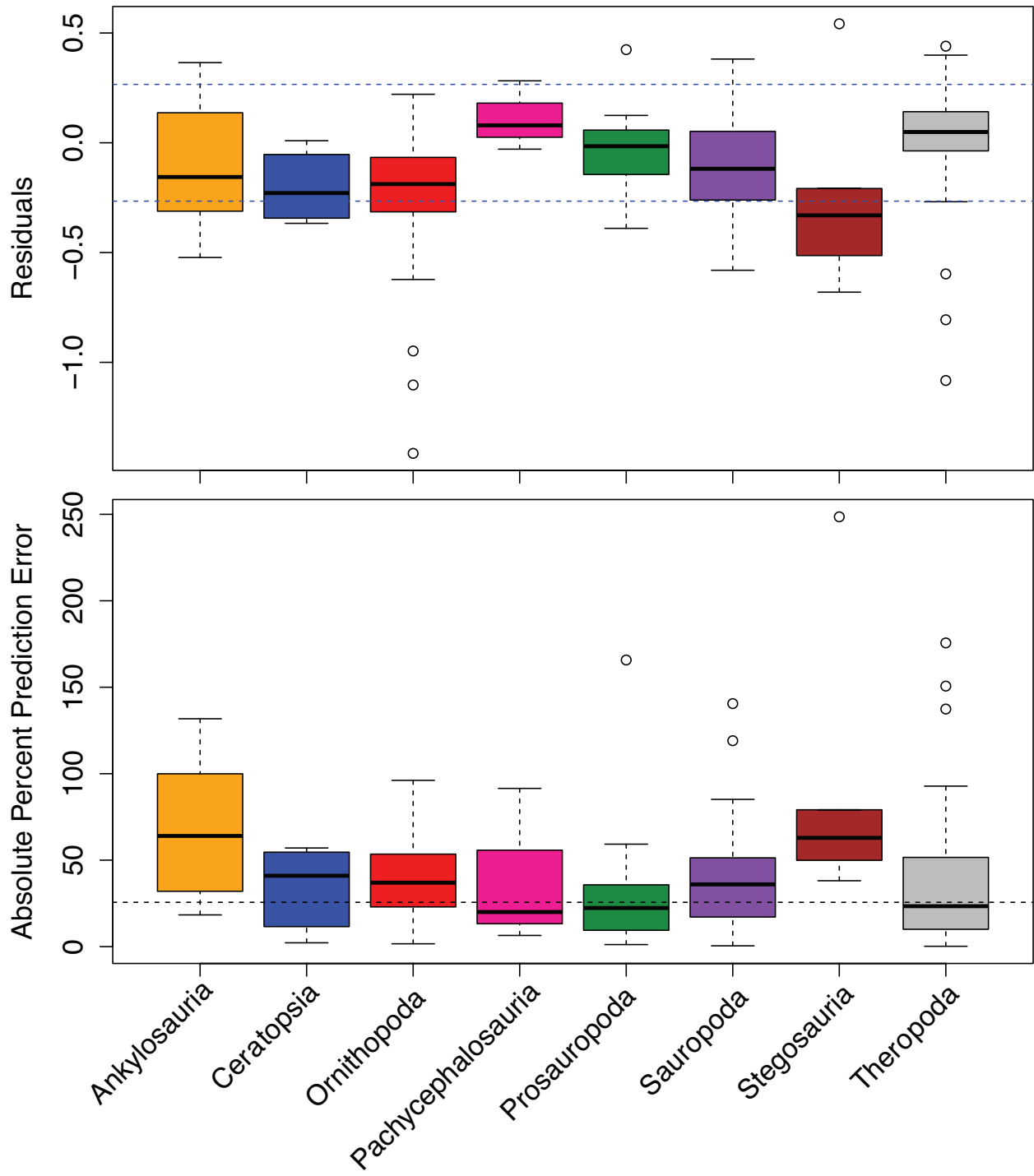


Figure 3-11. Plot of stylopodial circumferences against VD mass estimates or residuals grouped by methodology used to implement the model. Stylopodial circumference refers to the combined humeral and femoral circumference for assumed quadrupeds, whereas it refers to solely the femoral circumference for assumed bipeds (See Appendix 4 for full list of gait designations).

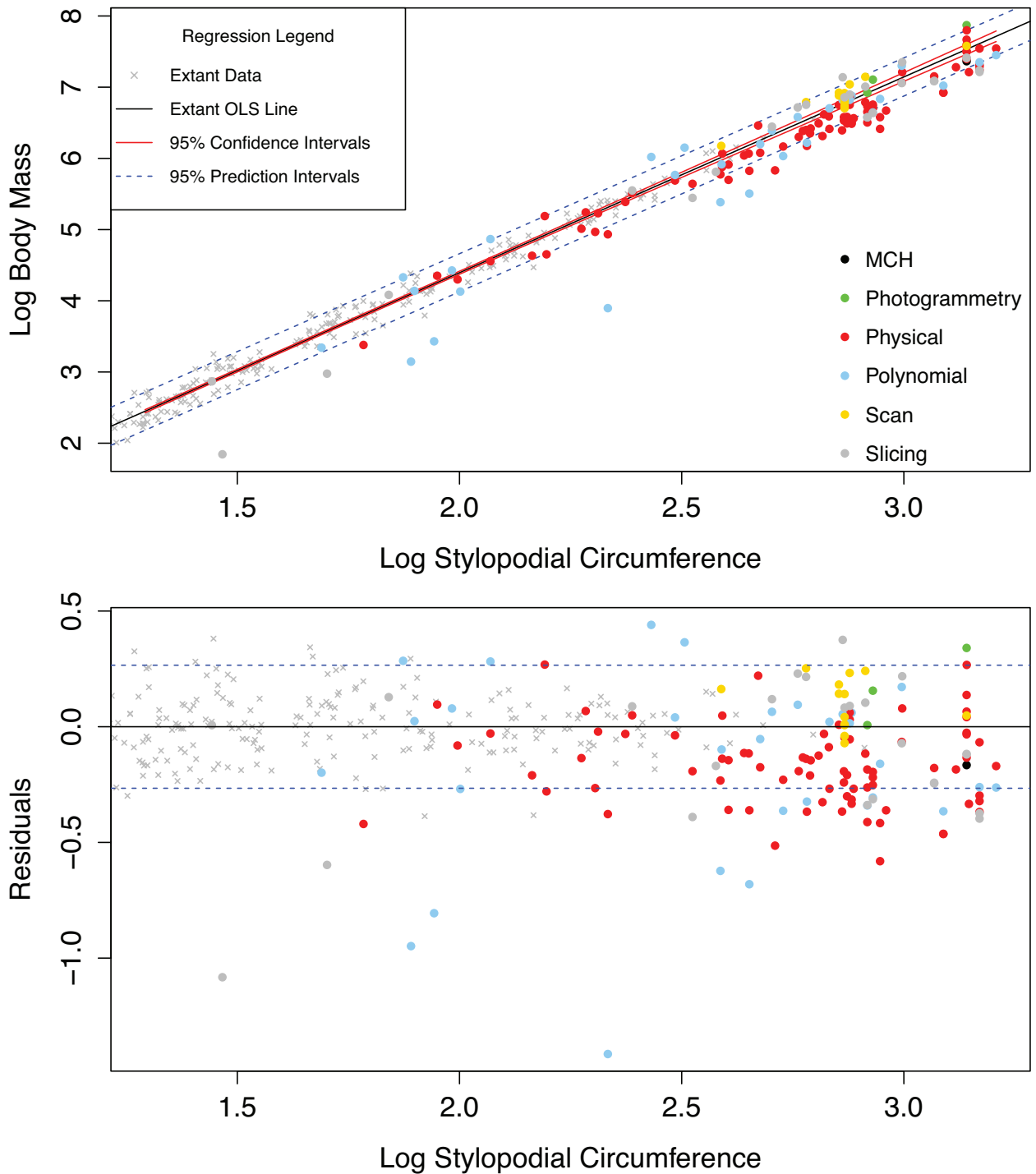


Figure 3-12. Boxplots of residuals and absolute percent prediction errors grouped by methodology used to measure the volume of a model. Dashed lines represent the 95% prediction intervals (top), and the ~25% mean PPE (bottom), both recovered from the extant terrestrial quadrupedal dataset. Colours correspond of the legend in Figure 3-11.

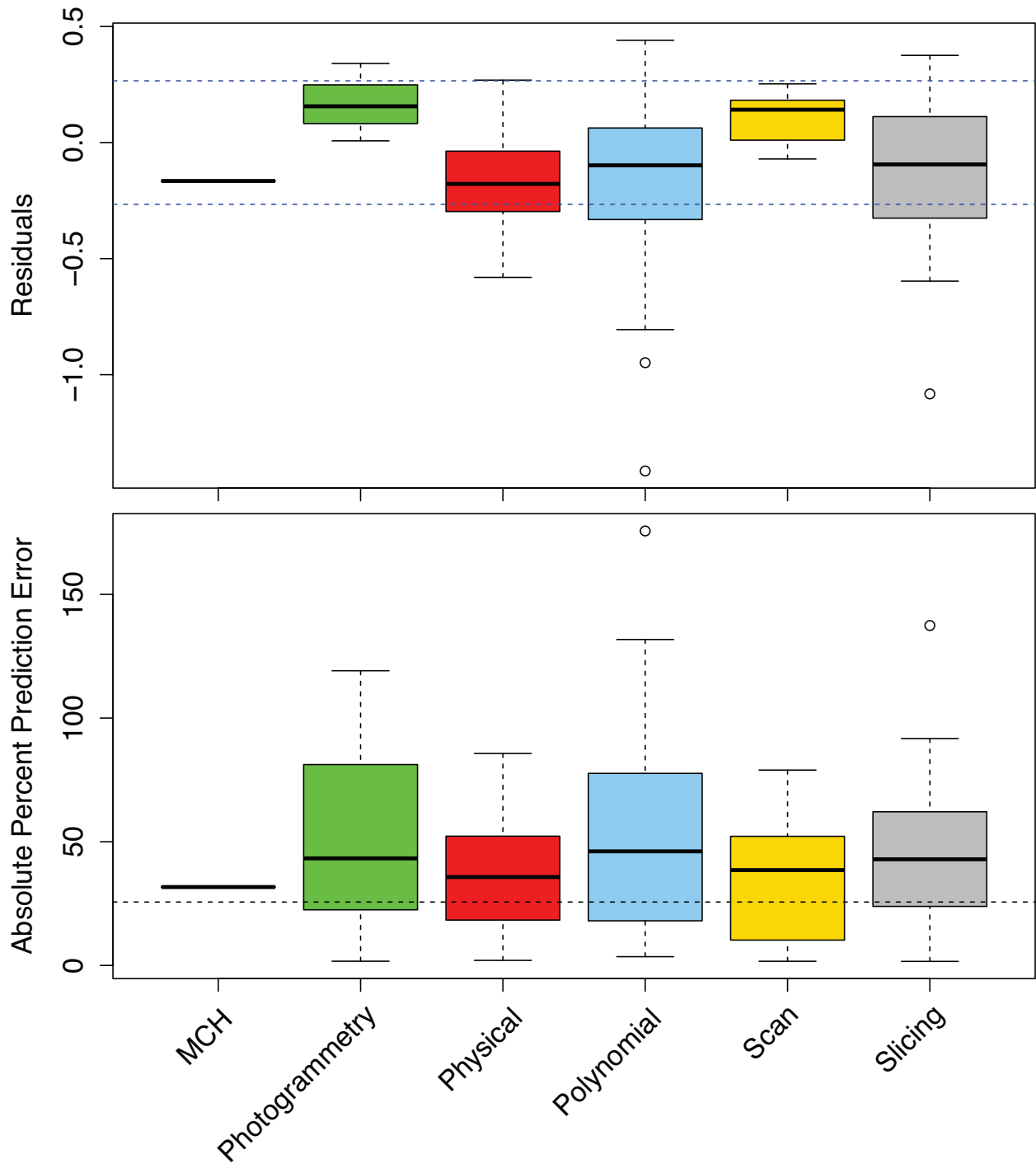
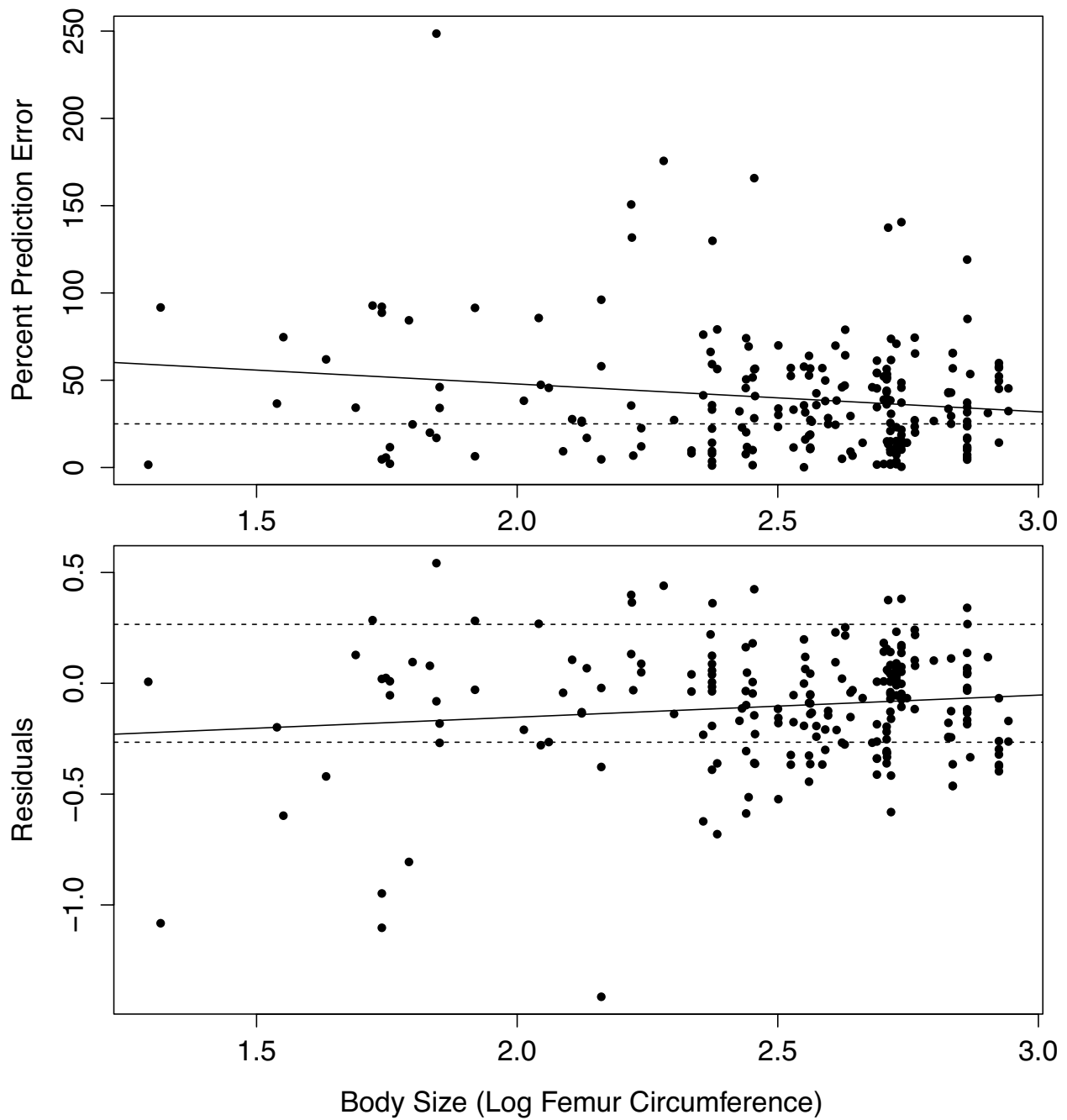


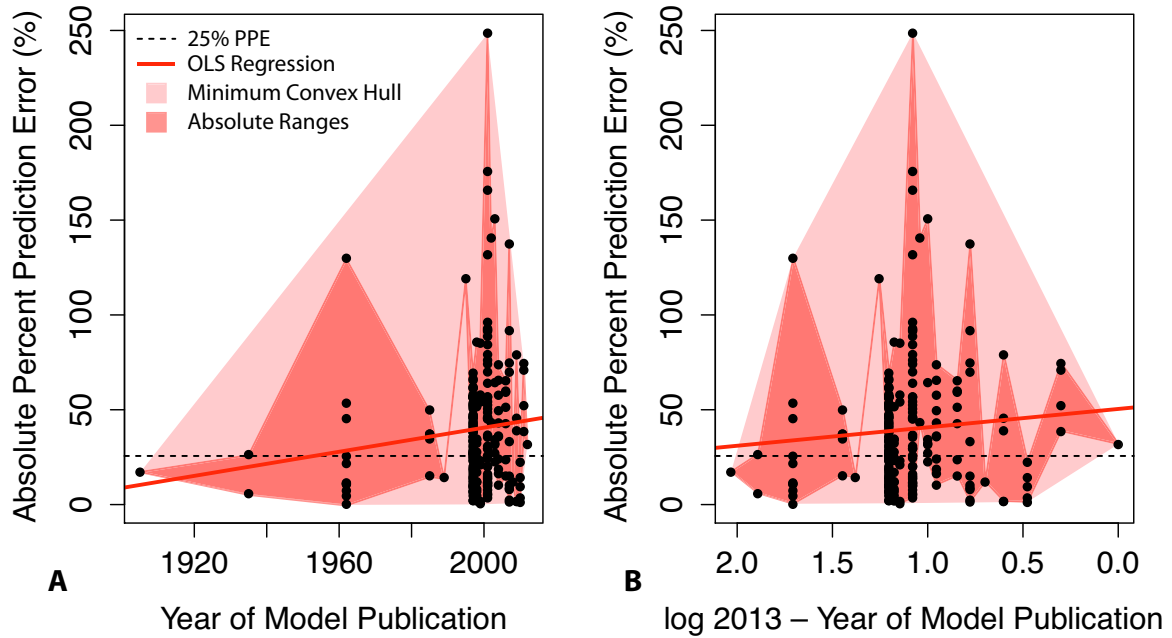
Figure 3-13. Relationship between size (femoral circumference) and the error between VD mass estimates and those derived from stylopodial circumference scaling. Percent prediction error (top) and residuals are expressed in absolute and relative terms, respectively. Dashed lines represent the 95% prediction intervals (top) and the ~25% mean PPE (bottom), both recovered from the extant terrestrial quadrupedal dataset. Table below the plots summarizes the regression statistics; * represents a significant relationship at p<0.05.



Regression Results

	N	Slope	95% CI	r ²	p-value
PPE plot	214	-15.9	-29.3 to -2.5	0.021	0.02*
Residual plot	214	0.1	-0.005 to 0.204	0.011	0.062

Figure 3-14. Relationship between year of model publication and absolute PPE. Dashed line represents the ~25% mean PPE that was recovered from the extant quadrupedal dataset.



Regression Results					
	N	Slope	95% CI	r ²	p-value
Year of Publication	214	0.318	-3.562 to 0.672	0.001	0.078
log Difference	214	-9.707	-26.247 to 6.834	0.002	0.249
Year of Publication	214	0.394	-0.005 to 0.838	0.013	0.082
log Difference	214	-14.27	-31.865 to 3.329	0.01	0.111

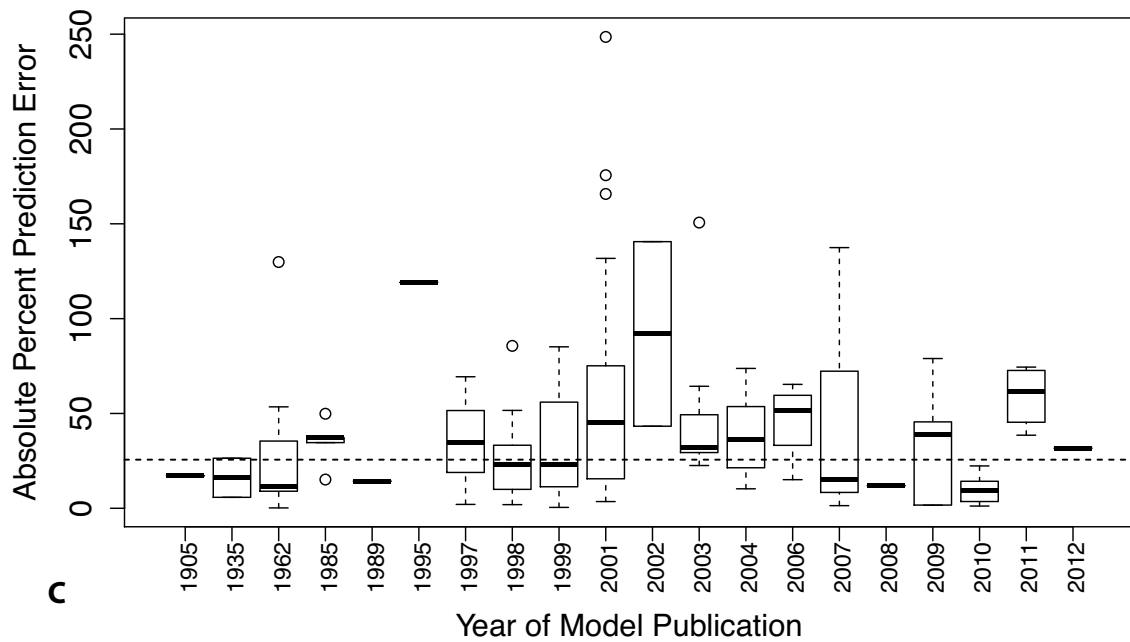
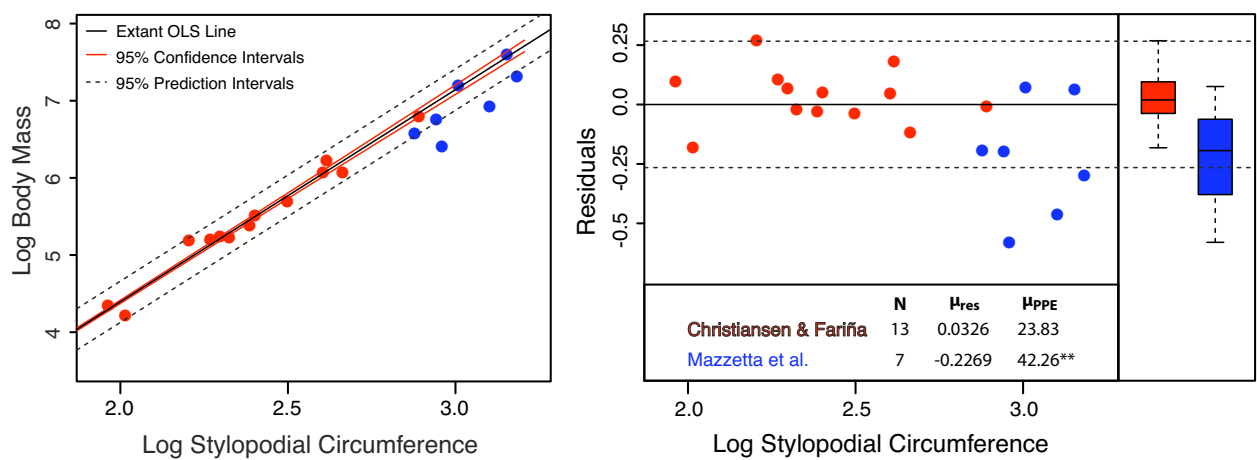


Figure 3-15. *Post hoc validation test of physical VD models presented in Christiansen and Fariña (2004) and Mazzetta *et al.* (2004). Extant OLS regression line derived from the extant terrestrial quadrupedal data used in Chapter 1 (Campione and Evans, 2012). Residuals (plot on right) derived from the extant OLS line. Table at the bottom of the residual plot provides the mean residual (statistically compared to a value of zero) and PPE (compared to the mean PPE of the extant quadrupedal data) for the VD models (**significance at p<0.01). Boxplots at the far right are those of the residual values.*



Chapter 4

The Evolution of Body Size in Ornithopod Dinosaurs: Testing Cope's Rule, Insular Dwarfism, and Upper Body Size Limits in Non-Avian Dinosaurs

4.1 Abstract

Dinosaurs span the largest size range of an terrestrial vertebrate group and are thus a model clade for investigating macroevolutionary patterns of body size in the fossil record of terrestrial vertebrates. Most studies, however, address this issue on a large scale and few have attempted to quantify finer-scale within clade patterns. This chapter utilizes ornithopod dinosaurs as a model for investigating finer-scale patterns in the evolution of their body size, the range of which spans four orders of magnitude. In addition, ornithopods exhibit multiple cases of gigantism (>5 tonnes) and putative cases of insular dwarfism making them ideal for testing Cope's Rule and the hypotheses forwarded by the Island Rule within a well defined, morphologically similar clade. Analyses of body size evolution within a detailed phylogenetic context reveal little to no support for the occurrence of insular dwarfs in Ornithopoda, in particular the most famous dinosaur "dwarf" *Telmatosaurus transsylvanicus*. Upper-body size limit analyses indicate that ornithopods plateaued early in their evolutionary history with the occurrence of giant iguanodontians in the Early Cretaceous (*Barilium* and *Iguanodon*). These limits do not appear to have been driven by environmental factors, such as sea level or atmospheric oxygen, but it is possible that the evolution towards this limit was driven by the marked decrease in sauropodomorph diversity in

Laurasia at the Jurassic-Cretaceous Boundary. Finally, several of the analyses suggest overall trends towards increasing body size in ornithopods. However, more detailed analyses within ornithopods indicate that designating the evolution of body size in this clade as strictly a trend represents an important oversimplification of the detailed pattern. These analyses suggest the occurrence of two early-burst (i.e., adaptive radiation) events in ornithopods: one in the initial stages of their evolution that correlates with the advent of upper-body size limits within this clade (and may be correlated with a shift from biped to quadruped), and then a subsequent event in the origin of Hadrosauridae (possibly associated with the evolution of dental batteries). The recovery of a possible early-burst model of evolution at certain times in the evolutionary history of ornithopods contradicts recent studies indicating a rarity of such models. However, such studies are based on extant datasets and the results presented here further emphasize the importance of investigating these models in fossil groups, which provide a deep time perspective.

4.2 Introduction

Body size is intimately associated with the ecology of extant vertebrates, including diversity (McClain and Boyer, 2009), population density (Damuth, 1981), home range (Brown *et al.*, 1993; Gaston and Blackburn, 1996; Burness *et al.*, 2001), and community structure (Eisenberg, 1990; Codron *et al.*, 2012b). In particular, community structure is often described by body size distributions, which (at least in mammals) are strongly dictated by trade-offs between short-term selective advantages for increases in body size (although these can purportedly lead to long-term trends, such as Cope's Rule) and long-term risks, with larger taxa exhibiting elevated levels of extinction, largely due to lower fecundity rates and hence longer recovery times following wanes in population numbers (Clauset and Erwin, 2008). These trade-offs, in association with

physiology- or morphology-driven lower body size limits, formulate the hypothesis for observed positively skewed size distributions in mammals (Elton, 1927; Colinvaux, 1978; Peters, 1983; Peters and Wassenberg, 1983; Griffiths, 1992; Blackburn and Gaston, 1994; Woodward *et al.*, 2005; Clauset and Erwin, 2008).

Non-avian dinosaurs exhibit a very large body size range, from ~500 g (Turner *et al.*, 2007; Chapter 2; Butler *et al.*, 2009) to well over 30,000 kg (see chapters 1 and 3) and in particular reached upper size bounds never again attained by terrestrial vertebrates. These have resulted in a generally opposite pattern of body size distribution in dinosaurs, compared to current mammalian faunas (Peczkis, 1994; Farlow *et al.*, 1995; Codron *et al.*, 2012b; O’Gorman and Hone, 2012; Brown *et al.*, 2013b), although this pattern is likely strongly affected by often unappreciated taphonomic biases against preserving small-bodied taxa (Behrensmeyer *et al.*, 1979; Kidwell and Flessa, 1996; Brown *et al.*, 2012b; Codron *et al.*, 2012a; Brown *et al.*, 2013b). Given their large size range and temporal duration, dinosaurs present a model system for investigating body size evolution on a macroevolutionary scale and the opportunity to study the evolution of short-term and long-term trade-offs of body size in fossil record, and whether their effects have varied over time. In order to begin to address these questions, however, fine-scale patterns of body size evolution need to be reconstructed in detail and investigated within the context of changing Earth Systems.

4.2.1 Body Size Evolution in Dinosauria

Attempts to quantify evolutionary patterns of body size in dinosaurs were first presented by Sereno (1997), who modeled dinosaur size as an ordered multistate discrete character. The author noted trends towards increases in size in multiple dinosaurian lineages (including thyreophorans, ornithopods, pachycephalosaurs, ceratopsians, sauropodomorphs, and basal

theropods). Decreases in size were rare, noted in certain pachycephalosaurs and certain theropod lineages, in particular preceding the origin of flight in dinosaurs; later supported by Turner *et al.* (2007).

Since Sereno (1997), the study of the evolution of body size in dinosaurs has been approached via different methods, but in general model body size as a continuous, rather than a discrete, variable. Hone *et al.* (2005) tested Cope's Rule in dinosaurs by reconstructing theoretical ancestor-descendant comparisons generated by contrasting (subtracting) closely related taxa at least 10 million years apart. The older taxon represents the putative ancestral stalk and overall contrasts (mean and median) were statistically tested against a null model of zero change in body size. Their results supported Sereno's (1997) trend towards increasing body size but did not support a size decrease in theropods leading up to the origin of birds. In addition, Hone *et al.* (2005) noted that although small taxa tended to get bigger, in general support for Cope's Rule, large taxa (above 7.8 m in length) trended towards smaller size, suggesting a possible optimal size. An alternative approach to *ad hoc* designations of particular species as ancestors is to estimate ancestral states. Methods, such as squared-change parsimony (SCP; Maddison, 1991), estimate ancestral states at a node by averaging values of the preceding node, along with succeeding nodes and terminal taxa. Ancestral states can be calculated without branch length information (Carrano, 2006; equivalent to assuming that all branches have a length of 1), or states can be weighted by branch length thereby maximizing the influence that closest nodes and/or terminal taxa have on ancestral reconstructions (Butler and Goswami, 2008; Ősi *et al.*, 2012). Based on resulting ancestral states, ancestor-descendant contrasts can be calculated and tested for trends.

To date, Carrano (2006) presents the most comprehensive study on body size evolution in a large sample of non-avian dinosaurs. The study utilized various approaches including, ancestor-descendant comparisons based on SCP, bivariate methods addressing both maximum and minimum size increases across time (age rank) and phylogeny (clade rank) (McShea, 1994; Alroy, 2000), and comparisons of size distributions between subclades and the overarching pattern. In general, Carrano (2006) obtained support for the occurrence of active trends when body size increases in non-avian dinosaurs. However, active trends were not supported in certain dinosaurian clades, and often depended on the methodology applied. In addition, the overall dinosaurian pattern is suggestive of passive trends throughout the Mesozoic. Analyses supported trends towards smaller body size in coelurosaurans (Sereno, 1997), a pattern also noted in macronarian sauropods indicating the presence of an upper body size bound in sauropodomorphs (Carrano, 2005; Sanders *et al.*, 2010).

The most recent studies forgo ancestor-descendant interpretations and apply model-fitting approaches that test the aptitude of evolutionary models (e.g., Brownian motion, directed trend, early-burst, single-stationary peak, and stasis) to particular datasets (Hunt and Carrano, 2010; Sookias *et al.*, 2012a; Sookias *et al.*, 2012b; Zanno and Makovicky, 2013). Hunt and Carrano (2010), largely based on the dataset of Carrano (2006), fit models of Brownian motion (with and without a trend) and stasis to a phylogenetic tree of ornithischian dinosaurs, and obtained greatest support for an overall trend model, indicating size increases in this clade (i.e., Cope's Rule). Similar methods were most recently applied by Sookias *et al.* (2012b) to test overall patterns in the evolution of size from the Late Permian to the Late Jurassic in archosauromorphs and synapsids. In contrast to previous studies, Sookias *et al.* (2012b) obtained little support for the trend model, suggesting that early body size evolution in archosauromorphs is largely passive followed by periods of stasis as clades become more exclusive. A subsequent study by this

research group recovered evidence for upper body size limits in archosauromorphs through this time interval, and found little support that this pattern was driven by environmental factors, including oxygen, temperature and land area (2012a).

Despite interest in understanding general patterns in the evolution of body size in dinosaurs, few studies have attempted to reconstruct smaller scale patterns within smaller clades as recommended by Alroy (2000). Patterns at lower taxonomic levels permit a better assessment of nuances in the data (e.g., taxonomic opinions and temporal occurrence) and in addition generally comprise morphologically similar taxa that may provide a more robust approach to understanding the mechanisms that have driven body size in the past. To date, studies reconstructing the evolution of body size in more exclusive dinosaur clades include: paravians (Turner *et al.*, 2007), sauropods (Carrano, 2005; Sanders *et al.*, 2010), herbivorous theropods (Zanno and Makovicky, 2013), rhabdodontid ornithopods (Ösi *et al.*, 2012), and Mesozoic birds (Butler and Goswami, 2008; Hone *et al.*, 2008). Overall patterns of body size evolution in Ornithischia were investigated by Hunt and Carrano (2010), but this study will focus on the evolution of body size in the more exclusive group, Ornithopoda, and reconstruct the detailed macroevolutionary patterns of body size within this clade.

4.2.2 Body Size Evolution in Ornithopoda

Ornithopod dinosaurs comprise a long-lived (~100 Ma) clade of herbivorous taxa that attained a cosmopolitan distribution throughout the Jurassic and Cretaceous (Sues and Averianov, 2009; Prieto-Márquez, 2010; McDonald, 2012). Importantly, they span a large size-range [four orders of magnitude, from thecelosaurids (~5 kg) to iguanodontians (>10,000 kg) (e.g., Paul, 1997; Seebacher, 2001)] and have been intensively sampled and researched (in particular hadrosaurids; Horner *et al.*, 2004). As a result, they represent a model clade within which to investigate

macroevolutionary patterns of body size. Ornithopods include multiple ‘giants’, such as *Iguanodon bernissartensis*, *Edmontosaurus regalis*, *E. annectens*, *Barsboldia sicinskii*, and *Magnapaulia laticaudus*, all of which approach 10 tonnes, and *Shantungosaurus giganteus*, which may have weighed almost 20 tonnes, greater than most sauropods (e.g., *Diplodocus*), and are therefore ideal for testing upper-body size limits in a dinosaur clade. Several ornithopod taxa have also been hypothesized to represent instances of insular nanism (dwarfism), including: *Telmatosaurus transsylvanicus*, *Zalmoxes robustus*, and *Tethyshadros insularis* (Weishampel *et al.*, 1993; Weishampel *et al.*, 2003; Dalla Vecchia, 2009; Benton *et al.*, 2010; Dalla Vecchia *et al.*, 2011; Ősi *et al.*, 2012). Insular dwarfism, in which species on an island are smaller than their continental counterparts, is one of the fundamental predictions made by the Island Rule, introduced by Foster (1964) and coined by Van Valen (1973). In general terms, and as defined in mammals, the Island Rule predicts that large-bodied taxa (such as elephants, artiodactyls, and carnivores) evolve towards smaller forms on islands, whereas the reverse occurs in small-bodied taxa, such as rodents, which tend towards larger size. Trends towards smaller size, such as those putatively recognized in ornithopods, are often explained by reduction in short-term advantages of larger body size, such as reductions in predation and/or interspecific competition when on an island (e.g., Damuth, 1993). Although it is still premature to hypothesize evolutionary mechanisms for insular dwarfism in dinosaurs, ornithopods are ideal for testing its occurrence earlier on in Earth’s history. Finally, ornithopods have a well-sampled rock record resulting in a large sample size of taxa that are well defined, phylogenetically and morphologically, and are therefore ideal for testing Cope’s Rule (Alroy, 1998).

4.2.3 Cope's Rule

Cope's Rule is one of the most investigated and tested macroevolutionary trends in dinosaurs and other fossil vertebrates (Alroy, 1998; Laurin, 2004; Hone and Benton, 2005; Hone *et al.*, 2005; Carrano, 2006; Butler and Goswami, 2008; Hone *et al.*, 2008; Hunt and Carrano, 2010; Sookias *et al.*, 2012b; Zanno and Makovicky, 2013), due to the fact that dinosaurs exhibit a very large range in size and are often regarded as the ‘poster-child’ of “increases of size in phyletic branches” (Depéret, 1907; pg. 193), the most common phraseology used to depict Cope’s Rule. However, Edward D. Cope, never formally defined this trend and only briefly mentions an overall tendency towards larger body sizes from ‘lower’ to ‘higher’ orders in his essay *The Origin of the Fittest: Essays on Evolution*:

“While the amount of simple growth-force, represented in adult living animals, has varied very irregularly throughout the animal kingdom, there being large and small in every division, it would seem to have *accumulated*, on the whole, with the *rising scale of animal types*. Thus the lower or Protozoa are the smallest; Radiates are next in size; Molluscs and Articulates reach nearly the same maximum, which exceeds that of the Radiates, and falls far below that of the Vertebrates. Among the last the Mammalia have attained as large if not larger size than any of the other orders (e.g., Cetacea). This is, however, *not necessary to the history of evolution.*” (Cope, 1887; pg. 204)

As defined by Cope (1887), a tendency towards large size need not be absolute, but rather represents an overarching tendency in animals. Furthermore, his reference to ‘accumulation’ may be better interpreted as increases in upper body size bounds, but not necessarily changes in lower bounds; a pattern suggestive of passive (or Brownian) rather than driven trends (as defined by McShea, 1994). The cooption of this overall tendency reported by Cope (1887) to reflect a biological ‘law’ was forwarded 20 years later by Depéret (1907; ch. 19), who referred to it as ‘la

loi d'augmentation de taille dans les rameaux phylétiques' or 'the law of increasing size in phyletic lineages'. Depéret (1907) described the evolution of large size as 'progressive' providing examples from all parts of Animalia, and contested phyletic decreases in body size, including the occurrence of insular dwarfism (Depéret, 1907; pg. 210). This led researchers, such as Simpson (1953) to refer to phyletic increases in size as 'Depéret's Rule' rather than 'Cope's Rule'. The use of 'Cope's Rule' to identify phyletic increases in size was proposed by Rensch (1943, 1948), who described size increases and decreases in insects, along with associated allometric affects (see also Newell, 1949). The difference between Cope's original broad depiction of body size increases throughout evolutionary history of animals and Depéret's precise phyletic interpretation was also noted by Stanley (1973), and most recently mentioned by Laurin (2010), whom opted instead to identify the trend as 'Cope-Depéret's Rule'. Despite noted differences between Cope and Depéret interpretations, most studies on body size evolution in dinosaurs still define Cope's Rule as *driven*, rather than passive, trend toward large body size throughout the evolutionary history of a lineage. (Hone and Benton, 2005; Hone *et al.*, 2005; Carrano, 2006; Butler and Goswami, 2008; Hone *et al.*, 2008; Hunt and Carrano, 2010; Sookias *et al.*, 2012b; Zanno and Makovicky, 2013). In order to be consistent with over a century of research on this pervasive trend, I have opted to define Cope's Rule, as a driven trend.

Traditional hypotheses for Cope's Rule included direct benefits of larger body size (see Hone and Benton, 2005) including inter/intraspecific competitive advantages, increased ability to capture prey/fend off predators due to increases in strength, increases in reproductive success, larger brain size, extended lifespan, increased ability to retain body heat that can lead to overall increased resistance to environmental changes, and increased variability in food choice to explain directed trends towards large body size (Depéret, 1907; Newell, 1949; Kurtén, 1953; Rensch, 1959; Gould, 1966; McLain, 1993). Any one of these hypotheses would predict a

driven, rather than passive, evolutionary trend towards large body size due to selective pressures acting against small-bodied exemplars. However, as first presented by Stanley (1973), evolution towards large body size need not result from benefits of larger size but rather the observation that the ancestors of higher taxonomic groups tend to be small-bodied. Given biological limitations of small-body size (such as the endoskeleton in vertebrates), body size evolution will tend towards increases, rather than decreases, in size (Stanley, 1973). Under this scenario, a trend towards increasing body size is considered to be passive, smaller-bodied taxa within a clade are not selected against, and lower body size bounds remain generally constant through time and phylogeny (McShea, 1994). Recently, Kingsolver and Pfennig (2007) compared the direction of selection on direct measurements of size (e.g., mass, length, *etc.*) compared to other morphological characters, which although likely related to size, are not directly associated. The authors observed that size measurements exhibited strong positive selection, whereas other traits exhibited both positive and negative selection. Based on these results, the authors predicted that Cope's Rule should be accompanied by a strong, driven trend towards large body size, a hypothesis that requires empirical testing.

Over the last several decades studies have attempted to quantify Cope's Rule utilizing various empirical datasets with results both supporting and rejecting this pattern in different groups (Newell, 1949; Jablonski, 1997; Alroy, 1998; Laurin, 2004; Van Valkenburgh *et al.*, 2004; Hone *et al.*, 2005; Carrano, 2006; Hunt and Roy, 2006; Butler and Goswami, 2008; Hone *et al.*, 2008; Novack-Gottshall, 2008; Hunt and Carrano, 2010; Raia *et al.*, 2012; Zanno and Makovicky, 2013). Support for this pattern has varied depending on the dataset (as expected), but also based on methodology applied (e.g., in Mesozoic birds: Butler and Goswami, 2008; Hone *et al.*, 2008). This level of variation has led researchers to either discount the universality of Cope's Rule, or to consider Cope's Rule as simply a pattern that can be explained by both

driven (i.e., selection) or passive (i.e., increases in variation) processes and that these require to be studied on a case-by-case basis (Jablonski, 1997). Importantly, Alroy (1998) suggested that within- vs. among-clade comparisons need to be considered when attempting to test for Cope's Rule, and that large sample sizes may obscure driven trends due to different mechanisms acting among lineages. As a result, in order to properly test for such patterns, analyses should be conducted at lower, rather than more inclusive, taxonomic scales (Alroy, 1998).

In keeping with Alroy's (1998) suggestion the final chapter of this dissertation will apply the results obtained in the previous chapters to reconstruct the macroevolutionary patterns of body size in Ornithopoda. Recent analyses recover a highly pectinate cladogram structure for ornithopods (i.e., successive sister-clade relationships; e.g., Prieto-Márquez, 2010; Han *et al.*, 2012; McDonald, 2012), with the exceptions of a major dichotomy within Hadrosauridae (Hadrosaurinae and Lambeosaurinae) and perhaps a few small clades near the base of the ornithopod tree, such as Rhabdodontidae (Han *et al.*, 2012; Ősi *et al.*, 2012) and Thescelosauridae (Brown *et al.*, 2013a). Given the current phylogenetic and temporal context known for ornithopods, I intend to explore the patterns of body size evolution in this clade and test for Cope's Rule and the occurrence of a driven, positive trend in body size through their evolutionary history. In addition, I will test hypotheses of insular dwarfism in ornithopod dinosaurs. Finally, I will explore upper body size limits and discuss potential factors (e.g., land area) that may have played a role in driving macroevolutionary patterns of body size in this group.

4.3 Methodology

4.3.1 Dataset Construction

Body size can be represented by various metrics (e.g., body height or total body length).

However, body mass is generally thought to represent the standard measure of size, as it forms the standard variable for most studies examining the correlations between ecological and physiological properties and size in extant taxa (e.g., Peters, 1983; Calder, 1984). Body mass cannot be directly measured in the fossil record and, as a result, must be estimated or approximated using a proxy. The latter represents the most common approach in studies attempting to reconstruct macroevolutionary scale patterns of vertebrate body size in deep-time (Laurin, 2004; Hone *et al.*, 2005; Carrano, 2006; Hunt and Carrano, 2010; O’Gorman and Hone, 2012; Ősi *et al.*, 2012; Sookias *et al.*, 2012a; Sookias *et al.*, 2012b). In particular, studies use femoral length as a measure of overall size (e.g., Carrano, 1998; Sookias *et al.*, 2012b), and although it likely represents a robust proxy for size at low taxonomic scales, the results of Chapter 1 (Campione and Evans, 2012) indicate that, in terms of body mass, femoral length represents a poor proxy for size when sampling a broad range of terrestrial mammals and reptiles. For example, *Panthera tigris* (Siberian tiger; CN 5698) and *Rhinoceros sondaicus* (Javan Rhinoceros; ZMUC uncataloged) have a similar femoral length, 411 mm and 515 mm respectively, but are almost an order of magnitude different in mass, 230 kg and 1,435 kg respectively (see Appendix 1). These discrepancies will have a particularly large effect on finer-scale interpretations, such as when comparing the sizes of herbivores and carnivores (Sookias *et al.*, 2012b). Finally, in datasets where both bipedal and quadrupedal taxa are sampled (as in Ornithopoda) using a single measurement proxy based on the hindlimb fails to incorporate data

on the forelimb, which in quadrupeds is also involved in weight support. Such an approach will underestimate the size of a quadruped relative to a biped.

In order to investigate the macroevolutionary patterns of body size in ornithopod dinosaurs I compiled an extensive dataset of limb measurements for 89 ornithopod species. Unlike previous studies of body size evolution, I use body mass estimates obtained from stylopodial circumferential measurements of the diaphysis and based on the phylogenetically corrected equations presented in chapters 1 and 2 for quadrupeds and bipeds respectively. These equations require the femoral and humeral circumferences to estimate mass. Unfortunately, a large number of taxa either do not preserve these elements, or their state of preservation precludes a robust and meaningful measure of circumference resulting in approximately 65% missing circumference data for the femur. As a result, the dataset includes a wide variety of limb bone measurements, as well as skull length, in order to provide as large a dataset possible to better estimate missing stylopodial circumferences. Measurements include the lengths and minimum circumferences of the humerus, radius, ulna, femur, tibia, fibula and metatarsal III (only length). Most measurements were taken via direct examination of specimens using callipers for lengths (<30 cm) and/or a tape measure for lengths (>30 cm) and minimum circumference. The dataset is extensively complemented by measurements provided in the literature for several taxa. All measurements and their sources are provided in Appendix 5.

This study samples the vast majority of known ornithopods. Fourteen taxa were not included due to their incomplete nature: *Blasisaurus canudoi* (Cruzado-Caballero *et al.*, 2010), *Fukuisaurus tetoriensis* (Kobayashi and Azuma, 2003), *Huehuecanauhtlus tiquichensis* (Ramirez-Velasco *et al.*, 2012), *Iguanacolossus fortis* (McDonald *et al.*, 2010b), *Jaxartosaurus aralensis* (Godefroit *et al.*, 2004), *Jeyawati rugoculus* (McDonald *et al.*, 2010a), *Kerberosaurus*

manakini (Bolotsky and Godefroit, 2004), *Lanzhousaurus magnidens* (You *et al.*, 2005), *Levnesovia transoxiana* (Sues and Averianov, 2009), *Macrogyphosaurus gondwanicus* (Calvo *et al.*, 2007), *Parasaurolophus tubicen* (Sullivan and Williamson, 1999), *Penelopognathus weishamplei* (Godefroit *et al.*, 2005), *Shuangmiaosaurus gilmorei* (You *et al.*, 2003), and *Zephyrosaurus schaffi* (Sues, 1980). These taxa are generally known from few skeletal remains and, most importantly, do not preserve any limb bones and thus the required measurements for mass estimation cannot be obtained or confidently approximated. In addition to the taxa listed above, ten taxa were not included due to their poorly resolved phylogenetic affinities: *Cedrorestes crichtoni* (McDonald *et al.*, 2010a), *Cumnoria prestwichii* (McDonald, 2011), *Draconyx loureiroi* (McDonald *et al.*, 2010b), *Gongbusaurus wucaiwanensis* (Dong, 1989), *Hypselospinus fittoni* (McDonald *et al.*, 2010b), *Lurdusaurus arenatus* (McDonald *et al.*, 2010b), *Nanningosaurus dashiensis* (Mo *et al.*, 2007), *Notohypsilophodon comodorensis* (Coria *et al.*, 2007), *Planicoxa vananica* (McDonald *et al.*, 2010b), *Yandusaurus hongheensis* (Butler *et al.*, 2008; Han *et al.*, 2012), and *Yueosaurus tiantaiensis* (Zheng *et al.*, 2012). Finally, ten taxa were excluded due to both a lack of limb bones and poorly resolved phylogenetic affinities: *Angulomastacator daviesi* (Wagner and Lehman, 2009), *Dakotadon lakotaensis* (McDonald *et al.*, 2010b), *Delapparentia turolensis* (Ruiz-Omeñaca, 2011), *Drinker nisti* (Galton, 2007), *Osmakasaurus depressus* (McDonald, 2011), *Qantassaurus intrepidus* (Agnolin *et al.*, 2010), *Ratchasimasaurus suranareae* (Shibata *et al.*, 2011), *Sellacoxa pauli* (Carpenter and Ishida, 2010), *Siamodon nimngami* (Buffetaut and Suteethorn, 2011). A complete list of the 89 ornithopod taxa used in this study is provided in Appendix 5.

4.3.1.1 Temporal Context

One of the main advantages of studying patterns of morphological evolution in the fossil record is that it permits these patterns to be investigated within a temporal context that can then be associated to environmental dynamics, including climatic and geographic changes. As a result, the dataset constructed here includes the ages for all taxa initially taken from the PaleoBiology Database (paleodb.org). Given the difficulties associated with constraining fossil ages (i.e., taxa are generally described from broad temporal stages that reflect a poorly constrained biostratigraphic framework), temporal data for most taxa are defined based on the start and end of stage(s) and/or sub-stage(s) from which they were described. For example, *Iguanodon bernissartensis* is described from the Barremian (age) to the Early Aptian (age) (Paul, 2008) and therefore its age is defined between 130 to 112 Ma, with a midpoint age of 121 Ma. These ages are obtained from Gradstein *et al.* (2004). The temporal occurrence of certain taxa, in particular those from well-sampled North American deposits (e.g., Dinosaur Park Formation), are better defined and a more precise age is adopted when possible (see Appendix 5 for age references).

4.3.1.2 Body Mass Estimation

The body mass of all ornithopod taxa included in this study was derived using the results of chapters 1 and 2, which provide phylogenetically corrected equations for estimating mass in quadrupeds, based on the relationship between humeral and femoral circumference and body mass in terrestrial quadrupeds, and bipeds, based on femoral circumference and a mathematical correction of the equation obtained for quadrupeds. Both equations are implemented in the R package ‘MASSTIMATE’ (Campione, 2013). Assessment of whether a species was bipedal or

quadrupedal is problematic in dinosaurs, especially among ornithischians in which quadrupedality has evolved multiple times (Maidment and Barrett, 2012). Quadrupedality evolved at least once in ornithopods, but the details of this transition have not been studied in detail. Nevertheless, small-bodied taxa, such as the celosaurids, *Hypsilophodon*, and *Gasparinisaura*, have long been considered to be bipedal based on the morphology of their manus and pelvic girdle (Norman *et al.*, 2004), and were regarded as such in this study. Although often regarded in the literature as facultatively bipedal (Horner *et al.*, 2004), postcranial anatomy and trackways now strongly support the notion that at least hadrosaurids, and potentially most iguanodontians, were predominantly quadrupedal (Dilkes, 2001; Lockley and Wright, 2001; Maidment and Barrett, 2012; Maidment *et al.*, 2012; Maidment *et al.*, in press). Given the transition from biped to quadruped in non-hadrosauriform iguanodontians, assessment of gait can be difficult in this grade of ornithopods. Designations of gait in this study follow in large part those of Maidment *et al.* (2012). In addition, the morphology of the distal manual phalanges, in particular whether the taxon possessed hooves or claws, aided gait assessments, as the presence of hooves was regarded as an indication of quadrupedality. In general, all non-iguanodontian ornithopods (i.e., Thescelosauridae and *Hypsilophodon*) were considered to be bipedal and all iguanodontians were considered to be quadrupedal, with a few exceptions (see Appendix 5). Despite the possibility of miscategorising the gait, or even the presence of varying degrees of quadrupedality in these taxa, its designation will likely not significantly affect the results of the evolutionary analyses. Mass estimation of the hadrosaurid sample using both the quadrupedal and bipedal equations reveals that the bipedal formula provided, on average, 20% lower estimates of body mass relative to the quadrupedal equation. That value is in terms of non-log body mass estimates; whereas logged estimates reveal only a 1.7% difference between mass

estimation equations. Given that all analyses are run using the logarithmically transformed data, this minor difference is unlikely to have a significant effect on the interpretation of the results.

As described earlier, the dataset is fraught with missing data due to the incomplete nature of most specimens. The circumference values could not always be directly obtained and were therefore estimated based on other known values. Numerous methods for estimating missing data have been discussed within the context of morphometric data and multivariate analyses (Rubin, 1976; Strauss *et al.*, 2003; Strauss and Atanassov, 2006; Nakagawa and Freckleton, 2008; Brown *et al.*, 2012a). Recently, Brown *et al.* (2012a) suggested that BPCA (Oba *et al.*, 2003) represents one of the better methods for estimating missing data, tested by degenerating a complete morphometric dataset and comparing estimated results with the original complete results. Although my dataset is not meant for multivariate analysis, I applied BPCA, implemented in the R package ‘pcaMethods’ (Stacklies *et al.*, 2007). In order to verify the estimated data, all measurements (including originals and estimates) were plotted against each other. Strong correlations exist between limb bone measurements (e.g., Chapter 1; Christiansen, 1999a, c; Carrano, 2001; Campione and Evans, 2012) and hence predict that there be no evidence of systematic biases between scaling of estimated and original values. In addition to BPCA, I implement another estimation technique that creates a correlation matrix derived from the original data and then estimates missing values from a bivariate regression equation with the strongest correlate. The latter is implemented in the package ‘LOST’ (Arbour and Brown, 2012). It is expected that the regression estimation technique may provide the most reliable results given that it assumes strong correlations between variables, such as those observed between limb measurements. However, it may reduce the overall variance in the dataset and reduce the probability of recovering outlier data-points.

4.3.2 Phylogenetic Context

Despite over a century of research on ornithopod dinosaurs, no complete phylogenetic analysis of Ornithopoda has ever been attempted. Therefore, a tree was manually constructed based on a compilation of recent analyses conducted at various regions within the ornithopod tree (Figure 4-1). Hadrosaurids are the best-studied ornithopod clade, and numerous phylogenies have been proposed for this clade. In order to retain a certain amount of resolution, the hadrosaurid portion of the tree is largely based on the topologies of Evans (2010), Godefroit *et al.* (2012), and Prieto-Márquez (2010), with additions and amendments made for particular species, including *Aristostavus gaglarseni* (Gates *et al.*, 2011), *Magnapaulia laticaudus* (Prieto-Márquez *et al.*, 2012), *Arenysaurus ardevoli* (Pereda-Suberbiola *et al.*, 2009), *Shantungosaurus giganteus* and *Wulagosaurus dongi* (Xing *et al.*, 2012), and *Barsboldia sicinskii* (Prieto-Márquez, 2011). The phylogeny of non-hadrosaurid iguanodontians is based on that proposed by McDonald *et al.* (2010b) and McDonald (2012). Finally, the base of the ornithopod tree is primarily derived from phylogenies proposed by Ősi *et al.* (2012), Han *et al.* (2012), Butler *et al.* (2008), Boyd *et al.* (2009), and Brown *et al.* (2013a). The tree was assembled in Mesquite version 2.74 (Maddison and Maddison, 2010).

In order to reconstruct ancestral states or fit models of evolution on a tree, branch lengths estimates are required to standardize for the expected variation between an ancestor-descendant pair (Garland *et al.*, 1992). Ideally branch lengths measure, or are at least directly related to the amount of evolutionary change that has occurred between nodes and between nodes and terminal taxa. These are relatively easy to generate via molecular data, when dealing with extant phylogenies (e.g., Bininda-Emonds *et al.*, 2007), however, molecular data are virtually impossible to obtain in deep time. Palaeontological studies should ideally rely on morphological

changes (as attempted by Brusatte *et al.*, 2008b); in practice, phylogenetic character matrices of extinct taxa are fraught with missing data (e.g., 36% missing data in the hadrosaurid matrix of Prieto-Márquez, 2010) that would result in incomplete and possibly biased representations of character evolution and thus inaccurate branch lengths. In this particular case, no complete character matrix yet exists for ornithopods and therefore consistent branch lengths cannot be determined through the use of character data. As a result, branches need to be estimated using other methods or assumptions, including assigning all branches a length of 1, which assumes equal evolutionary change along each branch, or the use of evolutionary time (in millions of years [Ma]), most commonly used (Laurin, 2004; Ruta *et al.*, 2006; Brusatte *et al.*, 2008b; Hunt and Carrano, 2010). The latter provides a proxy for how much evolutionary change has occurred along a branch by measuring the amount of time where change could have taken place; however, it assumes that the evolutionary rate is constant throughout the tree, which will not necessarily fit a punctuated model of evolution (Eldredge and Gould, 1972).

Given the current limitations of branch length estimation techniques available for palaeontological datasets, both uniform and time-based branch lengths were applied to the ornithopod tree in order to better understand their effects on the results. This is particularly important given that branch lengths are thought to have a stronger effect on results than tree topology (D. Bapst, Personal Communication). Uniform branch lengths (i.e., equal to 1; Figure 4-2A) were assigned in R (R Development Core Team, 2012) using the package ‘APE’ (Paradis *et al.*, 2004). Branch time-scaling was done using ‘paleotree’ (Bapst, 2012) based on the age-range of the terminal taxa. Time-scaling in the strictest sense (i.e., a traditional time-calibrated phylogeny; Figure 4-2B) results in several branch lengths of zero that will not allow several of the analyses to be carried out. As a result, four time-scaling methods were applied in order to assess their sensitivity: 1) the equal time-scaling adds a predetermined and arbitrary amount of

time (10 Ma is used here; Figure 4-2C) to the root of the tree, and then distributes this time equally to all zero-length branches (Brusatte *et al.*, 2008b); 2) the all branches additive (aba) method treats all branches evenly and adds a designated amount (here 1 Ma; Figure 4-2D); 3) the zero-length branches additive (zlba) method acts only on those branches with zero branch length and adds the desired time (here 1 Ma; Figure 4-2E); and 4) the minimum branch length (mbl) method is similar to zlba, however, it corrects the ages of terminal taxa in order their retain relative consistent with the original, time-calibrated tree.

Independent of time-scaling methodological details, the resulting branch lengths make particular assumptions about where evolutionary changes take place and where they are concentrated. For instance, by equally distributing time added to the root (equal-scaling method) it pulls back early, temporally non-resolved dichotomies (e.g., the clade of *Thescelosaurus neglectus* and *T. assiniboiensis*), thereby assuming that at least as much evolution has occurred within the species lineages than along the ancestral branch prior to the species dichotomy. Aba- and zlba-scaling retain dichotomous splits closer to their original temporal occurrence, however, depending on how much time is added, either to all branches (aba) or only zero-length branches (zlba) it has the potential to pull the origin of the tree back several 10s of millions of years. In addition, the latter scaling techniques have the potential to alter the relative temporal occurrence between taxa so that coeval taxa no longer occur at the same time. Finally, mbl makes the fewest number of assumptions relative to the original, time-calibrated tree. In addition to only affecting zero-length branches, it corrects the temporal ages of terminal taxa so not to alter their relative temporal occurrence. The latter time-scaling method provides the strongest nodal age correlation with the unaltered time-calibrated phylogeny ($r= 0.9963$), whereas the equal scaling method provides the lowest correlation coefficient ($r=0.969$; Appendix 6). The majority of analyses will

be run using the mbl method; however, certain analyses will be run using various other scaling techniques so as to assess their effect on final results.

4.3.3 Analyses

Here I use the ornithopod body mass and phylogenetic data described in the previous sections and apply a variety of analyses that have been applied in the last decade or so to comprehensively investigate the patterns of body size both in a broad context, and on a finer scale (Hone *et al.*, 2005; Carrano, 2006; Sookias *et al.*, 2012a; Sookias *et al.*, 2012b; Zanno and Makovicky, 2013). Given that all analyses will be conducted on the same dataset, it allows to better compare the results obtained from each and discuss their relative merits. All analyses and plots were carried out in R (R Development Core Team, 2012) through the use of various packages as specified.

4.3.3.1 Testing for Cope's Rule

Numerous studies have attempted to quantitatively test Cope's Rule in the vertebrate fossil record, and although the details may vary, most analyses attempt some form of ancestor-descendent comparison (Laurin, 2004; Hone *et al.*, 2005; Carrano, 2006; Hone *et al.*, 2008; Laurin, 2010). Methods for estimating ancestral states vary, but here I reconstruct ancestral states by using a maximum likelihood algorithm developed by Schluter *et al.* (1997) that is equivalent to the weighted squared-change parsimony (Maddison, 1991). This algorithm estimates ancestors based on an average of values in adjacent nodes or terminal taxa and then weights the relative effects of these values based on their distance (i.e., branch length) from the desired node. Contrasts were then calculated between ancestors and descendants by subtracting the descendant from the ancestor. Positive and negative values represent increases and decreases in body size,

respectively. If Cope's Rule (a driven trend) is to be supported, a distribution of contrasts should tend towards a negative skew that is driven by a significantly greater number of positive contrast values (Carrano, 2006). This pattern was tested by statistically comparing the mean contrast value to a null contrast of zero change using a two-tailed t-test, by comparing the observed distribution to a normal distribution *via* a Shapiro-Wilk Normality Test, and by comparing the observed ratio of positive to negative contrast values to an expected ratio of 1:1 through the use of a Chi-squared test. These analyses were run on the total ornithopod dataset, along with major ornithopod subclades: Iguanodontia, Hadrosauroidea, Hadrosauridae, Hadrosaurinae, and Lambeosaurinae.

Investigation of Cope's Rule in Ornithopods was also conducted by plotting mass against both time (measured in absolute terms or as ranked) and relative phylogenetic position [measured as the distance from the root, assuming uniform branch lengths; clade rank (patristic distance of Carrano, 2006)] through the use of bivariate plots. Age rank is measured based on the midpoint age of each species, and clade rank is measured as the number of nodes between the terminal taxon and the root node. Clade rank was calculated using the 'distRoot' function in the package 'adephylo' (Jombart and Dray, 2011).

Recent studies attempting to test for Cope's Rule adopt a likelihood approach (Hunt and Carrano, 2010; Sookias *et al.*, 2012b; Zanno and Makovicky, 2013) whereby models, defined by a suite of parameters that describe a particular pattern, are fit to the data. Models can then be compared (via the Akaike Information Criterion [AIC] and associated Akaike Weights [AW]) and the best-fit model is considered to represent the best explanation for a given dataset. Model fitting was implemented in the R package 'geiger' (Harmon *et al.*, 2009) through the 'fitContinuous' function where I fit a trend (Generalized Random Walk), Brownian motion

(Unbiased Random Walk), stasis, Ornstein-Uhlenbeck (single stabilizing selective peak), and early-burst (adaptive radiation) models of evolution. ‘fitContinuous’ permits incorporation of error associated with the modelled trait (i.e., body mass). Error was measured via the standard error of the estimate obtained for the phylogenetically corrected equation and the extant dataset of Chapter 1 (Table 1-9; SE=0.135). In order to support Cope’s Rule a trend model of evolution should be supported.

4.3.3.2 Testing for Insular Dwarfism

The Island Rule predicts that large-bodied animals will decrease in size upon entering an island habitat (Foster, 1964). As a result, putative ornithopod dwarfs should show a significant decrease in body size relative to the reconstructed ancestor. In order to test this I utilized the ancestor-descendent contrasts introduced in the previous section. Based on these contrasts it is possible to generate a 95% prediction range where the vast majority of data points are expected to lie. Contrasts outside these intervals represent significant shifts in body size. Therefore, I would predict that putative insular dwarfs, including *Telmatosaurus transylvanicus*, *Zalmoxes robustus*, and *Tethyshadros insularis* (Weishampel *et al.*, 1993; Weishampel *et al.*, 2003; Dalla Vecchia, 2009; Benton *et al.*, 2010), should occur either close to or even outside the 95% prediction intervals.

4.3.3.3 Assessing Upper Body Size Limits

Despite the interest in the evolution of body size in dinosaurs, only recently have upper body size limits been quantified, in this case across the Triassic and Jurassic (Sookias *et al.*, 2012a). The authors recovered an upper limit for all dinosaurs, but did not support the notion that these limits were driven by environmental factors. I will apply similar methods to test the presence of an

upper body size limit in ornithopods. The size data were temporally binned at 5 Ma and 10 Ma to assess possible effects of time-averaging. Taxa included within these bins were determined using two different age measures: 1) their midpoint age, where a taxon will only be counted in one bin; and 2) the age range, where a taxon will be included in all bins that it crosses.

In order to assess the presence of an upper size limit previous studies recommend the use a Gompertz model (Smith *et al.*, 2010; Sookias *et al.*, 2012a), which is similar to a logistic model, but is asymmetrical, with an initial rapid increase that quickly reaches an asymptote. The fit of the Gompertz model was compared to linear, logarithmic, and logistic models using AIC. Gompertz should represent the lowest AIC score.

4.3.3.4 Further Data Exploration

In addition to the analyses mentioned above, I will use the constructed dataset to explore the evolution of body size in ornithopods in more detail, by elaborating on the model fitting approaches discussed above. These models were fit in the same manner as that described above for the trend and Brownian motion models. However, instead of fitting the models for the entire ornithopod tree, I ran the model-fitting functions along the main spine of the tree, including all clades with at least 10 taxa (as recommended by Harmon *et al.*, 2010). This provides a measure of model stability within ornithopods and the ability to observe how preferred models change throughout the evolutionary history of this clade. This approach is analogous to that presented by Sookias *et al.* (2012b) that fit models at particular ‘important’ nodes within Archosauromorphs (e.g., Dinosauromorpha, Pterosauria, *etc.*) and Therapsida (e.g., Anomodontia, Cynodontia, *etc.*) however my approach does not make prior assumptions of node ‘importance’ and instead fit models in a more continuous fashion from the root of the tree to near the apex. This technique is more justified given that ‘important’ nodes, which simply represent those that, historically, were

deemed worthy of naming, are artificial constructs and just because a node is historically significant does not necessarily mean that it represents the region of greatest evolutionary change or diversification.

4.4 Results

4.4.1 Missing Data Estimation

Brown *et al.* (2012a) recommended BPCA as the preferred method for estimating missing morphometric data, but suggested that further tests with other datasets were still needed in order to more holistically confirm their conclusions. In particular, the authors found that errors associated with estimating missing data were highest when missing data were biased towards certain anatomical regions or taxonomic groups. Given the large amount of data missing from the present dataset (Appendix 5; 63.8% missing data overall) and the identification of anatomical biases (e.g., femoral length has 25% missing data and radial length is 68.2% missing data), I verified estimated values by generating bivariate plots and visually inspecting for systematic biases in estimates. Using BPCA revealed important systematic biases in humeral circumference estimates, which are systematically greater than data points based on original measured data (Figure 4-3). These systematic biases are unexpected between limb measurements given the strong correlations that are generally recovered between such variables across disparate taxa (Christiansen, 1999a; Carrano, 2001; Kilbourne and Makovicky, 2010; Campione and Evans, 2012) and would result in body mass over estimation in multiple taxa. In comparison, the use of a correlated-variable regression estimation technique results in no systematic biases (Figure 4-4), although the variation is highly reduced relative to the original data and BPCA estimates.

Nevertheless, given the lack of a systematic bias, it seems that the latter estimation technique is most appropriate here.

4.4.2 Trend Analyses

Ancestor-descendent reconstructions provide minor to no support for a directed trend towards large or small body size in ornithopods or any subclade therein (Figure 4-5; Table 4-1). Distributions, in general, centre on a mean zero-contrast, with the exception of a significantly greater than zero mean in Iguanodontia when analysed using certain trees (equal, aba, and zlba). A Chi-squared test of the positive/negative-contrast count data reveal a greater number of significant increases in body size when the tree is scaled using the ‘equal’ method, including directed trends in all clades except Hadrosaurinae, when 1 Ma is added to the root node. The addition of 10 Ma to the root node resulted in non-significance in ornithopods and iguanodontians, overall. In contrast to the t-test of mean, the Chi-squared test did not recover an increasing trend in Iguanodontia in the aba and zlba trees, a pattern it did recover in Hadrosauridae. No significant trends were noted using the preferred time-scaling method (mbl; Table 4-1).

Bivariate plots between age/clade-rank and body size reveal different patterns (Figure 4-6). Results based on age-rank do not indicate a strong directional trend towards large body size, but rather an initial increase in body size variance followed by relative stability through time. Despite this passive appearance, a spearman correlation including all ornithopod data indicates a strong significant relationship between axes ($\rho=0.339$, $S=75106.9$, $p=0.001$) indicative of an overall increase in body size through time (i.e., a driven trend). Subdivisions within ornithopods, such as Iguanodontia, Hadrosauroidea, and Thescelosauridae, also exhibit significant correlations between age rank and size ($\rho=0.385$, $S=46776.3$, $p=0.0005$; $\rho=0.412$,

$S=14584.6$, $p=0.002$; and $\rho=0.723$, $S=45.6$, $p=0.018$, respectively). The relationship between clade-rank and size exhibits a rapid initial increase in body size range within the initial 10 ranks (nodes) followed by a loss of smaller-bodied representative and a period of relative stasis; an increase in size also occurs in the final 10 ranks. This relationship is strongly indicative of a driven trend, whereby smaller taxa occur near the base of the tree and larger taxa occur near the apex. Not surprisingly this pattern results in very high spearman correlation coefficients, which are highly significant when analyzed at the ornithopod ($\rho=0.768$, $S=26391.1$, $p<<0.001$), iguanodontian ($\rho=0.679$, $S=24455.2$, $p<<0.001$), and hadrosauroid ($\rho=0.575$, $S=10540.8$, $p<<0.001$) levels. Despite the stark difference between the overall patterns recovered between age- and clade-rank, both recovered significant correlations within inclusive clades, and except for the age-rank of Thescelosauridae, body size in more exclusive clades were not significantly related to time or phylogeny. Caution, however, is warranted when interpreting the differences between age/clade-rank. Recent studies have noted important biases against the preservation of small-bodied dinosaur taxa (Brown *et al.*, 2013b; Brown *et al.*, 2013a), which are reflected by their long ghost-lineages (Evans *et al.*, 2013). Thescelosaurids, for instance, exhibit long ghost lineages that reflect the incompleteness of their record (Brown *et al.*, 2013a); however, these are not taken into account in analyses using clade rank, which treat all nodes equally. It is therefore possible, and likely, that this analysis undersamples nodes at this, and other parts of the tree thereby biasing the occurrence of certain taxa towards the root node, lowering their clade-rank.

The body size-space occupied by the different ornithopod subgroupings, assessed using minimum convex hulls (MCH; Figure 4-6), reveals a dichotomous pattern within this clade, especially when examined in terms of age-rank. Iguanodontians and thescelosaurids represent two phylogenetically distinct clades (Figure 4-1) yet they overlap in size space. However, hadrosauroids (a subclade within Iguanodontia that includes the diverse hadrosaurids) occupies a

distinct part of size-space relative to the scelosaurids. Hadrosaurids represents the upper limit of hadrosauroid body size and there appears to be no notable difference between its major diversifications (i.e., Hadrosaurinae and Lambeosaurinae).

4.4.2.1 Model-Fitting

A model fitting approach comparing five different models of evolution (Brownian motion, driven trend, stasis, Ornstein-Uhlenbeck, and early-burst; see Table 4-2) recovered the most variable results depending on whether branch lengths were estimated using time or assumed to be uniform. For instance, assumption of branch uniformity fails to support a trend model in any of the ornithopod clades analyzed here, preferring in general an early-burst model. Similar support for early-burst was obtained used the equal distribution time-scaling method (equal). In contrast, the final three time-scaled trees (i.e., aba, zlba, and mbl) on average support a driven trend in most clades, which based on the positive mean step value (μ) indicate overall increases in body size. Only in Thescelosauridae and Hadrosaurinae, do all trees (irrespective of how branch lengths were calculated) support a static or Brownian motion mode of evolution, respectively. Overall, the Ornstein-Uhlenbeck model received the lowest support of the five models tested here. Aba, zlba, and mbl time-scaled trees support a driven trend in the evolution of body size in ornithopods overall, as well as in Hadrosauroidea and Hadrosauridae.

Iguanodontians and lambeosaurines are the most variable in terms of model support. The uniform, equal (with 1 million years added to the root), all branched adjusted, and minimum branch length trees support an early-burst model of evolution in iguanodontians, whereas the other two trees support a driven trend model. The evolution of body size in lambeosaurines fits an early burst model of evolution best, except within the mbl tree that finds greater support for

Brownian motion. Regardless, the relative support is low and in all cases many of the models cannot be conclusively rejected.

Although certain models are observed to fit better, in almost all cases there is a secondary and maybe even a tertiary model that cannot be rejected outright given the dataset (Table 4-2). Given a set number of models, a particular model can be rejected if its Akaike weight is equal or larger than one-eighth the weight obtained for the best-fit model (Royall, 1997). Finally, two overall patterns emerged when comparing the results obtained using the different trees. Both equal trees exhibit the same overall results, and similarly both aba and zlba are virtually identical. As a result, subsequent analyses and interpretations will be based on the uniform, equal distribution adding 1 Ma to the base of the tree, zlba, and mbl trees. The latter remains the preferred tree based on the comments made in section 4.3.2 of this chapter.

4.4.3 Ancestor-Descendent Contrasts

Ancestor-descendent comparisons were generated by first reconstructing ancestral conditions via a maximum likelihood algorithm that assumes a Brownian motion model of evolution (Schluter *et al.*, 1997) and then calculating the difference between the ancestral and descendent body mass. Results from initial uses of contrasts to detect trends were mentioned in the previous section; however, contrasts can be used to recognize important, and potentially biologically significant shifts in body size (e.g., significant shifts in body size related to dispersal events onto islands). The contrasts include a range of values from which a prediction interval can be calculated to objectively identify statistically significant shifts in body mass within an ancestor-descendent pair. Results are shown for the preferred time-scaled tree (mbl; Table 4-3) and recovered 13 increases and 10 decreases that may represent important shifts in the evolution of body size in ornithopods. Of these contrasts four were recovered in all, independent of branch length

estimation method; including increases in body mass in the ancestor of *Thescelosaurus* (Node8), *Muttaburrasaurus langdoni* (5,808 kg), and *Barsboldia sicinskii* (16,174 kg), and a decrease in body mass in *Haya griva* (10.5 kg). An additional 11 size-contrasts were recovered as significant by all time-scaled trees, including increases in *Talenkauen santacrucensis* (564 kg), the ancestor of rhabdodontids (Node16), *Rhabdodon priscum* (863 kg), the ancestor of *Tenontosaurus* (Node22), and *Iguanodon bernissartensis* (8.680 kg); and decreases in *Hypsilophodon foxi* (25 kg), *Gasparinisaura cincosalensis* (12.9 kg), *Anabisetia saldiviae* (29.7 kg), *Bolong yixianensis* (558 kg), *Tethyshadros insularis* (411 kg), and *Aralosaurus tuberiferus* (596 kg).

4.4.4 Testing Upper Size Limits

Time-series analyses of upper size limits in ornithopods indicate that ornithopods reached an upper limit throughout their evolutionary history. Of the three models tested here (linear, power, and Gompertz), Gompertz was unanimously supported, independent of bin size (Figure 4-8). In all cases, the Akaike weight score was >0.9 , allowing confident rejection of the alternate models tested here. The body size asymptote is reached at a \log_{10} mass of 6.8534 to 6.952, which correspond to an absolute body mass of 7,135 kg to 8,954 kg. This asymptotic size crosses the upper limit size data between 136 Ma to 131.7 Ma, during the Early Cretaceous (Valanginian–Hauterivian). Although the overall pattern is indicative of a rapid initial increase in body size followed by a plateau, a second maximal size event is apparent between 95.7 Ma and 91.2 Ma, in the early Late Cretaceous (Cenomanian–Turonian). This period of time is marked by maximal sizes (approximately 2,000 kg) that are over half an order of magnitude smaller than the overall asymptotic size. It is important to note, that this time period exhibits low sample sizes compared to other time bins (especially at 2 Ma bins; Figure 4-8), a factor that may account for the drop in maximal size. However, an appreciable drop in size is also noted at 10 Ma size bins, where the

drop in sample size is not as pronounced. This lull in maximal size is followed by a rapid increase in maximal size during the Coniacian–Santonian (~85.7 Ma) at which point ornithopod body size reaches its zenith during the Campanian with the appearance of hadrosaurids, most notably *Shantungosaurus giganteus* (18,259 kg), the largest ornithischian.

4.5 Discussion

4.5.1 Insular Dwarfism in Ornithopoda

The Island Rule predicts that large-bodied animals will decrease in size upon colonization of an island, whereas the opposite pattern is expected in small-body taxa (Foster, 1964). This tendency is most noted in mammalian clades, but is also described in reptiles (including birds; Lomolino, 1985, 2005) and is thought to be driven by characteristics of island environments (e.g., reduction in competition and predation) that are in turn hypothesized to drive body size evolution towards optima that differ from their mainland relatives (Lomolino, 2005). In the fossil record of dinosaurs, patterns predicted by the Island Rule (i.e., insular dwarfism) were first forwarded by Nopcsa (1914), well before the Island Rule was formally defined by Foster (1964). Nopcsa's assertions were based on ornithopod remains from Eastern Europe, including *Telmatosaurus transsylvanicus*, and the observation that these remains were, on average, of smaller body size than those recovered elsewhere in the world. Numerous studies have since attempted to test this pattern with overall support for the occurrence of insular dwarfism in this clade (Weishampel *et al.*, 1993; Weishampel *et al.*, 2003; Benton *et al.*, 2010; Weishampel and Jianu, 2011; but see Ősi *et al.*, 2012).

In order to test cases of the Island Rule in the fossil record, four major pieces of data are required: 1) evidence of island habitation; 2) body masses of closely related taxa; 3) evidence that the representative specimen is of approximate adult size; and 4) a phylogenetic framework. Three ornithopod taxa (*Telmatosaurus transsylvanicus*, *Zalmoxes robustus*, and *Tethyshadros insularis*) are hypothesized to represent examples of insular dwarfism due to 1) their small size relative to closely related taxa, 2) the palaeoenvironmental reconstructions of the deposits in which they are found indicate an island habitat, and 3) recent histological data support the notion that they are at least close to fully grown adults and not juveniles of other larger contemporaries (Benton *et al.*, 2010; this data is not available for *T. insularis*). Although insular dwarfism in ornithopods has been discussed within the context of ornithopod phylogeny (Weishampel *et al.*, 1993; Weishampel *et al.*, 2003; Benton *et al.*, 2010; Weishampel and Jianu, 2011), it has not been properly quantified, except for recently in rhabdodontid ornithopods (Ósi *et al.*, 2012). Given the prediction made by the Island Rule, support for insular dwarfism should be manifested as significant decreases in body mass in descendants relative to the ancestral condition, and can be quantified and tested for by using ancestor-descendant contrasts.

Reconstructed ancestor-descendent size contrasts reveal numerous significant shifts towards both gigantism and dwarfism in ornithopods (Table 4-3; Figure 4-7). Of these significant shifts, *Tethyshadros insularis*, *Rhabdodon priscus*, and perhaps *Iguanodon bernissartensis* may have occurred on islands, and only *T. insularis* represents a significant shift towards small body size. *Iguanodon bernissartensis* and *Rhabdodon priscus* represent the inverse, significant increases in body size relative to their ancestral condition. Given that the size-contrast leading to *Tethyshadros* occurs below the 95% prediction intervals of contrasts, in all but one (uniform) of the trees (Figure 4-7; red square, where it still falls near the lower limit), this study finds quantitative, phylogenetic support for the hypothesis that *Tethyshadros* may be an island dwarf

(Dalla Vecchia, 2009). An important caveat, however, is that the ontogenetic status of *Tethyshadros* has not been conclusively established, other than a vague statement by the Dalla Vecchia (2009; pg. 1113) citing “[individuals] lack evidence of osteological immaturity suggestive of a juvenile condition.” Further histological data may yet reveal that the specimens on which this species was named represent immature individuals that have not yet reached their maximum size. Nevertheless, based on the current dataset *Tethyshadros* is the only ornithopod for which insular dwarfism is supported; neither *Telmatosaurus* nor *Zalmoxes* represent significant shifts towards small body size relative to their ancestral condition.

Telmatosaurus transsylvanicus was originally named and described by Franz Nopcsa in the early 20th century based on specimens recovered in the Hațeg region of Romania (Nopcsa, 1900, 1903). Since then, and largely due to pioneering studies in hadrosaurid systematics by David Weishampel, *Telmatosaurus* has become an icon of insular dwarfism in ornithopods and dinosaurs in general. In its first revision, subsequent to Nopcsa’s work, Weishampel *et al.* (1993) recovered the taxon as sister to all other hadrosaurids, and in addition to forming the basis for phylogenetically defining the clade, its island habitat in the European Archipelago of the Late Cretaceous and small size relative to its hadrosaurid sister-taxa, *T. transsylvanicus* was championed as strong evidence of the occurrence of insular dwarfism in non-avian dinosaurs. Given the advent of histological techniques for assessing relative ontogenetic age in dinosaurs (reviewed in Chinsamy-Turan, 2005; Erickson, 2005), Benton *et al.* (2010) conducted a thorough histological sampling of putative dinosaurian insular dwarfs (except for *T. insularis*) and supported an ontogenetically mature designation for *T. transsylvanicus* material thereby strengthening the dwarf hypothesis. Despite the large amount of research on *Telmatosaurus*, assessments of its body size evolution have remained largely qualitative, and to a certain degree speculative, and have not been explicitly tested within a phylogenetic framework. The

quantitative and more comprehensive phylogenetic context provided here failed to recover a significant shift in body mass leading to *T. transsylvanicus* as predicted by the Island Rule. Based on the four trees used in this study, the mean size contrast that leads to *T. transsylvanicus* (mean $\Delta_{AD}=0.004\pm0.094 \log_{10} g$) indicates almost no change from its most recent ancestor (ancestral BM_{mbl} \approx 1,900 kg; *Telmatosaurus* BM \approx 1,670 kg) with other hadrosaurids. This pattern is independent of method used to estimate branch length (Figure 4-7). As a result, I reject the hypothesis that *Telmatosaurus* was an island dwarf. Previous observations of small size, relative to other hadrosaurids (e.g., Weishampel *et al.*, 1993), were likely due to a trend towards larger body size in hadrosaurids (e.g., Table 4-2) and *Telmatosaurus* is better interpreted as plesiomorphically small-bodied, similar in size to many non-hadrosaurid hadrosauroids; a condition it retains into the Late Maastrichtian of Eastern Europe.

The most recent assessment of insular dwarfism in ornithopods was published by Ősi *et al.* (2012), focusing on rhabdodontid ornithopods from the European islands of the Late Cretaceous, including Hațeg in Romania. This clade includes *Rhabdodon priscus*, *Zalmoxes robustus*, *Z. shqiperorum*, *Mochlodon vorosi*, and *M. suessi* as well as *Muttaburrasaurus* from Australia, although the phylogenetic affinities of the latter remain contentious (McDonald *et al.*, 2010b). Ősi *et al.* (2012) present a comprehensive quantitative test of insular dwarfism in rhabdodontids, using a dataset of non-ankylopellexian ornithopods and methods similar to those applied here (i.e., ancestral state reconstruction). Based on their quantitative phylogenetic framework, the authors reject the hypothesis of Weishampel and Jianu (2011) that *Zalmoxes robustus* was an island dwarf and instead suggest that *Rhabdodon* is an island giant. Similar to *Telmatosaurus*, the results presented here (Figure 4-7) indicate that the body size of *Z. robustus* does not constitute significant shift relative to its immediate ancestor. However, neither *Z. robustus* nor its common ancestor with *Z. shqiperorum* constitutes the original island colonizer,

as all rhabdodontid species (with the exception of *Muttaburrasaurus*) occur on the Late Cretaceous European Archipelago. As a result, Ősi *et al.* (2012) suggest comparisons to be made with the colonizing ancestors (i.e., the common ancestor of *Rhabdodon*, *Zalmoxes*, and *Mochlodon*). Under these stipulations a significant shift towards small body size is obtained using the uniform tree ($\Delta_{AD} = -0.665 \log_{10} g$), however, all three time-scaled trees fail to recover a significant shift between the common ancestor of European rhabdodontids and *Z. robustus* (mean $\Delta_{AD} = -0.074 \log_{10} g$). Although this study also fails to support insular dwarfism in *Zalmoxes*, it is possible that comparisons are being made at the wrong phylogenetic level. Given the stipulations of the Island Rule, a significant decrease in body size would not necessarily be expected to occur within the contrast (or set of contrasts) leading to *Z. robustus*, but rather in the colonizing ancestor of the clade. This prediction is provisionally supported here, given that both the zlba and mbl trees recover a significant decrease in size in the common ancestor of *Rhabdodon*, *Zalmoxes*, and *Mochlodon* (Table 4-3; range $\Delta_{AD} = -0.98 \log_{10} g$ to $-0.94 \log_{10} g$) relative to its preceding ancestor. Unfortunately, the magnitude of the body size shift is equivocal at best, given the current available data. A significant dwarfing event in the ancestor of European rhabdodontids is contingent on the phylogenetic placement of *Muttaburrasaurus* as its sister-taxon. Removal of *Muttaburrasaurus* results in a non-significant shift in size in the European colonizing ancestor (range $\Delta_{AD} = -0.083 \log_{10} g$ to $-0.047 \log_{10} g$) and hence does not support the hypothesis of insular dwarfism in rhabdodontids.

In addition to *Zalmoxes robustus*, Ősi *et al.* (2012) found some support for the hypothesis that *Mochlodon*, the sister-taxon to *Zalmoxes*, is an island dwarf. Although the current study finds a decrease in size leading to *Mochlodon*, it is only significant when using the uniform tree. However, if the contrast is taken relative to the colonizing ancestor (Node17) all trees recover an appreciable, though not always significant, decrease in size leading to *Mochlodon* (range

$\Delta_{AD} = -0.938$ to $-0.194 \log_{10} g$), and to a greater extent *M. suessi* the smaller of the two *Mochlodon* species ($BM \approx 30.5$ kg). This study supports the recent conclusions of Ősi et al (2012) in rejecting insular dwarfism in *Zalmoxes* with some evidence suggesting a dwarfing event in the evolution of *Mochlodon*. However, at this time more data are needed on the phylogeny, systematics, and biogeography of rhabdodontids in order to better constrain the ancestral condition both in terms of body size and biogeographic origins and thus adequately test the patterns noted by Ősi et al. (2012) and supported here.

Overall, the results presented here suggest that insular dwarfism may not be as widespread in the European Archipelago of the Late Cretaceous as previously thought. In particular, this section of this chapter emphasizes the robusticity of the dataset needed to properly detect patterns predicted by the Island Rule in the fossil record. Although, relatively little support was obtained for dwarfism, both *Rhabdodon* and *Iguanodon* represent significant shifts towards large size, a transition that presumably occurred after island colonization, and may represent examples of insular gigantism. Previous interpretation of the Island Rule in dinosaurs assumed that given the large average sizes noted in dinosaurs (Peczkis, 1994; O’Gorman and Hone, 2012) insular dwarfism, rather than gigantism, is more likely; similar to that noted in large body terrestrial mammals (e.g., hippopotamus and elephants; Foster, 1964). However, the optimal body size for a given island will vary with the level of resources available and hence the size of the island (Burness et al., 2001). Although the palaeogeography of Europe in the Early Cretaceous remains poorly defined, the Maastrichtian island archipelago is comparatively well understood (Camoin et al., 1993). Within this archipelago, *R. priscus* occurred on what is thought to represent the largest of the islands (Weishampel and Jianu, 2011) and it is therefore conceivable that ancestor of European rhabdodontids was small, and given adequate resource

availability, subsequent colonization of larger islands may have resulted in a shift towards large, rather than small, body size.

4.5.2 Upper Size Limits in Ornithopoda

Reconstructing and understanding the upper body size limits in vertebrates has received recent attention in both Cenozoic mammals and Permian to Middle Jurassic amniotes (Smith *et al.*, 2010; Sookias *et al.*, 2012a). Both studies recover the presence of upper limits to body size in their respective research clades, but hypothesize alternate mechanisms driving these patterns. Smith *et al.* (2010) interpret the rapid increase in upper body size of Cenozoic mammals as being consistent with the hypothesis of rapid diversification and niche-filling following the extinction of non-avian dinosaurs at the Cretaceous-Tertiary boundary. The authors also recovered strong correlations between both temperature and land area that are interpreted as possible mitigators of the value at which the upper body size limit is set. In contrast, Sookias *et al.* (2012a) recovered no strong correlations between any of the abiotic factor they tested and suggest instead that biology, including physiological factors, might better explain the evolution of upper body size limits in tetrapods. The authors re-analyzed the data of Smith *et al.* (2010) noting that the original study had not considered possible autocorrelation between successive data points within their time series. Autocorrelation is generally present in time-series data given that the value at any given time will undoubtedly be related to the preceding value, except under a pure stasis model whereby all data point are independent from each other (Hunt and Carrano, 2010). In all cases reported by Smith *et al.* (2010), Sookias *et al.* (2012a) recovered a better fit when autocorrelation is taken into account indicating dependence between data points. Once autocorrelation is accounted for, abiotic factors no longer correlate as strongly with maximal size, and a null model of no relationship best explains the data (Sookias *et al.*, 2012a).

As in the previously discussed studies, ornithopods also exhibit a rapid initial burst in upper body size limits followed by a prolonged period of relative stability (Figure 4-8). These patterns are recovered using different time-bin sizes, and are best explained by a Gompertz model, which incurs a prolonged period of reduced growth rates at the beginning and/or end of a time series. It is the preferred model for testing the presence of upper size limits (Smith *et al.*, 2010; Sookias *et al.*, 2012a). According to these results, the asymptote size is reached in the Early Cretaceous, with the first occurrence of large bodied iguanodontians such as *Barilium dawsoni* and *Iguanodon bernissartensis*. In particular, body mass estimates in *I. bernissartensis* are here revised based on its stylopodial circumferential measurements. Mass estimates for *I. bernissartensis* have traditionally ranged between 3,200 and 4,500 kg (Colbert, 1962; Paul, 1997; Seebacher, 2001). However, the combined limb circumference for the holotype (IRSNB R51) is 826.5 mm, similar to that of large African elephants (see Appendix 1), and it is therefore not surprising that based on these measurements the body mass of *I. bernissartensis* is estimated at approximately 8,700 kg, almost double that of previous estimates, and heavier than most hadrosaurids (mean body mass ~5,000 kg). The holotype specimen was used here due to its well-preserved, complete skeleton; however, BMNH R 2502–2509 [originally assigned to *I. seelyi* but now a junior synonym of *I. bernissartensis* (Norman, 2004)], has much more robust limbs and hence was much heavier than the latter ($C_{H+F}=1036$ mm; $BM=16,100$ kg). Given these mass estimates it is not surprising that this study recovers the presence of an upper size limit that was reached early in the evolutionary history of ornithopods, as also noted in sauropods (Carrano, 2005).

The mechanisms that dictate the body size limits which a group can reach are often considered to be the result of intrinsic and/or extrinsic factors including physiological or life history qualities, resource availability (often measured as available land area) and climate

(Peters, 1983; Janis, 1993; Burness *et al.*, 2001; Payne *et al.*, 2009; Smith *et al.*, 2010; Sookias *et al.*, 2012a). These factors need not be mutually exclusive, given that extrinsic factors, such as atmospheric oxygen levels and temperature, are thought to affect the metabolic capabilities of an animal either by allowing greater metabolic efficiency or great levels of heat dissipation, respectively (Peters, 1983; Janis, 1993; Payne *et al.*, 2009; Smith *et al.*, 2010). However, these factors are generally investigated within the context of mammalian groups, and non-avian dinosaurs may not follow similar patterns (Sookias *et al.*, 2012a) given their oviparous reproductive strategy and likely metabolic differences (Bakker, 1972; Sanders *et al.*, 2010).

Preliminary analyses comparing abiotic factors, such as carbon-13 concentration [a model for atmospheric oxygen levels (Falkowski *et al.*, 2005)], reconstructed land area (Smith *et al.*, 1994; a proxy for resource availability), and atmospheric carbon dioxide [a proxy for palaeotemperature (Royer *et al.*, 2004)] recovered initial support for upper body size limits in ornithopods to be driven by land area and hence habitat/resource availability (Table 4-5). However, as was recovered by Sookias *et al.* (2012a), when autocorrelation between data points is accounted for, a null model of no association fits the size limit data better. Nevertheless, based on the Akaike weight scores, both land area and carbon-13 concentrations cannot be rejected outright (Table 4-5) and may have played an important role in dictating the upper limits reached by ornithopods.

One final point merits further discussion. Throughout the Jurassic period sauropodomorph dinosaurs represented the dominant megaherbivores (e.g., Upchurch and Barrett, 2005). However, the end of the Jurassic is marked by a significant dinosaur extinction event, in particular within the northern continent of Laurasia (Bambach, 2006). This extinction event is marked by a sudden decrease in the diversity of the large bodied sauropodomorph

dinosaurs in the north (Upchurch and Barrett, 2005; Barrett *et al.*, 2009; Mannion *et al.*, 2010; Lloyd, 2012), which would have theoretically resulted in the opening of various niche spaces. The sudden increase in upper body size limits in ornithopods, initially via *Barilium dawsoni*, and subsequently by *I. bernissartensis*, following the J-K extinction event can be readily associated with a significant decrease in sauropod diversity (Figure 4-9). As a result, the initial stages in the evolution of upper body size limits in ornithopods can be hypothesized to represent an ecological release event, similar to that observed in mammals, following the extinction of non-avian dinosaurs at the K-T extinction event (Smith *et al.*, 2010). It is important to note however, that although the ornithopod upper body size limits in the Early Cretaceous may be linked to sauropod diversity dynamics (significant negative correlation when autocorrelation is not taken into account; Table 4-5), the overall ornithopod size pattern is not well explained by sauropod diversity data (Lloyd, 2012). Although ornithopods never fully reached the sizes obtained by sauropodomorphs, some taxa, including the giant *I. bernissartensis* may have filled the sauropod niche-space that was left vacant. The hypothesis that ornithopods may represent an adaptive radiation, perhaps resulting from this ecological release, will be discussed further in the final section of this chapter (Section 4.6).

4.5.3 Cope's Rule in Ornithopoda

Cope's Rule was coined by Rensch (1943) in honour of Edward Drinker Cope, who is credited for first noting overall trends towards larger body size in extant animals. Edward D. Cope, however, is also known for copious amounts of research on North American fossils, in particular, non-avian dinosaurs and is particularly famous for his feud with Othniel C. Marsh (Colbert, 1984, 1997). It is therefore surprising that Cope never explicitly commented on dinosaurian evolution within the context body size evolution towards larger size. Perhaps even more

unexpected, Cope's Rule was not directly tested, nor even alluded to, in dinosaurs until less than a decade ago (although Sereno, 1997 discussed patterns towards larger size in multiple dinosaurian clades; Hone *et al.*, 2005; Carrano, 2006). Nevertheless, most studies support Cope's Rule in dinosaurs, as well as in some dinosaurian subclades (Hone *et al.*, 2005; Carrano, 2006; Hunt and Carrano, 2010).

The analyses presented here, in particular the Spearman rank and model-fitting (based on time-scaled trees) analyses support Cope's Rule in Ornithopoda (Table 4-4) and confirms the overall pattern that Carrano (2006) obtained for this clade. In particular, rank correlation analyses recovered a high *rho* value between clade-rank and body mass ($\rho=0.768$), that is only slightly lower than the value obtained by Carrano (2006) using femoral measurements as a proxy for size ($\rho=0.845–0.913$). A major difference between the results of the latter study to those obtained here includes the ancestor-descendent analysis. Carrano (2006) obtained significantly more increases in body size (femoral length) from ancestors to descendants, when all pairs are considered, than decreases (see tables 8.1–8.3 of that study). In contrast, this study recovered little support for such a pattern between ancestor-descendent contrasts, except for in one of the time-scaled trees using an equal time distribution (Table 4-1). However, this result is not robust, as it appears to be contingent on how the tree is scaled; other time-scaling techniques did not recover a significant difference between increases and decrease in body size in ornithopods. The reason for the differences between this analysis and that of Carrano (Carrano, 2006) are presently unclear but may be related to the different datasets utilized (e.g., femoral measurements vs. body mass estimates and differences in tree topology) or variances in the methodology used (e.g., unweighted vs. weighted square changed parsimony and the use of branch lengths in this study). Despite not recovering a significant increase in body size when utilizing ancestor-descendent contrasts, model-fitting approaches based on both the zlba and mbl trees (the latter being the

preferred tree as it makes the fewest *a priori* assumptions about branch lengths relative to the raw time-calibrated tree) support a trend model (i.e., Cope's Rule) of evolution in ornithopods overall compared to the four other models tested here (Brownian motion, stasis, Ornstein-Uhlenbeck, and early-burst). Based on the results of the mbl tree, the mean step ($\mu = \log_{10} BM_1 - \log_{10} BM_0$) is 0.0062 log g/Ma, which indicates an average increase in mass in ornithopods of about 0.62% per million years. Interestingly, this value is almost identical to that obtained for all ornithischians based on femoral length data (Hunt and Carrano, 2010). Given the 97.7 million year range currently known for ornithopod fossils a 0.62% rate of increase predicts over an 80% average increase in body mass throughout this time ($97.7 \text{ Ma} \times 0.0062 \text{ log}_{10} \text{ g/Ma} = 0.606 \text{ log g}$; $e^{0.606} = 1.833 = 83.2\%$). These results support the overall driven trend predicted by Cope's Rule in ornithopods, however support for Cope's Rule is limited in other ornithopod clades, except for Hadrosauropoda, in which a trend is supported by all time-scaled trees and rank correlations (Table 4-4). The hadrosauroid trend is slightly stronger than the overall ornithopod trend ($\mu = 0.0101 \log_{10} \text{ g/Ma}$, implying a 1% rate of increase) and represents an average increase of 104% over its 70.5 million year period. Although, a trend model is not the preferred in all ornithopod subclades, in no case, except in the uniform tree (that found very little support for a trend model), can it be definitively rejected (Table 4-2). As a result, overall support for Cope's Rule is documented here in ornithopods.

In his overall review of Cope's Rule in Cenozoic mammals, Alroy (1998) suggested that analysing overall patterns, for instance in all dinosaurs, may in itself mask driven trends towards increasing body size, and that future work should concentrate on more exclusive clades. The highly pectinate structure of the ornithopod cladogram (Figure 4-1), with the exception of a possible major dichotomy at the base of Ornithopoda (Thescelosauridae; Brown *et al.*, 2013a) and the well-recognized Hadrosaurinae-Lambeosaurinae dichotomy within Hadrosauridae,

allows for one of the first tests of Cope's Rule within what it is essentially a single lineage. The results, which in general support an overall increase in body size throughout the evolutionary history of ornithopods, confirms the predictions of Alroy (1998). That being said, it appears that dinosaurs in general may also show this pattern (Hone *et al.*, 2005; Carrano, 2006), although this remains to be tested using modern model-fitting techniques (but see Hunt and Carrano, 2010), especially since a dataset of dinosauromorphs spanning the Late Triassic to Middle Jurassic indicates that passive or more random patterns of evolution may better explain the evolution of body size early in dinosaurian evolutionary history (Sookias *et al.*, 2012b).

Support for Cope's Rule in ornithopods is in contrast to the conclusions of Sookias *et al.* (2012b), who found little to no support for trends in early archosauromorphs (Permian to Middle Jurassic) and, in addition, suggested that exclusive clades would exhibit a stable, and somewhat random, mode of evolution (i.e., stasis). In addition to supporting Cope's Rule, ornithopods present little to no support for stasis, except at small sample sizes (e.g., thecodontosaurs, N=10). Small sample size may itself be an important factor to consider when applying model-fitting techniques. Harmon *et al.* (2010; figure S1) found that at samples sizes less than 20, the chances of recovering an Ornstein-Uhlenbeck or early-burst model significantly declined, being replaced by a greater chance of recovering a more passive mode of evolution (i.e., Brownian motion). These results are supported by a random subsampling of the ornithopod dataset, which also recovered a significant drop in the recovery of early-burst, Ornstein-Uhlenbeck, and trend models at sample sizes less than 20 compared to an increase in recovery of Brownian motion or stasis models of evolution (discussed in section 4.6; see Figure 4-11). Caution should therefore be taken when interpreting evolutionary patterns among clades with less than 20 taxa, especially if passive (null-type) models are supported. For instance, in the study of Sookias *et al.* (2012b) all clades that support a stasis model of evolution have sample sizes <30, whereas support for an

early-burst or Ornstein-Uhlenbeck model occur in clades ≥ 30 . These results also suggest caution when interpreting the passive patterns recovered by Zanno and Makovicky (2013) given that all three theropod clades tested in that study have sample sizes of 20 or less.

Support for Cope's Rule is perhaps expected in ornithopods given the well-known occurrence of small taxa early in their evolutionary and temporal history (e.g., *Jeholosaurus shangyuanensis*, 10 kg; *Hypsilophodon foxi*, 25 kg; and *Callovosaurus leedsi*, 68.8 kg) followed by much larger taxa leading-up to the end of the Cretaceous, that is, the hadrosaurids (body mass between 596 kg [*Aralosaurus tuberiferus*] to 18,259 kg [*Shantungosaurus giganteus*]). However, to summarize the evolution of body size in ornithopods as simply an example of Cope's Rule represents a gross oversimplification of the macroevolutionary patterns of body size in this clade. The complex nature of body size evolution in ornithopods is apparent from the results of the upper body size analysis indicating that the upper body size limit in ornithopods was reached early in their evolutionary history, approximately 130 Ma during the Early Cretaceous (Hauterivian–Barremian). Such a pattern suggests that a gradual increase does not typify all aspects of body size evolution in this clade and that other models of evolution may also be invoked (Table 4-2).

4.6 Ornithopod Size Evolution: An Adaptive Radiation?

This chapter set out to demonstrate the utility of the body mass estimation techniques developed in chapters 1 and 2, and test Cope's Rule, upper size limits, and the occurrence of insular dwarfism in a model clade, Ornithopoda. Through these investigations however, it became clear that the evolutionary patterns of body size in this clade were too complex to be simply the result of single trend, as expected under Cope's Rule. In particular, it became evident that rates of body

size diversification may have varied through time and phylogeny thus suggesting that, while overall size may have increased, other models of evolution may better explain particular stages in the evolutionary history of ornithopods.

Although originally grounded in palaeontological research (Osborn, 1910; Simpson, 1944; Simpson, 1953), adaptive radiations have, as of late, received little attention within fossil groups compared to recent interest in modelling adaptive radiations (or early-burst evolutionary events) in extant animals (Losos and Miles, 2002; Harmon *et al.*, 2003; Harmon *et al.*, 2010; Yoder *et al.*, 2010; Ingram *et al.*, 2012). As conceived by George G. Simpson (1953) an adaptive radiation can be described in three main stages: 1) a population enters a new adaptive zone (a ‘quantum leap’). Such a shift may relate to ecological opportunity through the evolution of a key innovation, reduction in interspecific competitors and/or predation, invasion of a new geographical region, and/or the evolution of a new resource (Yoder *et al.*, 2010). 2) Preceding the invasion of a new zone, a population will spread geographically in an attempt to mitigate intraspecific competition, which may eventually result in 3) ecological specializations and thus speciation filling available niche space (Simpson, 1953). Given this scenario, a hypothesized adaptive radiation makes two predictions as to the pattern of evolution in an adaptively radiating clade (Schluter, 2000): 1) the rate of lineage diversification should be highest near the root of a clade, with a subsequent and gradual decline in diversification associated with niche filling; and 2) in relation to ecological specializations, the rate of morphological diversification (i.e., disparity) will similarly be highest near the origin of the clade and subsequently decline. The former pattern is the most commonly tested of the two predictions, but recent studies focus on the latter, which is thought to be more directly related to the adaptive zone model proposed by Simpson (Losos and Miles, 2002; Harmon *et al.*, 2010; Slater *et al.*, 2010).

In spite of the interest among quantitative biologists, testing the patterns predicted by an adaptive radiation model has been limited in the fossil record of vertebrates despite the fact that, in addition to the appearance of novel lineages and morphologies, it has the ability to integrate data on extinction, a factor that Simpson regularly cited when developing his adaptive zone model (Simpson, 1944). Inclusion of fossil data has been strongly advocated recently, in particular with regards to ancestral-state reconstruction (Finarelli and Flynn, 2006; Smaers and Vinicius, 2009) and modelling diversity dynamics of living taxa (Quental and Marshall, 2009, 2010). Non-avian dinosaurs were diverse, both taxonomically and morphologically, members of the Mesozoic terrestrial community and hence present a model clade with which to investigate evolutionary models, such as adaptive radiation. However, to date diversity and disparity dynamics in dinosaurs are investigated within the context of extinction events (e.g., Fastovsky *et al.*, 2004; Barrett *et al.*, 2009; Campione and Evans, 2011; Brusatte *et al.*, 2012) and comparatively minor attention has been given to evolutionary rates, although a couple of studies have attempted to reconstruct the rates of evolution during the early stages of dinosaur diversification (Brusatte *et al.*, 2008a; Lloyd *et al.*, 2008). Nevertheless, no study has directly investigated dinosaur diversification within the context of an adaptive radiation model. Given the ecological implications of body size (e.g., Peters, 1983), it can be used as a proxy for ecological diversity (LaBarbera, 1989; Slater *et al.*, 2010) thereby allowing to test the second and perhaps more important pattern predicted by the adaptive radiation model, that is, initial rapid ecological diversification followed by a period of relative stability. The ornithopod body mass dataset developed here presents the ideal opportunity to investigate this prediction.

Overall, the study presented here recovered considerable support for the notion that ornithopods get progressively larger, both through time and throughout their evolutionary history (Table 4-2, Table 4-4, and Figure 4-6); thus conforming to the pattern predicted by Cope's Rule.

However, given that Cope's Rule is not unambiguously supported at all levels within Ornithopoda (Table 4-2 and Figure 4-6), it is clear that the evolution of body size in ornithopods was complex and variable at different stages throughout their evolutionary history. Despite overall support for a trend model of evolution in some of the major ornithopod groups, model-fitting techniques were unable to conclusively reject other evolutionary models, including early-burst (Table 4-2). As a result, the hypothesis that ornithopods represent an adaptive radiation marked by the evolution of body size merits further investigation, especially given recent suggestions that early-burst (or adaptive radiations) are rare based on datasets of extant animals ranging from arthropods to mammals (Harmon *et al.*, 2010).

Typically, models are fitted at nodes that represent traditional and presumably evolutionarily 'important' taxonomic groupings, such as those applied in Table 4-2, as well as recent studies (Harmon *et al.*, 2010; Sookias *et al.*, 2012b; Zanno and Makovicky, 2013). However, taxonomic groupings are human constructs thereby necessitating a more iterative approach to model fitting on phylogenetic trees. The approach utilized here fits five major evolutionary models (Brownian motion, trend, stasis, Ornstein-Uhlenbeck, and early burst) at all nodes within the ornithopod tree that include more than 10 taxa (following Harmon *et al.*, 2010). This approach allows a more objective depiction of how support for particular evolutionary models varies as one assesses patterns within progressively more exclusive clades. Relative model support was measured using Akaike weight scores plotted on a proportional area plot. This approach finds overall support for trend models, as seen by the overall greater proportion of area taken up by the latter (Figure 4-10). However, some support is also recovered for early-burst, especially within the first dozen nodes, as well as more passive processes. This result suggests that despite overall trends towards large body mass in ornithopods, their early evolutionary history may also be characterized by rapid diversification of body sizes during the

Middle to Late Jurassic, subsequent to the evolution of iguanodontians. This pattern is supported by rank analyses (Figure 4-6), which depict non-iguanodontian ornithopods as exhibiting the lower body size limits within this clade and a shift in iguanodontians towards larger body size; this is most apparent in hadrosauroids that do not overlap size-space with the celosaurids. Support for early-burst is maintained leading up to the J-K boundary, although it becomes significantly reduced, and replaced instead by a period of Brownian motion. The evolution of body size throughout most of the Early Cretaceous follows a passive, Brownian mode of evolution, although support for a trend model remains also high throughout. In the late Aptian, however, ornithopods show strong support for another driven trend towards larger body size in the node that includes *Nanyangosaurus zhugeii*, *Tanis sinensis*, *Gilmoreosaurus mongolensis*, *Bactrosaurus johnsoni*, *Claosaurus agilis*, and Hadrosauridae. Support for a trend model decreases leading up to the evolution of hadrosaurids with increased support for both early-burst and a more passive model of evolution following the evolution of hadrosaurids in the clade that includes *Lophorhothon* and Saurolophidae (sensu Prieto-Márquez, 2010). Random (i.e., stasis) or passive (i.e., Brownian) models of evolution are best supported within the last few nodes, corresponding to Lambeosaurinae. Although relative stability within lambeosaurines makes intuitive sense, given that their mass estimates range approximately an order of magnitude compared to the 3.5 orders of magnitude spanned by all ornithopods, increased support for Brownian motion and stasis is also expected at lower sample sizes given associated reductions in statistical power (Harmon *et al.*, 2010). In light of this possibility, I randomly subsampled the ornithopod tree at sample sizes ranging from 11 to 87. The five models were fit to these subsamples and their relative support was tested against samples size in order to determine whether the patterns described above could be driven by a reduction in sample size alone; subsampling was carried out 1000 times and the mean support was plotted (Figure 4-11).

Subsampling results indicate overall increases in Brownian motion support with reduction in sample size and a corresponding gradual decrease in support for a trend model. In contrast, both early-burst and Ornstein-Uhlenbeck models show little variation in support values associated with sample size, despite previous assertions regarding their relative low statistical power (Harmon *et al.*, 2010). Reduction in support for these models occurs only in the smallest samples sizes ($N < 20$) and is associated with a rapid increase in support for stasis. Overall, the patterns described for ornithopods (Figure 4-10) are drastically different from those obtained from a randomly subsampling of the data and support overall biological interpretations. However, I cannot reject the possibility that support for stasis and Brownian motion within the final five to ten nodes is driven by small sample size.

Preliminary support for an early-burst model early in the evolutionary history of body size in ornithopods suggests that they may conform to the predictions outlined by the adaptive radiation model. To test this possibility further, I examined patterns of variance and rates of evolution (based on the Brownian step variance coefficient, σ^2) in body size at each node with sample sizes greater than 10 from the base of the tree towards the apex (Figure 4-12). Under an adaptive radiation model, both trait variance and evolutionary rate should decrease through time, depicting an initial burst of variation into new niche spaces early in the clade's history followed by reduction in these qualities as niche space is filled (Harmon *et al.*, 2003; Harmon *et al.*, 2010). Both variance and rate support the patterns predicted by an adaptive radiation model. In particular, node variance decreases sharply (associated with high support of early-burst model in Figure 4-10) followed by a prolonged period of stable variance. Importantly, this pattern does not appear to be driven by reduction in sample size, given that variance taken at random subsamples occur well above those obtained at each node (Figure 4-12 left). Evolutionary rates of body size do not always occur outside that expected given a random subsampling at 1000 replicates (Figure

4-12 right), however, given their consistent occurrence near the lower extreme of the subsampled area and the significant correlation to decrease with time ($r= 0.734$, $t=6.581$, $p<<0.001$) the observed pattern is here interpreted as real and again supports an adaptive radiation model of evolution for ornithopods.

Taken together, the evolution of body size in ornithopods can be potentially described as biphasic. The initial phase is characterized by rapid increases in body size towards the upper limit, high variance in size, and high diversification rates. Both evolutionary rates and variation in body size stabilize as upper size limits in ornithopods are approached at the beginning of the Cretaceous (Figure 4-8 and Figure 4-9), possibly associated with a significant decline in sauropodomorphs diversity in the northern hemisphere during this time (e.g., Mannion *et al.*, 2010). Body size evolution remained largely passive throughout most of the Early Cretaceous followed by a second phase characterized initially by a strong trend towards increasing body size and then a possible second body size diversification event in hadrosaurids, possibly associated with a key innovation: the evolution of dental batteries, highly complex dentition, and novel feeding mechanisms (Norman and Weishampel, 1985; Cuthbertson *et al.*, 2012; Erickson *et al.*, 2012).

4.7 Concluding Remarks

Over the last two decades there has been considerable interest in quantifying macroevolutionary patterns, and this has been particularly driven by the development of molecular phylogenetic methods that provide the context on which to investigate tempo and mode of evolution within large datasets (Maddison, 1991; Hansen, 1997; Schluter *et al.*, 1997; Pagel, 1999; Pybus and

Harvey, 2000; Losos and Miles, 2002; Harmon *et al.*, 2008). Despite being developed for molecular-based phylogenies, methods for quantifying evolution have also been applied to phylogenies of fossil taxa (e.g., Alroy, 1998; Laurin, 2004; Hone *et al.*, 2005; Carrano, 2006; Hunt and Roy, 2006; Hunt, 2007, 2008; Payne *et al.*, 2009). The most recent application of quantitative methods to the fossil record, involve model-fitting approaches, such as Brownian Motion, stasis, trend, Ornstein-Uhlenbeck, and early burst (Hunt and Carrano, 2010; Sookias *et al.*, 2012b; Zanno and Makovicky, 2013). These approaches are useful for testing expected patterns of evolution (Pagel, 1999), but have for the most part been developed with an ultrametric tree in mind (i.e., all the taxa on the tree occur at the same time). As a result, the effects of sampling taxa at different time periods, as is available in the fossil record, on the results obtained through model-fitting techniques remain poorly understood. Nevertheless, it is evident that the fossil record provides data on what actually happened in the past, without having to infer it (e.g., Finarelli and Flynn, 2006; Quental and Marshall, 2010).

This chapter utilized the body mass estimation methods developed in chapters 1 and 2 to build a dataset of body masses in ornithopod dinosaurs (Appendix 6), which, given their temporal and body size range, represent a model clade for investigating macroevolutionary patterns of body size in non-avian dinosaurs. Here I applied a variety of different methods from traditional correlation analyses, ancestor-descendant contrasts (based on ancestral state reconstructions) and finally newer model-fitting approaches to test for patterns associated with Cope's Rule, the Island Rule, and upper body size limits. Overall, this study found support for the pattern that ornithopods increased in body size throughout their evolutionary history (Table 4-4), reaching an upper body size bound in the Early Cretaceous, perhaps in association with significant decreases in sauropod diversity at the Jurassic-Cretaceous boundary (Figure 4-9). However, the data and detailed phylogenetic framework used in this study does not support the

hypothesis that the Island Rule was a major driver of body size evolution in ornithopods (Figure 4-7).

In addition to testing specific hypotheses of body size evolution in ornithopods, this clade serves as a good case study for discussing the application of phylogenetic comparative methods to phylogenies of fossil taxa. In particular, my results allow me to forward three important methodological issues to the forefront.

4.7.1 Branch Lengths

All phylogenetic comparative methods require measures of branch length; that is an estimate of how much evolution has occurred between an ancestor and a descendant. Molecular phylogenies calculate branch lengths by quantifying changes in DNA/RNA sequences that are then standardized with respect to time using fossil calibration points and the molecular clock (see Kumar, 2005 for a review of molecular clocks). Molecular data is not available for the majority of the fossil record, and, as a result, branch lengths must be estimated via other methods. The most common method is to use time (Laurin, 2004; Hunt and Carrano, 2010; Sookias *et al.*, 2012b; Zanno and Makovicky, 2013), as is the case for molecular phylogenies. However, unlike the molecular clock, which is at least in part based on the intrinsic genetic properties of an organism, branch lengths using time from the fossil record are extrinsic, and need not always represent a direct measure of evolution between an ancestor-descendant pair (see Phylogenetic Context section and Dececchi and Larsson, in press for further discussion on limitations associated with assessing branch lengths in a fossil dataset). The analyses carried out here indicate that further research is needed on measuring branch lengths within a fossil dataset. This is particularly evident when comparing the analysis that used uniform branch lengths (all equal to one) to the four others that utilize time (Table 4-2). Even when using time as a measure of

branch length, the scaling methods (i.e., equal, zlba, aba, and mbl) applied will also have a significant effect of the final results, and hence subsequent interpretations. Therefore, it is important that future studies not only investigate the sensitivity of analyses to topological uncertainty, but also ambiguity associates with branch lengths.

4.7.2 Model-Fitting at Nodes

Applications of the model-fitting approach in living taxa are generally carried out by fitting selected models at particular nodes within the tree of life (e.g., Harmon *et al.*, 2010). This node-biased approach may at first seem reasonable when interpreting the evolution of living taxa because one is often able to distinguish clearly between what are perceived as major radiations (e.g., birds, mammals, squamates, and clades therein). However, such an approach does not take into account the variability in preferred model within a clade, and will ignore many ‘stem’-based taxa. This is most evident in the fossil record, where broad levels of classification are not as easily defined. Despite efforts to classify ornithopods into what are often deemed ‘important’ groups (e.g., Thescelosauridae, Iguanodontia, and Hadrosauridae), these levels of classification simply represent historical constructs and in practice there are several paraphyletic clusters of taxa that represent successive grades from one taxonomic classification to another. For instance, Hadrosauroidae can be defined as all taxa more closely related to *Parasaurolophus* than to *Iguanodon* (stem-based; sensu Sereno, 1997), as was used in this study, or as the most recent common ancestor of *Bactrosaurus*, *Telmatosaurus*, and Hadrosauridae (node-based; sensu Godefroit *et al.*, 1998). These definitions are largely arbitrary and simply reflect qualitative assertions as to where major evolutionary shifts occurred. As a result, simply fitting models at specific node will not accurately reflect the changes in model support in other parts of the tree. My results strongly advocate that a more continuous approach be adopted in the future, for both

extinct and extant clades. In other words, models should be fit at all nodes for which an adequate sample size can be obtained. When this approach was used on the ornithopod tree, it became evident that although a trend model was supported for ornithopods overall, there were several instances in which other models, such as early-burst and Brownian Motion were the preferred model. These patterns would have been lost had the traditional discrete approach of fitting models and specific nodes been adopted.

4.7.3 Model-Fitting and Sample Size

Sample size and statistical power have been the subject of much discussion for almost 50 years, ever since the pioneering research of Jacob Cohen (e.g., Cohen, 1969). Its application is generally discussed within the null vs. alternative hypothesis paradigm, but is clearly applicable when comparing the fit of different models using a likelihood approach. Does the ability to support a particular model (say an early burst model) decrease or increase at lower sample sizes? This is a question that has yet to be studied in detail. Currently, there is only a single published study that attempts to address it (Harmon *et al.*, 2010; figure S1). The authors found that, based on simulated data, as sample size decreases the ability to recover more complex models (such as Ornstein-Uhlenbeck and early-burst) diminishes dramatically at sample sizes less than 20, whereas support for simpler models (such as Brownian Motion) significantly increases. The results of Harmon et al. (2010) are corroborated by the empirical data presented in this study. A random subsampling of the ornithopod dataset (1000 replicates) indicates that both Brownian Motion and stasis models of evolution will be preferred at low sample sizes ($N < 20$), whereas trend, early-burst, Ornstein-Uhlenbeck models will decrease (Figure 4-11). These results advocate for caution when interpreting patterns of evolution within small clades using the model-

fitting approach, in particular where simpler models, such as Brownian Motion and stasis are preferred (Sookias *et al.*, 2012b; Zanno and Makovicky, 2013).

4.8 Tables

Table 4-1. Statistical summary of ancestor-descendent contrasts in ornithopods.

Clade	Mean (μ)	Median	Sum	Skew	N	+	-
Uniform (all branches=1)							
Ornithopoda	0.0091	-0.007	1.579	0.1848	174	83	91
Thescelosauridae	0.0327	0.0905	0.5879	-0.1383	18	11	7
Iguanodontia	0.0067	-0.0132	1.0172	0.2595	152	70	82
Hadrosauroidea	0.007	-0.0109	0.7254	0.1395	104	47	57
Hadrosauridae	0.014	-0.0013	1.01	0.115	72	35	37
Hadrosaurinae	0.0129	0.0221	0.4136	0.3053	32	17	15
Lambeosaurinae	0.0155	-0.0052	0.5259	-0.066	34	15	19
Equal Distribution (1 Ma added)							
Ornithopoda	0.0396	0.0075	6.8877	0.5611	174	108	66*
Thescelosauridae	0.0096	0.0087	0.1721	-0.1133	18	9	9
Iguanodontia	0.0495*	0.0104	7.5216	0.7934	152	97	55*
Hadrosauroidea	0.014	0.0134	1.4537	-0.1408	104	68	36*
Hadrosauridae	0.0229	0.0188	1.6496	-0.1308	72	51	21*
Hadrosaurinae	0.0391	0.019	1.2515	0.9942	32	22	10
Lambeosaurinae	0.0161	0.0182	0.5476	-0.8385	34	26	8*
Equal Distribution (10 Ma added)							
Ornithopoda	0.0321	0.0151	5.591	0.4081	174	104	70
Thescelosauridae	0.0163	0.0189	0.2932	-0.095	18	9	9
Iguanodontia	0.0397	0.0151	6.027	0.5918	152	93	59
Hadrosauroidea	0.0126	0.013	1.3128	-0.1603	104	66	38
Hadrosauridae	0.0225	0.018	1.6199	-0.1295	72	51	21*
Hadrosaurinae	0.0376	0.0193	1.2048	0.9836	32	22	10
Lambeosaurinae	0.0166	0.0169	0.5635	-0.8265	34	26	8*
All Branches Adjusted (1 Ma added)							
Ornithopoda	0.0381	0.0117	6.6311	0.5124	174	106	68
Thescelosauridae	0.0999	0.0579	1.7979	0.3163	18	11	7
Iguanodontia	0.0388	0.0109	5.8932	0.5767	152	93	59
Hadrosauroidea	0.0167	0.01	1.7368	0.1148	104	65	39
Hadrosauridae	0.03	0.0205	2.1622	0.245	72	51	21*
Hadrosaurinae	0.0502	0.0397	1.6072	1.2005	32	24	8
Lambeosaurinae	0.0164	0.0103	0.5572	-0.4495	34	23	11
Zero-Length Branches Adjusted (1 Ma added)							
Ornithopoda	0.0387	0.0135	6.7391	0.5038	174	106	68
Thescelosauridae	0.101	0.0517	1.8188	0.3468	18	11	7
Iguanodontia	0.0393	0.0131	5.978	0.5523	152	93	59
Hadrosauroidea	0.017	0.0103	1.7681	0.0778	104	64	40

Clade	Mean (μ)	Median	Sum	Skew	N	+	-
Hadrosauridae	0.031	0.0163	2.2329	0.2067	72	50	22*
Hadrosaurinae	0.0549	0.0407	1.7583	1.1708	32	24	8
Lambeosaurinae	0.0156	0.0103	0.531	-0.5002	34	22	12
Minimum Branch Length (all branched\geq1)							
Ornithopoda	0.0308	0.01	5.359	0.4776	174	103	71
Thescelosauridae	0.1023	0.0415	1.8415	0.3673	18	11	7
Iguanodontia	0.0305	0.0087	4.6341	0.5081	152	90	62
Hadrosauroidae	0.0039	0.0067	0.4006	-0.2334	104	62	42
Hadrosauridae	0.0172	0.0169	1.2418	-0.1579	72	48	24
Hadrosaurinae	0.0332	0.0288	1.0624	1.1137	32	21	11
Lambeosaurinae	0.011	0.0128	0.3745	-0.7772	34	23	11

Positive/negative columns represent the number of positive and negative ancestor-descendent constraints, respectively. Means and counts were tested for significance using a two-tailed t-test ($H_0: \mu=0$; $H_A: \mu\neq0$) and Chi-squared test ($H_0: + = -$; $H_A: + \neq -$), respectively. (*) Denote significance between $p=0.05$ and $p=0.01$ and (**) denote significance at $p<0.01$.

Table 4-2. Results of phylogenetic model-fitting analyses for Ornithopoda and certain clades therein.

			Models Tested									
Tree	Clade	N	Brownian Motion		Driven Trend		Stasis		Ornstein-Uhlenbeck		Early Burst	
			σ^2	AW	σ^2, μ	AW	θ, ω	AW	α, ω	AW	ω, r	AW
Uniform	Ornithopoda	88	0.0805	0.0002	0.0799, 0.0259	0.0001	5.9735, 0.6939	0.0000	0.0817, 0.0059	0.0001	0.2124, -0.0601	0.9996
	Thescelosauridae	10	0.1712	0.1566	0.1631, 0.1517	0.0177	4.6531, 0.2833	0.7440	20, 35.3033	0.0675	0.1712, 0	0.0142
	Iguanodontia	77	0.0710	0.0006	0.0706, 0.0186	0.0002	6.1654, 0.461	0.0000	0.0714, 0.0019	0.0002	0.2011, -0.0629	0.9989
	Hadrosauroidea	53	0.0335	0.3063	0.0324, 0.0286	0.1576	6.4605, 0.1179	0.0023	0.0567, 0.2221	0.3709	0.062, -0.0383	0.1629
	Hadrosauridae	37	0.0315	0.1270	0.0291, 0.0466	0.0837	6.5841, 0.0903	0.0652	0.0789, 0.4175	0.0697	0.1979, -0.3009	0.6544
	Hadrosaurinae	17	0.0218	0.4496	0.0207, -0.0496	0.1380	6.6924, 0.0663	0.1785	0.0388, 0.2542	0.1362	0.0262, -0.0492	0.0978
	Lambeosaurinae	18	0.0295	0.1089	0.0239, 0.0779	0.0698	6.5428, 0.075	0.1514	3.4566, 23.0424	0.0340	0.2374, -0.5424	0.6359
Equal Distribution	Ornithopoda	88	0.0075	0.0760	0.0073, 0.0054	0.1313	5.9735, 0.6939	0.0000	0.0075, 0	0.0260	0.0166, -0.015	0.7668
	Thescelosauridae	10	0.0065	0.1873	0.0038, 0.0171	0.1980	4.6531, 0.2833	0.5480	20, 35.3033	0.0497	0.0065, 0	0.0170
	Iguanodontia	77	0.0070	0.1119	0.0067, 0.0068	0.3459	6.1654, 0.461	0.0000	0.007, 0	0.0378	0.016, -0.0146	0.5044
	Hadrosauroidea	53	0.0046	0.2701	0.0043, 0.0122	0.5537	6.4605, 0.1179	0.0012	0.0046, 0	0.0875	0.0046, 0	0.0875
	Hadrosauridae	37	0.0059	0.0982	0.0052, 0.0264	0.3162	6.5841, 0.0903	0.0880	0.0059, 0	0.0298	0.0553, -0.2186	0.4678
	Hadrosaurinae	17	0.0042	0.4348	0.0041, 0.0099	0.1018	6.6924, 0.0663	0.2066	0.0042, 0	0.0934	0.0234, -0.3145	0.1635
	Lambeosaurinae	18	0.0056	0.2238	0.0051, 0.0215	0.1260	6.5428, 0.075	0.2545	7.5005, 50	0.0571	0.1422, -0.7484	0.3385
Equal Distribution	Ornithopoda	88	0.0069	0.1429	0.0066, 0.0063	0.3413	5.9735, 0.6939	0.0000	0.0069, 0	0.0489	0.0146, -0.012	0.4669
	Thescelosauridae	10	0.0061	0.1883	0.0036, 0.0168	0.1695	4.6531, 0.2833	0.5731	20, 35.3033	0.0520	0.0061, 0	0.0171
	Iguanodontia	77	0.0066	0.1859	0.0064, 0.0063	0.3452	6.1654, 0.461	0.0000	0.0066, 0	0.0628	0.0143, -0.0121	0.4061
	Hadrosauroidea	53	0.0046	0.2700	0.0043, 0.0122	0.5539	6.4605, 0.1179	0.0012	0.0046, 0	0.0874	0.0046, 0	0.0874
	Hadrosauridae	37	0.0059	0.0982	0.0052, 0.0264	0.3162	6.5841, 0.0903	0.0880	0.0059, 0	0.0298	0.0553, -0.2186	0.4678
	Hadrosaurinae	17	0.0042	0.4348	0.0041, 0.0099	0.1018	6.6924, 0.0663	0.2066	0.0042, 0	0.0934	0.0234, -0.3145	0.1635
	Lambeosaurinae	18	0.0056	0.2238	0.0051, 0.0215	0.1260	6.5428, 0.075	0.2545	7.5005, 50	0.0571	0.1422, -0.7484	0.3385
All Branches Adjusted	Ornithopoda	88	0.0089	0.1375	0.0085, 0.0075	0.5041	5.9735, 0.6939	0.0000	0.0089, 0	0.0470	0.0181, -0.0091	0.3113
	Thescelosauridae	10	0.0118	0.2184	0.0078, 0.0155	0.1024	4.6531, 0.2833	0.5900	0.0707, 0.1268	0.0694	0.0118, 0	0.0198
	Iguanodontia	77	0.0083	0.2048	0.008, 0.0065	0.3275	6.1654, 0.461	0.0000	0.0083, 0	0.0692	0.0175, -0.0095	0.3985
	Hadrosauroidea	53	0.0045	0.1407	0.004, 0.0129	0.7679	6.4605, 0.1179	0.0003	0.0045, 0	0.0456	0.0045, 0	0.0456

			Models Tested									
			Brownian Motion		Driven Trend		Stasis		Ornstein-Uhlenbeck		Early Burst	
Tree	Clade	N	σ^2	AW	σ^2, μ	AW	θ, ω	AW	α, ω	AW	ω, r	AW
	Hadrosauridae	37	0.0056	0.0222	0.0041, 0.0303	0.7649	6.5841, 0.0903	0.0115	0.0056, 0	0.0067	0.0434, -0.1746	0.1947
	Hadrosaurinae	17	0.0036	0.4950	0.0036, 0.0078	0.1138	6.6924, 0.0663	0.1699	0.0036, 0	0.1063	0.0067, -0.0656	0.1150
	Lambeosaurinae	18	0.0052	0.1929	0.004, 0.0265	0.2859	6.5428, 0.075	0.1288	0.0052, 0	0.0433	0.0671, -0.2965	0.3492
	Ornithopoda	88	0.0094	0.1475	0.0089, 0.0079	0.5729	5.9735, 0.6939	0.0000	0.0094, 0	0.0504	0.0179, -0.0089	0.2292
	Thescelosauridae	10	0.0120	0.2221	0.0078, 0.0164	0.1121	4.6531, 0.2833	0.5778	0.0712, 0.1279	0.0678	0.012, 0	0.0201
	Iguanodontia	77	0.0087	0.2288	0.0084, 0.0069	0.3773	6.1654, 0.461	0.0000	0.0087, 0	0.0774	0.0174, -0.0093	0.3165
	Hadrosauroidea	53	0.0048	0.1288	0.0043, 0.0142	0.7873	6.4605, 0.1179	0.0004	0.0048, 0	0.0417	0.0048, 0	0.0417
	Hadrosauridae	37	0.0061	0.0201	0.0045, 0.0326	0.7387	6.5841, 0.0903	0.0138	0.0061, 0	0.0061	0.0516, -0.2042	0.2213
	Hadrosaurinae	17	0.0038	0.5008	0.0038, 0.008	0.1141	6.6924, 0.0663	0.1651	0.0038, 0	0.1075	0.0064, -0.0572	0.1125
	Lambeosaurinae	18	0.0056	0.1872	0.0044, 0.0278	0.2368	6.5428, 0.075	0.1288	0.0056, 0	0.0420	0.0775, -0.3558	0.4053
	Ornithopoda	88	0.0084	0.2394	0.0081, 0.0062	0.4247	5.9735, 0.6939	0.0000	0.009, 0.0022	0.0916	0.0154, -0.009	0.2444
	Thescelosauridae	10	0.0119	0.2225	0.0078, 0.0159	0.1068	4.6531, 0.2833	0.5816	0.0692, 0.1244	0.0690	0.0119, 0	0.0202
	Iguanodontia	77	0.0077	0.2943	0.0076, 0.0051	0.2634	6.1654, 0.461	0.0000	0.0077, 0	0.0995	0.0155, -0.0105	0.3428
	Hadrosauroidea	53	0.0038	0.3375	0.0036, 0.0101	0.4438	6.4605, 0.1179	0.0001	0.0038, 0	0.1093	0.0038, 0	0.1093
	Hadrosauridae	37	0.0045	0.2535	0.0041, 0.0215	0.3685	6.5841, 0.0903	0.0241	0.0045, 0	0.0769	0.0198, -0.1075	0.2771
	Hadrosaurinae	17	0.0034	0.4960	0.0034, 0.0089	0.1158	6.6924, 0.0663	0.1573	0.0034, 0	0.1065	0.0089, -0.1006	0.1244
	Lambeosaurinae	18	0.0042	0.4211	0.0039, 0.017	0.1648	6.5428, 0.075	0.1679	0.0042, 0	0.0945	0.0194, -0.1621	0.1518

Ornithopod clades represent major subdivisions discussed in the literature. Green shading represents the best-fit model (highest Akaike weight score), orange shading represents models that cannot be rejected outright ($AK \geq 0.125$ that of the best-fit model), and no colour represents models that can be rejected. σ^2 , step variance (in \log_{10} mm); μ , step mean (in \log_{10} mm); θ , stasis body mass mean (in \log_{10} mm); ω , stasis body mass variance.

Table 4-3. Ancestor-descendent body mass (in \log_{10} g) contrasts based on the ‘mbl’ ornithopod tree.

Ancestor	Descendent	Ancestral Mass	Descendent Mass	Size Contrast
Node1	Node2	4.887	4.2357	-0.6513 ^z
Node2	Node3	4.2357	4.1835	-0.0522
Node3	<i>Gideonmantellia amosanjuanae</i>	4.1835	3.8481	-0.3354 ^{e,u}
Node3	Node4	4.1835	4.6653	0.4818
Node4	<i>Oryctodromeus cubicularis</i>	4.6653	4.7278	0.0626
Node4	Node5	4.6653	4.7694	0.1041
Node5	<i>Koreanosaurus boseongensis</i>	4.7694	5.2393	0.4699 ^{e,u}
Node5	<i>Orodromeus makelai</i>	4.7694	4.3103	-0.4591 ^{z,u}
Node2	Node6	4.2357	4.2593	0.0236
Node6	<i>Parksosaurus warreni</i>	4.2593	4.8609	0.6015 ^z
Node6	Node7	4.2593	4.2723	0.0129
Node7	Node8	4.2723	5.2732	1.0009 ^{z,e,u}
Node8	<i>Thescelosaurus neglectus</i>	5.2732	5.5483	0.2751 ^u
Node8	<i>Thescelosaurus assiniboiensis</i>	5.2732	5.0535	-0.2197
Node7	Node9	4.2723	4.269	-0.0033
Node9	<i>Jeholosaurus shangyuanensis</i>	4.269	4.0013	-0.2677 ^{e,u}
Node9	Node10	4.269	4.5354	0.2665
Node10	<i>Changchunsaurus parvus</i>	4.5354	4.9198	0.3844 ^u
Node10	<i>Haya griva</i>	4.5354	4.0213	-0.5141 ^{z,e,u}
Node1	Node11	4.887	4.9027	0.0157
Node11	<i>Hypsilophodon foxi</i>	4.9027	4.3989	-0.5038 ^{z,e}
Node11	Node12	4.9027	4.9294	0.0267
Node12	<i>Gasparinisaura cincosalensis</i>	4.9294	4.1105	-0.8189 ^{z,e}
Node12	Node13	4.9294	4.9669	0.0375
Node13	<i>Anabisetia saldiviae</i>	4.9669	4.4734	-0.4934 ^{z,e}
Node13	Node14	4.9669	5.0099	0.043 ^u
Node14	<i>Talenkauen santacruzensis</i>	5.0099	5.7513	0.7414 ^{z,e}
Node14	Node15	5.0099	5.0455	0.0356
Node15	Node16	5.0455	6.0063	0.9608 ^{z,e}
Node16	<i>Muttaburrasaurus langdoni</i>	6.0063	6.764	0.7577 ^{z,e,u}
Node16	Node17	6.0063	5.0657	-0.9406 ^z
Node17	<i>Rhabdodon priscum</i>	5.0657	5.9361	0.8703 ^{z,e}
Node17	Node18	5.0657	4.9698	-0.0959 ^u
Node18	Node19	4.9698	5.0752	0.1054
Node19	<i>Zalmoxes robustus</i>	5.0752	5.0924	0.0172
Node19	<i>Zalmoxes shqiperorum</i>	5.0752	5.0828	0.0076
Node18	Node20	4.9698	4.8681	-0.1017 ^u
Node20	<i>Mochlodon seussi</i>	4.8681	4.4839	-0.3842
Node20	<i>Mochlodon vorosi</i>	4.8681	4.7377	-0.1304
Node15	Node21	5.0455	5.0637	0.0182
Node21	Node22	5.0637	6.0092	0.9455 ^{z,e}
Node22	<i>Tenontosaurus tilletti</i>	6.0092	6.028	0.0188
Node22	<i>Tenontosaurus dossi</i>	6.0092	6.075	0.0659
Node21	Node23	5.0637	5.0622	-0.0015
Node23	Node24	5.0622	4.9884	-0.0739 ^u
Node24	<i>Callovosaurus leedsi</i>	4.9884	4.8374	-0.1509 ^u
Node24	Node25	4.9884	5.0828	0.0944

Node25	<i>Dryosaurus altus</i>	5.0828	5.2107	0.1279
Node25	Node26	5.0828	5.0869	0.0041
Node26	<i>Dysalotosaurus lettowvorbecki</i>	5.0869	5.1756	0.0887
Node26	Node27	5.0869	4.7965	-0.2904
Node27	<i>Kangnasaurus coetzeei</i>	4.7965	5.4025	0.606 ^z
Node27	Node28	4.7965	4.7763	-0.0202
Node28	<i>Elrhazosaurus nigeriensis</i>	4.7763	4.6995	-0.0768
Node28	<i>Valdosaurus canaliculatus</i>	4.7763	4.6995	-0.0768
Node23	Node29	5.0622	5.6121	0.5499 ^z
Node29	<i>Campitosaurus dispar</i>	5.6121	6.1416	0.5295 ^e
Node29	Node30	5.6121	5.6418	0.0297
Node30	<i>Uteodon aphanoecetes</i>	5.6418	5.4447	-0.197 ^u
Node30	Node31	5.6418	6.2918	0.6501 ^z
Node31	Node32	6.2918	6.023	-0.2688
Node32	<i>Hippodraco scutodens</i>	6.023	5.8695	-0.1536
Node32	<i>Theiophytalia kerri</i>	6.023	6.1561	0.1331
Node31	Node33	6.2918	6.3579	0.0661 ^u
Node33	<i>Barilium dawsoni</i>	6.3579	6.764	0.4061 ^e
Node33	Node34	6.3579	6.3457	-0.0122
Node34	<i>Iguanodon bernissartensis</i>	6.3457	6.9385	0.5929 ^{z,e}
Node34	Node35	6.3457	6.3184	-0.0273
Node35	<i>Ouranosaurus nigeriensis</i>	6.3184	6.4588	0.1405
Node35	Node36	6.3184	6.2873	-0.0311
Node36	<i>Mantellisaurus atherfieldensis</i>	6.2873	6.1749	-0.1124
Node36	Node37	6.2873	6.2642	-0.0231
Node37	<i>Jinzhousaurus yangi</i>	6.2642	6.0977	-0.1664
Node37	Node38	6.2642	6.2476	-0.0166
Node38	<i>Bolong yixianensis</i>	6.2476	5.7467	-0.501 ^{z,e}
Node38	Node39	6.2476	6.2516	0.0039
Node39	<i>Altirhinus kurzanovi</i>	6.2516	6.6548	0.4033
Node39	Node40	6.2516	6.2437	-0.0079
Node40	Node41	6.2437	6.2312	-0.0125
Node41	<i>Equijubus normani</i>	6.2312	6.3083	0.0771
Node41	<i>Xuwulong yueluni</i>	6.2312	6.0005	-0.2307
Node40	Node42	6.2437	6.2404	-0.0033
Node42	<i>Probactrosaurus mazongshanensis</i>	6.2404	6.1925	-0.0478
Node42	Node43	6.2404	6.2393	-0.0011
Node43	Node44	6.2393	6.2455	0.0061
Node44	<i>Eolambia caroljonesa</i>	6.2455	6.4725	0.2271
Node44	<i>Probactrosaurus gobiensis</i>	6.2455	6.2539	0.0084
Node43	Node45	6.2393	6.1196	-0.1197
Node45	<i>Protohadros byrdi</i>	6.1196	6.4622	0.3426
Node45	Node46	6.1196	6.0955	-0.0241
Node46	<i>Tethyshadros insularis</i>	6.0955	5.6136	-0.4819 ^{z,e}
Node46	Node47	6.0955	6.0821	-0.0135
Node47	<i>Nanyangosaurus zhugeii</i>	6.0821	5.7301	-0.352
Node47	Node48	6.0821	6.2402	0.1581
Node48	<i>Tanius sinensis</i>	6.2402	6.5667	0.3266
Node48	Node49	6.2402	6.2424	0.0022
Node49	<i>Gilmoreosaurus mongolensis</i>	6.2424	6.1331	-0.1093
Node49	Node50	6.2424	6.2517	0.0093
Node50	<i>Bactrosaurus johnsoni</i>	6.2517	6.2746	0.0229

Node50	Node51	6.2517	6.2595	0.0078
Node51	<i>Claosaurus agilis</i>	6.2595	6.11	-0.1495
Node51	Node52	6.2595	6.2761	0.0166
Node52	<i>Telmatosaurus transsylvanicus</i>	6.2761	6.2226	-0.0535
Node52	Node53	6.2761	6.2946	0.0185
Node53	<i>Lophorhothon atopus</i>	6.2946	5.8501	-0.4445 ^e
Node53	Node54	6.2946	6.3426	0.048
Node54	Node55	6.3426	6.5784	0.2358
Node55	Node56	6.5784	6.5755	-0.0029
Node56	<i>Wulagasaurus dongi</i>	6.5755	6.4852	-0.0903
Node56	Node57	6.5755	6.5789	0.0034
Node57	<i>Acristavus gaglarsoni</i>	6.5789	6.534	-0.0449
Node57	Node58	6.5789	6.5852	0.0062
Node58	<i>Brachylophosaurus canadensis</i>	6.5852	6.6698	0.0847
Node58	<i>Maiasaura peeblesorum</i>	6.5852	6.5836	-0.0016
Node55	Node59	6.5784	6.6265	0.0481
Node59	<i>Barsboldia sicinskii</i>	6.6265	7.2088	0.5823 ^{z,e,u}
Node59	Node60	6.6265	6.6447	0.0182
Node60	Node61	6.6447	6.621	-0.0236
Node61	<i>Kritosaurus navajovius</i>	6.621	6.661	0.04
Node61	Node62	6.621	6.5956	-0.0254
Node62	Node63	6.5956	6.6039	0.0083
Node63	<i>Gryposaurus notabilis</i>	6.6039	6.6553	0.0513
Node63	<i>Gryposaurus latidens</i>	6.6039	6.647	0.0431
Node62	Node64	6.5956	6.327	-0.2686
Node64	<i>Secernosaurus koernerri</i>	6.327	6.3921	0.0651
Node64	<i>Willinakage salitralensis</i>	6.327	5.9667	-0.3603 ^e
Node60	Node65	6.6447	6.6863	0.0416
Node65	Node66	6.6863	6.6445	-0.0419
Node66	<i>Prosaurolophus maximus</i>	6.6445	6.5135	-0.131
Node66	Node67	6.6445	6.6773	0.0329
Node67	<i>Sauropodus osborni</i>	6.6773	6.8316	0.1543
Node67	<i>Sauropodus angustirostris</i>	6.6773	6.7901	0.1127
Node65	Node68	6.6863	6.7335	0.0472
Node68	<i>Kundurosaurus nagornyi</i>	6.7335	6.8276	0.0941
Node68	Node69	6.7335	6.7768	0.0432
Node69	<i>Shantungosaurus giganteus</i>	6.7768	7.2615	0.4847 ^e
Node69	Node70	6.7768	6.8755	0.0988
Node70	<i>Edmontosaurus annectens</i>	6.8755	6.8412	-0.0344
Node70	<i>Edmontosaurus regalis</i>	6.8755	6.9011	0.0256
Node54	Node71	6.3426	6.3431	0.0005
Node71	<i>Aralosaurus tuberiferus</i>	6.3431	5.7756	-0.5673 ^{z,e}
Node71	Node72	6.3431	6.3876	0.0445
Node72	Node73	6.3876	6.431	0.0434
Node73	<i>Pararhabdodon isonensis</i>	6.431	6.1553	-0.2757
Node73	<i>Tsintaosaurus spinorhinus</i>	6.431	6.6949	0.2639
Node72	Node74	6.3876	6.4264	0.0388
Node74	<i>Arenysaurus ardevoli</i>	6.4264	6.0528	-0.3736 ^e
Node74	Node75	6.4264	6.4797	0.0533
Node75	Node76	6.4797	6.721	0.2413
Node76	<i>Charonosaurus jiayinensis</i>	6.721	6.9785	0.2575
Node76	Node77	6.721	6.7222	0.0012

Node77	<i>Parasaurolophus walkeri</i>	6.7222	6.7298	0.0076
Node77	<i>Parasaurolophus cyrtocristatus</i>	6.7222	6.7142	-0.008
Node75	Node78	6.4797	6.5127	0.033
Node78	Node79	6.5127	6.4272	-0.0855
Node79	<i>Amurosaurus riabinini</i>	6.4272	6.669	0.2418
Node79	<i>Sahaliyenia elunchunorum</i>	6.4272	6.1679	-0.2592
Node78	Node80	6.5127	6.5505	0.0378
Node80	<i>Magnapaulia laticaudus</i>	6.5505	6.9855	0.4349
Node80	Node81	6.5505	6.5641	0.0136
Node81	Node82	6.5641	6.5474	-0.0167
Node82	<i>Lambeosaurus lambei</i>	6.5474	6.539	-0.0084
Node82	Node83	6.5474	6.5484	0.001
Node83	<i>Lambeosaurus clavintialis</i>	6.5484	6.5606	0.0122
Node83	<i>Lambeosaurus magnicristatus</i>	6.5484	6.5394	-0.009
Node81	Node84	6.5641	6.5802	0.0161
Node84	Node85	6.5802	6.6218	0.0416
Node85	<i>Corythosaurus casuarius</i>	6.6218	6.6909	0.0691
Node85	<i>Corythosaurus intermedius</i>	6.6218	6.559	-0.0628
Node84	Node86	6.5802	6.5914	0.0112
Node86	<i>Olorotitan arharensis</i>	6.5914	6.6368	0.0454
Node86	Node87	6.5914	6.6006	0.0092
Node87	<i>Hypacrosaurus altispinus</i>	6.6006	6.5874	-0.0131
Node87	<i>Hypacrosaurus stebingeri</i>	6.6006	6.733	0.1324

Colour shaded cells represent contrasts that occur above (green=giants) or below (orange=dwarfs) the 95% prediction intervals derived from the entire list of contrast from the ‘mbl’ ornithopod tree (intervals: -0.453 to 0.516). Node numbers follows the default settings used by ‘class.phylo’ in R. Superscripts indicate significant shifts recovered by other ornithopod trees that vary in how branch lengths were calculated: z, zero-length branch adjustment; e, equal; u, uniform.

Table 4-4. Summary of analyses supporting a trend in body size evolution in ornithopods (i.e., Cope's Rule).

		Analyses														
		Spearman Rank Correlation		Tree (i.e., branch length estimation method)												
				Uniform				Equal Distribution				Zero-Length Branch Adjustment				
Clade	N	Age	Clade	Δ_{AD}		MF	Δ_{AD}		MF	Δ_{AD}		MF	Δ_{AD}		Trend Support	
				μ	\pm		μ	\pm	MF	μ	\pm	MF	μ	\pm		
Ornithopoda	88	*	*					*				*			*	5
Thescelosauridae	10	*														1
Iguanodontia	77	*	*				*	*				*				5
Hadrosauroidea	53	*	*					*	*			*			*	6
Hadrosauridae	37							*			*	*			*	4
Hadrosaurinae	17															0
Lambeosaurinae	18							*								1

Each set of shaded columns represent different analyses or suite of analyses based on the same set of assumptions, and the final column provides the total number to analyses that support a directed trends towards increasing body size (i.e., Cope's Rule). Δ_{AD} , results based on the ancestor-descendent contrasts; μ , mean contrast t-test against a value of zero (=no trends); \pm , positive/negative count Chi-squared test against equal number of positive and negative shifts; MF, model-fitting results. Asterisks (*) indicate significant p-values in Δ_{AD} analyses and a preferred trend model in MF.

Table 4-5. Preliminary results modeling the evolution of upper body size limits within the context of extrinsic factors.

Model	<i>m</i>	SE <i>m</i>	<i>b</i>	SE <i>b</i>	AIC	A.W.
Autocorrelation: Negligible						
C-13	0.1007	0.0954	9.1243	2.3891	44.3	0.0397
CO ₂	0.0002	0.0001	6.2293	0.2528	55.6	0.0001
GLA	-0.0456**	0.013	12.3177	1.6317	39.5	0.4317
SD	-0.0295**	0.0084	6.5182	0.1068	40.5	0.2695
Null	-	-	6.6064	0.1308	40.5	0.2589
Autocorrelation: ARD1						
C-13	0.0596	0.057	7.5652	12237.9	35.8	0.0757
CO ₂	0.0001	0	5.9507	7622.9	48.4	0.0001
GLA	-0.0457*	0.0195	12.2072	2.445	35.8	0.0778
SD	-0.0091	0.011	5.9576	3657.3	39.5	0.0119
Null	-	-	6.0231	9920	31	0.8345

Results are those obtained from a generalized least regression implemented in the R package ‘nlme’ that allows for autocorrelation between successive data points to be corrected. Regression equation in the format: $y=mx+b$. Green shaded models represent the best-fit models with the highest Akaike weights (A.W.) and lowest AIC scores. Upper body size limits were modelled within the context of carbon-13 concentrations (C-13; Falkowski *et al.*, 2005), atmospheric carbon dioxide (CO₂; Royer *et al.*, 2004), global land area (GLA; Smith *et al.*, 1994), sauropodomorphs diversity (modelled relative to dinosaur bearing formations, SD; Lloyd, 2012), and null model that incurs independence of size (follows Sookias *et al.*, 2012a).

1.1 Figures

Figure 4-1. Phylogenetic tree of Ornithopoda. The topology is derived from various analyses of Hadrosauridae, Iguanodontia, and non-iguanodontian ornithopods outlined in the text.

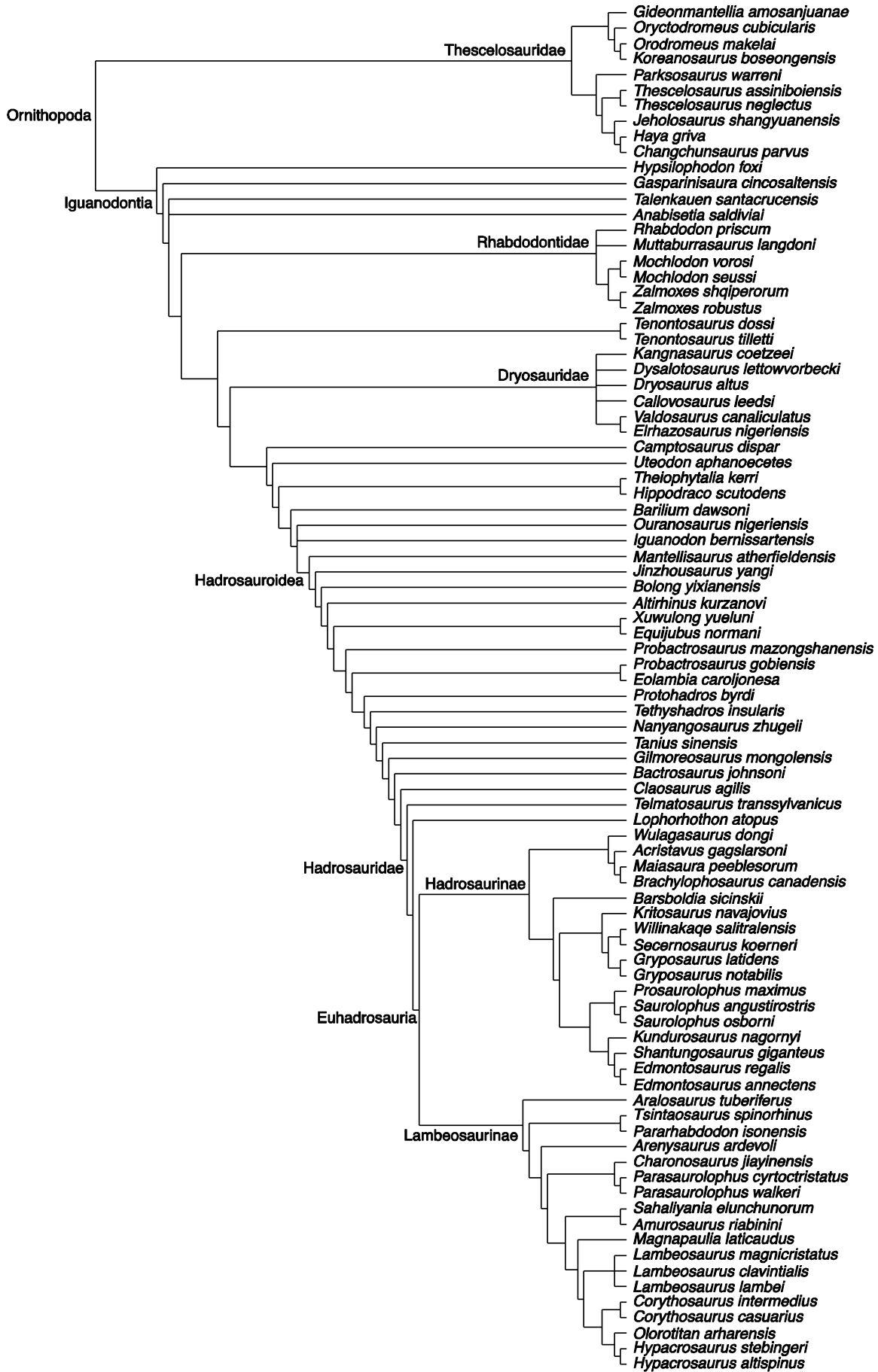


Figure 4-2. Phylogeny of Hadrosauridae showing the effects of different scaling methods on reconstructed branch lengths. Time-scaling methods are those described by Bapst (2012). A, branch lengths are uniform (equal to 1); B, a time calibrated phylogeny, lack of phylogenetic resolution results from zero-branch lengths; C, ‘equal’ with 10 Ma added to the root; D, All branch additive method with 1 Ma added to each branch; E, Zero-length branch additive method with all zero-length branches assigned a length of 1 Ma; and F, Minimum branch length method with a minimum branch lengths of 1 Ma.

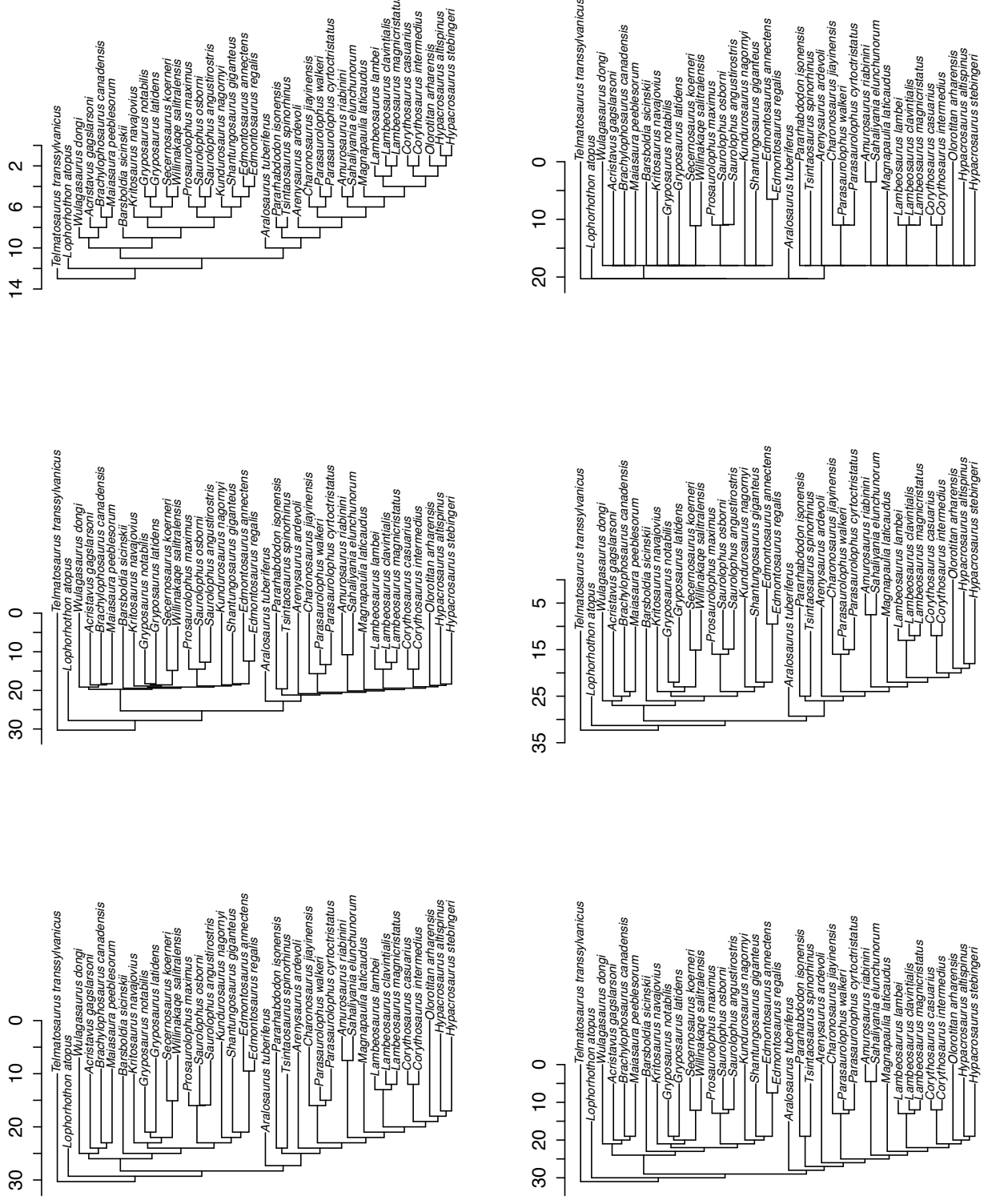


Figure 4-3. Bivariate plots of humeral and femoral length and circumference including both original data and estimated missing data via the BPCA method of Oba *et al.* (2003). In order for estimated data to be considered valid it is expected that it not show evidence of a systematic bias.

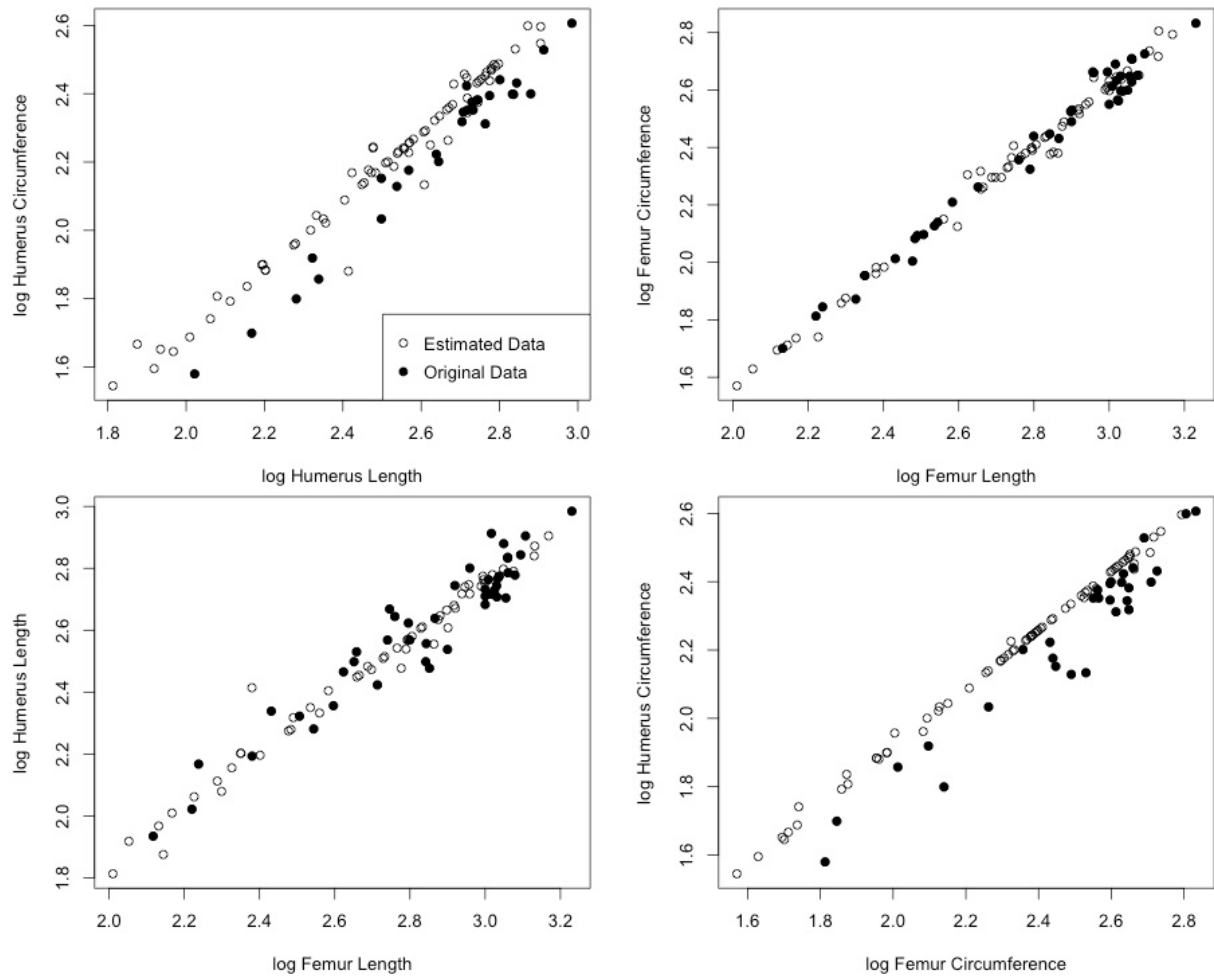


Figure 4-4. Bivariate plots of humeral and femoral length and circumference including both original data and estimated missing data via the best-fit regression method of Brown et al. (2012a). In order for estimated data to be considered valid it is expected that it not show evidence of a systematic bias.

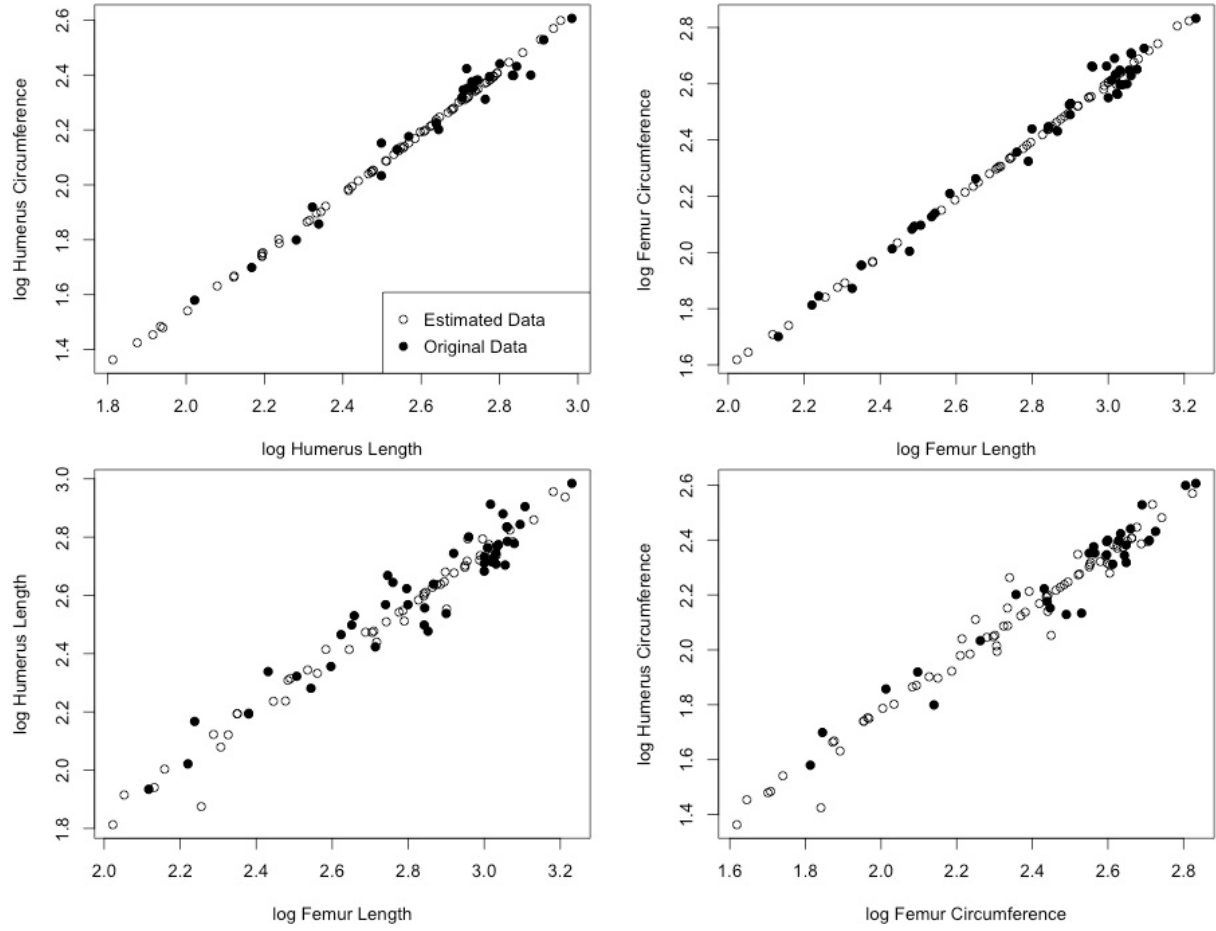


Figure 4-5. Distribution of ancestor-descendent contrasts in ornithopods. Ancestral states are estimated through a maximum likelihood approach that assumed a Brownian motion model of evolution. Tree time-scaling is based on the minimum branch length method (mbl).

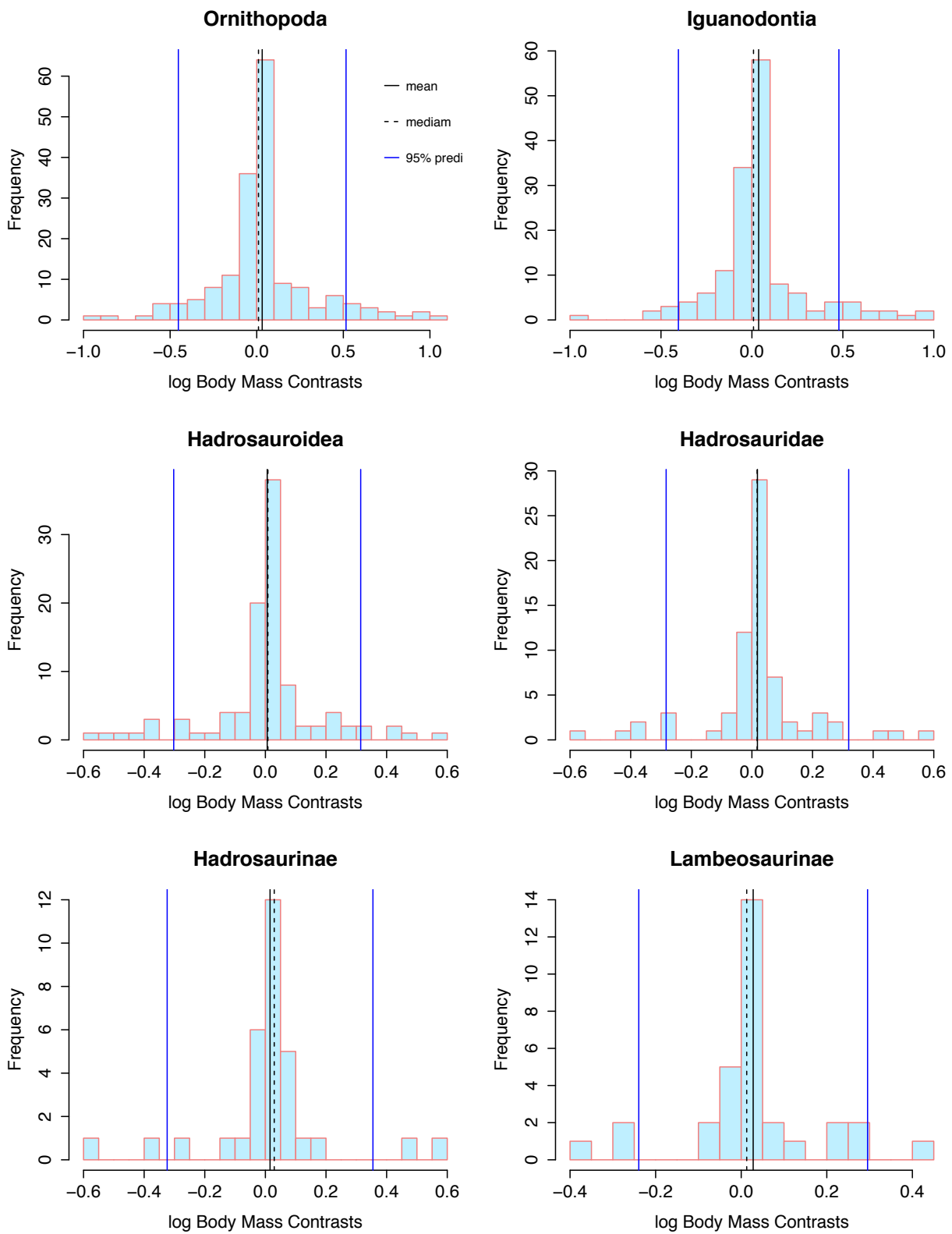
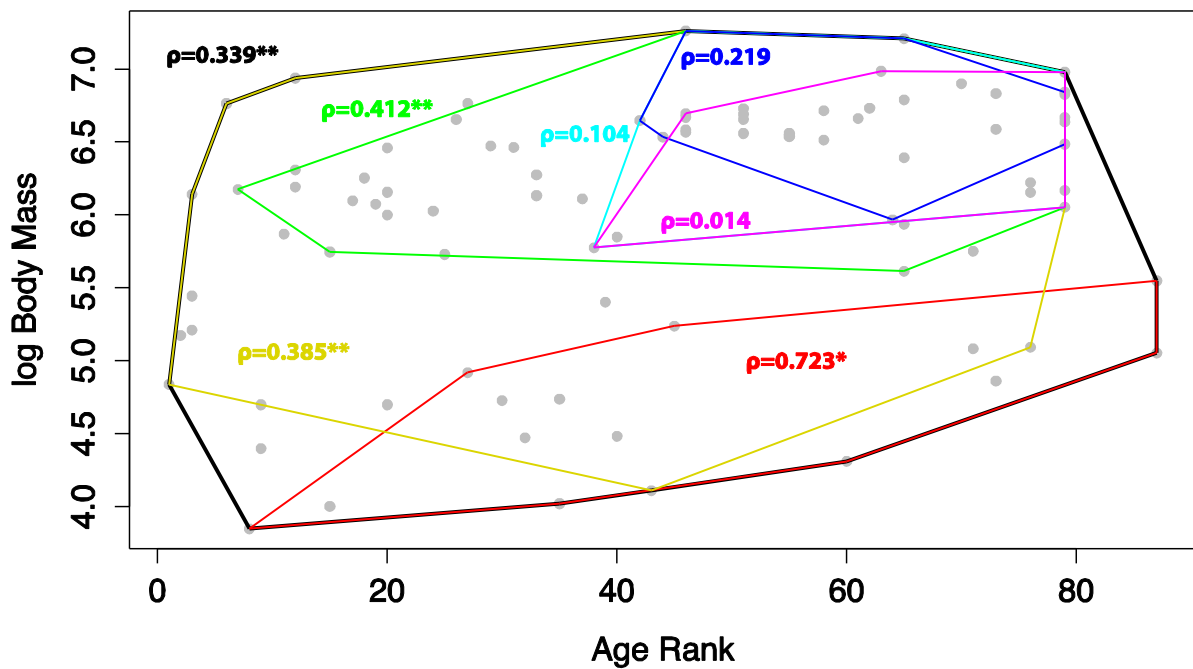


Figure 4-6. Relationship between age/clade-rank and body mass in ornithopods. Coloured minimum convex hulls reflect ornithopod clades, shown with their corresponding spearman rank correlation coefficients (ρ). Asterisks denote significant between 0.05 and 0.01 (*) and <0.01 (**).

Age Rank vs. Body Mass



Clade Rank vs. Body Mass

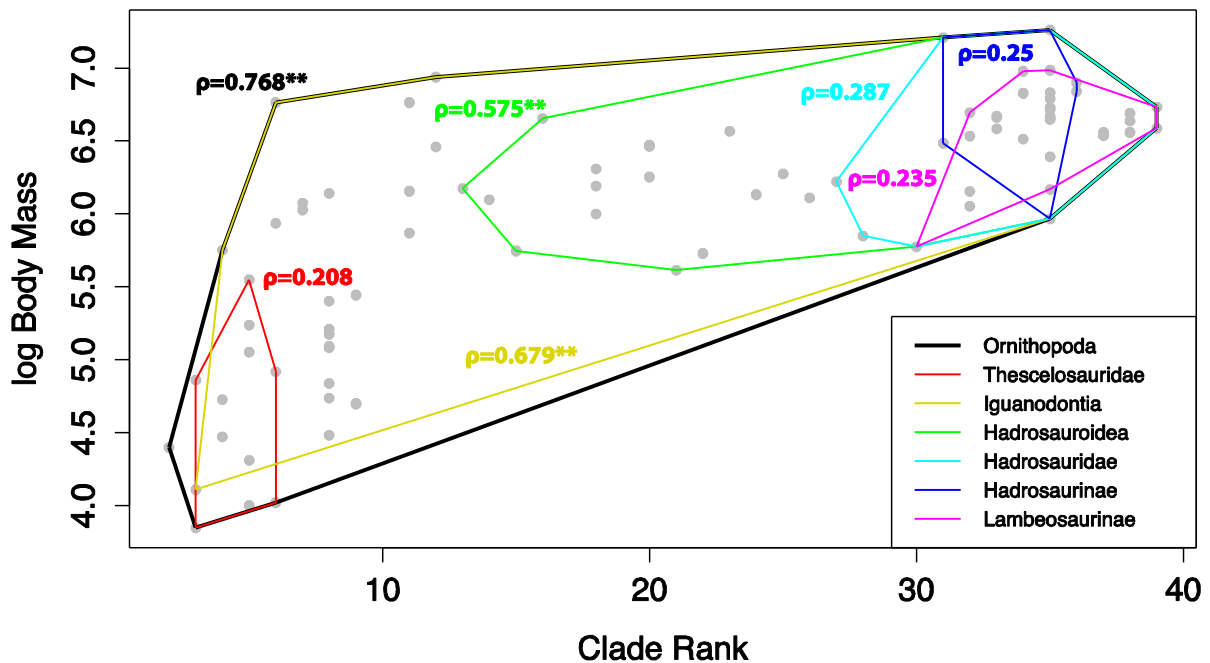


Figure 4-7. Boxplots of ancestor-descendent contrasts based on four branch length estimation methods. Whiskers of the boxplots represent the 95% prediction intervals of the contrast data and datapoints shown indicate outliers with either large or small contrasts relative to the overall pattern. In addition to showing outliers, the plot also indicates the contrasts for ornithopod taxa hypothesized to be insular dwarfs.

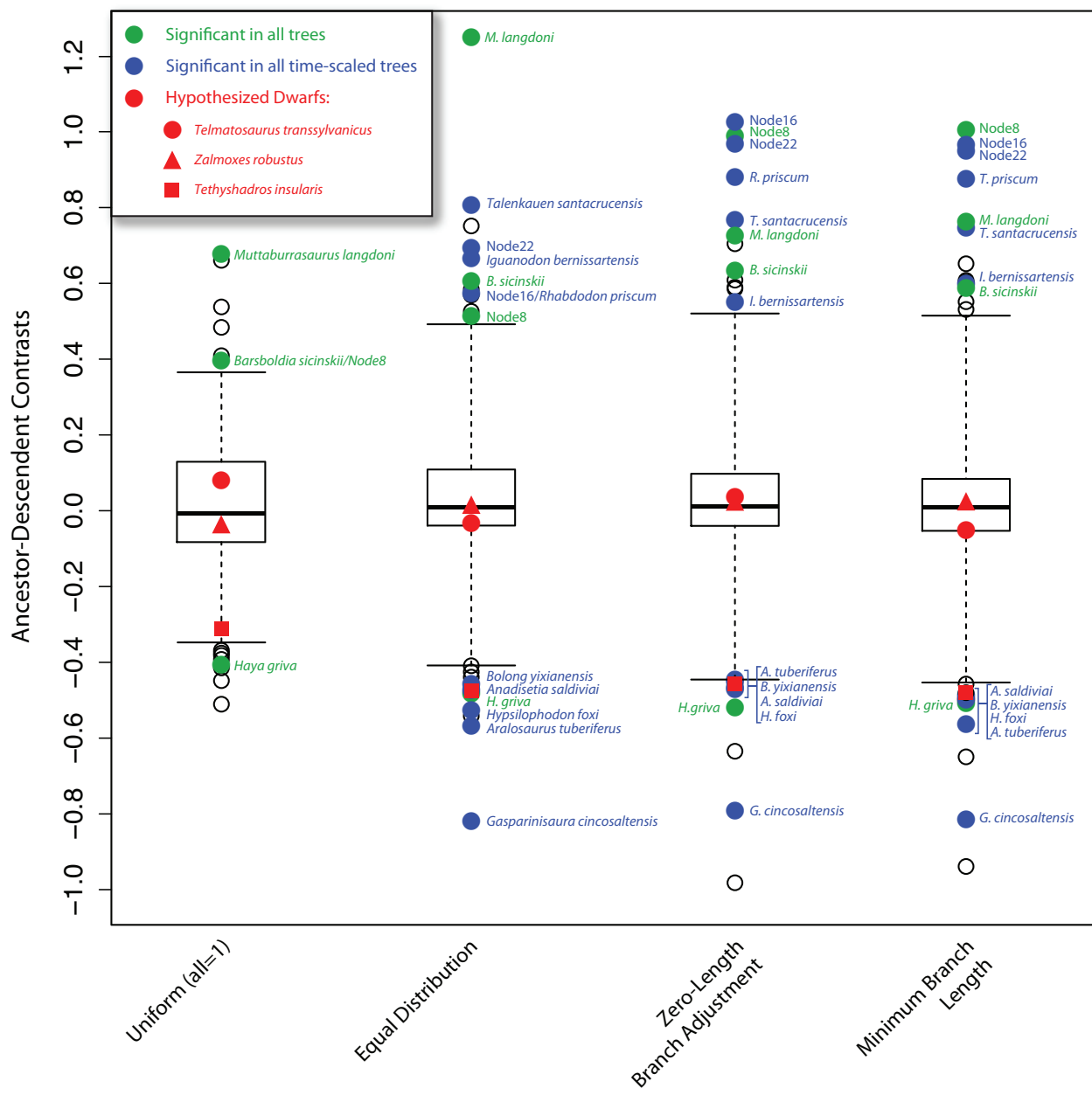
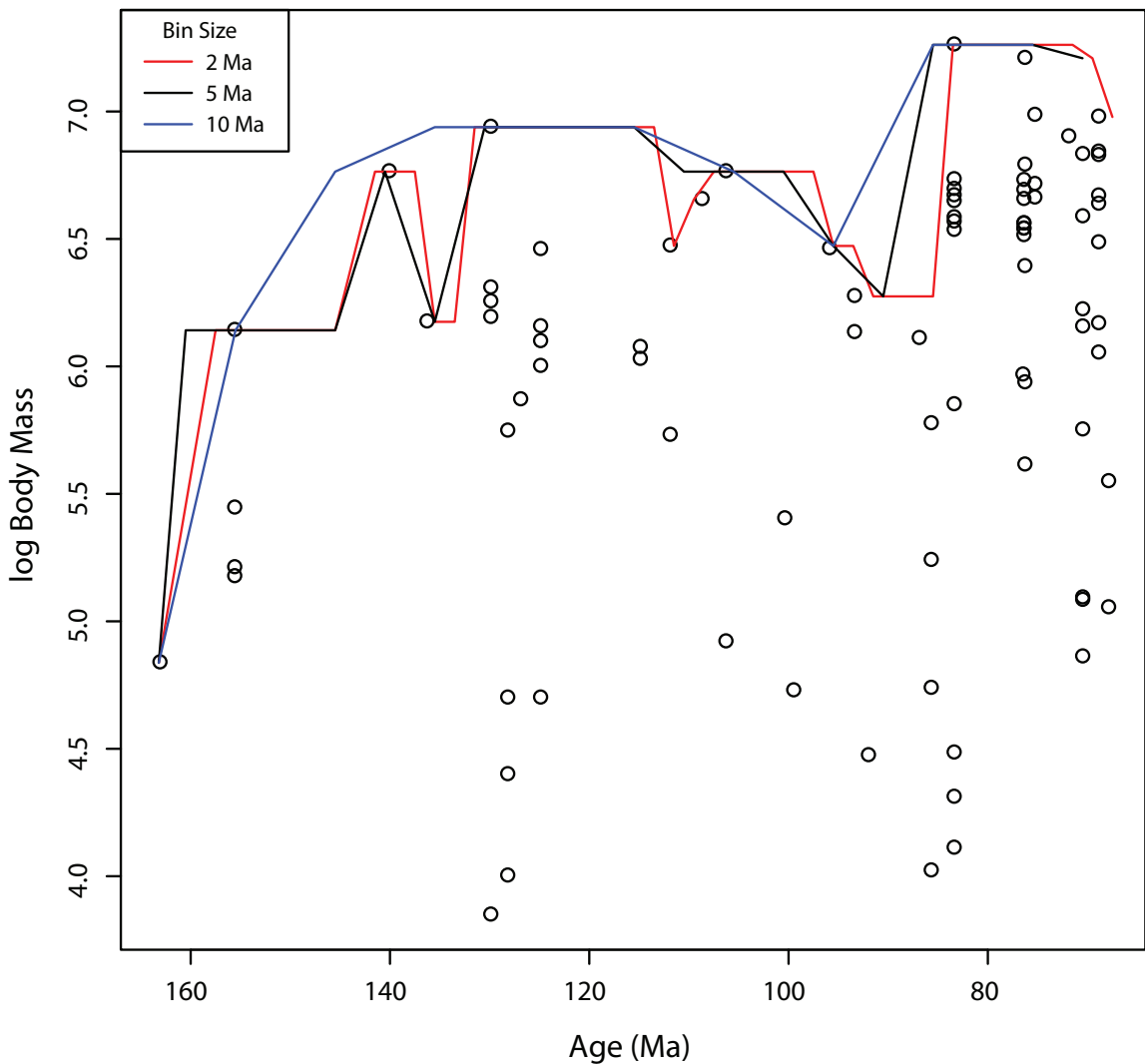


Figure 4-8. Upper body size limits in ornithopods relative to time. Analyses were carried out by binning taxa at three different bin sizes (2, 5, and 10 million years) and taxa are counted in each bin that their range crosses. Three models were fit to the upper size-limit data (linear, power, and Gompertz) and their strength, given the data, was assessed using the Akaike Information Criterion (AIC) and associated weights (AW). The linear model follows the classic format: $\log y = m \log x + b$, where m is the slope and b is the intercept. The power model follows the standard format: $\log y = b \log x^m$. Finally, the Gompertz model follows Smith *et al.* (2010) and Sookias *et al.* (2012a): $\log y = BM_{asym} - BM_o e^{-\alpha x}$, where BM_{asym} is the asymptotic body mass, BM_o is the initial body mass (oldest occurrence), and α is the rate of the curve (equivalent to the slope, in linear terms). In all cases, x is time (in millions of years) and y is log body mass. Coloured text corresponds to the coloured lines in the graph and shaded region within the tables represents the preferred model.



2 Ma Bins (n=45)			Model Parameters					
Model	AIC	AW	<i>m</i>	<i>b</i>	<i>BM_{asym}</i>	<i>BM_o</i>	<i>a</i>	
Linear	44.6	0.001	0.0108	6.1241	-	-	-	
Power	112.9	0	0.0517	5.5221	-	-	-	
Gompertz	30.6	0.999	-	-	6.8534	1.787	0.0838	

5 Ma Bins (n=20)			Model Parameters					
Model	AIC	AW	<i>m</i>	<i>b</i>	<i>BM_{asym}</i>	<i>BM_o</i>	<i>a</i>	
Linear	25	0.066	0.0145	5.948	-	-	-	
Power	67.2	0	0.0501	5.5926	-	-	-	
Gompertz	19.7	0.934	-	-	6.9388	1.6194	0.0632	

10 Ma Bins (n=9)			Model Parameters					
Model	AIC	AW	<i>m</i>	<i>b</i>	<i>BM_{asym}</i>	<i>BM_o</i>	<i>a</i>	
Linear	19.9	0.001	0.0167	5.9157	-	-	-	
Power	43.1	0	0.0464	5.7653	-	-	-	
Gompertz	5.6	0.999	-	-	6.952	2.1203	0.1292	

Figure 4-9. Upper body size limits in ornithopods within the context of sauropodomorph diversity dynamics. Sauropodomorph diversity curves are based on those obtained by Barrett *et al.* (2009) and Lloyd (2012); blue arrows show the sauropod diversity nadir. Green lines indicate the Jurassic-Cretaceous (dashed) and Cretaceous-Tertiary (solid) boundaries. Upper size limit plot is derived using five million year bins; red arrows show particular ornithopod taxa that reflect the upper body size limit in this clade.

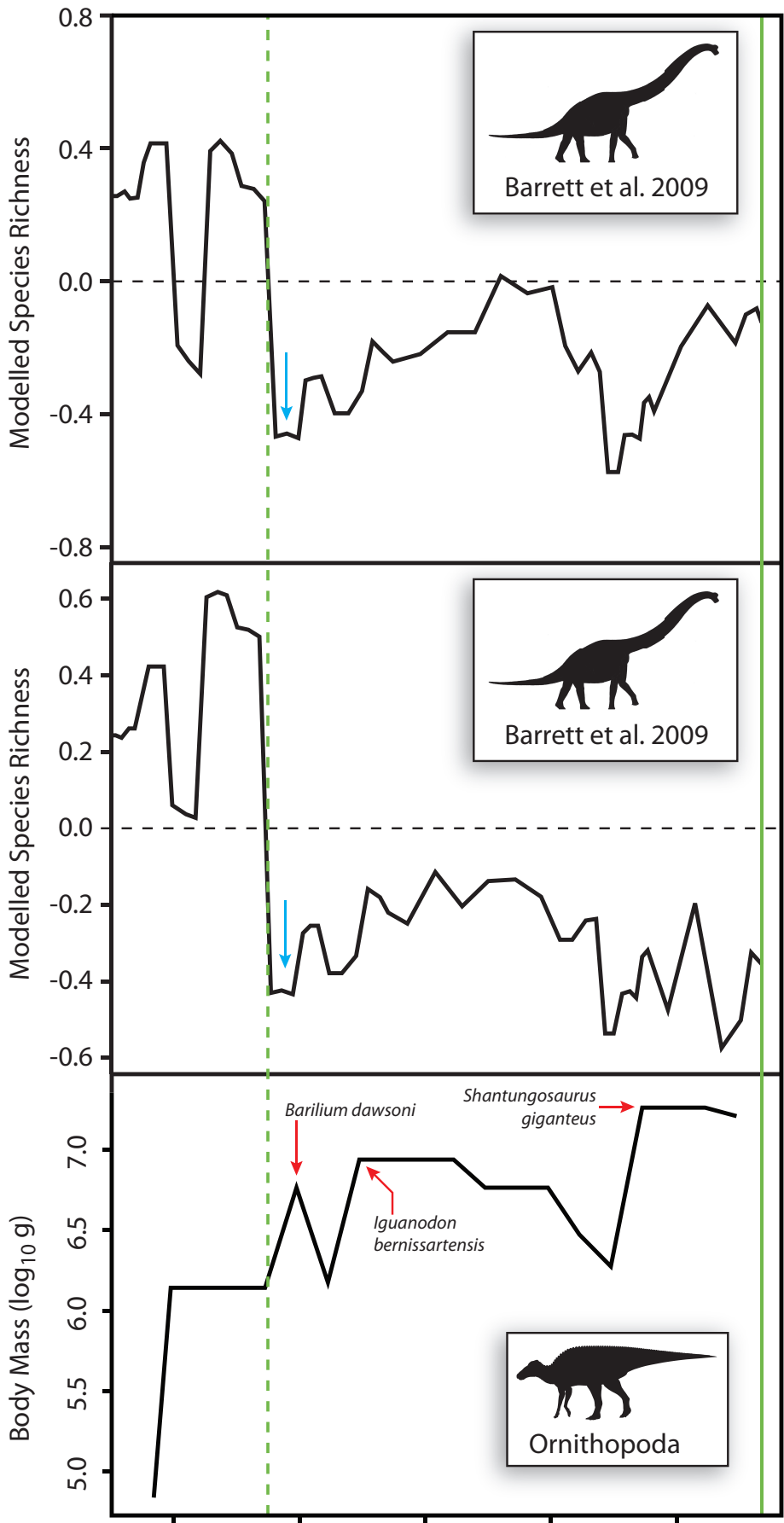


Figure 4-10. Sequential model-fitting to the mbl ornithopod tree. Models were fitted starting from the root node (Ornithopoda) and iterated up the tree for all nodes including more than 10 taxa (following Harmon *et al.*, 2010). Relative model support is measured using Akaike weight scores based on the five models that are tested here. Ancestral state reconstruction at the associated node is presented by the black line, along with its 95% confidence intervals (dashed lines). Results are plotted against sequential node number (above) as well as time, in which the nodes are scaled relative to estimated derived from the time-scaled tree. Thicker weighted lines represent the Jurassic-Cretaceous and Early to Late Cretaceous boundaries. Time scale abbreviations: Ael, Aalenian; Ba, Bathonian; Baj, Bajocian; Bar, Barremian; Ber, Berriasian; Cal, Callovian; Cen, Cenomanian; Haut, Hauterivian; Kim, Kimmeridgian; Oxf, Oxfordian; Tith, Tithonian; Tur, Turonian; Val, Valanginian.

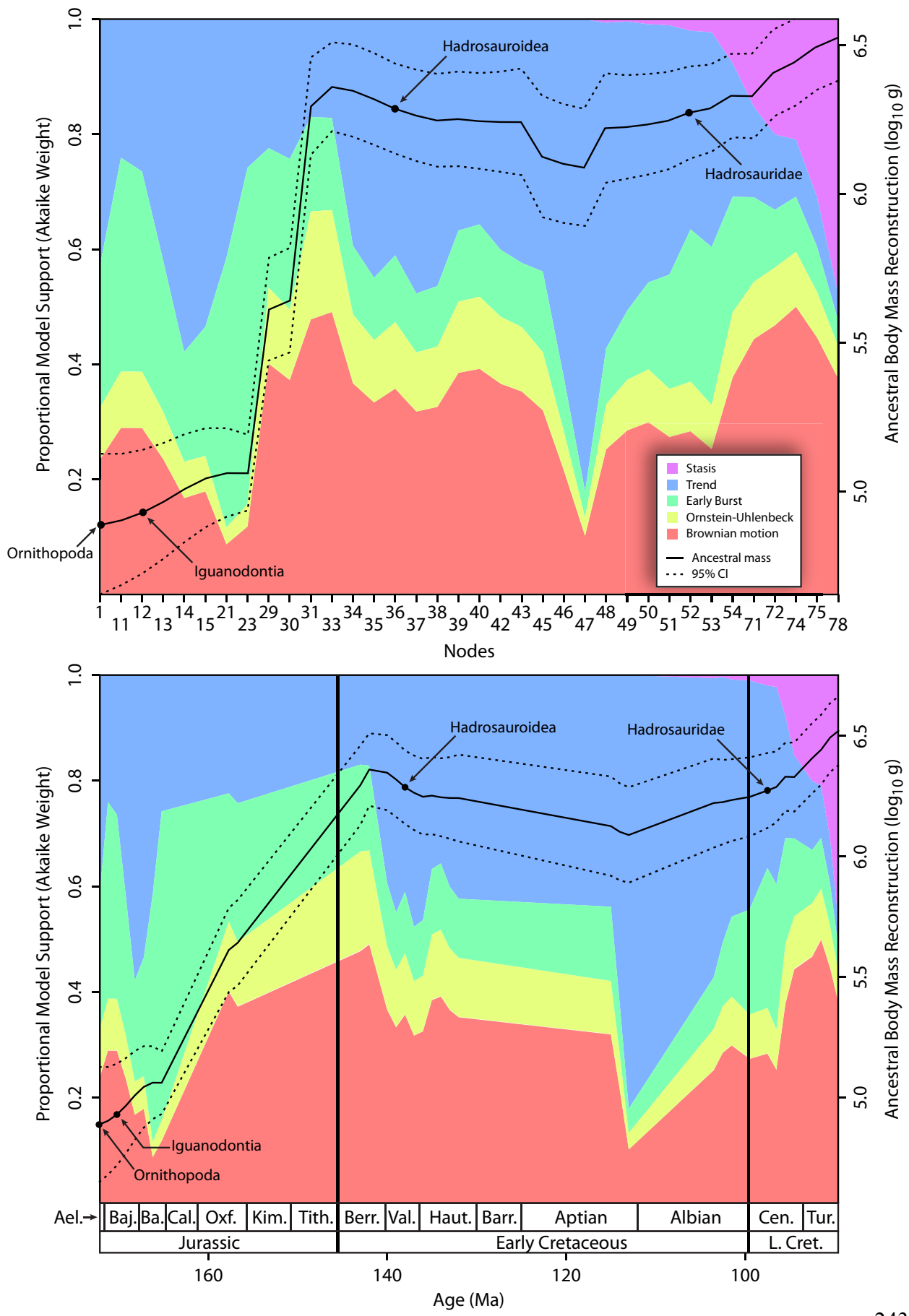


Figure 4-11. Sequential model-fitting of subsampled data based on the mbl ornithopod tree.
The ornithopod sample size ($N=88$) was subsampled at sample sizes between 87 and 11 taxa. The mbl tree was then pruned to match the subsampled taxa and all five models were fitted. The subsampling procedure was carried out 1000 times and averages are plotted for all subsamples (87–11; above) as well as a restricted set of subsamples, the sample sizes of which match those of Figure 4-10(below). Relative model support is measured using Akaike weight scores based on the five models that are tested here.

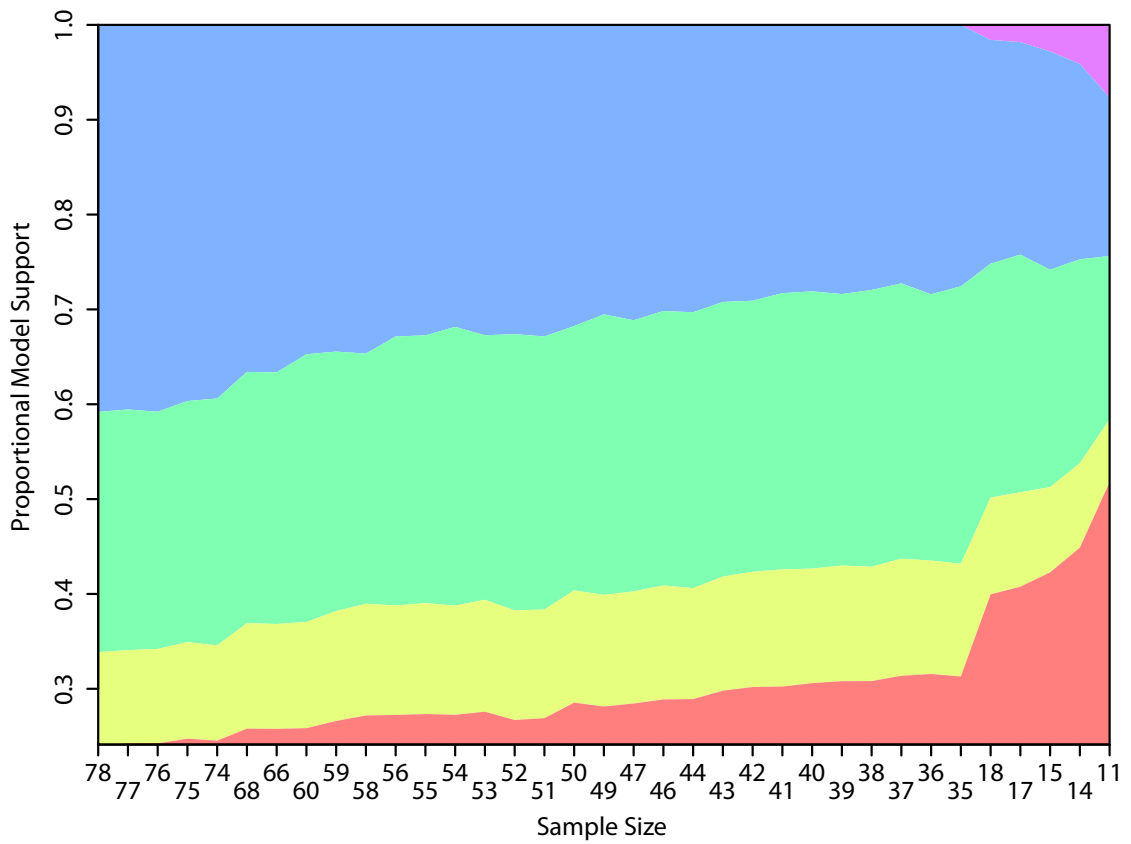
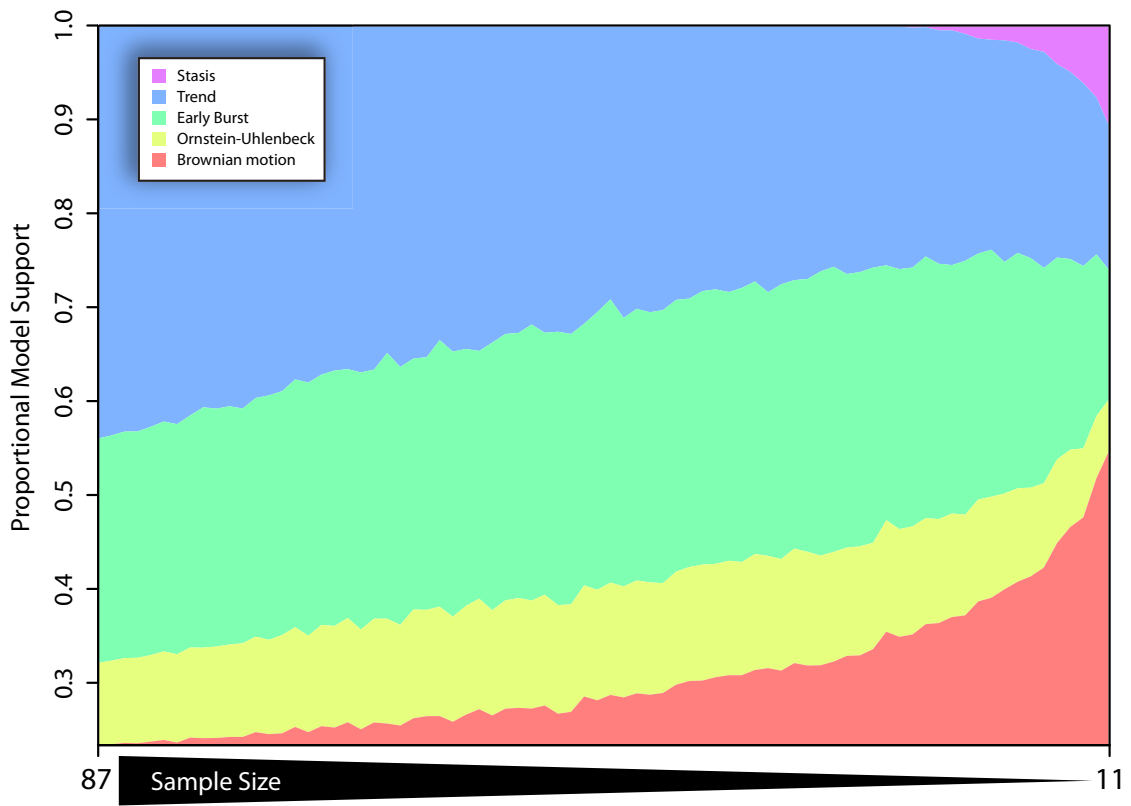
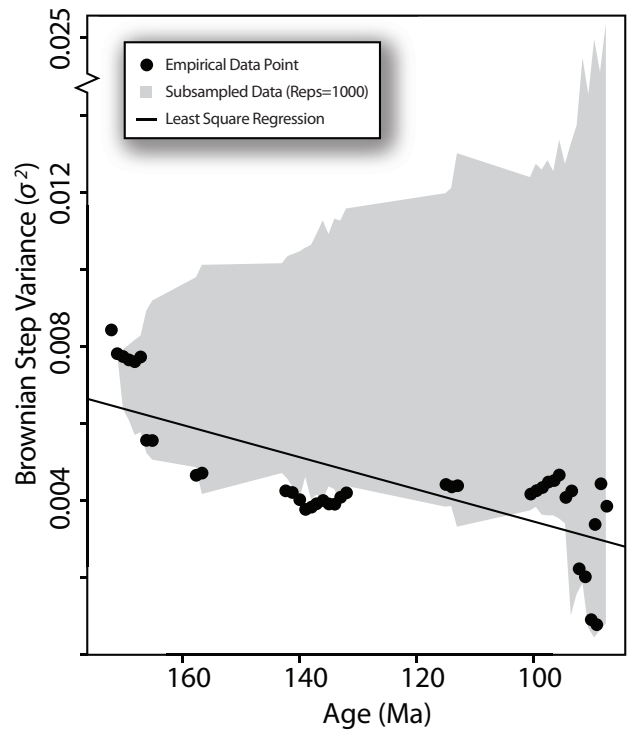
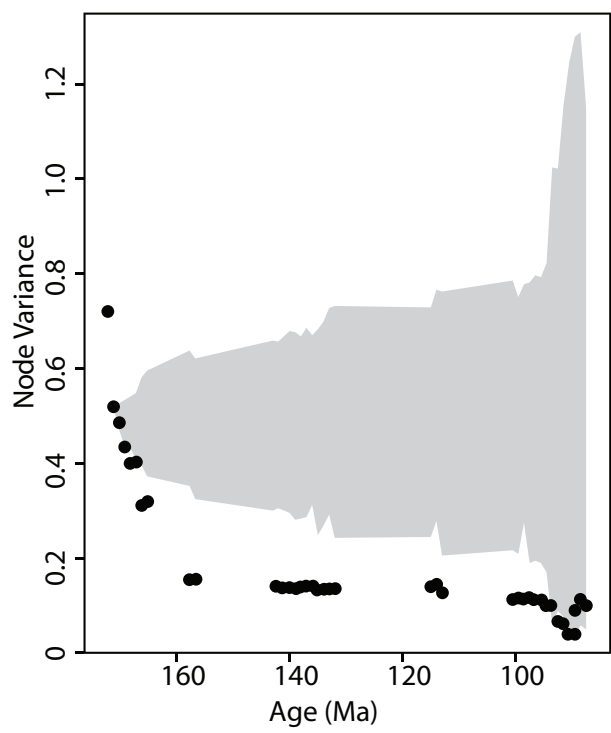


Figure 4-12. Body mass variance and evolutionary rates based on the mbl ornithopod tree.
Variances and rates are determined based on the same nodes used to fit the models in
Figure 4-10, hence sample sizes are limited to clades with greater than 10 taxa. Empirically
derived results are plotted (black dots) relative to their estimated age. Grey area represents
subsampled data (replicates=1000), following the methods described in Figure 4-10.
Regression between time and evolutionary rate (i.e., Brownian step variance) was regressed
using ordinary least squares.



References

- Agnolin, F. L., M. D. Ezcurra, D. F. Pais, and S. W. Salisbury. 2010. A reappraisal of the Cretaceous non-avian dinosaur faunas from Australia and New Zealand: evidence for their Gondwanan affinities. *Journal of Systematic Palaeontology* 8:257–300.
- Albert, E. A., D. San Mauro, M. García-París, L. Rüber, and R. Zardoya. 2009. Effect of taxon sampling on recovering the phylogeny of squamate reptiles based on complete mitochondrial genome and nuclear gene sequence data. *Gene* 441:12-21.
- Alexander, R. M. 1985. Mechanics of posture and gait of some large dinosaurs. *Zoological Journal of the Linnean Society* 83:1-25.
- Alexander, R. M. 1989. Dynamics of Dinosaurs and Other Extinct Giants. Columbia University Press, New York, 167 pp.
- Alexander, R. M., A. S. Jayes, G. M. O. Maloiy, and E. M. Wathuta. 1979. Allometry of the limb bones of mammals from shrews (*Sorex*) to elephant (*Loxodonta*). *Journal of Zoology* 189:305-314.
- Allen, V., H. Paxton, and J. R. Hutchinson. 2009. Variation in center of mass estimates for extant sauropsids and its importance for reconstructing inertial properties of extinct archosaurs. *The Anatomical Record: Advances in Integrative Anatomy and Evolutionary Biology* 292:1442-1461.
- Allen, V., K. T. Bates, Z. Li, and J. R. Hutchinson. 2013. Linking the evolution of body shape and locomotor biomechanics in bird-line archosaurs. *Nature* 497:104–107.
- Alroy, J. 1998. Cope's rule and the dynamics of body mass evolution in North American fossil mammals. *Science* 280:731-734.
- Alroy, J. 2000. Understanding the dynamics of trends within evolving lineages. *Paleobiology* 26:319-329.

- Amer, S. A. M., and Y. Kumazawa. 2005. Mitochondrial DNA sequences of the Afro-Arabian spiny-tailed lizards (genus *Uromastyx*; family Agamidae): phylogenetic analyses and evolution of gene arrangements. *Biological Journal of the Linnean Society* 85:247–260.
- Anderson, J. F., A. Hall-Martin, and D. A. Russell. 1985. Long-bone circumference and weight in mammals, birds and dinosaurs. *Journal of the Zoological Society of London A* 207:53–61.
- Andrews, R. M. 1982. Patterns of growth in reptiles; pp. 273–320 in C. Gans and F. H. Pough (eds.), *Biology of the Reptilia: Physiology* D. Academic Press, London, U.K.
- Andrews, R. M., and F. H. Pough. 1985. Metabolism of squamate reptiles: allometric and ecological relationships. *Physiological Zoology* 58:214–231.
- Arbour, J. H., and C. M. Brown. 2012. LOST: Missing morphometric data simulation and estimation. Version 1.0.
- Ast, J. C. 2001. Mitochondrial DNA evidence and evolution in Varanoidea (Squamata). *Cladistics* 17:211-226.
- Bakker, R. T. 1972. Anatomical and ecological evidence of endothermy in dinosaurs. *Nature* 239:81-85.
- Bakker, R. T. 1986. *The Dinosaur Heresies*. Citadel Press Books, 481 pp.
- Bambach, R. K. 2006. Phanerozoic biodiversity mass extinctions. *Annual Review of Earth and Planetary Science* 34:127–155.
- Bapst, D. W. 2012. paleotree: Paleontological and Phylogenetic Analyses of Evolution. 1.3. R-Project.
- Barrett, P. M., A. J. McGowan, and V. Page. 2009. Dinosaur diversiy and the rock record. *Proceedings of the Royal Society B* 276:2667-2674.

- Bates, K. T., P. L. Manning, D. Hodgetts, and W. I. Sellers. 2009a. Estimating mass properties of dinosaurs using laser imaging and 3D computer modelling. *PLoS ONE* 4:e4532. doi:10.1371/journal.pone.0004532.
- Bates, K. T., P. L. Falkingham, B. H. Breithaupt, D. Hodgetts, W. I. Sellers, and P. L. Manning. 2009b. How big was 'Big Al'? Quantifying the effects of soft tissue and osteological unknowns on mass predictions for *Allosaurus* (Dinosauria: Theropoda). *Palaeontologia Electronica* 12:33p.
- Behrensmeyer, A. K., D. Western, and D. E. D. Boaz. 1979. New perspectives in vertebrate paleoecology from a recent bone assemblage. *Paleobiology*:12-21.
- Benjamini, Y., and Y. Hochberg. 1995. Controlling the false discovery rate: a practical and powerful approach to multiple testing. *Journal of the Royal Statistical Society. Series B (Methodological)* 57:289–300.
- Benson, R. B. J., R. J. Butler, M. T. Carrano, and P. M. O'Connor. 2011. Air-filled postcranial bones in theropod dinosaurs: physiological implications and the 'reptile'-bird transition. *Biological Reviews* 87:168–193.
- Benton, M. J. 2008. How to find a dinosaur, and the role of synonymy in biodiversity studies. *Journal Information* 34.
- Benton, M. J., Z. Csiki, D. Grigorescu, R. Redelstorff, P. M. Sanders, K. Stein, and D. B. Weishampel. 2010. Dinosaurs and the island rule: the dwarfed dinosaurs from Hateg Island. *Palaeogeography, Palaeoclimatology, Palaeoecology*:17p.
- Bertram, J. E. A., and A. A. Biewener. 1990. Differential scaling of the long bones in the terrestrial Carnivora and other mammals. *Journal of Morphology* 204:157-169.
- Biewener, A. A. 1983. Allometry of quadrupedal locomotion: the scaling of duty factor, bone curvature and limb orientation to body size. *Journal of Experimental Biology* 105:147-171.
- Biewener, A. A. 1989. Scaling body support in mammals: limb posture and muscle mechanics. *Science* 245.

- Bininda-Emonds, O. R., M. Cardillo, K. E. Jones, R. D. E. MacPhee, R. M. D. Beck, R. Grenyer, S. A. Price, R. A. Vos, J. L. Gittleman, and A. Purvis. 2007. The delayed rise of present-day mammals. *Nature* 446:507-512.
- Blackburn, T. M., and K. J. Gaston. 1994. Animal body size distributions: patterns, mechanisms and implications. *Trends in Ecology and Evolution* 9:471-474.
- Blob, R. W. 2000. Interspecific scaling of the hindlimb skeleton in lizards, crocodilians, felids and canids: does limb bone shape correlate with limb posture? *Journal of Zoology* 250:507-531.
- Blob, R. W. 2001. Evolution of hindlimb posture in nonmammalian therapsids: biomechanical tests of paleontological hypotheses. *Paleobiology* 27:14-38.
- Blob, R. W., and A. A. Biewener. 1999. *In vivo* locomotor strain in the hindlimb bones of *Alligatos mississippiensis* and *Iguana iguana*: implications for the evolution of limb bone safety factor and non-sprawling limb posture. *The Journal of Experimental Biology* 202:1023-1046.
- Blob, R. W., and A. A. Biewener. 2001. Mechanics of limb bone loading during terrestrial locomotion in the green iguana (*Iguana iguana*) and American alligator (*Alligatos mississippiensis*). *The Journal of Experimental Biology* 204:1099-1122.
- Bolotsky, Y. L., and P. Godefroit. 2004. A new hadrosaurine dinosaur from the Late Cretaceous of far Eastern Russia. *Journal of Vertebrate Paleontology* 24:351-365.
- Bou, J., A. Casinos, and J. Ocaña. 1987. Allometry of the limb long bones of insectivores and rodents. *Journal of Morphology* 192:113-123.
- Boyd, C. A., C. M. Brown, R. D. Scheetz, and J. A. Clarke. 2009. Taxonomic revision of the basal neornithischian taxa *Thescelosaurus* and *Bugenasaura*. *Journal of Vertebrate Paleontology* 29:758-770.
- Boyer, A. G., and W. Jetz. 2010. Biogeography of body size in Pacific island birds. *Ecography* 33:369–379.

- Brown, C. M., J. H. Arbour, and D. A. Jackson. 2012a. Testing of the Effect of Missing Data Estimation and Distribution in Morphometric Multivariate Data Analyses. *Systematic Biology*.
- Brown, C. M., D. C. Evans, M. J. Ryan, and A. P. Russell. 2013a. New data on the diversity and abundance of small-bodied ornithopods (Dinosauria: Ornithischia) from the Belly River Group (Campanian) of Alberta. *Journal of Vertebrate Paleontology* 33:495–520.
- Brown, C. M., D. C. Evans, N. E. Campione, L. J. O'Brien, and D. A. Eberth. 2013b. Evidence for taphonomic size bias in the Dinosaur Park Formation (Campanian, Alberta), a model Mesozoic terrestrial alluvial-paralic system. *Palaeogeography, Palaeoclimatology, Palaeoecology* 372:108–122.
- Brown, C. M., N. E. Campione, H. Corrêa Giacomini, L. J. O'Brien, M. J. Vavrek, and D. C. Evans. 2012b. Ecological modelling, size distributions and taphonomic size bias in dinosaur faunas: a comment on Codron et al. (2012). *Biology Letters* 20120582.
- Brown, J. H., and B. A. Maurer. 1986. Body size, ecological dominance and Cope's rule. *Nature* 324:248–250.
- Brown, J. H., P. A. Marquet, and M. L. Taper. 1993. Evolution of body size: consequences of an energetic definition of fitness. *The American Naturalist* 142:573–584.
- Brusatte, S. L., M. J. Benton, M. Ruta, and G. T. Lloyd. 2008a. The first 50 Myr of dinosaur evolution: macroevolutionary pattern and morphological disparity. *Biology Letters* 4:733–736.
- Brusatte, S. L., M. J. Benton, M. Ruta, and G. T. Lloyd. 2008b. Superiority, competition, and opportunism in the evolutionary radiation of dinosaurs. *Science* 321:1485–1488.
- Brusatte, S. L., R. J. Butler, A. Prieto-Márquez, and M. A. Norell. 2012. Dinosaur morphological diversity and the end-Cretaceous extinction. *Nature Communications* 3.
- Buffetaut, E., and V. Suteethorn. 2011. A new iguanodontian dinosaur from the Khok Kruat Formation (Early Cretaceous, Aptian) of northeastern Thailand. *Annales de Paléontologie* 97:51–62.

- Burness, G. P., J. Diamond, and T. Flannery. 2001. Dinosaurs, dragons, and dwarfs: The evolution of maximal body size. *Proceedings of the National Academy of Science* 98:14518-14523.
- Butcher, M. T., N. R. Espinoza, S. R. Cirilo, and R. W. Blob. 2008. In vivo strains in the femur of river cooter turtles (*Pseudemys concinna*) during terrestrial locomotion: tests of force-platform models of loading mechanics. *Journal of Experimental Biology* 211:2397–2407.
- Butler, R. J., and A. Goswami. 2008. Body size evolution in Mesozoic birds: little evidence for Cope's rule. *Journal of Evolutionary Biology* 21:1673-1682.
- Butler, R. J., P. Upchurch, and D. B. Norman. 2008. The phylogeny of the ornithischian dinosaurs. *Journal of Systematic Palaeontology* 6:1-40.
- Butler, R. J., P. M. Galton, L. B. Porro, L. M. Chiappe, D. M. Henderson, and G. M. Erickson. 2009. Lower limits of ornithischian dinosaur body size inferred from a new Upper Jurassic heterodontosaurid from North America. *Proceedings of the Royal Society B* 277:375–381.
- Calder, W. A. I. 1984. *Size, Function, and Life History*. Harvard University Press, Cambridge, Massachusetts, 431 pp.
- Calder, W. A. I. 1996. *Size, Function, and Life History*. Dover Publications, Mineola, NY, 448 pp.
- Calvo, J. O., J. D. Porfiri, and F. E. Novas. 2007. Discovery of a new ornithopod dinosaur from the Portezuelo Formation (Upper Cretaceous), Neuquén, Patagonia, Argentina. *Arquivos do Museu Nacional, Rio de Janeiro* 65:471-483.
- Camoin, G., Y. Bellion, J. Benkhelil, J. J. Cornee, J. Dercourt, R. Guiraud, A. Poisson, and B. Vrielynck. 1993. Late Maastrichtian Paleoenvironments (69.5-65 Ma); pp. in J. Dercourt, L. E. Ricou, and B. Vrielynck (eds.), *Atlas Tethys Paleoenvironmental Maps*. BEICIP-FRANLAB, Rueil-Malmaison.
- Campbell Jr, K. E., and E. P. Tonni. 1983. Size and locomotion in teratorns (Aves: Teratornithidae). *The Auk* 100:390-403.

Campbell Jr, K. E., and L. Marcus. 1992. The relationships of hindlimb bone dimensions to body weight in birds. Natural History Museum of Los Angeles County Science Series 36:395-412.

Campione, N. E. 2013. MASSTIMATE: Body Mass Estimation Equations for Vertebrates. Verson 1.0. R Project for Statistical Computing, Comprehensive R Archive Network (CRAN).

Campione, N. E. in press. Postcranial anatomy of *Edmontosaurus regalis* (Hadrosaurinae) from the Horseshoe Canyon Formation, Alberta, Canada: description and photographic atlas of the paratype; pp. in D. C. Evans and D. A. Eberth (eds.), HADROSAURS: Proceedings of the International Hadrosaur Symposium at the Royal Tyrrell Museum. Indiana University Press, Bloomington, Indiana.

Campione, N. E., and D. C. Evans. 2011. Cranial growth and variation in edmontosaurs (Dinosauria: Hadrosauridae): implications for latest Cretaceous megaherbivore diversity in North America. PLoS ONE 6:e25186.

Campione, N. E., and D. C. Evans. 2012. A universal scaling relationship between body mass and proximal limb bone dimensions in quadrupedal terrestrial tetrapods. BMC Biology 10:60.

Capellini, I., and L. M. Gosling. 2007. Habitat primary production and the evolution of body size within the hartebeest clade. Biological Journal of the Linnean Society 92:431-440.

Carpenter, K., and Y. Ishida. 2010. Early and “Middle” Cretaceous iguanodonts in time and space. Journal of Iberian Geology 36:145–164.

Carrano, M. T. 1998. Locomotion in non-avian dinosaurs: integrating data from hindlimb kinematics, in vivo strains, and bone morphology. Paleobiology 24:450-469.

Carrano, M. T. 1999. What, if anything, is a cursor? Categories versus continua for determining locomotor habit in mammals and dinosaurs. Journal of Zoology 247:29-42.

Carrano, M. T. 2001. Implications of limb bone scaling, curvature and eccentricity in mammals and non-avian dinosaurs. Journal of Zoology 254:41-55.

- Carrano, M. T. 2005. The evolution of sauropod locomotion: morphological diversity of a secondarily quadrupedal radiation; pp. 229-251 in K. C. Rogers and J. A. Wilson (eds.), *The Sauropods: Evolution and Paleobiology*. University of California Press, Berkeley, CA.
- Carrano, M. T. 2006. Body-size evolution in the Dinosauria; pp. 225-268 in M. T. Carrano, R. W. Blob, T. J. Gaudin, and J. R. Wible (eds.), *Amniote Paleobiology: Perspectives on the Evolution of Mammals, Birds, and Reptiles*. University of Chicago Press, Chicago, Illinois.
- Casinos, A. 1996. Bipedalism and quadrupedalism in *Megatherium*: an attempt at biomechanical reconstruction. *Lethaia* 29:87-96.
- Casinos, A., and J. Cubo. 2001. Avian long bones, flight and bipedalism. *Comparative Biochemistry and Physiology Part A* 131:159-167.
- Cawley, G. C., and G. J. Janacek. 2009. On allometric equations for predicting body mass of dinosaurs. *Journal of Zoology* 280:355-361.
- Chinsamy-Turan, A. 2005. *The Microstructure of Dinosaur Bone: Deciphering Biology with Fine-Scale Techniques*. Johns Hopkins University Press, Baltimore, MD.
- Christian, A., W. D. Heinrich, and W. Golder. 1999. Posture and mechanics of the forelimbs of *Brachiosaurus brancai* (Dinosauria: Sauropoda). *Mitteilungen aus dem Museum für Naturkunde in Berlin, Geowissenschaftliche Reihe* 2:63–73.
- Christiansen, P. 1997. Locomotion in sauropod dinosaurs. *Gaia* 14:45-75.
- Christiansen, P. 1998. Strength indicator values of theropod long bones, with comments on limb proportions and cursorial potential. *Gaia* 15:241-255.
- Christiansen, P. 1999a. Scaling of mammalian long bones: small and large mammals compared. *Journal of Zoology* 247:333-348.
- Christiansen, P. 1999b. Scaling of the limb long bones to body mass in terrestrial mammals. *Journal of Morphology* 239:167-190.

- Christiansen, P. 1999c. Long bone scaling and limb posture on non-avian theropods: evidence for differential allometry. *Journal of Vertebrate Paleontology* 19:666-680.
- Christiansen, P., and R. A. Fariña. 2004. Mass prediction in theropod dinosaurs. *Historical Biology* 16:85-92.
- Christiansen, P., and J. M. Harris. 2005. Body size of *Smilodon* (Mammalia: Felidae). *Journal of Morphology* 266:369-384.
- Clauset, A., and D. H. Erwin. 2008. The evolution and distribution of species body size. *Science* 321:399-401.
- Clemente, C. J., P. C. Withers, G. Thompson, and D. Lloyd. 2011. Evolution of limb bone loading and body size in varanid lizards. *Journal of Experimental Biology* 214:3013–3020.
- Codron, D., C. Carbone, D. W. H. Müller, and M. Clauss. 2012a. Ecological modelling, size distributions and taphonomic size bias in dinosaur faunas: reply to Brown et al. *Biology Letters* 20120926.
- Codron, D., C. Carbone, D. W. H. Müller, and M. Clauss. 2012b. Ontogenetic niche shifts in dinosaurs influenced size, diversity and extinction in terrestrial vertebrates. *Biology Letters* 8:620-623.
- Cohen, J. 1969. Statistical Power Analysis for the Behavioral Sciences. 1st Edition. Routledge Academic, New York, NY, 415 pp.
- Colbert, E. H. 1962. The weights of dinosaurs. *American Museum Novitates* 2076:1-16.
- Colbert, E. H. 1984. The great dinosaur hunters and their discoveries. Dover Publications Inc., New York, NY, 283 pp.
- Colbert, E. H. 1997. North American dinosaur hunters; pp. 24–33 in J. O. Farlow and M. K. Brett-Surman (eds.), *The Complete Dinosaur*. Indiana University Press, Bloomington, ID.

- Colinvaux, P. 1978. Why big fierce animals are rare. Princeton University Press, Princeton, New Jersey, 256 pp.
- Cope, E. D. 1887. The origin of the fittest: essay on evolution. D. Appleton and Company, New York, NY, 467 pp.
- Coria, R. A., A. V. Cambiaso, and L. Salgado. 2007. New records of basal ornithopod dinosaurs in the Cretaceous of North Patagonia. *Ameghiniana* 44:473–477.
- Cruzado-Caballero, P., X. Pereda-Suberbiola, and J. I. Ruiz-Omeñaca. 2010. *Blasisaurus canudoi* gen. et sp. nov., a new lambeosaurine dinosaur (Hadrosauridae) from the Latest Cretaceous of Arén (Huesca, Spain). *Canadian Journal of Earth Sciences* 47:1507–1517.
- Cubo, J., and A. Casinos. 1998. Biomechanical significance of cross-sectional geometry of avian long bones. *European Journal of Morphology* 36:19-28.
- Cubo, J., and A. Casinos. 2000. Incidence and mechanical significance of pneumatization in the long bones of birds. *Zoological Journal of the Linnean Society* 130:499-510.
- Curran-Everett, D. 2000. Multiple comparisons: philosophies and illustrations. *American Journal of Physiology-Regulatory, Integrative and Comparative Physiology* 279:R1–R8.
- Cuthbertson, R. S., A. Tirabasso, N. Rybczynski, and R. B. Holmes. 2012. Kinetic limitations of intracranial joints in *Brachylophosaurus canadensis* and *Edmontosaurus regalis* (Dinosauria: Hadrosauridae), and their implications for the chewing mechanics of hadrosaurids. *The Anatomical Record* 295:968–979.
- Dalla Vecchia, F. M. 2009. *Tethyshadros insularis*, a new hadrosauroid dinosaur (Ornithischia) from the Upper Cretaceous of Italy. *Journal of Vertebrate Paleontology* 29:1110–1116.
- Dalla Vecchia, F. M., R. Gaete, V. Riera, O. Oms, A. Prieto-Márquez, B. Vila, A. Garcia Sellés, and A. Galobart. 2011: The hadrosaurid record in the Maastrichtian of the eastern Tremp Syncline (Northern Spain). International Hadrosaur Symposium, Royal Tyrrell Museum of Palaeontology, Drumheller, Alberta, 2011.
- Damuth, J. 1981. Population density and body size in mammals. *Nature* 290:699-700.

- Damuth, J. 1993. Cope's rule, the island rule and the scaling of mammalian population density. *Nature* 365:748–750.
- Damuth, J., and B. J. MacFadden (eds.) 1990. Body Size in Mammalian Paleobiology: Estimation and Biological Implications. Cambridge University Press, Cambridge, U.K., 397 pp.
- De Esteban-Trivigno, S., and M. Köhler. 2011. New equations of body mass estimation in bovids: testing some procedures when constructing regression functions. *Mammalian Biology* 76:755–761.
- De Esteban-Trivigno, S., M. Mendoza, and M. De Renzi. 2008. Body mass estimation in Xenarthra: a predictive equation suitable for all quadrupedal terrestrial placentals? *Journal of Morphology* 269:1276-1293.
- Dececchi, T. A., and H. C. E. Larsson. in press. Body and limb size dissociation at the origin of birds: uncoupling allometric constraints across a macroevolutionary transition. *Evolution*.
- Depéret, C. J. J. 1907. Les transformations du monde animal. Ernest Flammarion, Paris, France, 358 pp.
- Dilkes, D. W. 2001. An ontogenetic perspective on locomotion in the Late Cretaceous dinosaur *Maiasaura peeblesorum* (Ornithischia: Hadrosauridae). *Canadian Journal of Earth Sciences* 38:1205-1227.
- Dong, Z.-M. 1989. On a small ornithopod (*Gongbusarus wucaiwanensis*) from Kelamaili, Junggar Basin, Xinjiang, China. *Vertebrata PalAsiatica* 27:140–146.
- Doube, M., S. C. W. Yen, M. M. Kłosowski, A. A. Farke, J. R. Hutchinson, and S. J. Shefelbine. 2012. Whole-bone scaling of the avian pelvic limb. *Journal of Anatomy* 221:21–29.
- Economos, A. C. 1983. Elastic and/or Geometric Similarity in Mammalian Design? *Journal of Theoretical Biology* 103:167-172.

- Eisenberg, J. F. 1990. The behavioral/ecological significance of body size in the Mammalia; pp. 25–37 in J. Damuth and B. J. MacFadden (eds.), *Body Size in Mammalian Paleobiology: Estimation and Biological Implications*. Cambridge University Press, Cambridge, UK.
- Eldredge, N., and S. J. Gould. 1972. Punctuated equilibria: an alternative to phyletic gradualism; pp. 82-115 in T. J. M. Schopf (ed.), *Models in Paleobiology*. Freeman Cooper, San Francisco, CA, U.S.A.
- Elton, C. 1927. *Animal Ecology*. Macmillan, New York, 209 pp.
- Engstrom, T. N., H. B. Shaffer, and W. P. McCord. 2004. Multiple data sets, high homoplasy, and the phylogeny of softshell turtles (Testudineae: Trionychidae). *Systematic Biology* 53:693-710.
- Erickson, G. M. 2005. Assessing dinosaur growth patterns: a microscopic revolution. *Trends in Ecology and Evolution* 20:677-684.
- Erickson, G. M., K. C. Rogers, and S. A. Yerby. 2001. Dinosaurian growth patterns and rapid avian growth rates. *Nature* 412:429-433.
- Erickson, G. M., P. J. Makovicky, P. J. Currie, M. A. Norell, S. A. Yerby, and C. A. Brochu. 2004. Gigantism and comparative life-history parameters of tyrannosaurid dinosaurs. *Nature* 430:772-775.
- Erickson, G. M., B. A. Krick, M. Hamilton, G. R. Bourne, M. A. Norell, E. Lilleodden, and W. G. Sawyer. 2012. Complex Dental Structure and Wear Biomechanics in Hadrosaurid Dinosaurs. *Science* 338:98–101.
- Evans, D. C. 2010. Cranial anatomy and systematics of *Hypacrosaurus altispinus*, and a comparative analysis of skull growth in lambeosaurine hadrosaurids (Dinosauria: Ornithischia). *Zoological Journal of the Linnean Society* 159:398-434.
- Evans, D. C., R. Ridgely, and L. M. Witmer. 2009. Endocranial anatomy of lambeosaurine hadrosaurids (Dinosauria: Ornithischia): A sensorineural perspective on cranial crest function. *The Anatomical Record* 292:1315-1337.

- Evans, D. C., R. K. Schott, D. W. Larson, C. M. Brown, and M. J. Ryan. 2013. The oldest North American pachycephalosaurid and the hidden diversity of small-bodied ornithischian dinosaurs. *Nature Communications*.
- Falkowski, P. G., M. E. Katz, A. J. Milligan, K. Fennel, B. S. Cramer, M. P. Aubry, R. A. Berner, M. J. Novacek, and W. M. Zapol. 2005. The rise of oxygen over the past 205 million years and the evolution of large placental mammals. *Science* 309:2202–2204.
- Fariña, R. A., S. F. Vizcaíno, and M. S. Bargo. 1998. Body mass estimations in Lujanian (late Pleistocene-early Holocene of South America) mammal megafauna. *Mastozoología Neotropical* 5:87-108.
- Farke, A. A., and J. Alicea. 2009. Femoral strength and posture in terrestrial birds and non-avian theropods. *The Anatomical Record* 292:1406-1411.
- Farlow, J. O. 1976. A consideration of the trophic dynamics of a Late Cretaceous large-dinosaur community (Oldman Formation). *Ecology* 57:841-857.
- Farlow, J. O., P. Dodson, and A. Chinsamy. 1995. Dinosaur biology. *Annual Review of Ecology and Systematics* 26:445-71.
- Fastovsky, D. E., Y. Huang, J. Hsu, J. Martin-McNaughton, P. M. Sheehan, and D. B. Weishampel. 2004. Shape of Mesozoic dinosaur richness. *Geology* 32:877-880.
- Felsenstein, J. 1985. Phylogenies and the comparative method. *The American Naturalist* 125:1-15.
- Finarelli, J. A. 2008. Hierarchy and the reconstruction of evolutionary trends: evidence for constraints on the evolution of body size in terrestrial caniform carnivorans (Mammalia). *Paleobiology* 34:553-563.
- Finarelli, J. A., and J. J. Flynn. 2006. Ancestral state reconstruction of body size in the Caniformia (Carnivora, Mammalia): the effects of incorporating data from the fossil record. *Systematic Biology* 55:301–313.

- Finnegan, S., and M. L. Droser. 2008. Body size, energetics, and the Ordovician restructuring of marine ecosystems. *Paleobiology* 34:342-359.
- Fortelius, M., and J. Kappelman. 1993. The largest land mammal ever imagined. *Zoological Journal of the Linnean Society* 108:85-101.
- Foster, J. B. 1964. The evolution of mammals on islands. *Nature* 202:234-235.
- Franz, R., J. Hummel, E. Kiensle, P. Kölle, H.-C. Gunga, and M. Clauss. 2009. Allometry of visceral organs in living amniotes and its implications for sauropod dinosaurs. *Proceedings of the Royal Society B* 276:1731-1736.
- Fröbisch, J. 2006. Locomotion in derived dicynodonts (Synapsids, Anomodontia): a functional analysis of the pelvis girdle and hind limb of *Tetragonia njalilus*. *Canadian Journal of Earth Sciences* 43:1297–1308.
- Gaffney, E. S., and P. A. Meylan. 1988. A phylogeny of turtles; pp. 157-219 in M. J. Benton (ed.), *The Phylogeny and Classification of Tetrapods*. Clarendon Press, Oxford, U.K.
- Galton, P. M. 2007. Teeth of ornithischian dinosaurs (mostly Ornithopoda) from the Morrison Formation (Upper Jurassic) of the western United States; pp. 17–47 in K. Carpenter (ed.), *Horns and Beaks: Ceratopsian and Ornithopod Dinosaurs*. Indiana University Press, Bloomington, Indiana.
- Garcia, G. J. M., and J. K. L. da Silva. 2006. Review: Interspecific allometry of bone dimensions: a review of the theoretical models. *Physics of Life Reviews* 3:188-209.
- Garland, T. J., P. H. Harvey, and A. R. Ives. 1992. Procedures for the analysis of comparative data using phylogenetically independent contrasts. *Systematic Biology* 41:18-32.
- Gaston, K. J., and T. M. Blackburn. 1996. Range size-body size relationships: evidence of scale dependence. *Oikos* 1996:479-485.
- Gates, T. A., J. R. Horner, R. R. Hanna, and C. R. Nelson. 2011. New unadorned hadrosaurine hadrosaurid (Dinosauria, Ornithopoda) from the Campanian of North America. *Journal of Vertebrate Paleontology* 31:798–811.

Gillooly, J. F., A. P. Allen, and E. L. Charnov. 2006. Dinosaur fossils predict body temperatures.

PLoS Biology 4:e248.

Gillooly, J. F., J. H. Brown, G. B. West, V. M. Savage, and E. L. Charnov. 2001. Effects of size and temperature on metabolic rate. Science 293:2248-2251.

Gillooly, J. F., E. L. Charnov, G. B. West, V. M. Savage, and J. H. Brown. 2002. Effects of size and temperature of developmental time. Nature 417:70-73.

Gingerich, P. D. 1990. Prediction of body mass in mammalian species from long bone lengths and diameters. Contributions from the Museum of Paleontology, University of Michigan 28:79-92.

Godefroit, P., V. Alifanov, and Y. Bolotsky. 2004. A re-appraisal of *Aralosaurus tuberiferus* (Dinosauria, Hadrosauridae) from the Late Cretaceous of Kazakhstan. Bulletin de l'Institut Royal des Sciences Naturelles de Belgique 74-Suppl:139–154.

Godefroit, P., H. Li, and C. Y. Shang. 2005. A new primitive hadrosauroid dinosaur from the Early Cretaceous of Inner Mongolia (PR China). Comptes Rendus Palevol 4:697-705.

Godefroit, P., Y. L. Bolotsky, and P. Lauters. 2012. A New Saurolophine Dinosaur from the Latest Cretaceous of Far Eastern Russia. PLoS ONE 7:e36849.

Godefroit, P., Z.-M. Dong, P. Bultynck, H. Li, and L. Feng. 1998. Sino-Belgian Cooperation Program "Cretaceous dinosaurs and mammals from Inner Mongolia" 1. New Bactrosaurus (Dinosauria: Hadrosauridae) material from Iren Dabasu (Inner Mongolia, P. R. China). Bulletin de l'Institut Royal des Sciences Naturelles de Belgique 68, Supplement:3-70.

Gould, S. J. 1966. Allometry and size in ontogeny and phylogeny. Biological Reviews 41:587-640.

Gradstein, F. M., J. G. Ogg, and A. G. Smith (eds.) 2004. A Geologic Time Scale 2004. Cambridge University Press, Cambridge, U.K., 589 pp.

- Grand, T. I. 1990. The functional anatomy of body mass; pp. 39-47 in J. Damuth and B. J. MacFadden (eds.), *Body Size in Mammalian Paleobiology: Estimation and Biological Implications*. Cambridge University Press, Cambridge, U.K.
- Greenewalt, C. H. 1975. The flight of birds: the significant dimensions, their departure from the requirements for dimensional similarity, and the effect on flight aerodynamics of that departure. *Transactions of the American Philosophical Society* 65:1-67.
- Gregory, W. K. 1905. The weight of *Brontosaurus*. *Science, New Series* 22:572.
- Griffiths, D. 1992. Size, abundance and energy use in communities. *Journal of Animal Ecology* 61:307-315.
- Gunga, H.-C., K. Kirsch, F. Baartz, and L. Röcker. 1995. New data on the dimensions of *Brachiosaurus brancai* and their physiological implications. *Naturwissenschaften* 82:190-192.
- Gunga, H.-C., T. Suthau, A. Bellmann, S. Stoinski, A. Friedrich, T. Trippel, K. Kirsch, and O. Hellwich. 2008. A new body mass estimation of *Brachiosaurus brancai* Janensch, 1914 mounted and exhibited at the Museum of Natural History (Berlin, Germany). *Fossil Record* 11:33-38.
- Gunga, H.-C., K. Kirsch, J. Rittweger, A. Clarke, J. Albertz, A. Wiedemann, A. Wehr, W.-D. Heinrich, and H.-P. Schultze. 2002. Dimensions of *Brachiosaurus brancai*, *Dicraeosaurus hansemanni* and *Diplodocus carnegii* and their implications for gravitational physiology. *Adaptation Biology and Medicine* 3:156-169.
- Gunga, H.-C., T. Suthau, A. Bellmann, F. Andreas, T. Schwanebeck, S. Stoinski, T. Trippel, K. Kirsch, and O. Hellwich. 2007. Body mass estimations for *Plateosaurus engelhardti* using laser scanning and 3D reconstruction methods. *Naturwissenschaften* 94:623-630.
- Gunga, H.-C., K. Kirsch, J. Rittweger, L. Röcker, A. Clarke, J. Albertz, A. Wiedemann, S. Mokry, T. Suthau, A. Wehr, W.-D. Heinrich, and H.-P. Schultze. 1999. Body size and body volume distribution in two sauropods from the Upper Jurassic of Tendaguru

(Tanzania). Mitteilungen aus dem Museum für Naturkunde der Humboldt-Universität Berlin, Geowissenschaftliche Reihe 2:91-102.

Han, F.-L., P. M. Barrett, R. J. Butler, and X. Xu. 2012. Postcranial anatomy of *Jeholosaurus shangyuanensis* (Dinosauria, Ornithischia) from the Lower Cretaceous Yixian Formation of China. Journal of Vertebrate Paleontology.

Hansen, T. F. 1997. Stabilizing selection and the comparative analysis of adaptation. Evolution:1341-1351.

Hansen, T. F., and K. Bartoszek. 2012. Interpreting the evolutionary regression: the interplay between observational and biological errors in phylogenetic comparative studies. Systematic Biology 61:413–425.

Harmon, L. J., J. A. Schulte II, A. Larson, and J. B. Losos. 2003. Tempo and mode of evolutionary radiation in iguanian lizards. Science 301:961–964.

Harmon, L. J., J. T. Weir, C. D. Brock, R. E. Glor, and W. Challenger. 2008. GEIGER: investigating evolutionary radiations. Bioinformatics 24:129–131.

Harmon, L. J., J. Weir, C. Brock, R. Glor, W. Challenger, and G. Hunt. 2009. geiger: analysis of evolutionary diversification. Version 1.3-1. Comprehensive R Archive Network (CRAN).

Harmon, L. J., J. B. Losos, T. Jonathan Davies, R. G. Gillespie, J. L. Gittleman, W. Bryan Jennings, K. H. Kozak, M. A. McPeek, F. Moreno-Roark, and T. J. Near. 2010. Early bursts of body size and shape evolution are rare in comparative data. Evolution 64:2385-2396.

Hazlehurst, G. A., and J. M. V. Rayner. 1992. Flight characteristics of Triassic and Jurassic Pterosauria: an appraisal based on wing shape. Paleobiology 18:447–463.

Head, J. J., J. I. Bloch, A. K. Hastings, J. R. Bourque, E. A. Cadena, F. A. Herrera, P. D. Polly, and C. A. Jaramillo. 2009. Giant boid snake from the Palaeocene neotropics reveals hotter past equatorial temperatures. Nature 457:715-718.

- Hemmingsen, A. M. 1960. Energy metabolism as related to body size and respiratory surfaces, and its evolution. Steno Memorial Hospital and Nordinsk Insulin Laboratosium 9:6-110.
- Henderson, D. 2003. Footprints, trackways, and hip heights of bipedal dinosaurs—testing hip height predictions with computer models. *Ichnos* 10:99-114.
- Henderson, D. M. 1999. Estimating the masses and centers of mass of extinct animals by 3-D mathematical slicing. *Paleobiology* 25:88-106.
- Henderson, D. M. 2004. Tipsy punters: sauropod dinosaur pneumaticity, buoyancy and aquatic habits. *Biology Letters* 271:S180–S183.
- Henderson, D. M. 2006. Burly gaits: centers of mass, stability, and the trackways of sauropod dinosaurs. *Journal of Vertebrate Paleontology* 26:907–921.
- Henderson, D. M. 2010. Pterosaur body mass estimates from three-dimensional mathematical slicing. *Journal of Vertebrate Paleontology* 30:768-785.
- Henderson, D. M. in press. The floating fates of Dinosaur Provincial Park hadrosaurs and ceratopsians during largescale flooding events; pp. in D. C. Evans and D. A. Eberth (eds.), HADROSAURS: Proceedings of the International Hadrosaur Symposium at the Royal Tyrrell Museum. Indiana University Press, Bloomington, Indiana.
- Henderson, D. M., and E. Snively. 2004. *Tyrannosaurus* en pointe: allometry minimized rotational inertia of large carnivorous dinosaurs. *Biology Letters* 271:S57-S60.
- Hohn, B. 2011. Walking with the Shoulder of Giants: Biomechanical Conditions in the Tetrapod Shoulder Girdle as a Basis for Sauropod Shoulder Reconstruction; pp. 182–196 in N. Klein, K. Remes, C. T. Gee, and P. M. Sander (eds.), Biology of the Sauropod Dinosaurs: Understanding the Life of Giants. Indiana University Press, Bloomington, ID.
- Hone, D. W. E., and M. J. Benton. 2005. The evolution of large size: how does Cope's Rule work? *Trends in ecology & evolution* 20:4–6.
- Hone, D. W. E., T. M. Keesey, D. Pisani, and A. Purvis. 2005. Macroevolutionary trends in the Dinosauria: Cope's rule. *Journal of Evolutionary Biology* 18:587-595.

- Hone, D. W. E., G. J. Dyke, M. Haden, and M. J. Benton. 2008. Body size evolution in Mesozoic birds. *Journal of Evolutionary Biology* 21:618-624.
- Hopson, J. A. 1977. Relative brain size and behavior in archosaurian reptiles. *Annual Review of Ecology and Systematics* 8:429-448.
- Hopson, J. A. 1979. Paleoneurology; pp. 39-146 in C. Gans, R. G. Northcutt, and P. Ulinski (eds.), *Biology of the Reptilia, Neurology A*. Academic Press, New York, U.S.A.
- Horner, J. R., D. B. Weishampel, and C. A. Forster. 2004. Hadrosauridae; pp. 438-463 in D. B. Weishampel, P. Dodson, and H. Osmolska (eds.), *The Dinosauria* (2nd ed.). University of California Press, Berkeley, CA.
- Hunt, G. 2007. The relative importance of directional change, random walks, and stasis in the evolution of fossil lineages. *Proceedings of the National Academy of Science* 104:18404-18408.
- Hunt, G. 2008. Gradual or pulsed evolution: when should punctuational explanations be prepared? *Paleobiology* 34:360-377.
- Hunt, G., and K. Roy. 2006. Climate change, body size evolution, and Cope's Rule in deep-sea ostracodes. *Proceedings of the National Academy of Science* 103:1347-1352.
- Hunt, G., and M. T. Carrano. 2010. Models and methods for analyzing phenotypic evolution in lineages and clades; pp. 245–269 in J. Alroy and G. Hunt (eds.), *Quantitative Methods in Paleobiology*. The Paleontological Society Papers.
- Hurlburt, G. 1999. Comparison of body mass estimation techniques, using recent reptiles and the pelycosaur *Edaphosaurus boanerges*. *Journal of Vertebrate Paleontology* 19:338-350.
- Hutchinson, J. R. 2001. The evolution of femoral osteology and soft tissues on the line to extant birds (Neornithes). *Zoological Journal of the Linnean Society* 131:169-197.
- Hutchinson, J. R. 2006. The evolution of locomotion in archosaurs. *Comptes Rendus Palevol* 5:519–530.

- Hutchinson, J. R., V. Ng-Thow-Hing, and F. C. Anderson. 2007. A 3D interactive method for estimating body segmental parameters in animals: application to the turning and running performance of *Tyrannosaurus rex*. Journal of Theoretical Biology 246:660-680.
- Hutchinson, J. R., K. T. Bates, J. Molnar, V. Allen, and P. J. Makovicky. 2011. A Computational Analysis of Limb and Body Dimensions in *Tyrannosaurus rex* with Implications for Locomotion, Ontogeny, and Growth. PLoS ONE 6:e26037.
- Ingram, T., L. J. Harmon, and J. B. Shurin. 2012. When should we expect early bursts of trait evolution in comparative data? Predictions from an evolutionary food web model. Journal of Evolutionary Biology.
- Jablonski, D. 1997. Body-size evolution in Cretaceous molluscs and the status of Cope's rule. Change 385:250–252.
- Janensch, W. 1935. Die Schädel der Sauropoden *Brachiosaurus*, *Barosaurus* und *Dicraeosaurus* aus den Tendaguruschichten Deutsch-Ostafrikas. Palaeontographica, Supplement 7:147–298.
- Janis, C. M. 1993. Tertiary mammal evolution in the context of changing climates, vegetation, and tectonic events. Annual Review of Ecology and Systematics 24:467–500.
- Janis, C. M., and M. T. Carrano. 1992. Scaling of reproductive turnover in archosaurs and mammals: why are large terrestrial mammals so rare? Annales Zoologici Fennici 28:201–216.
- Jenkins, F. A. 1971. Limb posture and locomotion in the Virginia opossum (*Didelphis marsupialis*) and in other non-cursorial mammals. Journal of Zoology 165:303-315.
- Jerison, H. J. 1969. Brain evolution and dinosaur brains. The American Naturalist 103:575-588.
- Jerison, H. J. 1973. Evolution of the Brain and Intelligence. Academic Press, New York, U.S.A., 482 pp.
- Jombart, T., and S. Dray. 2011. adephylo: exploratory analyses for the phylogenetic comparative method. Bioinformatics 26:1907–1909.

- Jones, K. E., J. Bielby, M. Cardillo, S. A. Fritz, J. O'Dell, C. D. L. Orme, K. Safi, W. Sechrest, E. H. Boakes, and C. Carbone. 2009. PanTHERIA: a species-level database of life history, ecology, and geography of extant and recently extinct mammals. *Ecology* 90:2648.
- Kidwell, S. M., and K. W. Flessa. 1996. The quality of the fossil record: populations, species, and communities. *Annual Review of Earth and Planetary Science* 24:433-464.
- Kilbourne, B. M., and P. J. Makovicky. 2010. Limb bone allometry during the postnatal ontogeny in non-avian dinosaurs. *Journal of Anatomy* 217:135-152.
- Kingsolver, J. G., and D. W. Pfennig. 2007. Individual-level selection as a cause of Cope's Rule of phyletic size increase. *Evolution* 58:1608–1612.
- Kleiber, M. 1947. Body Size and Metabolic Rate. *Physiological Reviews* 27:511-541.
- Kobayashi, Y., and Y. Azuma. 2003. A new iguanodontian (dinosauria: ornithopoda) from the Lower Cretaceous Kitadani Formation of Fukui Prefecture, Japan. *Journal of Vertebrate Paleontology* 23:166–175.
- Kumar, S. 2005. Molecular clocks: four decades of evolution. *Nature Reviews Genetics* 6:654–662.
- Kurtén, B. 1953. On the variation and population dynamics of fossil and Recent mammal populations. *Acta Zoologica Fennica* 76:1–122.
- LaBarbera, M. 1989. Analyzing body size as a factor in ecology and evolution. *Annual Review of Ecology and Systematics* 20:97-117.
- Laurin, M. 2004. The evolution of body size, Cope's rule and the origin of amniotes. *Systematic Biology* 53:594-622.
- Laurin, M. 2010. Assessment of the relative merits of a few methods to detect evolutionary trends. *Systematic Biology* 59:689.

- Le, M., C. J. Raxworthy, W. P. McCord, and L. Mertz. 2006. A molecular phylogeny of tortoises (Testudines: Testudinidae) based on mitochondrial and nuclear genes. *Molecular Phylogenetics and Evolution* 40:517-531.
- Lehman, T. M., and H. N. Woodward. 2008. Modeling growth rates for sauropod dinosaurs. *Paleobiology* 34:264-281.
- Lloyd, G. T. 2012. A refined modelling approach to assess the influence of sampling on palaeobiodiversity curves: new support for declining Cretaceous dinosaur richness. *Biology Letters* 8:123–126.
- Lloyd, G. T., K. E. Davies, D. Pisani, J. E. Tarver, M. Ruta, M. Sakamoto, D. W. E. Hone, R. Jennings, and M. J. Benton. 2008. Dinosaurs and the Cretaceous terrestrial revolution. *Proceedings of the Royal Society B*.
- Lockley, M., and J. L. Wright. 2001. Trackways of large quadrupedal ornithopods from the Cretaceous: A Review; pp. 428–442 in D. H. Tanke and K. Carpenter (eds.), *Mesozoic Vertebrate Life*. Indiana University Press, Bloomington, Indiana.
- Lomolino, M. V. 1985. Body size of mammals on islands: the island rule reexamined. *The American Naturalist* 125:310–316.
- Lomolino, M. V. 2005. Body size evolution in insular vertebrates: generality of the island rule. *Journal of Biogeography* 32:1683–1699.
- Losos, J. B., and D. B. Miles. 2002. Testing the hypothesis that a clade has adaptively radiated: iguanid lizard clades as a case study. *The American Naturalist* 160:147–157.
- Maddison, W. P. 1991. Squared-change parsimony reconstructions of ancestral states for continuous-valued characters on a phylogenetic tree. *Systematic Zoology* 40:304-314.
- Maddison, W. P., and D. R. Maddison. 2010. Mesquite: A modular system for evolutionary analysis. Version 2.74 (build 500). mesquiteproject.org.

- Maidment, S. C. R., and P. M. Barrett. 2012. Does morphological convergence imply functional similarity? A test using the evolution of quadrupedalism in ornithischian dinosaurs. *Proceedings of the Royal Society B: Biological Sciences* 279:3765-3771.
- Maidment, S. C. R., K. T. Bates, and P. M. Barrett. in press. Three-dimensional computational modeling of locomotor muscle moment arms in *Edmontosaurus* (Dinosauria, Hadrosauridae) and comparisons with other archosaurs; pp. in D. C. Evans and D. A. Eberth (eds.), HADROSAURS: Proceedings of the International Hadrosaur Symposium at the Royal Tyrrell Museum. Indiana University Press, Bloomington, Indiana.
- Maidment, S. C. R., D. H. Linton, P. Upchurch, and P. M. Barrett. 2012. Limb-Bone Scaling Indicates Diverse Stance and Gait in Quadrupedal Ornithischian Dinosaurs. *PLoS ONE* 7:e36904.
- Mallison, H. 2010. The digital *Plateosaurus* I: body mass, mass distribution, and posture assessed using CAD and CAE on a digitally mounted complete skeleton. *Palaeontologia Electronica* 13:26p.
- Mallison, H. 2011a. Plateosaurus in 3D: how CAD models and kinetic-dynamic modeling bring an extinct animal to life; pp. 219–236 in N. Klein, K. Remes, C. T. Gee, and P. M. Sander (eds.), *Biology of the Sauropod Dinosaurs: Understanding the Life of Giants*. Indiana University Press, Bloomington, ID.
- Mallison, H. 2011b. Defense capabilities of *Kentrosaurus aethiopicus* Hennig, 1915. *Palaeontologia Electronica* 14:1-25.
- Mallison, H. 2011c. Rearing giants: kinetic-dynamic modeling of sauropod bipedal and tripodal poses; pp. 237–250 in N. Klein, K. Remes, C. T. Gee, and P. M. Sander (eds.), *Biology of the Sauropod Dinosaurs: Understanding the Life of Giants*. Indiana University Press, Bloomington, ID.
- Mannion, P. D., and P. Upchurch. 2010. Completeness metrics and the quality of the sauropodomorph fossil record through geological and historical time. *Journal Information* 36:283–302.

- Mannion, P. D., P. Upchurch, M. T. Carrano, and P. M. Barrett. 2010. Testing the effects of the rock record on diversity: a multidisciplinary approach to elucidating the generic richness of sauropodomorph dinosaurs through time. *Biological Reviews*.
- Marquet, P. A., R. A. Quiñones, S. Abades, F. Labra, M. Tognelli, M. Arim, and M. Rivadeneira. 2005. Review: scaling and power-laws in ecological systems. *The Journal of Experimental Biology* 208:1749-1769.
- Martins, E. P., and T. F. Hansen. 1997. Phylogenies and the comparative method: a general approach to incorporating phylogenetic information into the analysis of interspecific data. *The American Naturalist* 149:647–667.
- Mazzetta, G. V., P. Christiansen, and R. A. Fariña. 2004. Giants and bizarres: body size of some southern South American Cretaceous dinosaurs. *Historical Biology* 16:71-83.
- McClain, C. R., and A. G. Boyer. 2009. Biodiversity and body size are linked across metazoans. *Proceedings of the Royal Society B* 276:2209-2215.
- McDonald, A. T. 2011. The taxonomy of species assigned to *Camptosaurus* (Dinosauria: Ornithopoda). *Zootaxa* 2783:52–68.
- McDonald, A. T. 2012. Phylogeny of basal iguanodonts (Dinosauria: Ornithischia): an update. *PLoS ONE* 7:e36745.
- McDonald, A. T., D. G. Wolfe, and J. I. Kirkland. 2010a. A new basal hadrosauroid (Dinosauria: Ornithopoda) from the Turonian of New Mexico. *Journal of Vertebrate Paleontology* 30:799-812.
- McDonald, A. T., J. I. Kirkland, D. D. DeBlieux, S. K. Madsen, J. Cavin, A. R. Milner, and L. Panzarini. 2010b. New basal iguanodonts from the Cedar Mountain Formation of Utah and the evolution of thumb-spikes dinosaurs. *PLoS ONE* 5:e14075.
- McLain, D. K. 1993. Cope's rules, sexual selection, and the loss of ecological plasticity. *Oikos* 68:490–500.
- McMahon, T. 1973. Size and shape in biology. *Science* 179:1201-1204.

- McMahon, T. A. 1975a. Allometry and biomechanics: limb bones in adult ungulates. *The American Naturalist* 109:547–563.
- McMahon, T. A. 1975b. Using body size to understand the structural design of animals: quadrupedal locomotion. *Journal of Applied Physiology* 39:619-627.
- McShea, D. W. 1994. Mechanisms of large-scale evolutionary trends. *Evolution* 48:1747–1763.
- Millien, V. 2008. Comment: The largest among the smallest: the body mass of the giant rodent *Josephoatigasia monesi*. *Proceedings of the Royal Society B* 275:1953-1955.
- Millien, V., and H. Bovy. 2010. When teeth and bones disagree: body mass estimates in a giant extinct rodent. *Journal of Mammalogy* 91:11-18.
- Mo, J., Z. Zhao, W. Wang, and X. Xu. 2007. The first hadrosaurid dinosaur from southern China. *Acta Geologica Sinica-English Edition* 81:550–554.
- Motani, R. 2001. Estimating body mass from silhouettes: testing the assumption of elliptical body cross-sections. *Paleobiology* 27:735-750.
- Nakagawa, S., and R. P. Freckleton. 2008. Missing inaction: the dangers of ignoring missing data. *Trends in ecology & evolution* 23:592–596.
- Naro-Maciel, E., M. Le, N. N. FitzSimmons, and G. Amato. 2008. Evolutionary relationships of marine turtles: a molecular phylogeny based on nuclear and mitochondrial genes. *Molecular Phylogenetics and Evolution* 49:659–662.
- Near, T. J., P. A. Meylan, and H. B. Shaffer. 2005. Assessing concordance of fossil calibration points in molecular clock studies: an example using turtles. *The American Naturalist* 165:137–146.
- Newell, N. D. 1949. Phyletic size increase, an important trend illustrated by fossil invertebrates. *Evolution*:103-124.

- Nopcsa, F. 1900. Dinosaurierreste aus Siebenbürgen. I. Schädel von *Limnosaurus transsylvaniaicus* nov. gen. et spec. Denkschriften der königlichen Akademie der Wissenschaften 68:555–591.
- Nopcsa, F. 1903. *Telmatosaurus*, new name for the dinosaur *Limnosaurus*. Geological Magazine (Series 5) 2:241–295.
- Nopcsa, F. 1914. Über das Vorkommen der Dinosaurier in Siebenbürgen. Verhandlungen der Zoologischen und Botanischen gessellschaft 54:12–14.
- Norman, D. B. 2004. Basal Iguanodontia; pp. 413-437 in D. B. Weishampel, P. Dodson, and H. Osmolska (eds.), *The Dinosauria* (2nd ed.). University of California Press, Berkeley, CA.
- Norman, D. B., and D. B. Weishampel. 1985. Ornithopod Feeding Mechanisms: Their Bearing on the Evolution of Herbivory. *The American Naturalist* 126:151-164.
- Norman, D. B., H.-D. Sues, L. M. Witmer, and R. A. Coria. 2004. Basal Ornithopoda; pp. 393–412 in D. B. Weishampel, H. Osmólska, and P. Dodson (eds.), *The Dinosauria* (2nd ed.). University of California Press, Berkeley, CA.
- Novack-Gottshall, P. M. 2008. Ecosystem-wide body-size trends in Cambrian–Devonian marine invertebrate lineages. *Paleobiology* 34:210–228.
- Novas, F. E., S. Valais, P. Vickers-Rich, and T. Rich. 2005. A large Cretaceous theropod from Patagonia, Argentina, and the evolution of carcharodontosaurids. *Naturwissenschaften* 92:226-230.
- O'Connor, P. M. 2006. Postcranial pneumaticity: An evaluation of soft-tissue influences on the postcranial skeleton and the reconstruction of pulmonary anatomy in archosaurs. *Journal of Morphology* 267:1199–1226.
- O'Gorman, E. J., and D. W. E. Hone. 2012. Body Size Distribution of the Dinosaurs. *PLoS ONE* 7:e51925.

- Oba, S., M. Sato, I. Takemasa, M. Monden, K. Matsubara, and S. Ishii. 2003. A Bayesian missing value estimation method for gene expression profile data. *Bioinformatics* 19:2088-2096.
- Okajima, Y., and Y. Kumazawa. 2009. Mitogenomic perspectives into iguanid phylogeny and biogeography: Gondwana vicariance for the origin of Madagascan oplurines. *Gene* 441:28-35.
- Okajima, Y., and Y. Kumazawa. 2010. Mitochondrial genomes of acrodont lizards: timing of gene rearrangements and phylogenetic and biogeographic implications. *BMC Evolutionary Biology* 10:141.
- Osborn, H. F. 1910. The age of mammals in Europe, Asia and North America. The Macmillan Co., New York, NY, 635 pp.
- Ősi, A., E. Prondvai, R. Butler, and D. B. Weishampel. 2012. Phylogeny, histology and inferred body size evolution in a new rhabdodontid dinosaur from the Late Cretaceous of Hungary. *PLoS ONE* 7:e44318.
- Packard, G. C., T. J. Boardman, and G. F. Birchard. 2009. Allometric equations for predicting body mass of dinosaurs. *Journal of Zoology* 279:102-111.
- Pagel, M. 1999. Inferring the historical patterns of biological evolution. *Nature* 401:877–884.
- Paradis, E., J. Claude, and K. Strimmer. 2004. APE: analyses of phylogenetics and evolution in R language. *Bioinformatics* 20:289-290.
- Paul, G. 1997. Dinosaur models: the good, the bad, and using them to estimate the mass of dinosaurs; pp. 39-45 in D. L. Wolberg, E. Stump, and G. D. Rosenberg (eds.), *Dinofest International*. The Academy of Natural Sciences, Arizona State University.
- Paul, G. S. 1998. Terramegathermy and Cope's Rule in the lane of titans. *Modern Geology* 23:179–218.
- Paul, G. S. 2008. A revised taxonomy of the iguanodont dinosaur genera and species. *Cretaceous Research* 29:192–216.

- Payne, J. L., A. G. Boyer, J. H. Brown, S. Finnegan, M. Kowalewski, R. A. Krause Jr, S. K. Lyons, C. R. McClain, D. W. McShea, and P. M. Novack-Gottshall. 2009. Two-phase increase in the maximum size of life over 3.5 billion years reflects biological innovation and environmental opportunity. *Proceedings of the National Academy of Sciences* 106:24–27.
- Peczkis, J. 1994. Implications of body-mass estimates for dinosaurs. *Journal of Vertebrate Paleontology* 14:520-533.
- Pereda-Suberbiola, X., J. I. Canudo, P. Cruzado-Caballero, J. L. Barco, N. López-Martínez, O. Oms, and J. I. Ruiz-Omeñaca. 2009. The last hadrosaurid of Europe: a new lambeosaurine from the Uppermost Cretaceous of Aren (Huesca, Spain). *Comptes Rendus Palevol*.
- Peters, R. H. 1983. *The Ecological Implications of Body Size*. Cambridge University Press, New York, New York, 329 pp.
- Peters, R. H., and K. Wassenberg. 1983. The effect of body size on animal abundance. *Oecologia* 60:89-96.
- Pontzer, H., V. Allen, and J. R. Hutchinson. 2009. Biomechanics of running indicates endothermy in bipedal dinosaurs. *PLoS ONE* 4:1-9.
- Prieto-Márquez, A. 2010. Global phylogeny of hadrosauridae (Dinosauria: Ornithopoda) using parsimony and Bayesian methods. *Zoological Journal of the Linnean Society* 159:435-502.
- Prieto-Márquez, A. 2011. A reappraisal of *Barsboldia sicinskii* (Dinosauria: Hadrosauridae) from the Late Cretaceous of Mongolia. *Journal of Paleontology* 85:468-477.
- Prieto-Márquez, A., L. M. Chiappe, and S. H. Joshi. 2012. The Lambeosaurine Dinosaur *Magnapaulia laticaudus* from the Late Cretaceous of Baja California, Northwestern Mexico. *PLoS ONE* 7:e38207.

- Pybus, O. G., and P. H. Harvey. 2000. Testing macro–evolutionary models using incomplete molecular phylogenies. *Proceedings of the Royal Society of London. Series B: Biological Sciences* 267:2267–2272.
- Quental, T. B., and C. R. Marshall. 2009. Extinction during evolutionary radiations: reconciling the fossil record with molecular phylogenies. *Evolution* 63:3158–3167.
- Quental, T. B., and C. R. Marshall. 2010. Diversity dynamics: molecular phylogenies need the fossil record. *Trends in Ecology and Evolution* 25:434–441.
- R Development Core Team. 2012. R: a language and environment for statistical computing. 2.15.2. R Foundation for Statistical Computing, Vienna, Austria.
- Raia, P., F. Carotenuto, F. Passaro, D. Fulgione, and M. Fortelius. 2012. Ecological specialization in fossil mammals explains Cope's rule. *American Naturalist* 179:328–337.
- Ramirez-Velasco, A. A., M. Benammi, A. Prieto-Márquez, J. A. Ortega, and R. Hernandez-Rivera. 2012. *Huehuecanauhtlus tiquichensis*, a new hadrosauroid dinosaur (Ornithischia: Ornithopoda) from the Santonian (Late Cretaceous) of Michoacan, Mexico. *Canadian Journal of Earth Sciences* 49:379–395.
- Redelstorff, R., and P. M. Sanders. 2009. Long and girdle bone histology of *Stegosaurus*: implications for growth and life history. *Journal of Vertebrate Paleontology* 29:1087–1099.
- Rensch, B. 1943. Die paläontologischen Evolutionsregeln in zoologischer Betrachtung. *Biologia Generalis* 17:1–55.
- Rensch, B. 1948. Histological changes correlated with evolutionary changes of body size. *Evolution* 2:218–230.
- Rensch, B. 1959. Evolution above the species level. Columbia University Press, New York, NY.
- Rinderknecht, A., and R. E. Blanco. 2008. The largest fossil rodent. *Proceedings of the Royal Society B: Biological Sciences* 275:923–928.

- Romer, A. S., and L. I. Price. 1940. Review of the Pelycosauria. Geological Society of America Special Paper 28.
- Roos, J., R. K. Aggarwal, and A. Janke. 2007. Extended mitogenomic phylogenetic analyses yield new insight into crocodylian evolution and their survival of the Cretaceous-Tertiary boundary. *Molecular Phylogenetics and Evolution* 45:663–673.
- Royall, R. M. 1997. Statistical evidence: likelihood paradigm, Monographs of Statistics and Applied Probability, Volume 71. Chapman & Hall/CRC, London, UK.
- Royer, D. L., R. A. Berner, I. P. Montañez, N. J. Tabor, and D. J. Beerling. 2004. CO₂ as a primary driver of Phanerozoic climate. *Geological Society of America Today* 14:4-10.
- Rubin, C. T., and L. E. Lanyon. 1982. Limb mechanics as a function of speed and gait: a study of functional strains in the radius and tibia of horse and dog. *Journal of Evolutionary Biology* 101:187-211.
- Rubin, C. T., and L. E. Lanyon. 1984. Dynamic strain similarity in vertebrates: an alternative to allometric limb bone scaling. *Journal of Theoretical Biology* 107:321-327.
- Rubin, D. B. 1976. Inference and missing data. *Biometrika* 63:581–592.
- Ruiz-Omeñaca, J. I. 2011. *Delapparentia turolensis* nov. gen et sp., un nuevo dinosaurio iguanodontideo (Ornithischia: Ornithopoda) en el Cretácico Inferior de Galve. *Estudios Geológicos* 67:83–110.
- Ruta, M., P. J. Wagner, and M. I. Coates. 2006. Evolutionary patterns in early tetrapods. I. Rapid initial diversification followed by decrease in rates of character change. *Proceedings of the Royal Society B: Biological Sciences* 273:2107–2111.
- Sampson, S. D. 2009. *Dinosaur Odyssey: Fossil Threads in the Web of Life*. University of California Press, Berkeley, CA, 332 pp.
- Sanders, P. M., A. Christian, M. Clauss, R. Fechner, C. T. Gee, E.-M. Griebeler, H.-C. Gunga, J. Hummel, H. Mallison, S. F. Perry, H. Preuschoft, O. W. M. Rauhut, K. Remes, T.

- Tütken, O. Wings, and U. Witzel. 2010. Biology of the sauropod dinosaurs: the evolution of gigantism. *Biological Reviews* 86:117–155.
- Schluter, D. 2000. *The Ecology of Adaptive Radiation*. Oxford University Press, Oxford, UK, 292 pp.
- Schluter, D., T. Price, A. Ø. Mooers, and D. Ludwig. 1997. Likelihood of ancestor states in adaptive radiation. *Evolution* 51:1699–1711.
- Seebacher, F. 2001. A new method to calculate allometric length-mass relationships of dinosaurs. *Journal of Vertebrate Paleontology* 21:51-60.
- Seebacher, F. 2003. Dinosaur body temperatures: the occurrence of endothermy and ectothermy. *Paleobiology* 29:105–122.
- Sellers, W. I., J. Hepworth-Bell, P. L. Falkingham, K. T. Bates, C. A. Brassey, V. M. Egerton, and P. L. Manning. 2012. Minimum convex hull mass estimations of complete mounted skeletons. *Biology Letters*.
- Sereno, P. C. 1997. The origin and evolution of dinosaurs. *Annual Review of Earth and Planetary Science* 25:435-489.
- Shibata, M., P. Jintasakul, and Y. Azuma. 2011. A New Iguanodontian Dinosaur from the Lower Cretaceous Khok Kruat Formation, Nakhon Ratchasima in Northeastern Thailand. *Acta Geologica Sinica* 85:969–976.
- Simpson, G. G. 1944. *Tempo and mode in evolution*. Columbia University Press, New York, NY, 235 pp.
- Simpson, G. G. 1953. *The Major Features of Evolution*. Columbia University Press, New York, NY.
- Slater, G. J., S. A. Price, F. Santini, and M. E. Alfaro. 2010. Diversity versus disparity and the radiation of modern cetaceans. *Proceedings of the Royal Society B: Biological Sciences* 277:3097–3104.

- Smaers, J. B., and L. Vinicius. 2009. Inferring macro-evolutionary patterns using an adaptive peak model of evolution. *Evolutionary Ecology Research* 11:991–1015.
- Smith, A. G., D. G. Smith, and B. M. Funnell. 1994. *Atlas of Mesozoic and Cenozoic coastlines*. Cambridge University Press, Cambridge, UK.
- Smith, F. A., A. G. Boyer, J. H. Brown, D. P. Costa, D. T., S. K. M. Ernest, A. R. Evans, M. Fortelius, J. L. Gittleman, M. J. Hamilton, L. E. Harding, K. Lintulaakso, S. K. Lyons, C. McCain, J. G. Okie, J. J. Saarinen, R. M. Sibly, P. R. Stephens, J. Theodor, and M. D. Uhen. 2010. The evolution of maximum body size of terrestrial mammals. *Science* 330:1216-1219.
- Smith, R. J. 1984. Allometric scaling in comparative biology: problems of concept and method. *American Journal of Physiology - Regulatory, Integrative and Comparative Physiology* 246:R152-R160.
- Smith, R. J. 2002. Lead review: Estimation of body mass in paleontology. *Journal of Human Evolution* 43:271-287.
- Sokal, R. R., and F. J. Rohlf. 1969. *Biometry: The Principles and Practice of Statistics in Biological Science*. W. H. Freeman and Company, San Francisco, CA, 776 pp.
- Sookias, R. B., R. B. J. Benson, and R. J. Butler. 2012a. Biology, not environment, drives major patterns in maximum tetrapod body size through time. *Biology Letters* 8:674–677.
- Sookias, R. B., R. J. Butler, and R. B. J. Benson. 2012b. Rise of dinosaurs reveals major body-size transitions are driven by passive processes of trait evolution. *Proceedings of the Royal Society B: Biological Sciences* 279:2180-2187.
- Spinks, P. Q., and H. B. Shaffer. 2009. Conflicting mitochondrial and nuclear phylogenies for the widely disjunct *Emys* (Testunides: Emydidae) species complex, and what they tell us about biogeography and hybridization. *Systematic Biology* 58:1-20.
- Stacklies, W., H. Redestig, M. Scholz, D. Walther, and J. Selbig. 2007. *pcaMethods* - a biconductor package providing PCA methods for incomplete data. *Bioinformatics* 23:1164-1167.

- Stanley, S. M. 1973. An explanation for Cope's rule. *Evolution* 27:1–26.
- Stoinski, S., T. Suthau, and H.-C. Gunga. 2011. Reconstructing Body Volume and Surface Area of Dinosaurs Using Laser Scanning and Photogrammetry; pp. 94–104 in N. Klein, K. Remes, C. T. Gee, and P. M. Sander (eds.), *Biology of the Sauropod Dinosaurs: Understanding the Life of Giants*. Indiana University Press, Bloomington, Indiana.
- Strauss, R. E., and M. N. Atanassov. 2006. Determining best complete subsets of specimens and characters for multivariate morphometric studies in the presence of large amounts of missing data. *Biological Journal of the Linnean Society* 88:309–328.
- Strauss, R. E., M. N. Atanassov, and J. A. De Oliveira. 2003. Evaluation of the principal-component and expectation-maximization methods for estimating missing data in morphometric studies. *Journal of Vertebrate Paleontology* 23:284–296.
- Sues, H.-D. 1980. Anatomy and relationships of a new hypsilophodontid dinosaur from the Lower Cretaceous of North America. *Palaeontographica Abt. A* 169:51-72.
- Sues, H.-D., and A. Averianov. 2009. A new basal hadrosauroid dinosaur from the Late Cretaceous of Uzbekistan and the early readiation of duck-billed dinosaurs. *Proceedings of the Royal Society B* 276:2549-2555.
- Sullivan, R. M., and T. E. Williamson. 1999. A new skull of *Parasaurolophus* (Dinosauria: Hadrosauridae) from the Kirtland Formation of New Mexico and a revision of the genus. *New Mexico Museum of Natural History and Science Bulletin* 15:1-41.
- Therrien, F., and D. M. Henderson. 2007. My theropod is bigger than yours...or not: estimating body size from skull length in theropods. *Journal of Vertebrate Paleontology* 27:108-115.
- Townsend, T. M., A. Larson, E. Louis, and J. R. Macey. 2004. Molecular phylogenetics of Squamata: the position of snakes, amphisbaenians, and didamids, and the root of the squamate tree. *Systematic Biology* 53:735-757.
- Turner, A. H., D. Pol, J. A. Clarke, G. M. Erickson, and M. A. Norell. 2007. A basal dromaeosaurid and size evolution preceding avian flight. *Science* 317:1378-1381.

- Upchurch, P., and P. M. Barrett. 2005. Phylogenetic and Taxix Perspectives on Sauropod Diversity; pp. 104-124 in K. Curry Rogers and J. A. Wilson (eds.), *The Sauropods: Evolution and Paleobiology*. University of California Press, Berkeley, CA.
- Van Valen, L. 1973. Pattern and the balance of nature. *Evolutionary Theory* 1:31–49.
- Van Valkenburgh, B., X. Wang, and J. Damuth. 2004. Cope's rule, hypercarnivory, and extinction in North American canids. *Science* 306:101–104.
- Varricchio, D. J., F. Jackson, J. J. Borkowski, and J. R. Horner. 1997. Nests and egg clutches of the dinosaur *Troodon formosus* and the evolution of avian reproductive traits. *Nature* 385:247-250.
- Varricchio, D. J., J. R. Moore, G. M. Erickson, M. A. Norell, F. D. Jackson, and J. J. Borkowski. 2008. Avian paternal care had dinosaur origin. *Science* 322:1826-1828.
- Vidal, N., and S. B. Hedges. 2005. The phylogeny of squamate reptiles lizards, snakes, and amphisbaenians) inferred from nine nuclear protein-coding genes. *Comptes Rendus Biologies* 328:1000-1008.
- Wagner, J. R., and T. M. Lehman. 2009. An enigmatic new lambeosaurine hadrosaur (Reptilia: Dinosauria) from the upper shale member of the Campanian Aguja Formation of Trans-Pecos Texas. *Journal of Vertebrate Paleontology* 29:605-611.
- Warton, D. I., I. J. Wright, D. S. Falster, and M. Westoby. 2006. Bivariate line-fitting methods for allometry. *Biological Reviews* 81:259-291.
- Warton, D. I., R. A. Duursma, D. S. Falster, and S. Taskinen. 2011. smatr 3-an R package for estimation and inference about allometric lines. *Methods in Ecology and Evolution* 3:257–259.
- Wedel, M. J. 2003. Vertebral pneumaticity, air sacs, and the physiology of sauropod dinosaurs. *Paleobiology* 29:243-255.
- Weishampel, D. B., and C.-M. Jianu. 2011. *Transylvanian Dinosaurs*. John Hopkins University Press, Baltimore, MD, 301 pp.

- Weishampel, D. B., D. B. Norman, and D. Grigorescu. 1993. *Telmatosaurus transsylvanicus* from the Late Cretaceous of Romania: the most basal hadrosaurid dinosaur. *Palaeontology* 36:361-385.
- Weishampel, D. B., C.-M. Jianu, Z. Csiki, and D. B. Norman. 2003. Osteology and phylogeny of *Zalmoxes* (n. g.), an unusual euornithopod dinosaur from the latest Cretaceous of Romania. *Journal of Systematic Palaeontology* 1:65-123.
- Wiedemann, A., T. Suthau, and J. Albertz. 1999. Photogrammetric survey of dinosaur skeletons. *Mitteilungen aus dem Museum für Naturkunde der Humboldt-Universität Berlin, Geowissenschaftliche Reihe* 2:113-119.
- Wiens, J. J., M. C. Brändle, and T. W. Reeder. 2006. Why does a trait evolve multiple times with a clade? Repeated evolution of snakelike body form in squamate reptiles. *Evolution* 60:123–141.
- Wilson, J. A., and M. T. Carrano. 1999. Titanosaurs and the origin of “wide-gauge” trackways: a biomechanical and systematic perspective on sauropod locomotion. *Journal Information* 25.
- Wilson, J. A., and P. Upchurch. 2009. Redescription and reassessment of the phylogenetic affinities of *Euhelopus zdanskyi* (Dinosauria: Sauropoda) from the Early Cretaceous of China. *Journal of Systematic Palaeontology* 7:199–239.
- Woodward, A. R., J. H. White, and S. B. Linda. 1995. Maximum size of the alligator (*Alligator mississippiensis*). *Journal of Herpetology* 29:507–513.
- Woodward, G., B. Ebenman, M. Emmerson, J. M. Montoya, J. M. Olesen, A. Valido, and P. H. Warren. 2005. Body size in ecological networks. *Trends in Ecology and Evolution* 20:402-409.
- Xing, H., A. Prieto-Márquez, S.-L. Hai, and T.-X. Yu. 2012. Re-evaluation and phylogenetic analysis of the hadrosaurine dinosaur *Wulagasaurus dongi* from the Maastrichtian of northeast China. *Vertebrata PalAsiatica* 50:160–169.

- Yoder, J. B., E. Clancey, S. Des Roches, J. M. Eastman, L. Gentry, W. Godsoe, T. J. Hagey, D. Jochimsen, B. P. Oswald, J. Robertson, B. A. J. Sarver, J. J. Schenk, S. F. Spear, and L. J. Harmon. 2010. Ecological opportunity and the origin of adaptive radiations. *Journal of Evolutionary Biology* 23:1581–1596.
- You, H. L., Q. Ji, and D. Li. 2005. *Lanzhousaurus magnidens* gen. et sp. nov. from Gansu Province, China: the largest-toothed herbivorous dinosaur in the world. *Geological Bulletin of China* 24:785–794.
- You, H. L., J. I. Qiang, L. I. Jinglu, and L. I. Yinxian. 2003. A New Hadrosauroid Dinosaur from the Mid-Cretaceous of Liaoning, China. *Acta Geologica Sinica* 77:148–154.
- Young, M. T., M. A. Bell, M. B. De Andrade, and S. L. Brussatte. 2011. Body size estimation and evolution in metriorhynchid crocodylomorphs: implications for species diversification and niche partitioning. *Zoological Journal of the Linnean Society* 163:1199–1216.
- Zanno, L. E., and P. J. Makovicky. 2013. No evidence for directional evolution of body mass in herbivorous theropod dinosaurs. *Proceedings of the Royal Society B: Biological Sciences* 280.
- Zar, J. H. 1968. Calculation and miscalculation of the allometric equation as a model in biological data. *BioScience* 18:118-1120.
- Zheng, W., X. Jin, M. Shibata, Y. Azuma, and F. Yu. 2012. A new ornithischian dinosaur from the Cretaceous Liangtoutang Formation of Tiantai, Zhejiang Province, China. *Cretaceous Research*.

Appendices

Appendix 1. Limb measurement and body mass data in extant mammals and reptiles.

Table of measurements of all the extant taxa used in Chapter 1 (Campione and Evans, 2012), as well as the limb measurements of the non-avian dinosaurian taxa used in Table 1-10.

Higher Clade	Species	SP#	BM	HL	HC	FL	FC
Afrotheria	<i>Elephas maximus</i>	ZMUC1399	3534000	830	310	980	315
Afrotheria	<i>Loxodonta africana</i>	ROM R6000	6435000	1035	416.3	1147.5	399
Afrotheria	<i>Petrodromus tetradactylus</i>	ROM 85723	275	33.7	9.5	47.3	12.5
Afrotheria	<i>Rhynchocyon cirnei</i>	ROM 47023	445		9.5	55.45	13.75
Afrotheria	<i>Heterohyrax brucei</i>	ROM 64992	3650	78.2	21.75	79.5	24.25
Carnivora	<i>Alopex lagopus</i>	ROM 105014	3710	112.15	23	114.68	24.85
Carnivora	<i>Canis latrans</i>	ROM R6654	13608	166.2	41	178.35	40.6
Carnivora	<i>Canis lupus</i>	ROM 101841	32000	211	53.25	226.5	51.75
Carnivora	<i>Cuon alpinus</i>	ROM 105074	15400	158.3	42.35	173.75	44.15
Carnivora	<i>Nyctereutes procyonoides</i>	ROM 94037	3500	84.3	25.25	89.74	25.75
Carnivora	<i>Urocyon cinereoargentus</i>	ROM 14309	4800	102.74	24.1	115	27.15
Carnivora	<i>Vulpes velox</i>	ROM 105398	2300	99.88	21.55	99.17	23.3
Carnivora	<i>Vulpes vulpes</i>	ROM 28025	6000	125.1	26.25	127.62	26.95
Carnivora	<i>Vulpes zerda</i>	ROM 91467	1000	68.2	16.25	70.4	16.25
Carnivora	<i>Acinonyx jubatus</i>	ROM 111488	60400	243.5	62.5	268.5	67.5
Carnivora	<i>Felis catus</i>	ZMUC 3629*	8400	104	28.5	119.5	30
Carnivora	<i>Leopardus pardalis</i>	ZMUC 1111*	13900	144.5	40.5	165	42
Carnivora	<i>Lynx canadensis</i>	ROM 74772	17710	178.75	38.75	215.55	40.85
Carnivora	<i>Lynx lynx</i>	ZMUC 120*	9700	170.5	38	202.5	39
Carnivora	<i>Lynx rufus</i>	ROM 67947	8800	151.25	36.5	175.95	38.25
Carnivora	<i>Neofelis nebulosa</i>	AHR1985	13478		44.7		41.4
Carnivora	<i>Panthera leo</i>	ZMUC 7231*	203000	366	116	401	109
Carnivora	<i>Panthera onca</i>	ZMUC 6221*	71000	239	76	265.5	72.5
Carnivora	<i>Panthera pardus</i>	ZMUC 5661*	61000	200	62	231	61
Carnivora	<i>Panthera tigris_altaica</i>	ZMUC 5698*	230000	350	113	411	102.5
Carnivora	<i>Panthera tigris_tigris</i>	ZMUC 5667*	145000	310	94	360.5	90.5
Carnivora	<i>Panthera unica</i>	ZMUC 6047*	43100	208.5	63.5	234.5	63
Carnivora	<i>Puma concolor</i>	ZMUC 5663*	47000	231.5	65.5	276.5	62.5
Carnivora	<i>Crossarchus obscurus</i>	ROM 89636	1190	48.86	14.9	54.76	15.5
Carnivora	<i>Galerella sanguinea</i>	ROM 58390	1100	45.5	14	51.25	14.5
Carnivora	<i>Helogale parvula</i>	ROM 58387	450	34.6	11	36	12
Carnivora	<i>Herpestes javanicus</i>	ROM 74045	384	42.2	11.6	46.84	12.5
Carnivora	<i>Ichneumia albicauda</i>	ROM 58383	4760	93.3	23.1	108.72	27.05
Carnivora	<i>Liberiictis kuhni</i>	ROM 102286	2430	68	20.5	76.1	22.25
Carnivora	<i>Suricata suricata</i>	ROM 74547	717	50.74	13.2	55.83	13.65
Carnivora	<i>Arctonyx collaris</i>	ROM 97264	5900	96.56	32.1	109.04	29.3
Carnivora	<i>Gulo gulo</i>	ROM 32287	16556	136.25	39.75	141.5	35
Carnivora	<i>Lutra canadensis</i>	ROM R6629	6400	74.66	26.1	73.69	24.4
Carnivora	<i>Martes pennanti</i>	ROM 87320	6160	96.4	22.25	102.45	24.5

Carnivora	<i>Mephitis mephitis</i>	ROM 98961	6500	62.15	24.05	71.25	22.05
Carnivora	<i>Mustela erminea</i>	ROM 77158	145	29.2	7	30.6	7.7
Carnivora	<i>Mustela frenata</i>	ROM 94414	260	34.98	9.55	38.48	10.2
Carnivora	<i>Mustela nigripes</i>	ROM R6743	694	48.8	12.15	49.9	13.05
Carnivora	<i>Mustela putorius</i>	ROM 88373	1100	47.3	12.95	51.97	12.5
Carnivora	<i>Mustela vison</i>	ROM 111439	1135	47.76	14.65	50.87	14.7
Carnivora	<i>Taxidea taxus</i>	ROM 58275	9900	103.1	33	100.8	27.75
Carnivora	<i>Arctocephalus pusillus</i>	ROM R5607	43000	141.35	83.95	81.75	48.75
Carnivora	<i>Phoca groenlandica</i>	ROM R1665	42000	128.5	68.85	90.55	70
Carnivora	<i>Procyon lotor</i>	ROM 88247	7000	114.7	31.05	132.75	33.25
Carnivora	<i>Ursus americanus</i>	ROM 71435	204000	296	101.5	302	96.5
Carnivora	<i>Ursus arctos</i>	ROM 35699	435500	400.5	146.25	445.5	126.25
Carnivora	<i>Ursus maritimus</i>	AHR1985	447695		158		135
Carnivora	<i>Viverricula indica</i>	ROM R629	2600	78.3	21.2	92.95	24.1
Euarchonta	<i>Aotus trivirgatus</i>	ROM 94422	1050	68.465	15	91.14	16.85
Euarchonta	<i>Callithrix jacchus</i>	ROM 101192	270	45.04	11.05	56.175	11.85
Euarchonta	<i>Cebuella pygmaea</i>	ROM 97068	178	35.77	8.75	40.615	8.85
Euarchonta	<i>Saguinus sp.</i>	ROM 20131	422	52.625	12.2	66.32	13.35
Euarchonta	<i>Cercopithecus neglectus</i>	ROM 111045	11450	149.43	36.95	184.4	39.05
Euarchonta	<i>Macaca fuscata</i>	ROM 112298	3500	135.9	30	152.5	31.5
Euarchonta	<i>Papio cynocephalus</i>	AHR1985	28576		55		57
Euarchonta	<i>Papio hamadryas</i>	ROM 91308	14700	190.85	42.25	224.4	44.5
Euarchonta	<i>Euoticus elegantulus</i>	ROM 55711	260	38.26	11.2	65.34	12
Euarchonta	<i>Otolemur crassicaudatus</i>	ROM 64976	950	59.915	16	90.14	19
Euarchonta	<i>Pongo Pygmaeus</i>	ROM 82830	155000	368.5	98.5	273	88
Euarchonta	<i>Hylobates lar</i>	ROM 77534	6400	238.05	28.5	203.6	31.45
Euarchonta	<i>Eulemur fulvus</i>	ROM 68120	1192	74.095	16.05	116.44	19.8
Euarchonta	<i>Lemur catta</i>	ROM 114614	2300	89.39	21	143.39	26.8
Euarchonta	<i>Tupaia glis</i>	ROM 75961	176	27.3	7	35.85	9.35
Eulipotyphla	<i>Atelerix albiventris</i>	ROM R6167	360	33.45	10.95	34.3	15.15
Eulipotyphla	<i>Atelerix algirus</i>	ROM 111451	415	33.8	10.2	34.25	11.7
Eulipotyphla	<i>Echinosorex gymnura</i>	ROM 36803	610	45	11	49.45	13.05
Eulipotyphla	<i>Erinaceus europaeus</i>	ROM 79166	717	44.65	15.5	41.35	16.75
Eulipotyphla	<i>Condylura cristata</i>	ROM 77166	59	13.9	10.05	15.9	6.3
Eulipotyphla	<i>Parascalops breweri</i>	ROM 90471	56	14.1	12.3	14.35	5.9
Glires	<i>Aplodontia rufa</i>	ROM R6571	953	45.55	15	52.75	15.75
Glires	<i>Castor canadensis</i>	ROM 111459	12500	78.8	34.5	104.2	49.75
Glires	<i>Cavia porcellus</i>	ROM 98958	1200	40.45	12.6	48.5	16
Glires	<i>Dolichotis patagonum</i>	ROM 90847	8950	113.6	28.6	129.35	35.35
Glires	<i>Chinchilla lanigera</i>	ROM R5786	462	33.3	8.85	54.7	14.8
Glires	<i>Dicrostonyx groenlandicus</i>	ROM 96599	103	19.85	6.9	23	7.15
Glires	<i>Dicrostonyx hudsonius</i>	ROM 63549	108.8	20	7.1	24.15	8
Glires	<i>Dicrostonyx richardsoni</i>	ROM 96743	95	19.5	5.8	23.35	5.6
Glires	<i>Melanomys caliginosus</i>	ROM 99943	64	16.95	6	23.35	8.2
Glires	<i>Mesocricetus auratus</i>	ROM R5623	198	24.3	8.85	29	11
Glires	<i>Microtus chrotorrhinus</i>	ROM 90185	67	15.05	4.85	18.35	5.6
Glires	<i>Microtus pennsylvanicus</i>	ROM 87854	70	14.6	4.5	18.1	5.7
Glires	<i>Microtus richardsoni</i>	ROM 83701	61	16.2	5.2	18.95	6.75
Glires	<i>Nectomys squamipes</i>	ROM 98049	235	24.45	7.6	37.5	11.8
Glires	<i>Neotoma albigula</i>	ROM 87452	188.1	27.5	8.45	35.4	11.05

Glires	<i>Oryzomys albicularis</i>	ROM 97316	106	22.5	6	30.35	8
Glires	<i>Oryzomys couesi</i>	ROM 97756	102	19.4	7.05	28.7	9.85
Glires	<i>Oryzomys megacephalus</i>	ROM 106329	86	19.65	5.75	29.15	7.5
Glires	<i>Peromyscus zephynchus</i>	ROM 97525	78	19.95	5.55	27.5	7
Glires	<i>Rhipidomys leucodactylus</i>	ROM 107873	110	22.85	7.9	32	10
Glires	<i>Sigmodon hispidus</i>	ROM 95215	163	22.95	6.75	33.6	10
Glires	<i>Dasyprocta aguti</i>	ROM 90845	2230	74.5	20.5	93.95	28
Glires	<i>Echimys didelphoides</i>	ROM 107837	375	30.4	10.1	39.3	13.5
Glires	<i>Echimys semivillosus</i>	ROM 107955	350	31.85	10.5	40.75	14.25
Glires	<i>Proechimys cuvieri</i>	ROM 98086	400	33.35	9.05	45	13.5
Glires	<i>Erethizon dorsatum</i>	ROM R1949	9051	105.1	29.65	121.3	37.4
Glires	<i>Geomys bursarius</i>	ROM 72875	167.6	23.25	10.25	26.45	9.15
Glires	<i>Orthogeomys hispidus</i>	ROM 96303	490	34.45	13.95	42.05	14.05
Glires	<i>Thomomys Talpoides</i>	ROM 102659	210	25.65	10.7	28.9	10.3
Glires	<i>Dipodomys ordii</i>	ROM 91990	67	15.8	5.1	29.18	7.35
Glires	<i>Heteromys gaumeri</i>	ROM 95659	81	19.6	6	28.1	8.2
Glires	<i>Heteromys goldmani</i>	ROM 97674	82	20.65	6.1	29.1	8.7
Glires	<i>H. desmarestianus</i>	ROM 96134	94	19.3	6.15	28.8	8.9
Glires	<i>Hydrochaeris hydrochaeris</i>	ROM 73588	56500	191.5	60.5	223.5	70.5
Glires	<i>Lepus americanus</i>	ROM 82454	1294	75.7	14.5	98.25	19.65
Glires	<i>Lepus arcticus</i>	ROM 94615	4500	109.15	22	129.2	30
Glires	<i>Lepus californicus</i>	ROM R6444	1535	83.6	17.8	107.55	12.3
Glires	<i>Lepus europaeus</i>	ROM 93105	3402	108.1	24.75	137.9	33.75
Glires	<i>Lepus townsendii</i>	ROM 91969	4300	102.6	20.75	125.85	28.25
Glires	<i>Oryctolagus cuniculus</i>	ROM 84051	1900	68.55	15.5	88.8	20
Glires	<i>Sylvilagus floridanus</i>	ROM R2974	1057	61.9	14.85	82.4	18.35
Glires	<i>Acomys cahirinus</i>	ROM 87683	56	16.7	4.36	21.65	6.225
Glires	<i>Arvicantis niloticus</i>	ROM 82849	120	21	6.5	28.65	9.05
Glires	<i>Gerbillus gerbillus</i>	ROM 88169	79	16.3	5.1	25.45	8
Glires	<i>Gerbillus pyramidum</i>	ROM 88173	62	16.5	5.2	25.1	7.3
Glires	<i>Malacomys cansdalei</i>	ROM 100502	70	21.05	5.25	30.1	7.1
Glires	<i>Meriones unguiculatus</i>	ROM R1689	61	16	5.1	22.95	7
Glires	<i>Ondatra zibethicus</i>	ROM 111463	1200	41.25	14	50.45	16.65
Glires	<i>Rattus norvegicus</i>	ROM R5644	464	31.5	10.9	41.65	14.25
Glires	<i>Myocastor coypus</i>	ROM 90843	8130	77.55	25.5	100.95	32.7
Glires	<i>Cricetomys emini</i>	ROM 100511	550	46	12.65	61.15	16
Glires	<i>Octodon degus</i>	ROM R7876	238	25.25	7.05	34.8	9.45
Glires	<i>Cynomys leucurus?</i>	ROM 79165	1130	40	13.5	48.25	13.5
Glires	<i>Funisciurus pyrrhopus</i>	ROM 100573	190	31.8	9.1	41.55	10.25
Glires	<i>Marmota caligata</i>	ROM 92037	6250	90.05	28.4	99.2	25.1
Glires	<i>Marmota monax</i>	ROM R1938	3012	68.95	24.15	80.85	22
Glires	<i>Sciurus carolinensis</i>	ROM 21472	765	44.7	13.1	57.4	14.6
Glires	<i>Sciurus niger</i>	ROM R6166	1109	57.8	16.85	72.75	18.25
Glires	<i>Spermophilus adocetus</i>	ROM R810	345	30.3	8.9	37.1	10.05
Glires	<i>Spermophilus franklinii</i>	ROM 43326	475	34	11.9	43.9	12
Glires	<i>Spermophilus lateralis</i>	ROM R7280	159	26	7.3	35.2	8.7
Glires	<i>Spermophilus richardsonii</i>	ROM 91974	345	31.95	10.1	38.75	10.9
Glires	<i>S. tridecemlineatus</i>	ROM 102662	195	26.65	9.7	34.1	8.8
Glires	<i>Tamias amoenus</i>	ROM 80704	52.9	18.25	5.25	24.7	6
Glires	<i>Tamias minimus</i>	ROM 83120	60.5	18.1	5.6	24.05	5.95

Glires	<i>Tamiasciurus hudsonicus</i>	ROM 81437	260	31.4	10	40.2	9.95
Marsupialia	<i>Dasyuroides byrnei</i>	ROM 101190	133	27.35	7.15	34.6	8.7
Marsupialia	<i>Sarcophilus harrisii</i>	ROM 101196	8490	99.95	27.25	103.75	27.45
Marsupialia	<i>Chironectes minimus</i>	ROM 98855	700	45.065	12.25	57.715	14.95
Marsupialia	<i>Didelphis marsupialis</i>	ROM 96214	1500	63.05	17	80.855	18.8
Marsupialia	<i>Didelphis virginiana</i>	ROM 75749	7500	75.7	26.5	90.85	26.25
Marsupialia	<i>Marmosa murina</i>	ROM 98151	59	21.45	6.2	25.75	6.1
Marsupialia	<i>Metachirus nudicaudatus</i>	ROM 114155	235	35.35	9.25	51.15	11.45
Marsupialia	<i>Monodelphis brevicaudata</i>	ROM 98909	77	20.75	6.9	24.55	6.8
Marsupialia	<i>Philander opossum</i>	ROM 90841	600	45.6	10.95	55.95	12.85
Marsupialia	<i>Bettongia penicillata</i>	ROM 111476	1120	33.67	12.95	80.32	21.45
Marsupialia	<i>Dendrolagus inustus</i>	ROM 86035	18200	140.7	48.25	183.5	56.25
Marsupialia	<i>Macropus fuliginosus</i>	ROM 93766	22730	117.4	31	214.35	57.5
Marsupialia	<i>Macropus rufus</i>	ROM 31178	38000	154.7	55.75	251.1	71.5
Marsupialia	<i>Gymnobelideus leadbeateri</i>	ROM 101194	106.7	24.2	7.75	34.9	8.2
Ungulata	<i>Aepycoerus malampus</i>	AHR1985	60500		65		69
Ungulata	<i>Ammotragus lervia</i>	ROM 92686	49200	181	65.75	212.5	67.25
Ungulata	<i>Antilope cervicapra</i>	ROM 74199	22000	137.85	47.4	176.5	47.55
Ungulata	<i>Bison bison</i>	AHR1985	1179000		191.5		167.5
Ungulata	<i>Bison bonasus</i>	ZMUC M2270	310000	350	130	418	122
Ungulata	<i>Bos gaurus</i>	ROM 82965	545000	343.5	154.5	429	156.5
Ungulata	<i>Capra aegagrus</i>	ROM 66884	29500	165.1	58	183.65	58.95
Ungulata	<i>Capra caucasica</i>	ROM 88431	116800	240	89	271.5	88
Ungulata	<i>Capra ibex</i>	ROM 78825	25420	156.25	54.1	188.9	52.65
Ungulata	<i>Connochaetes gnou</i>	ROM 88076	108500	209	85.5	251	87
Ungulata	<i>Connochaetes taurinus</i>	AHR1985	256500		115		100
Ungulata	<i>Hemitragus jemlahicus</i>	ROM 69484	31100	172.5	61.4	184.8	57.8
Ungulata	<i>Oryx dammah</i>	ROM 94512	117900	225	95	278	92.5
Ungulata	<i>Ovibos moschatus</i>	ROM 90469	315000	315.5	128	350.5	111
Ungulata	<i>Ovis aries</i>	ROM 53974	76600	158	74.5	188	79
Ungulata	<i>Ovis dalli</i>	ROM R2980	76200	214.5	82.5	254	81.5
Ungulata	<i>Sylvicapra grimmia</i>	AHR1985	13860		31		46
Ungulata	<i>Tragelaphus angasii</i>	AHR1985	134500		99		97
Ungulata	<i>Tragelaphus scriptus</i>	AHR1985	50900		56		62
Ungulata	<i>Tragelaphus strepsiceros</i>	AHR1985	301000		140		135
Ungulata	<i>Camelus bactrianus</i>	ROM 77458	680400	386	220	485	139.5
Ungulata	<i>Lama guanicoe</i>	ROM 33659	123800	253	100	315	95
Ungulata	<i>Alces alces</i>	ROM 18516	523000	393	145.5	440	144
Ungulata	<i>Cervus duvaucelii</i>	ROM 94093	225000	265.5	101.5	343	105
Ungulata	<i>Cervus nippon</i>	ROM 88428	82200	215	70	263.5	73
Ungulata	<i>Elaphurus davidianus</i>	ROM 62744	158800	271.5	112.5	340.5	112
Ungulata	<i>Hydropotes inermis</i>	ROM 75959	24290	117.95	33.95	153.7	43.65
Ungulata	<i>Odocoileus virginianus</i>	ROM 59338	66100	216	72	279	77
Ungulata	<i>Rangifer tarandus</i>	ROM 88934	131900	261.5	90.5	304.5	85.5
Ungulata	<i>Equus burchelli?</i>	ROM 72119	272400	259	118	363.5	137.5
Ungulata	<i>Equus caballus</i>	ROM R8138	350000	261.5	118.25	362	139.85
Ungulata	<i>Equus zebra</i>	AHR1985	262000		132		143
Ungulata	<i>Giraffa camelopardalis</i>	ROM 99207	990000	495	218	520	188
Ungulata	<i>Okapia johnstoni</i>	ZMUC M4221	310000	332	131	355	128
Ungulata	<i>Choeropsis liberiensis</i>	ZMUC M4117	250000	245	101	268.7	107

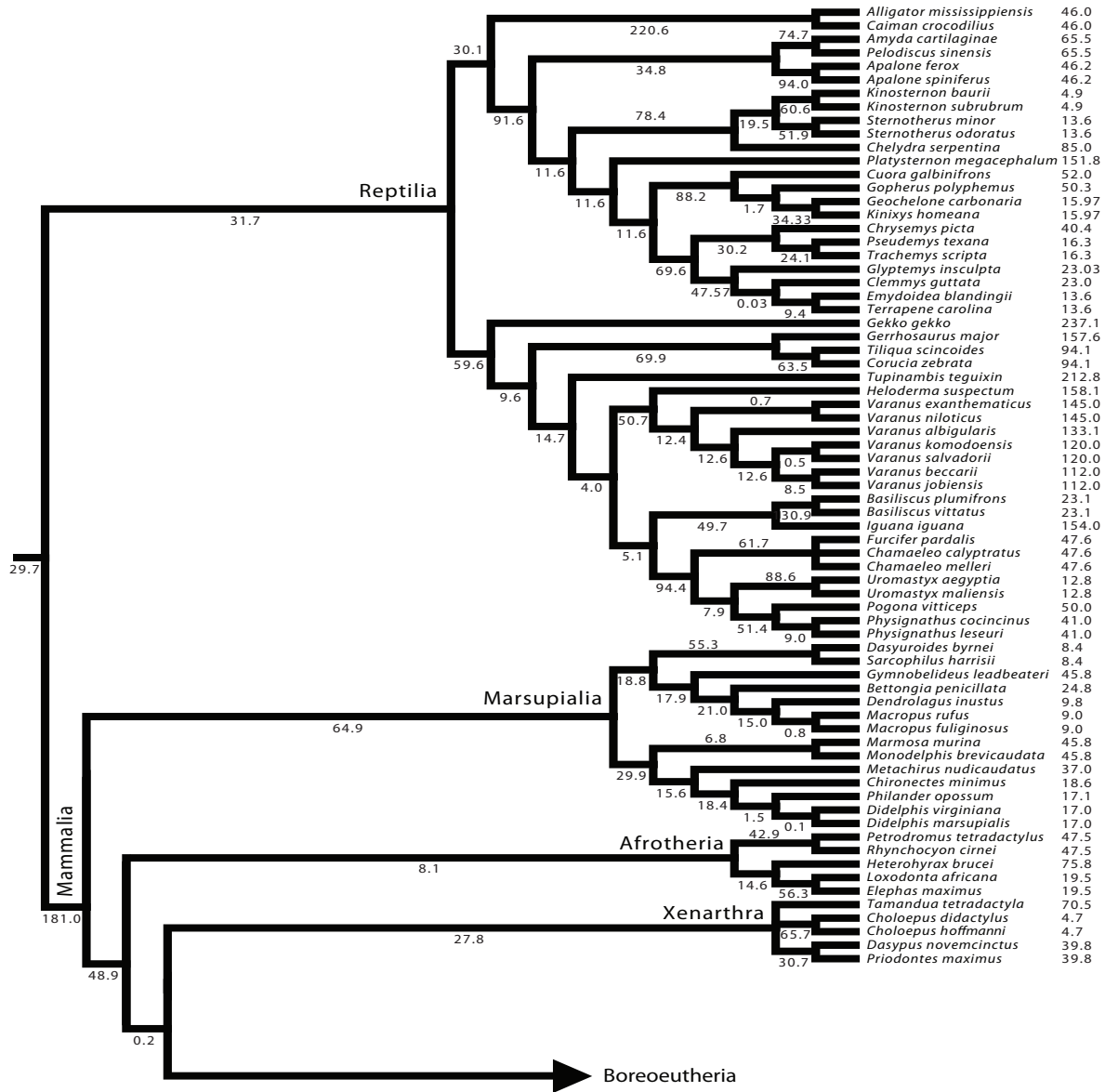
Ungulata	<i>Hippopotamus amphibius</i>	ROM 94513	1264000	422.5	182.5	467	188.5
Ungulata	<i>Ceratotherium simum</i>	ZMUC M4324	1900000	457	257	559	225
Ungulata	<i>Rhinoceros sondaicus</i>	Copenhagen	1435000	425	213	515	206
Ungulata	<i>Phacochoerus africanus</i>	AHR1985	90500		83		72
Ungulata	<i>Tapirus indicus</i>	ROM 94410	250000	257	109	330	115
Ungulata	<i>Tapirus terrestris</i>	ROM 66623	139300	235.5	94.5	307.5	106
Xenarthra	<i>Dasyurus novemcinctus</i>	ROM R2385	3077	55.16	22.25	83	29.9
Xenarthra	<i>Priodontes maximus</i>	ROM 46260	29500	125.05	68.25	167.7	78.5
Xenarthra	<i>Choloepus didactylus</i>	ROM 31160	6200	166.2	40.25	157.85	43.25
Xenarthra	<i>Choloepus hoffmanni</i>	ROM 89635	4500	140.65	32.75	133.45	34.5
Xenarthra	<i>Tamandua tetradactyla</i>	ROM 113857	5470	90.7	34.6	91.2	29.8
Reptilia	<i>Alligator mississippiensis</i>	ROM R4411	167830	201.2	88.5		86
Reptilia	<i>Caiman crocodilius</i>	ROM R6872	22050	91.75	37.3	117.75	43
Reptilia	<i>Physignathus cocincinus</i>	ROM R7460	259	33.15	8.05	48.7	10.1
Reptilia	<i>Physignathus leseuri</i>	ROM R7463	440	39.7	9.1	55.3	10.9
Reptilia	<i>Pogona vitticeps</i>	ROM R7400	511	34.65	9.05	38.7	9.5
Reptilia	<i>Uromastyx aegyptia</i>	ROM SD 107	610	46.7	14	50.57	16.1
Reptilia	<i>Uromastyx maliensis</i>	ROM R7867	512	30.7	9.55	33.85	10.2
Reptilia	<i>Chamaeleo calyptratus</i>	ROM R7875	199	33.75	7.05	33.65	6.5
Reptilia	<i>Chamaeleo melleri</i>	ROM R7977	258	42.7	8.65	43.65	9.5
Reptilia	<i>Furcifer pardalis</i>	ROM R7479	99	30.47	7.3	31.03	7.5
Reptilia	<i>Basiliscus plumifrons</i>	ROM R7455	199	31.2	7.55	49.15	9.5
Reptilia	<i>Basiliscus vittatus</i>	ROM R4660	112	22.2	5.95	40.85	7.5
Reptilia	<i>Gekko gekko</i>	ROM R7489	96	20.65	5.45	24.9	5.75
Reptilia	<i>Gerrhosaurus major</i>	ROM R3558	227	22.6	6.5	25.2	7.8
Reptilia	<i>Heloderma suspectum</i>	ROM R8142	406	35.85	10.25	37.15	10.85
Reptilia	<i>Iguana iguana</i>	ROM R5821	2700	68.8	20.25	82.7	22.75
Reptilia	<i>Corucia zebrata</i>	ROM R7868	374	36.05	10.15	36.5	10.95
Reptilia	<i>Tiliqua scincoides</i>	ROM R7535	243	27.16	7.75	25.97	8.1
Reptilia	<i>Tupinambis teguixin</i>	ROM R8380	1207	48.52	15	57.07	17.85
Reptilia	<i>Varanus albigularis</i>	ROM R8243	1358	52.9	16.8	60.8	18.6
Reptilia	<i>Varanus beccarii</i>	ROM R7483	133	34.3	7.25	36.6	8.6
Reptilia	<i>Varanus exanthematicus</i>	ROM R8034	5063	64.9	25	68.35	27.4
Reptilia	<i>Varanus jobiensis</i>	ROM R7950	1100	54.2	16.75	65.9	21
Reptilia	<i>Varanus komodoensis</i>	ZMUC R 4235	72000	141.6	62	173.4	67
Reptilia	<i>Varanus niloticus</i>	ROM R7287	8645	78.45	29.75	92.35	34
Reptilia	<i>Varanus salvatorii</i>	ROM R7926	4839	73.35	25.1	80.5	25.75
Reptilia	<i>Chelydra serpentina</i>	ROM R4101	5372	64.595	29.5	68.2	27.25
Reptilia	<i>Chrysemys picta</i>	ROM R7204	537	30.86	10	34.525	10
Reptilia	<i>Clemmys guttata</i>	ROM R1898	79	21.715	6.65	22.4	7
Reptilia	<i>Cuora galbinifrons</i>	ROM R5346	555	40.34	12.95	36.69	11.95
Reptilia	<i>Emydoidea blandingii</i>	ROM R3539	1588	52.55	15	56.155	16
Reptilia	<i>Glyptemys insculpta</i>	ROM R7991	766	44.37	12.45	46.87	13.15
Reptilia	<i>Pseudemys texana</i>	ROM R6766	185	31.17	9.05	35.65	10
Reptilia	<i>Terrapene carolina</i>	ROM R5214	460	33.76	11.85	37.2	11.45
Reptilia	<i>Trachemys scripta</i>	ROM R2083	1790	43.2	13.75	46.65	14.2
Reptilia	<i>Kinosternon baurii</i>	ROM R1877	121	17.08	7.25	17.5	6.4
Reptilia	<i>Kinosternon subrubrum</i>	ROM R2932	138	18.84	7	19.9	6.8
Reptilia	<i>Sternotherus minor</i>	ROM R7993	173	20.64	7.2	21.21	7
Reptilia	<i>Sternotherus odoratus</i>	ROM R7342	193	23.88	8	24.12	7

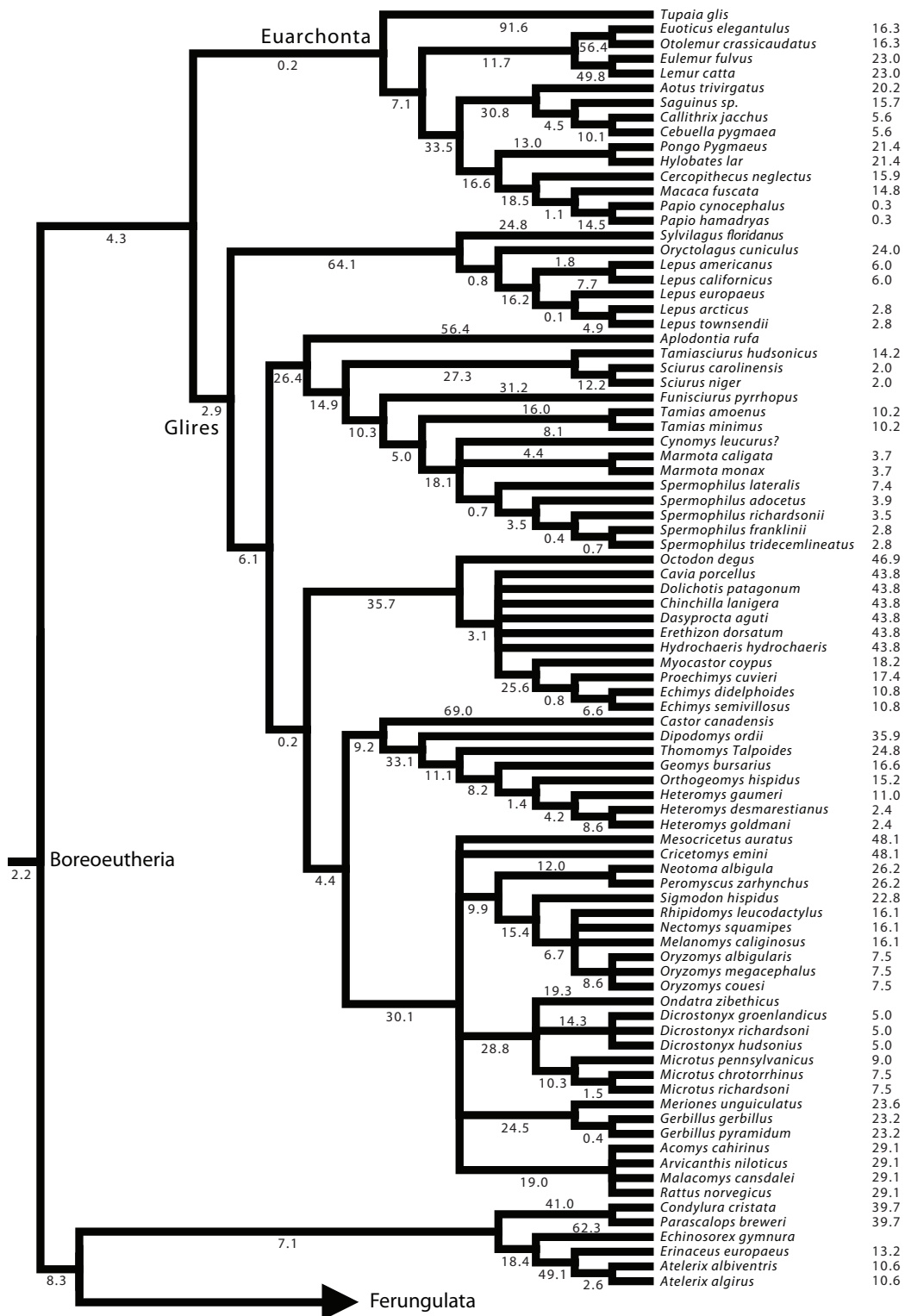
Reptilia	<i>Platysternon megacephalum</i>	ROM R5331	629	34.95	12.75	36.7	12
Reptilia	<i>Geochelone carbonaria</i>	ROM R8015	1181	52	19	43.72	15.65
Reptilia	<i>Gopherus polyphemus</i>	ROM R1915	2825	63.6	24	48.01	19.9
Reptilia	<i>Kinixys homeana</i>	ROM R7992	1485	51.99	17.9	44.39	15.95
Reptilia	<i>Amyda cartilaginea</i>	ROM R8016	962	39.38	16.35	39.68	14
Reptilia	<i>Apalone ferox</i>	ROM R7757	3836	58.56	22.25	61.12	23.6
Reptilia	<i>Apalone spiniferus</i>	ROM R2674	278	28.27	10.3	30.11	11
Reptilia	<i>Pelodiscus sinensis</i>	ROM R6026	1380.25	42.21	15.3	43.55	13.05
Amphibia	<i>Ambystoma tigrinum</i>	ROM R7713	59	15.3	6	16.3	4
Amphibia	<i>Ceratophrys cranwelli</i>	ROM R8421	129	23.3	8.65	27.8	8.45
Amphibia	<i>Litoria caerulea</i>	ROM R8261	51	18.5	6	30	5
Amphibia	<i>Rhinella schneideri</i>	ROM R7877	538	45.05	11.9	52.2	12.15
Amphibia	<i>Lepidobatrachus laevis</i>	ROM R8152	166.8	32.4	8.5	35.7	8.5
Amphibia	<i>Osteopilus septentrionalis</i>	ROM R2457	117	32.1	8.5	53.8	7.7
Amphibia	<i>Xenopus laevis</i>	ROM R7302	109.5	14.8	5.4	30	7.9
Amphibia	<i>Dyscophus guineti</i>	ROM R7295	76	19.5	6.6	28	6.2
Dinosaur Taxa							
Ornithischia	<i>Iguanodon bernissartensis</i>	IRSNB R51		337.5		490	
Ornithischia	<i>Corythosaurus casuarius</i>	ROM 845		237.5		365	
Ornithischia	<i>Protoceratops andrewsi</i>	MPC-D 100/504		64		86	
Ornithischia	<i>Styracosaurus albertensis</i>	AMNH 5372		280		365	
Ornithischia	<i>Triceratops horridus</i>	NSM PV 20379		345		436	
Ornithischia	<i>Stegosaurus mjosi</i>	SMA 0018		330		345	
Saurischia	<i>Diplodocus longus</i>	USNM 10865		410		490	
Saurischia	<i>Brachiosaurus brancai</i>	HMN SII		654		730	

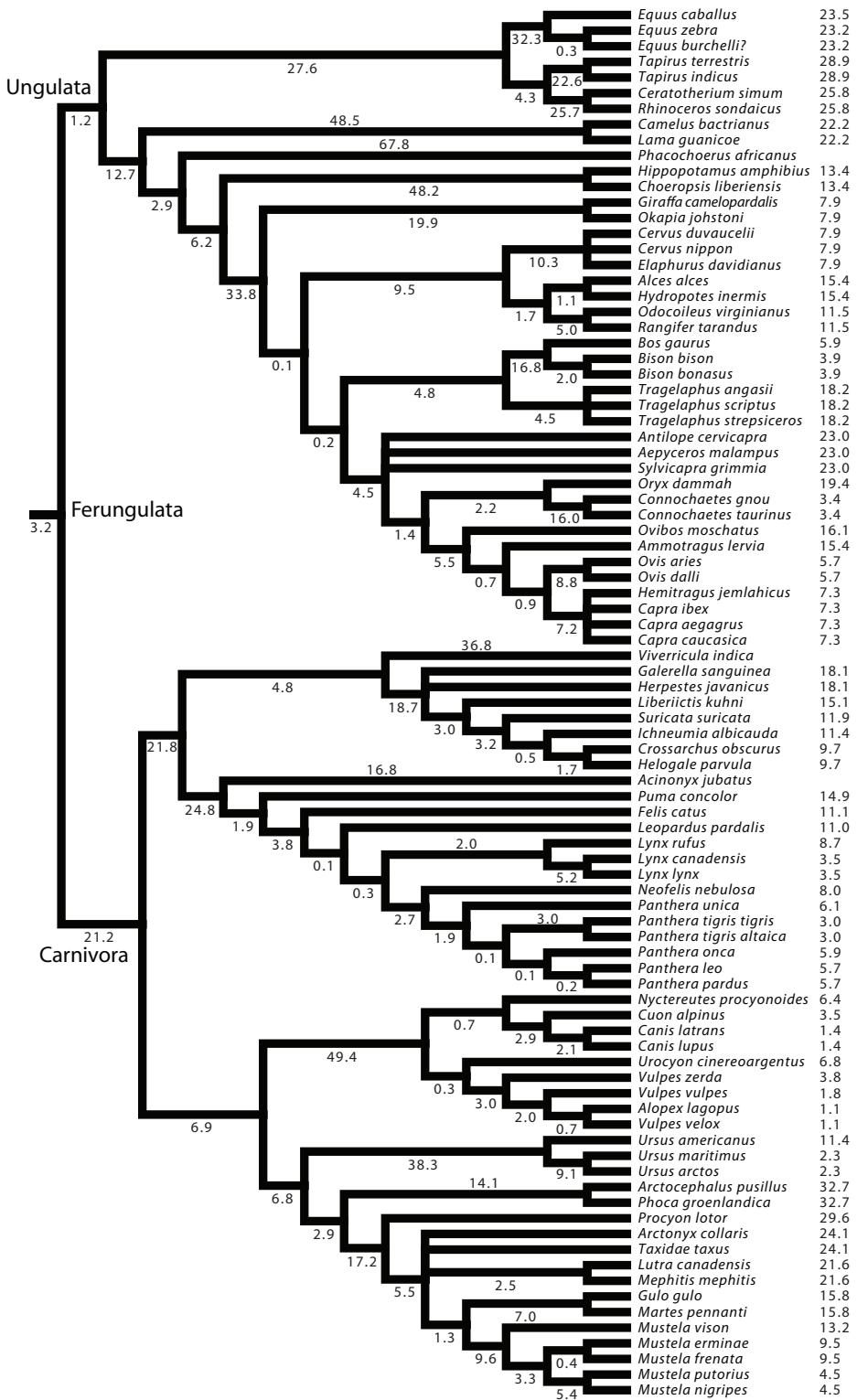
Legend

- * from Christiansen (2005)
- AHR1985 from Anderson *et al.* (1985)

Appendix 2. Phylogenetic tree of mammalian and reptilian taxa included in Chapter 1
(Campione and Evans, 2012). Topology is based on multiple published analyses mentioned
in the text. Numbers indicate the branch lengths used in this study, measured in millions of
years. Terminal branch lengths are most often given next to the species name.







Appendix 3. Limb measurement and body mass data in extant birds. Table of measurements of all the extant taxa used in Chapter 2.

Higher Clade	Species	SP #	BM	FL	FC	TL	TC
Anseriformes	<i>Anas discors</i>	ROM 80560	450	36.55	11	57.8	9
Anseriformes	<i>Anser caerulescens</i>	ROM 128667	2495	71.3	24	127.7	21
Anseriformes	<i>Anser indicus</i>	ROM 90956	2177	74.15	25.75	133.05	21
Anseriformes	<i>Anser rossii</i>	ROM 95694	1615	61.8	21.25		
Anseriformes	<i>Branta canadensis</i>	ROM 115311	5630	89.15	30	163.5	26.25
Anseriformes	<i>Cygnus buccinator</i>	ROM 33734	9000	119.2	44.15	218.5	38
Charadriiformes	<i>Calidris alpina</i>	ROM 123374	72.2	23.15	9		8
Charadriiformes	<i>Calidris canutus</i>	ROM 152718	139	31.3	9.3		
Charadriiformes	<i>Cephus grylle</i>	ROM 126414	489	37.2	13	59.9	11.25
Charadriiformes	<i>Himantopus leucocephalus</i>	ROM 102232	225	35.68	10.2	121.24	9.4
Charadriiformes	<i>Himantopus mexicanus</i>	ROM 150807	163	33.11	9.5	116.88	9
Charadriiformes	<i>Larus minutus</i>	ROM 124006	115.3	22.65	9.25	50.8	8
Charadriiformes	<i>Uria aalge</i>	ROM 109942	1020.3	47.85	15	83.7	12.5
Charadriiformes	<i>Vanellus armatus</i>	ROM 114673	150	33.75	11.5	86.3	11
Ciconiiformes	<i>Ardeola striata</i>	ROM 150928	245.8	49.3	12.5	79.5	11.5
Ciconiiformes	<i>Ciconia episcopus</i>	ROM 96598	1871.1	77.05	31.75	218.15	23.5
Ciconiiformes	<i>Ephippiorhynchus senegalensis</i>	ROM 35467	4210	112.62	43.6	365.5	35
Ciconiiformes	<i>Eudocimus albus</i>	ROM 112456	690	74.15	21.95	146.8	19.4
Ciconiiformes	<i>Ixobrychus exilis</i>	ROM 156801	87.2	41.1	8.5	64.9	8
Ciconiiformes	<i>Platalea alba</i>	ROM 157311	1440	80.26	23.4	188.25	21.4
Ciconiiformes	<i>Threskiornis aethiopicus</i>	ROM 124083	1247	67.18	18.3	142.05	16.95
Columbiformes	<i>Columba oenas</i>	ROM 122191	283.5	39.5	13	53.5	12
Columbiformes	<i>Streptopelia tranquebarica</i>	ROM 125565	79	24.3	9	31.9	8.5
Coraciiformes	<i>Bycanistes subcylindricus</i>	ROM 126588	1360.8	76.2	26.5	105.4	21.5
Cuculiformes	<i>Coccyzus americanus</i>	ROM 31822	95.1	29.8	10	41.7	9
Cuculiformes	<i>Coccyzus melacoryphus</i>	ROM 158342	53	26.9	9	37.6	8
Cuculiformes	<i>Geococcyx californiana</i>	ROM 128876	308	56.5	15.05	85.73	13
Falconiformes	<i>Accipiter gentilis</i>	ROM 158425	1010	85.3	24	110.35	20
Falconiformes	<i>Aquila chrysaetos</i>	ROM 72072	6577.1	133.7	44	172.5	37.35
Falconiformes	<i>Buteo platypterus</i>	ROM 74193	530	55.75	18.1	79.6	16.75
Falconiformes	<i>Buteogallus anthracinus</i>	ROM 109238	690	79.1	23	114.1	20
Falconiformes	<i>Falco sparverius</i>	ROM 159786	130.5	37.55	10.5	50.1	10.25
Falconiformes	<i>Haliaeetus leucocephalus</i>	ROM 105446	4309	118.2	41	154.4	33
Falconiformes	<i>Melierax gabar</i>	ROM 121031	220	48.05	12.85	66	11.25
Falconiformes	<i>Sagittarius serpentarius</i>	ROM 78897	3175.1	109.5	38.5	285	31.5
Galliformes	<i>Alectoris graeca</i>	ROM 29173	515	59.28	16.2	79.17	13.1
Galliformes	<i>Argusianus argus</i>	ROM 102133	1580	86.49	27.3	127.08	19.05
Galliformes	<i>Chrysolophus amherstiae</i>	ROM 124082	682	76.31	19.85		
Galliformes	<i>Dendragapus obscurus</i>	ROM 146117	1321	75.25	21.5	95.25	17.25

Galliformes	<i>Lophophorus impejanus</i>	ROM 29223	765.4	94.7	23	125.75	20.75
Galliformes	<i>Pavo cristatus</i>	ROM 105480	6945.6	120.55	38.75	200	31
Galliformes	<i>Phasianus colchicus</i>	ROM 111948	1226.3	84.97	21.3	111.85	18
Galliformes	<i>Phasianus versicolor</i>	ROM 111947	1543.4	90.75	25.5	120.9	22
Galliformes	<i>Tetraogallus himalayensis</i>	ROM 157320	1450	93.2	28	128.77	23.3
Galliformes	<i>Tympanuchus cupido</i>	ROM 148226	846	65.75	16.25		
Galliformes	<i>Tympanuchus phasianellus</i>	ROM 80796	940	70	18.5		
Gruiformes	<i>Bugeranus carunculatus</i>	ROM 124447	4989.5	141.85	39.25	364.5	39.45
Gruiformes	<i>Grus</i>	ROM 96150	6550	143.45	39.25	375	37.25
Pelecaniformes	<i>Pelecanus onocrotalus</i>	ROM 102334	8530	108.3	38.5	186	40.5
Pelecaniformes	<i>Phalacrocorax penicillatus</i>	ROM 138102	2360	61.4	26	125.1	21.4
Pelecaniformes	<i>Sula bassana</i>	ROM 94356	2891.7	72.35	24	105.35	21.75
Psittaciformes	<i>Cyanoramphus novaezelandiae</i>	ROM 102174	55.7	27.45	10.25	43.65	9
Psittaciformes	<i>Lorius lory</i>	ROM 157426	187.1	39.5	11	53.8	9.5
Sphenisciformes	<i>Megadyptes antipodes</i>	ROM 157401	4989.5	84.6	29.5	125.05	25
Strigiformes	<i>Aegolius funereus</i>	ROM 74337	169.6	36.95	11.75	48.7	11
Strigiformes	<i>Asio flammeus</i>	ROM 34389	370	57.8	14	83.8	13.25
Strigiformes	<i>Asio otus</i>	ROM 109101	396.9	57.8	14.5	85.15	12.5
Strigiformes	<i>Bubo bubo</i>	ROM 125641	1924.4	94.15	26.25	136.35	25.25
Strigiformes	<i>Bubo virginianus</i>	ROM 159789	1880.7	85.15	24.5	123.7	22.9
Strigiformes	<i>Nyctea scandiaca</i>	ROM 156270	1788.2	87.5	24.5	116.8	21.5
Strigiformes	<i>Otus asio</i>	ROM 102336	241	42.5	11.5	60.15	11
Struthioniformes	<i>Casuarius casuarius</i>	AHR1985	36571		94		
Struthioniformes	<i>Dromaius nocae</i> <i>hollandiae</i>	AHR1985	40667		95		
Struthioniformes	<i>Pterocnemia pennata</i>	ROM 106235	17746.8	209	71		
Struthioniformes	<i>Struthio camelus</i>	ROM 102298	139026.1	321	143	538	109
Tinamiformes	<i>Crypturellus boucardi</i>	ROM 112832	460	55.49	14	80.94	12.4
Tinamiformes	<i>Crypturellus cinnamomeus</i>	ROM 104348	350	52.82	13	72.27	11.4
Tinamiformes	<i>Crypturellus variegatus</i>	ROM 125757	260	41.97	11.1	63.76	9.9
Tinamiformes	<i>Eudromia elegans</i>	ROM 128924	1769	58.82	16.05	81.95	13.2
Tinamiformes	<i>Nothoprocta cinerascens</i>	ROM 28511	470	52.98	14.7	69.76	12.1

Appendix 4. Dataset of body mass estimates of non-avian dinosaurs derived from volumetric-density models.

Higher Clade	Species	Model Reference	Year	Modeled Specimen	Method	Body Mass	Measured Specimen	Match	Gait	C _{H+F}	C _H	C _F
Ankylosauria	<i>Ankylosaurus magniventris</i>	Paul	1997	AMNH 5214	(1)	3900000	AMNH 5214	X	quad	678	315	363
Ankylosauria	<i>Ankylosaurus magniventris</i>	Seebacher	2001		(2)	1719200	AMNH 5214		quad	678	315	363
Ankylosauria	<i>Edmontonia</i>	Colbert	1962	Palaeoscincus Type	(1)	3472000	ROM 1215		quad	446	209	237
Ankylosauria	<i>Saichania</i>	Seebacher	2001	MPC-D 100/1305	(2)	1417200	MPC-D 100/1305	X	quad	321	155	166
Ankylosauria	<i>Sauropelta</i>	Paul	1997	AMNH 3030	(1)	2100000	AMNH 3032		quad	573	256	317
Ankylosauria	<i>Sauropelta edwardsi</i>	Paul	1997	AMNH 3030	(1)	1990000	AMNH 3032		quad	573	256	317
Ankylosauria	<i>Sauropelta edwardsi</i>	Seebacher	2001	AMNH 3035/3056	(2)	902900	AMNH 3032		quad	573	256	317
Ceratopsia	<i>Centrosaurus apertus</i>	Paul	1997	YPM 2015	(1)	1470000	YPM 2015	X	quad	535	249	286
Ceratopsia	<i>Centrosaurus apertus</i>	Seebacher	2001	YPM 2015	(2)	1079700	YPM 2015	X	quad	535	249	286
Ceratopsia	<i>Chasmosaurus</i>	Seebacher	2001	CMN 2280	(2)	1658700	CMN 2280		quad	605	270	335
Ceratopsia	<i>Chasmosaurus belli</i>	Paul	1997	ROM 843	(1)	2060000	ROM 843	X	quad	656	293	363
Ceratopsia	<i>Chasmosaurus russelli</i>	Paul	1997	CMN 2280	(1)	1500000	CMN 2280	X	quad	605	270	335
Ceratopsia	<i>Leptoceratops gracilis</i>	Paul	1997	CMN 8889	(1)	93000	CMN 8889	X	quad	202	87	115
Ceratopsia	<i>Montanoceratops</i>	Paul	1997	AMNH 5464	(1)	170000	MOR 300		quad	208.8	86.3	122.5
Ceratopsia	<i>Pentaceratops sternbergii</i>	Paul	1997	OMNH 10165	(1)	4700000	OMNH 10165	X	quad	912	400.5	511.5
Ceratopsia	<i>Psittacosaurus mongoliensis</i>	Paul	1997	AMNH 6253	(1)	14000	AMNH 6537		bip			57
Ceratopsia	<i>Psittacosaurus mongoliensis</i>	Seebacher	2001	AMNH 6253	(2)	12100	AMNH 6537		bip			57
Ceratopsia	<i>Styracosaurus</i>	Colbert	1962		(1)	3686000	CMN 344		quad	645	280	365
Ceratopsia	<i>Styracosaurus</i>	Paul	1997	AMNH 5372	(1)	1800000	CMN 344		quad	645	280	365
Ceratopsia	<i>Triceratops</i>	Colbert	1962		(1)	8478000	BHI 6220		quad	930	410	520
Ceratopsia	<i>Triceratops</i>	Paul	1997	USNM 4842	(1)	6400000	NSM PV 20379		quad	781	345	436
Ceratopsia	<i>Triceratops horridus</i>	Seebacher	2001	BSP1964 I458 USNM 4842	(2)	4964000	NSM PV 20379		quad	781	345	436
Ornithopoda	<i>Bactrosaurus johnsoni</i>	Paul	1997	AMNH 6553	(1)	1200000	AMNH 6553	X	quad	475	136	339
Ornithopoda	<i>Bactrosaurus johnsoni</i>	Seebacher	2001	AMNH 6553	(2)	1588900	AMNH 6553	X	quad	475	136	339
Ornithopoda	<i>Brachylophosaurus canadensis</i>	Paul	1997	MOR 794	(1)	4150000	MOR 794	X	quad	661	221	440
Ornithopoda	<i>Campitosaurus dispar</i>	Paul	1997	USNM 5818	(1)	513000	YPM 1880		quad	389	114	275
Ornithopoda	<i>Campitosaurus prestwichii</i>	Seebacher	2001	OUM J.3303	(2)	268400	YPM 1880		quad	389	114	275
Ornithopoda	<i>Corythosaurus</i>	Colbert	1962		(1)	3820000	ROM 845		quad	602.5	237.5	365
Ornithopoda	<i>Corythosaurus</i>	Paul	1997	AMNH 5240	(1)	2800000	ROM 845		quad	602.5	237.5	365

Higher Clade	Species	Model Reference	Year	Modeled Specimen	Method	Body Mass	Measured Specimen	Match	Gait	C _{H+F}	C _H	C _F
Ornithopoda	<i>Corythosaurus casuarius</i>	Seebacher	2001	AMNH 5240	(2)	3078500	ROM 845		quad	602.5	237.5	365
Ornithopoda	<i>Corythosaurus intermedius</i>	Paul	1997	ROM 845	(1)	2510000	ROM 845	X	quad	602.5	237.5	365
Ornithopoda	<i>Dollodon bampingi</i>	Paul	1997	IRSNB 1551	(1)	1100000	IRSNB R57	X	quad	437	167	270
Ornithopoda	<i>Dryosaurus altus</i>	Paul	1997	YPM 1876	(1)	103000	YPM 1876	X	bip			133
Ornithopoda	<i>Dryosaurus altus</i>	Seebacher	2001	Several	(2)	104300	YPM 1876		bip			133
Ornithopoda	<i>Dryosaurus lettowvorbecki</i>	Paul	1997	HMN ??	(1)	45000	HMN Display	X	bip			111
Ornithopoda	<i>Edmontosaurus annectens</i>	Colbert	1962	AMNH 5730	(1)	3071000	AMNH 5730	X	quad	762.8	250.5	512.3
Ornithopoda	<i>Edmontosaurus annectens</i>	Paul	1997	AMNH 5730	(1)	3200000	AMNH 5730	X	quad	762.8	250.5	512.3
Ornithopoda	<i>Edmontosaurus annectens</i>	Seebacher	2001	YPM 1190 USNM 2414	(2)	4964000	SM R 4050		quad	727	267	460
Ornithopoda	<i>Edmontosaurus annectens</i>	Seebacher	2001	AMNH 5730	(2)	7594400	AMNH 5730	X	quad	762.8	250.5	512.3
Ornithopoda	<i>Edmontosaurus regalis</i>	Paul	1997	CMN 8399	(1)	2900000	CMN 8399	X	quad	470	235	235
Ornithopoda	<i>Edmontosaurus regalis</i>	Paul	1997	ROM 801	(1)	3670000	ROM 801	X	quad	771	291	480
Ornithopoda	<i>Fruitadens haagarorum</i>	Butler et al	2009	LACM 115727	(3)	740	LACM 115727	X	bip			19.6
Ornithopoda	<i>Gasparinisaura</i>	Paul	1997	MUCPv-215	(1)	13000	MUCPv-219		bip			55
Ornithopoda	<i>Gasparinisaura cincosalensis</i>	Seebacher	2001	MUCPv-208	(2)	980	MUCPv-219		bip			55
Ornithopoda	<i>Hypacrosaurus altispinus</i>	Paul	1997	CMN 8501	(1)	2640000	CMN 8501	X	quad	617	222	395
Ornithopoda	<i>Hypsilophodon foxii</i>	Seebacher	2001	BMNH R196	(2)	1400	BMNH R196	X	bip			55
Ornithopoda	<i>Iguanodon bernisartensis</i>	Colbert	1962	IRSNB R51	(1)	4514000	IRSNB R51	X	quad	827.5	337.5	490
Ornithopoda	<i>Iguanodon bernisartensis</i>	Alexander	1985	IRSNB R51	(1)	5400000	IRSNB R51	X	quad	827.5	337.5	490
Ornithopoda	<i>Iguanodon bernisartensis</i>	Paul	1997	IRSNB R51	(1)	3200000	IRSNB R51	X	quad	827.5	337.5	490
Ornithopoda	<i>Iguanodon bernisartensis</i>	Gunga et al	1999	IRSNB R51	(5)	8400000	IRSNB R51	X	quad	827.5	337.5	490
Ornithopoda	<i>Iguanodon bernisartensis</i>	Henderson	1999	IRSNB R51	(3)	3790000	IRSNB R51	X	quad	827.5	337.5	490
Ornithopoda	<i>Iguanodon bernisartensis</i>	Seebacher	2001	IRSNB R51	(2)	3775700	IRSNB R51	X	quad	827.5	337.5	490
Ornithopoda	<i>Lambeosaurus lambei</i>	Paul	1997	ROM 1218	(1)	2430000	ROM 1218	X	quad	592.5	225	367.5
Ornithopoda	<i>Lesothosaurus</i>	Paul	1997	BMNH RUB17	(1)	2400	BMNH RUB17	X	bip			43
Ornithopoda	<i>Maiasaura peeblesorum</i>	Paul	1997	ROM 44770	(1)	2250000	ROM 44770	X	quad	615	205	410
Ornithopoda	<i>Olorotitan</i>	Paul	1997	AEHM 2/845	(1)	3100000	IRSNB cast	X	quad	643	248	395
Ornithopoda	<i>Parasaurolophus</i>	Seebacher	2001	ROM 768	(2)	5056800	ROM 768	X	quad	680	260	420
Ornithopoda	<i>Parasaurolophus walkeri</i>	Paul	1997	ROM 768	(1)	2600000	ROM 768	X	quad	680	260	420
Ornithopoda	<i>Parksosaurus</i>	Paul	1997	ROM 804	(1)	43000	ROM 804	X	bip			103
Ornithopoda	<i>Prosauropodus</i>	Paul	1997	ROM 787	(1)	2000000	ROM 787	X	quad	580	225	355
Ornithopoda	<i>Shantugosaurus</i>	Paul	1997	PMNH 1	(1)	13000000	composite		quad	1084	404	680

Higher Clade	Species	Model Reference	Year	Modeled Specimen	Method	Body Mass	Measured Specimen	Match	Gait	C _{H+F}	C _H	C _F
Ornithopoda	<i>Shantugosaurus giganteus</i>	Paul	1997	PMNH 5	(1)	9900000	composite		quad	1084	404	680
Ornithopoda	<i>Shantugosaurus giganteus</i>	Seebacher	2001		(2)	22467100	composite		quad	1084	404	680
Ornithopoda	<i>Tenontosaurus</i>	Paul	1997	OMNH 11	(1)	597000	OMNH 11	X	quad	386.5	159	227.5
Ornithopoda	<i>Tenontosaurus</i>	Seebacher	2001	OMNH 11	(2)	242900	OMNH 11	X	quad	386.5	159	227.5
Ornithopoda	<i>Thescelosaurus neglectus</i>	Paul	1997	USNM 7757	(1)	86000	USNM 7757	X	quad	215.7	70.7	145
Ornithopoda	<i>Thescelosaurus neglectus</i>	Seebacher	2001	USNM 7757	(2)	7900	USNM 7757	X	quad	215.7	70.7	145
Ornithopoda	<i>Tsintaosaurus</i>	Paul	1997	PMNH V725	(1)	2500000	IVPP mount		quad	675	250	425
Pachycephalosauria	<i>Homalocephale</i>	Paul	1997	GI SPS 100/51	(1)	36000	MPC-D 100/1201	X	bip			83
Pachycephalosauria	<i>Homalocephale</i>	Seebacher	2001	MPC-D 100/1201	(2)	73700	MPC-D 100/1201	X	bip			83
Pachycephalosauria	<i>Stegoceras</i>	Seebacher	2001	UALVP 2	(2)	26700	UALVP 2	X	bip			68
Prosauropoda	<i>Anchisaurus sinensis</i>	Paul	1997	YPM 1883	(1)	20000	YPM 1883	X	bip			70
Prosauropoda	<i>Plateosaurus engelhardti</i>	Henderson	2006	HMN XXV	(3)	279000	HMN Skelett 25	X	bip		139.5	236.5
Prosauropoda	<i>Plateosaurus engelhardti</i>	Gunga et al	2007	GPIT1	(4)	630000	HMN Skelett 25		bip		139.5	236.5
Prosauropoda	<i>Plateosaurus engelhardti</i>	Gunga et al	2007	GPIT1	(4)	912000	HMN Skelett 25		bip		139.5	236.5
Prosauropoda	<i>Plateosaurus engelhardti</i>	Mallison	2010	GPIT1	(4)	660240	HMN Skelett 25		bip		139.5	236.5
Prosauropoda	<i>Plateosaurus engelhardti</i>	Mallison	2010	GPIT1	(4)	692640	HMN Skelett 25		bip		139.5	236.5
Prosauropoda	<i>Plateosaurus engelhardti</i>	Mallison	2010	GPIT1	(4)	782070	HMN Skelett 25		bip		139.5	236.5
Prosauropoda	<i>Plateosaurus engelhardti</i>	Mallison	2010	GPIT1	(4)	749340	HMN Skelett 25		bip		139.5	236.5
Prosauropoda	<i>Plateosaurus engelhardti</i>	Mallison	2010	GPIT1	(4)	837500	HMN Skelett 25		bip		139.5	236.5
Prosauropoda	<i>Plateosaurus longiceps</i>	Paul	1997	HMN XXV	(1)	440000	HMN Skelett 25	X	bip		139.5	236.5
Prosauropoda	<i>Riojasaurus</i>	Paul	1997	PVL 3808	(1)	500000	PVL 3808	X	bip		229	285
Prosauropoda	<i>Riojasaurus</i>	Paul	1997	PVL 3808	(1)	820000	PVL 3808	X	bip		229	285
Prosauropoda	<i>Riojasaurus</i>	Seebacher	2001		(2)	3038700	PVL 3808		bip		229	285
Sauropoda	<i>Alamosaurus</i>	Paul	1997	TMM 41541	(1)	16300000	TMM 41541	X	quad	1401	661	740
Sauropoda	<i>Amargasaurus cazaui</i>	Paul	1997	MACN-N 15	(1)	3800000	CMN cast	X	quad	884	362.5	521.5
Sauropoda	<i>Amargasaurus cazaui</i>	Seebacher	2001	MACN-N 15	(2)	6852900	CMN cast	X	quad	884	362.5	521.5
Sauropoda	<i>Amargasaurus cazaui</i>	Mazzetta et al	2004	MACN-N 15	(1)	2600000	CMN cast	X	quad	884	362.5	521.5
Sauropoda	<i>Apatosaurus excelsius</i>	Gregory	1905	AMNH mount	(1)	34200000	YPM 1980		quad	1310	580	730
Sauropoda	<i>Apatosaurus excelsius</i>	Colbert	1962	AMNH mount	(1)	27869000	YPM 1980		quad	1310	580	730
Sauropoda	<i>Apatosaurus excelsius</i>	Colbert	1962	AMNH mount	(1)	32418000	YPM 1980		quad	1310	580	730
Sauropoda	<i>Apatosaurus excelsius</i>	Paul	1998	YPM 1980	(1)	19100000	YPM 1980	X	quad	1310	580	730
Sauropoda	<i>Apatosaurus louisae</i>	Alexander	1989	CM 3018	(1)	35000000	CM 3018	X	quad	1480	640	840
Sauropoda	<i>Apatosaurus louisae</i>	Christiansen	1997	CM 3018	(1)	19500000	CM 3018	X	quad	1480	640	840

Higher Clade	Species	Model Reference	Year	Modeled Specimen	Method	Body Mass	Measured Specimen	Match	Gait	C _{H+F}	C _H	C _F
Sauropoda	<i>Apatosaurus louisae</i>	Paul	1997	CM 3018	(1)	17500000	CM 3018	X	quad	1480	640	840
Sauropoda	<i>Apatosaurus louisae</i>	Seebacher	2001	CM 3018	(2)	22407200	CM 3018	X	quad	1480	640	840
Sauropoda	<i>Apatosaurus louisae</i>	Mazzetta et al	2004	CM 3018	(1)	20600000	CM 3018	X	quad	1480	640	840
Sauropoda	<i>Apatosaurus louisae</i>	Henderson	2004	CM 3018	(3)	17273000	CM 3018	X	quad	1480	640	840
Sauropoda	<i>Apatosaurus louisae</i>	Henderson	2006	CM 3018	(3)	16381000	CM 3018	X	quad	1480	640	840
Sauropoda	<i>Barosaurus</i>	Paul	1997	AMNH 6341	(1)	11600000	AMNH 6341	X	quad	989	443	546
Sauropoda	<i>Barosaurus</i>	Seebacher	2001	AMNH 6341	(2)	20039500	AMNH 6341	X	quad	989	443	546
Sauropoda	<i>Brachiosaurus altithorax</i>	Paul	1997	FMNH P 25107	(1)	35000000	FMNH P 25107	X	quad	1613	737	876
Sauropoda	<i>Brachiosaurus altithorax</i>	Seebacher	2001	FMNH P 25107	(2)	28264600	FMNH P 25108	X	quad	1613	737	876
Sauropoda	<i>Camarasaurus</i>	Paul	1997	AMNH 5761	(1)	23000000	GMNH 101		quad	1102	472	630
Sauropoda	<i>Camarasaurus lentus</i>	Paul	1997	CM 11393	(1)	14200000	CM 11393	X	quad	1170	498	672
Sauropoda	<i>Camarasaurus lentus</i>	Henderson	2004	CM 11393	(3)	12177000	CM 11393	X	quad	1170	498	672
Sauropoda	<i>Camarasaurus lentus</i>	Henderson	2006	CM 11393	(3)	12262000	CM 11393	X	quad	1170	498	672
Sauropoda	<i>Dicraeosaurus</i>	Seebacher	2001	HMN on display	(2)	4421500	HMN on display	X	quad	851.5	340	511.5
Sauropoda	<i>Dicraeosaurus hansemanni</i>	Christiansen	1997	HMN on display	(1)	5400000	HMN on display	X	quad	851.5	340	511.5
Sauropoda	<i>Dicraeosaurus hansemanni</i>	Paul	1997	HMN on display	(1)	5000000	HMN on display	X	quad	851.5	340	511.5
Sauropoda	<i>Dicraeosaurus hansemanni</i>	Gunga et al	2002	HMN on display	(5)	12800000	HMN on display	X	quad	851.5	340	511.5
Sauropoda	<i>Dicraeosaurus hansemanni</i>	Mazzetta et al	2004	HMN on display	(1)	5700000	HMN on display	X	quad	851.5	340	511.5
Sauropoda	<i>Dicraeosaurus hansemanni</i>	Henderson	2006	HMN on display	(3)	4349000	HMN on display	X	quad	851.5	340	511.5
Sauropoda	<i>Diplodocus carnegiei</i>	Colbert	1962		(1)	10562000	AMNH 6341		quad	989	443	546
Sauropoda	<i>Diplodocus carnegiei</i>	Alexander	1985	CM 84	(1)	18500000	AMNH 6341		quad	989	443	546
Sauropoda	<i>Diplodocus carnegiei</i>	Christiansen	1997	CM 84	(1)	15200000	AMNH 6341		quad	989	443	546
Sauropoda	<i>Diplodocus carnegiei</i>	Paul	1997	CM 84	(1)	11400000	AMNH 6341		quad	989	443	546
Sauropoda	<i>Diplodocus carnegiei</i>	Henderson	1999	CM 84	(3)	13421000	AMNH 6341		quad	989	443	546
Sauropoda	<i>Diplodocus carnegiei</i>	Seebacher	2001	CM 84	(2)	19654600	AMNH 6341		quad	989	443	546
Sauropoda	<i>Diplodocus carnegiei</i>	Gunga et al	2002	CM 84	(5)	32440000	AMNH 6341		quad	989	443	546
Sauropoda	<i>Diplodocus carnegiei</i>	Mazzetta et al	2004	CM 84	(1)	16000000	AMNH 6341		quad	989	443	546
Sauropoda	<i>Diplodocus carnegiei</i>	Henderson	2004	CM 84	(3)	12099000	AMNH 6341		quad	989	443	546
Sauropoda	<i>Diplodocus carnegiei</i>	Henderson	2006	AMNH 6341	(3)	11449000	AMNH 6341	X	quad	989	443	546
Sauropoda	<i>Euhelopus zdanskyi</i>	Paul	1997	PMU R233	(1)	3400000	PMU 233, 234	X	quad	733	358	375
Sauropoda	<i>Euhelopus zdanskyi</i>	Mazzetta et al	2004	PMU 233	(1)	3800000	PMU 233, 234	X	quad	733	358	375
Sauropoda	<i>Europasaurus</i>	Paul	1997	composite	(1)	760000	composite	X	quad	390	190	200
Sauropoda	<i>Futalognkosaurus</i>	Paul	1997	MUCPv-323	(1)	50000000			quad	1443	643	800

Higher Clade	Species	Model Reference	Year	Modeled Specimen	Method	Body Mass	Measured Specimen	Match	Gait	C _{H+F}	C _H	C _F
Sauropoda	<i>Giraffatitan brancai</i>	Janensch	1935	HMN SKII	(1)	32000000	HMN SKII	X	quad	1384	654	730
Sauropoda	<i>Giraffatitan brancai</i>	Janensch	1935	HMN SKII	(1)	25000000	HMN SKII	X	quad	1384	654	730
Sauropoda	<i>Giraffatitan brancai</i>	Alexander	1985	HMN SKII	(1)	46600000	HMN SKII	X	quad	1384	654	730
Sauropoda	<i>Giraffatitan brancai</i>	Gunga et al	1995	HMN SKII	(5)	74420000	HMN SKII	X	quad	1384	654	730
Sauropoda	<i>Giraffatitan brancai</i>	Christiansen	1997	HMN SKII	(1)	37400000	HMN SKII	X	quad	1384	654	730
Sauropoda	<i>Giraffatitan brancai</i>	Paul	1997	HMN SKII	(1)	31500000	HMN SKII	X	quad	1384	654	730
Sauropoda	<i>Giraffatitan brancai</i>	Christian	1999	HMN SKII	(1)	63000000	HMN SKII	X	quad	1385	654	731
Sauropoda	<i>Giraffatitan brancai</i>	Mazzetta et al	2004	HMN SKII	(1)	39500000	HMN SKII	X	quad	1384	654	730
Sauropoda	<i>Giraffatitan brancai</i>	Henderson	2004	HMN SKII	(3)	25789000	HMN SKII	X	quad	1384	654	730
Sauropoda	<i>Giraffatitan brancai</i>	Henderson	2006	HMN SKII	(3)	25922000	HMN SKII	X	quad	1384	654	730
Sauropoda	<i>Giraffatitan brancai</i>	Gunga et al	2008	HMN SKII	(4)	38000000	HMN SKII	X	quad	1384	654	730
Sauropoda	<i>Giraffatitan brancai</i>	Sellers et al	2012	HMN SKII	(6)	23200000	HMN SKII	X	quad	1384	654	730
Sauropoda	<i>Jobaria</i>	Paul	1997	MNN TIG3	(1)	16300000	SAM Cast	X	quad	991.5	411.5	580
Sauropoda	<i>Jobaria tiguidensis</i>	Henderson	2006	MNN TIG 3-5	(3)	22448000	SAM Cast	X	quad	991.5	411.5	580
Sauropoda	<i>Mamenchisaurus hochuanensis</i>	Christiansen	1997	IVPP specimens	(1)	14300000	LACM ??	quad	1068.5	509	559.5	
Sauropoda	<i>Opisthocoelicaudia</i>	Paul	1997	ZPAL MgD-I/84	(1)	8400000	ZPAL MgD-I/84	X	quad	1227	542	685
Sauropoda	<i>Opisthocoelicaudia skarzynskii</i>	Seebacher	2001	ZPAL MgD-I/84	(2)	10522200	ZPAL MgD-I/84	X	quad	1227	542	685
Sauropoda	<i>Opisthocoelicaudia skarzynskii</i>	Mazzetta et al	2004	ZPAL MgD-I/84	(1)	8400000	ZPAL MgD-I/84	X	quad	1227	542	685
Sauropoda	<i>Saltasaurus</i>	Paul	1997	PVL 4017-79	(1)	2480000	PVL 4017-80	X	quad	726	341	385
Stegosauria	<i>Anchisaurus sinensis</i>	Seebacher	2001		(2)	84000	YPM 1883	bip				70
Stegosauria	<i>Gigantospinosaurus</i>	Paul	1997	ZDM 0019	(1)	680000	ZDM 0019	X	quad	513	235	278
Stegosauria	<i>Kentrosaurus</i>	Paul	1997	HMN MTD	(1)	670000	HMN on display	X	quad	449	207	242
Stegosauria	<i>Kentrosaurus</i>	Seebacher	2001	HMN	(2)	321100	HMN on display	X	quad	449	207	242
Stegosauria	<i>Stegosaurus ungulatus</i>	Alexander	1985	YPM 1853	(1)	3100000	YPM 1853	X	quad	745	355	390
Stegosauria	<i>Stegosaurus ungulatus</i>	Paul	1997	YPM 1853	(1)	3830000	YPM 1853	X	quad	745	355	390
Theropoda	<i>Acrocanthosaurus atokensis</i>	Henderson	2003	NCSM 14345	(3)	5672000	NCSM 14345	X	bip			426
Theropoda	<i>Acrocanthosaurus atokensis</i>	Bates et al	2009	NCSM 14345	(4)	6177040	NCSM 14345	X	bip			426
Theropoda	<i>Afrovenator abakensis</i>	Seebacher	2001	UC OBA 1	(2)	826600	UC OBA 1	X	bip			275
Theropoda	<i>Albertosaurus sarcophagus</i>	Christiansen	1997	TMP 81.10.1	(1)	1170000	TMP 81.10.1	X	bip			316.5
Theropoda	<i>Allosaurus fragilis</i>	Colbert	1962		(1)	2087000	AMNH 275	bip				355
Theropoda	<i>Allosaurus fragilis</i>	Gunga et al	1999		(5)	3300000	AMNH 275	bip				355
Theropoda	<i>Allosaurus fragilis</i>	Seebacher	2001	USNM 4734	(2)	952000	MOR 693	bip				274.5
Theropoda	<i>Allosaurus fragilis</i>	Bates et al	2009	MOR 693	(4)	1500910	MOR 693	X	bip			274.5

Higher Clade	Species	Model Reference	Year	Modeled Specimen	Method	Body Mass	Measured Specimen	Match	Gait	C _{H+F}	C _H	C _F
Theropoda	<i>Anserimimus planinya</i> chus	Christiansen	1998	GI 100/300	(1)	170000	GI 100/300	X	bip			145
Theropoda	<i>Avimimus portentosus</i>	Seebacher	2001	PIN 3907-1/3907-3	(2)	21400	PIN 3907-1/3907-3	X	bip			52.8
Theropoda	<i>Ceratosaurus nasicornis</i>	Henderson	2003	USNM 4735	(3)	647500	USNM 4735	X	bip			267
Theropoda	<i>Coelophysis bauri</i>	Henderson	2003	AMNH 7223	(3)	12140	AMNH 7223	X	bip			49
Theropoda	<i>Deltadromeus agilis</i>	Seebacher	2001	SGM-Din2	(2)	1048900	SGM-Din2	X	bip			191
Theropoda	<i>Dilophosaurus wetherilli</i>	Christiansen	1998	UCMP 37302	(1)	325000	UCMP 37302	X	bip			173
Theropoda	<i>Dilophosaurus wetherilli</i>	Henderson	2003	UCMP 37302	(3)	355200	UCMP 37302	X	bip			173
Theropoda	<i>Dromiceiomimus brevitertius</i>	Christiansen	1998	CMN 12228	(1)	160000	ROM 852		bip			127.5
Theropoda	<i>Dryptosaurus aquilunguis</i>	Christiansen	1998	TMP 84.181.2 (Cast of ANSP 9995/10006)	(1)	1170000	TMP 84.181.2 (Cast of ANSP 9995/10006)	X	bip			276
Theropoda	<i>Elaphrosaurus bambergi</i>	Christiansen	1998	HMN Gr. S. 38-44	(1)	245000	HMN Gr. S. 38-44	X	bip			167
Theropoda	<i>Eoraptor lunensis</i>	Seebacher	2001	PVSJ 512	(2)	2700	PVSJ 512	X	bip			62
Theropoda	<i>Gallimimus bullatus</i>	Christiansen	1998	GI 100/11	(1)	490000	GI 100/11	X	bip			216
Theropoda	<i>Gallimimus bullatus</i>	Seebacher	2001	GI 100/11	(2)	585700	GI 100/11	X	bip			216
Theropoda	<i>Giganotosaurus carolinii</i>	Seebacher	2001	MUCPv-CH-1	(2)	6594800	MUCPv-CH-1	X	bip			515
Theropoda	<i>Giganotosaurus carolinii</i>	Therrien & Henderson	2007	MUCPv-CH-1	(3)	13807000	MUCPv-CH-1	X	bip			515
Theropoda	<i>Gorgosaurus libratus</i>	Seebacher	2001	AMNH 5458	(2)	2465000	AMNH 5458	X	bip			357
Theropoda	<i>Gorgosaurus libratus</i>	Henderson	2003	AMNH 5458	(3)	2795000	AMNH 5458	X	bip			357
Theropoda	<i>Herrerasaurus ischigualastensis</i>	Henderson	2003	Several	(3)	643300	PVL 2566		bip			165.5
Theropoda	<i>Herrerasaurus ischigualastensis</i>	Seebacher	2001	Several	(2)	347800	PVL 2566		bip			165.5
Theropoda	<i>Mei long</i>	Therrien & Henderson	2007	IVPP V12733	(3)	70	IVPP V12733	X	bip			20.7
Theropoda	<i>Ornitholestes hermanni</i>	Christiansen	1998		(1)	16500	TMP 66.2.3 (cast of AMNH 619)		bip			71
Theropoda	<i>Ornitholestes hermanni</i>	Seebacher	2001	AMNH 619	(2)	13500	TMP 66.2.3 (cast of AMNH 619)	X	bip			71
Theropoda	<i>Ornithomimus edmontonensis</i>	Christiansen	1998	ROM 851	(1)	155000	ROM 851	X	bip			110
Theropoda	<i>Sauornitholestes langstoni</i>	Christiansen	1998	TMP 88.121.39	(1)	22500	TMP 88.121.39	X	bip			63
Theropoda	<i>Sinornithoides youngi</i>	Seebacher	2001	IVPP V9612	(2)	2200	IVPP V9612	X	bip			34.6
Theropoda	<i>Sinornithoides youngi</i>	Therrien & Henderson	2007	IVPP V9612	(3)	950	IVPP V9613	X	bip			35.6
Theropoda	<i>Sinraptor dongi</i>	Christiansen	1998		(1)	1700000	TMP 93.115.1 (cast of IVPP 87001)		bip			283
Theropoda	<i>Sinraptor dongi</i>	Seebacher	2001	IVPP 10600	(2)	1009000	TMP 93.115.1 (cast of IVPP 87001)		bip			283
Theropoda	<i>Sinraptor dongi</i>	Therrien & Henderson	2007	IVPP 10600	(3)	1136890	TMP 93.115.1 (cast of IVPP 87001)		bip			283
Theropoda	<i>Struthiomimus altus</i>	Christiansen	1998	AMNH 5339	(1)	175000	AMNH 5339	X	bip			136
Theropoda	<i>Suchomimus tenerensis</i>	Seebacher	2001	MNN GDF 500	(2)	3816100	MNN GDF 500	X	bip			408

Higher Clade	Species	Model Reference	Year	Modeled Specimen	Method	Body Mass	Measured Specimen	Match	Gait	C_{H+F}	C_H	C_F
Theropoda	<i>Suchomimus tenerensis</i>	Therrien & Henderson	2007	MNN GDF 500	(3)	5206560	MNN GDF 500	X	bip			408
Theropoda	<i>Syntarsus rhodesiensis</i>	Seebacher	2001	QG 1	(2)	13800	QG 1	X	bip			56
Theropoda	<i>Tyrannosaurus rex</i>	Colbert	1962	CM 9380 AMNH 5027	(1)	6895000	CM 9380	X	bip			534
Theropoda	<i>Tyrannosaurus rex</i>	Alexander	1985	CM 9380 AMNH 5027	(1)	7400000	CM 9380	X	bip			534
Theropoda	<i>Tyrannosaurus rex</i>	Paul	1997	BHI 3033	(1)	5622000	BHI 3033	X	bip			505
Theropoda	<i>Tyrannosaurus rex</i>	Paul	1997	MOR 555	(1)	5355000	MOR 555	X	bip			520
Theropoda	<i>Tyrannosaurus rex</i>	Paul	1997	CM 9380 AMNH 5027	(1)	5670000	CM 9380	X	bip			534
Theropoda	<i>Tyrannosaurus rex</i>	Paul	1997	FMNH PR 2081	(1)	6140000	FMNH PR 2081	X	bip			579
Theropoda	<i>Tyrannosaurus rex</i>	Christiansen	1998	AMNH 5027	(1)	6300000	CM 9380		bip			534
Theropoda	<i>Tyrannosaurus rex</i>	Henderson	1999	MOR 555	(3)	7224000	MOR 555	X	bip			520
Theropoda	<i>Tyrannosaurus rex</i>	Henderson	1999	CM 9380 AMNH 5027	(3)	7908000	CM 9380	X	bip			534
Theropoda	<i>Tyrannosaurus rex</i>	Seebacher	2001	CM 9380 AMNH 5027	(2)	6650900	CM 9380	X	bip			534
Theropoda	<i>Tyrannosaurus rex</i>	Henderson	2003	FMNH PR 2081	(3)	10200000	FMNH PR 2081	X	bip			579
Theropoda	<i>Tyrannosaurus rex</i>	Hutchinson et al	2007	MOR 555	(4)	5450000	MOR 555	X	bip			520
Theropoda	<i>Tyrannosaurus rex</i>	Hutchinson et al	2007	MOR 555	(4)	5074000	MOR 555	X	bip			520
Theropoda	<i>Tyrannosaurus rex</i>	Hutchinson et al	2007	MOR 555	(4)	6113000	MOR 555	X	bip			520
Theropoda	<i>Tyrannosaurus rex</i>	Hutchinson et al	2007	MOR 555	(4)	6583000	MOR 555	X	bip			520
Theropoda	<i>Tyrannosaurus rex</i>	Bates et al	2009	BHI 3033	(4)	7654710	BHI 3033	X	bip			505
Theropoda	<i>Tyrannosaurus rex</i>	Bates et al	2009	MOR 555	(4)	6071820	MOR 555	X	bip			520
Theropoda	<i>Tyrannosaurus rex</i>	Hutchinson et al	2011	BHI 3033	(4)	8385000	BHI 3033	X	bip			505
Theropoda	<i>Tyrannosaurus rex</i>	Hutchinson et al	2011	MOR 555	(4)	8272000	MOR 555	X	bip			520
Theropoda	<i>Tyrannosaurus rex</i>	Hutchinson et al	2011	CM 9380 AMNH 5027	(4)	10979000	CM 9380	X	bip			534
Theropoda	<i>Tyrannosaurus rex</i>	Hutchinson et al	2011	FMNH PR 2081	(4)	13996000	FMNH PR 2081	X	bip			579

Legend:

quad assumed quadrupedal stance

bip assumed bipedal stance

C_{F+H} Combined minimum humeral and femoral circumference

C_F Minimum femoral circumference

C_H Minimum humeral circumference

(1) Physical reconstruction and water displacement methods

(2) ‘Polynomial’ method of Seebacher (2001)

(3) 3D mathematical slicing method of Henderson (1999)

(4) 3D specimen scanning techniques

(5) Photogrammetry

(6) Minimum convex hull method of Sellers *et al.* (2012)

Appendix 5. Limb measurements of ornithopod dinosaurs used to derive body mass estimates.

Ornithopod Species	Source	SP#	Gait	hl	hc	hap	hml	ul	uc	rl	rc	fl	fc	fap	fml	tl	tc	fil	fic	MTHII	SKL	
<i>Aristastus gaglarsoni</i>	EAF	MOR 1155	quad													975	318			400		
<i>Altirhinus kurzanovi</i>	Norman 1998	PIN 3386/8	quad	595			92															
<i>Anurosaurus riabinini</i>	PG	PIN? 1/283	quad	550	240																	
<i>Anabisetia saldiviae</i>	DCE	MCF-PVPH-74	bip							212	74.5					230						
<i>Aralosaurus tuberiferus</i>	Rozhdestvensky 1968	PIN 2229/1	quad	300																210	650	
<i>Arenysaurus ardevoli</i>	Pereda-Suberbiola et al 2009	MPZ2008/336 MPZ2008/337	quad	300							711											
<i>Bactrosaurus johnsoni</i>	NEC/MTC	AMNH 6553	quad		136						796	339	103			655	246					
<i>Barilium dawsoni</i>	DCE	BMNH M2848	quad								905	460										
<i>Barsboldia sicinskii</i>	Prieto-Marquez 2011	Unspecified	quad													1400						
<i>Bolong yixianensis</i>	Wu et al 2010	YHZ-001	quad			237		198								510	448					
<i>Brachylophosaurus canadensis</i>	NEC	MOR 794	quad	221							440											
<i>Callovosaurus leedsi</i>	RJB	BMNH R1993	bip								300	101	29	26								
<i>Campitosaurus dispar</i>	NEC	ROM 5090	quad	370	150	39.8	47.5	255	109	222	84	630	275	80.3	107.9	520	203	480	102	199.6	260.5	
<i>Changchunsaurus parvus</i>	Butler et al 2011	JLUM L0403-j-Zn2	bip																138	67	115	
<i>Charonosaurus jiayinensis</i>	Godefroit et al 2000	Referred Specimens	quad								1350											
<i>Claosaurus agilis</i>	Lull & Wright 1942 MTC	YPM 1190	quad	360.5		46		330.5		271		697		99		572					216	
<i>Corythosaurus casuarinus</i>	Brown 1916 MTC	AMNH 5240	quad	585			660				1080		130		1000							
<i>Corythosaurus intermedius</i>	NEC MTC Evans 2010	ROM 845	quad	536.3	237.5	69.2	79.5	707.5	161	635	146	1058.8	365	108	86.6	940	370	955	160	370	702	
<i>Dryosaurus altus</i>	NEC MTC	YPM 1876	bip	191	63	18.8	20.8	150.2	43	146.2	40	350	138	40.3	42.1	393	115					
<i>Dysalotosaurus lettowvorbecki</i>	MTC	BMNH R12777	bip									343	134	36	45							
<i>Edmontosaurus annectens</i>	NEC MTC	AMNH 5730	quad	680.5	250.5	64.7	84.7	698	182.5	621.5	160	1147.7	512.3	140		968	381	929	179	407.5	1175	
<i>Edmontosaurus regalis</i>	NEC	CMN 2289	quad	697.5	270	97.3	64.5	775.5	186	673	167	1242.5	532	146.5	147	1174	405	1070	193		1065	
<i>Elrhazosaurus nigeriensis</i>	MTC	MHN GDF 332	bip								224	90	26.8	26.3								
<i>Eolambia caroljonesae</i>	Kirkland 1998	CEUM 5212	quad			520																
<i>Equijubus normani</i>	You et al 2003	IVPP V12534	quad																	570		
<i>Gasparinisaura cincosaltensis</i>	DCE	MUCPv-219	bip										55									
<i>Gideonmantellia amosanjuanae</i>	Ruiz-Omenaca et al 2012	MPG-PBCH	bip								112.9		13.2	11.5	132		112.3		60.9			
<i>Gilmoreosaurus</i>	DCE	AMNH FARB	quad	315	142		370	112	309	86	695	280				615	234					

Ornithopod Species	Source	SP#	Gait	hl	hc	hap	hml	ul	uc	rl	rc	fl	fc	fap	fml	tl	tc	fil	fic	MTHII	SKL	
<i>mongolensis</i>		30728 AMNH FARB 30741																				
<i>Gryposaurus latidens</i>	NEC MTC	AMNH 5465	quad	758	251	98.8						1120	397.5	137.8		1074	376					
<i>Gryposaurus notabilis</i>	NEC MTC	AMNH 5350	quad	506	208	57.7						1135	445	128.6		1012	358					
<i>Haya griva</i>	Makovicky et al 2011	IGM 100/2015	bip	86		10			66			131		17.5		155				93		
<i>Hippodraco scutodens</i>	McDonald et al 2010	UMNH VP 20208	quad	323																210		
<i>Hypacosaurus altispinus</i>	DCE Evans 2010	CMN 8501	quad	510	222	92		665	627.5			1074	395			995	350	932		350	710	
<i>Hypacosaurus stebingeri</i>	MTC	MOR 773	quad									1190	448	100.1	142.4							
<i>Hypsilophodon foxi</i>	NEC RBJB	BMNH R192	bip	147	50							173	70	22.2	21.2							
<i>Iguanodon bernissartensis</i>	NEC	IRSNB R51	quad	818	337.5	89.9	116.3	655	216	495	212.5	1038.8	490	144.1	153.7	852.5	388	845	155	342.5		
<i>Jeholosaurus shangyuensis</i>	NEC	IVPP V???	bip									135.5	50.2			160	41	151	19	75.5		
<i>Jinzhousaurus yangi</i>	Wang et al 2011	IVPP V12691	quad	420		58.5			265			625										
<i>Kangnasaurus coetzei</i>	NEC	SAM-PK-2731	bip									383	162									
<i>Koreanosaurus boseongensis</i>	Huh et al 2011	KDRC BB2	bip	215		26																
<i>Kritosaurus navajovius</i>	Lull & Wright 1942	AMNH 5799	quad									1045				943				363	1065	
<i>Kundurosaurus nagornyi</i>	Goderfroit et al 2012	AENM 2/904	quad						607													
<i>Lambeosaurus clavifrons</i>	Lull & Wright 1942 Evans 2010 NEC	CMN 8703	quad	520		660		616		1050		114.6		1045		960	147			748		
<i>Lambeosaurus lambei</i>	NEC MTC Evans 2010	ROM 1218	quad	522.5	225	74.8	62.4	681.5	172.5	305	138	1052.5	367.5	104.7	116.1	900	338	905	136	378	747	
<i>Lambeosaurus magnicristatus</i>	MTC Evans 2010	TMP 66.4.1	quad	482		53.5	60.7	665				1000		102.8		1010				371	733	
<i>Lophorhothon atopus</i>	MTC	FMNH P27383	quad									616	211	45	78.3	574	180	537		237.5		
<i>Magnapaulia laticaudus</i>	Prieto-Marquez 2012	LACM 17712	quad	803		128.5	85.1					1280										
<i>Maiasaura peeblesorum</i>	NEC Taquet & Russell 1999	ROM 44770	quad	580	205	56	63.2	615	145.5	565	121.5	1020	410						985	151	410	690
<i>Mantellisaurus atherfieldensis</i>	NEC MTC	IRSNB R57	quad	435	167	43.8	61	390	112	335	110	735	270	75.3	95.4	677.5	240.5	642	109	266.5		
<i>Mochlodon seussi</i>	Osi et al 2012	PIUW 2349/35	bip									194				181						
<i>Mochlodon vorosi</i>	Osi et al 2012	MTM 2012.23.1	bip	156								240										
<i>Muttaburrasaurus langdoni</i>	MTC	BMNH R.9604	quad									990	460	108.9	168.8							
<i>Nanyangosaurus zhugeii</i>	Xu et al. 2000	IVPP V11821	quad	265		41	243					517		57		548		503		193		
<i>Olorotitan arharensis</i>	DCE	Cast at IRSNB	quad	595	248							1090	395			1120		1020		369		

Ornithopod Species	Source	SP#	Gait	hl	hc	hap	hml	ul	uc	rl	rc	f1	fc	fap	fml	tl	tc	fil	fic	MTHII	SKL
<i>Orodromeus makelai</i>	MTC	MOR 473	bip	105.1	38	9.1	13.7	75.2	20			166.1	65	15.9	20.4	202.9	51.8				
<i>Oryctodromeus cubicularis</i>	Varricchio et al 2007	MOR 1636a	bip	157			16												254		
<i>Ouranosaurus nigriensis</i>	Taquet 1976	MNN GDF 300/381	quad	555			50					830.7		86.2	99.7	767.3				286.6	732
<i>Pararhabdodon isonensis</i>	Casanovas et al 1999	IPS SRA 15	quad	404			65														
<i>Parasaurolophus cyrtocristatus</i>	DCE MTC	FMNH P27393	quad	555	241	69.5	88.8	670	193.5	585		1072.5	445	124.5	142.4	975	366	890		395	
<i>Parasaurolophus walkeri</i>	NEC MTC Evans 2010	ROM 768	quad	520	265	83.2	75.5	559	189.5	494.5	142.5	1045	430	146.8	98.7					745	
<i>Parksosaurus warreni</i>	CMB NEC	ROM 804	bip	218	72	21.6	21	140.2		127		270	103	34	30	312.5	83	298	37	151	
<i>Probactrosaurus gobiensis</i>	Norman 2002	PIN 2232/18-9	quad									750		79	114						
<i>Probactrosaurus mazongshanensis</i>	NEC	IVPP V12060	quad	345	134.5			351		325	73	794	309			630	216				
<i>Prosaurolophus maximus</i>	NEC MTC	ROM 787	quad	540	225	48.8	71.9	546	166	478.5	130.5	1000	355	107.9	90.1	825.5	310	865	134	313.5	872.6
<i>Protohadros byrdi</i>	Head 1998	SMU 74582	quad																	700	
<i>Rhabdodon priscum</i>	Lapparent 1947	MNHN uncat.	quad	370			330		320		550		92		500		470				
<i>Sahaliyania elunchunorum</i>	Godefroit et al 2008	GMH W453	quad	408		63															
<i>Sauropodus angustirostris</i>	Maryanska & Osmolska 1984	PIN 551-8	quad	600								1200				1000				330	
<i>Sauropodus osborni</i>	Brown 1912, 1913	AMNH 5220	quad	610			680					1150	509			1020				370	1010.5
<i>Secernosaurus koernerri</i>	MTC	MACN-N 02	quad									790	335	80.7	109.2						
<i>Shantungosaurus giganteus</i>	NEC	ZJZ 1-1626 ZJZ 1-1610	quad	965	404							1700	680								
<i>Talenkauen santacruzensis</i>	Novas et al 2004	MPM-10001	quad	339				292				455				456		452			
<i>Tanios sinensis</i>	Wiman 1929	IVPP ???	quad	513				565				1000				945		910			
<i>Telmatosaurus transylvanicus</i>	Weishampel & Norman 1995	MAFI v.10338	quad									731			104					440	
<i>Tenontosaurus dossi</i>	Winkler et al 1997	FWMSH 93B1	quad	466	33.6		359		341		557		84.6	565		520		226			
<i>Tenontosaurus tilletti</i>	Ostrom 1970	OU 11	quad	441	159		340		330		575	227.5			535		510		215		
<i>Tethyshadros insularis</i>	Dalla Vecchia 2009	SC 57021	quad	292			285		277		420				550				193	475	
<i>Theiophytalia kerri</i>	Brill & Carpenter 2007	YPM 1887	quad																	466	
<i>Thescelosaurus assiniboiensis</i>	CMB	RSM 1225.1	bip									304.5	121			282	105	261		125	
<i>Thescelosaurus neglectus</i>	MTC	AMNH 5891	bip	315	108	28.3	38.7					448	183	56.3	61.2						
<i>Tsintaosaurus spinorhinus</i>	NEC	IVPP Mount IVPP V729	quad	685	250							1148	425			1120	378	160		380	
<i>Uteodon aploanoecetes</i>	Gilmore 1925	CM 11337	quad	227			160		143		395				360		320				
<i>Valdosaurus canaliculatus</i>	MTC	MNHN GDF 332	bip									224	90	26.8	26.3						

Ornithopod Species	Source	SP#	Gait	hl	hc	hap	hml	ul	uc	rl	rc	fl	fc	fap	fml	tl	tc	fil	fic	MTIII	SKL
<i>Willinakage salitratensis</i>	Juarez Valieri et al 2010	MPCA-Pv SM 33	quad	348.6			50.5														
<i>Wulagasaurus dongi</i>	Godefroit et al 2008	GMH W184	quad	522		76															
<i>Xuvulong yueluni</i>	You et al 2011	GSGM-F00001	quad																	380	
<i>Zalmoxes robustus</i>	MTC	BMNH 3814	bip	210	83	23.3	27	181.8	60			321	125	31	43						
<i>Zalmoxes shqiperorum</i>	MTC	BMNH 4900	bip									309	124	30.8	41.9						

Legend for Appendix 5:

Personal Observations: CMB, Caleb M. Brown; DCE, David C. Evans; EAF, Elizabeth A. Freeman; MTC, Matthew T. Carrano; NEC, Nicolás E. Campione; PG, Pascal Godefroit; RBJB, Roger, B. J. Benson.

Abbreviations: bip, biped; fap, femoral anteroposterior diameter; fc, femoral circumference; fic, fibular circumference; fil, fibular length; fl, femoral length; fml, femoral mediolateral diameter; hap, humeral anteroposterior diameter; hc, humeral circumference; hl, humeral length; hml, humeral mediolateral diameter; MTIII, metatarsal III length; quad, quadruped; rc, radial circumference; rl, radial length; SKL, skull length; tc, tibial circumference; tl, tibial length; uc, ulnar circumference; ul, ulnar length.

Appendix 6. Ages and body mass estimates of ornithopod dinosaurs. Ages are in millions of years, and body mass estimates are based on the phylogenetically corrected regression between combined humeral and femoral circumference and body mass (Chapter 1; Campione and Evans, 2012).

Ornithopod Species	Lower Age	Upper Age	Midpoint Age	\log_{10} BM	BM	BM+25%	BM-25%
<i>Acristavus gagoslarseni</i>	83.5	70.6	79.43	6.534012	3419889.6	4275888	2563891.2
<i>Altirhinus kurzanovi</i>	108.8	99.6	104.2	6.654845	4516948.3	5647540.5	3386356.1
<i>Amurosaurus riabinini</i>	69	65.5	67.25	6.669004	4666632.8	5834691	3498574.6
<i>Anabisetia saldiviae</i>	92.1	89.3	90.7	4.473437	29746.6	37192.2	22301
<i>Aralosaurus tuberiferus</i>	85.8	80.6	83.2	5.775589	596470.5	745767.1	447173.9
<i>Arenysaurus ardevoli</i>	69	65.5	67.25	6.052828	1129349.6	1412025.8	846673.4
<i>Bactrosaurus johnsoni</i>	93.5	83.5	88.5	6.274614	1881976.5	2353035.2	1410917.8
<i>Barilium dawsoni</i>	140.2	136.4	138.3	6.764024	5807960.9	7261693.5	4354228.3
<i>Barsboldia sicinskii</i>	76.4	69	72.7	7.208805	16173538.6	20221775.3	12125301.9
<i>Bolong yixianensis</i>	128.3	112	120.15	5.74665	558020.7	697693.3	418348.1
<i>Brachylophosaurus canadensis</i>	83.5	70.6	77.05	6.669835	4675572.8	5845868.7	3505276.9
<i>Callovosaurus leedsi</i>	163.2	162.5	162.85	4.837419	68773.2	85987.1	51559.3
<i>Camptosaurus dispar</i>	155.7	145.5	150.6	6.141583	1385425.3	1732197.3	1038653.3
<i>Changchunsaurus parvus</i>	106.4	96	101.2	4.919795	83137.2	103946.4	62328
<i>Charonosaurus jiayinensis</i>	69	65.5	67.25	6.978494	9516867.4	11898939.3	7134795.5
<i>Claosaurus agilis</i>	87	80.6	83.8	6.110003	1288258.9	1610710.1	965807.7
<i>Corythosaurus casuarius</i>	76.5	75	76.2	6.690882	4907748.6	6136158.1	3679339.1
<i>Corythosaurus intermedius</i>	76.5	75	76.2	6.559002	3622444.3	4529142.1	2715746.5
<i>Dryosaurus altus</i>	155.7	145.5	150.6	5.210745	162459.6	203123.2	121796
<i>Dysalotosaurus lettowvorbecki</i>	155.7	150.8	153.25	5.175565	149818.3	187317.8	112318.8
<i>Edmontosaurus annectens</i>	69	65.5	67.25	6.841159	6936797.6	8673078	5200517.2
<i>Edmontosaurus regalis</i>	72	71	71.5	6.901096	7963357.4	9956585.8	5970129
<i>Elrhazosaurus nigeriensis</i>	125	99.6	112.3	4.699502	50061.3	62591.6	37531
<i>Eolambia caroljonesa</i>	112	93.5	97.5	6.472546	2968561	3711591.8	2225530.2
<i>Equijubus normani</i>	130	112	121	6.308303	2033777	2542831.4	1524722.6
<i>Gasparinisaura cincosalensis</i>	83.5	76.4	79.95	4.110477	12896.7	16124.7	9668.7
<i>Gideonmantellia amosanjuanae</i>	130	125	127.5	3.84812	7048.9	8813.2	5284.6
<i>Gilmoreosaurus mongolensis</i>	93.5	83.5	88.5	6.13311	1358659.1	1698731.5	1018586.7
<i>Gryposaurus latidens</i>	83.5	70.6	80	6.647	4436087.3	5546440	3325734.6
<i>Gryposaurus notabilis</i>	76.5	75	76.2	6.655271	4521378.9	5653080	3389677.8
<i>Haya griva</i>	85.8	83.5	84.65	4.021291	10502.5	13131.3	7873.7
<i>Hippodraco scutodens</i>	127	121	124	5.869472	740409.8	925734.4	555085.2
<i>Hypacrosaurus altispinus</i>	70.6	69	69	6.587445	3867633.8	4835702.5	2899565.1
<i>Hypacrosaurus stebingeri</i>	83.5	70.6	74	6.733002	5407565.2	6761078.8	4054051.6
<i>Hypsilophodon foxii</i>	128.3	125	126.65	4.398918	25056.4	31328	18784.8
<i>Iguanodon bernissartensis</i>	130	112	121	6.938533	8680266.9	10852937.7	6507596.1
<i>Jeholosaurus shangyuanensis</i>	128.3	112	120.15	4.001256	10029	12539.3	7518.7
<i>Jinzousaurus yangi</i>	125	112	118.5	6.097748	1252414.9	1565894.3	938935.5
<i>Kangnasaurus coetzeei</i>	100.5	65.5	83	5.402523	252651.9	315890.7	189413.1
<i>Koreanosaurus boseongensis</i>	85.8	70.6	78.2	5.239309	173503.7	216931.7	130075.7
<i>Kritosaurus navajovius</i>	75.4	70.6	74.25	6.661029	4581719.8	5728524.3	3434915.3

<i>Kundurosaurus nagornyi</i>	69	65.5	67.25	6.82762	6723877.7	8406864.3	5040891.1
<i>Lambeosaurus clavintialis</i>	76.5	75	75.5	6.560631	3636057.4	4546162.6	2725952.2
<i>Lambeosaurus lambei</i>	76.5	75	75.5	6.538984	3459264.2	4325118	2593410.4
<i>Lambeosaurus magnicristatus</i>	76.5	75	75.5	6.539405	3462618.2	4329311.5	2595924.9
<i>Lophorhothon atopus</i>	83.5	80.6	82.05	5.850108	708121.6	885364.4	530878.8
<i>Magnapaulia laticaudus</i>	75.4	70.6	73.3	6.985477	9671125.4	12091808.1	7250442.7
<i i="" maiasaura="" peeblesorum<=""></i>	83.5	70.6	77.05	6.583562	3833205.2	4792656.5	2873753.9
<i>Mantellisaurus atherfieldensis</i>	136.4	125	130.7	6.174886	1495842.5	1870251.9	1121433.1
<i>Mochlodon seussi</i>	83.5	80.6	82.05	4.483893	30471.5	38098.5	22844.5
<i>Mochlodon vorosi</i>	85.8	83.5	84.65	4.737668	54659.8	68341.1	40978.5
<i>Muttaburrasaurus langdoni</i>	106.4	96	101.2	6.764024	5807960.9	7261693.5	4354228.3
<i>Nanyangosaurus zhugeii</i>	112	99.6	105.8	5.730107	537164.3	671616.5	402712.1
<i>Olorotitan arharensis</i>	69	65.5	67.25	6.636813	4333242.8	5417853.5	3248632.1
<i>Orodromeus makelai</i>	83.5	65.5	74.5	4.310282	20430.6	25544.4	15316.8
<i>Oryctodromeus cubicularis</i>	99.6	93.5	96.55	4.72782	53434.3	66808.9	40059.7
<i>Ouranosaurus nigeriensis</i>	125	99.6	112.3	6.458803	2876092.3	3595978.2	2156206.4
<i>Pararhabdodon isonensis</i>	70.6	65.5	68.05	6.1553	1429881.8	1787781.2	1071982.4
<i>Parasaurolophus cyrtocristatus</i>	75.4	70.6	75	6.714237	5178889.1	6475165	3882613.2
<i>Parasaurolophus walkeri</i>	76.5	75	76.2	6.729826	5368168.7	6711821.3	4024516.1
<i>Parksosaurus warreni</i>	70.6	69	69	4.860872	72589.2	90758.3	54420.1
<i>Probactrosaurus gobiensis</i>	130	99.6	114.8	6.253919	1794397.6	2243535.3	1345259.9
<i>Probactrosaurus mazongshanensis</i>	130	112	121	6.192545	1557919.6	1947866.9	1167972.3
<i>Prosaurolophus maximus</i>	76.5	75	75	6.513481	3261975.5	4078448	2445503
<i>Protohadros byrdi</i>	96	94.8	95.4	6.462165	2898444.4	3623925	2172963.8
<i>Rhabdodon priscum</i>	76.4	69	72.7	5.936072	863122.2	1079161.7	647082.7
<i>Sahaliyenia elunchunorum</i>	69	65.5	67.25	6.167935	1472090.6	1840554.9	1103626.3
<i>Saurolophus angustirostris</i>	76.4	69	72.7	6.790067	6166899.5	7710474.4	4623324.6
<i>Saurolophus osborni</i>	70.6	69	69	6.831619	6786078.8	8484634.3	5087523.3
<i>Secernosaurus koernerri</i>	76.4	69	72.7	6.392068	2466424.2	3083770.2	1849078.2
<i>Shantungosaurus giganteus</i>	83.5	70.6	77.05	7.261471	18258733.2	22828894.1	13688572.3
<i>Talenkauen santacrucensis</i>	70.6	69	69.8	5.751279	563999.7	705168.8	422830.6
<i>Tanius sinensis</i>	83.5	70.6	77.05	6.566746	3687615.3	4610625.4	2764605.2
<i>Telmatosaurus transsylvanicus</i>	70.6	65.5	68.05	6.222622	1669637.6	2087547.9	1251727.3
<i>Tenontosaurus dossi</i>	115	112	113.5	6.075022	1188562.9	1486060.2	891065.6
<i>Tenontosaurus tilletti</i>	115	108.8	111.9	6.02801	1066620	1333595	799645
<i>Tethyshadros insularis</i>	76.4	69	72.7	5.613641	410810.4	513636.2	307984.6
<i>Theiophytalia kerri</i>	125	99.6	112.3	6.156084	1432463.3	1791008.9	1073917.7
<i>Thescelosaurus assiniboiensis</i>	68	65.5	66.75	5.053509	113112.1	141424.1	84800.1
<i>Thescelosaurus neglectus</i>	68	65.5	66.75	5.548309	353434.2	441898.8	264969.6
<i>Tsintaosaurus spinorhinus</i>	83.5	70.6	77.05	6.694903	4953390.8	6193224.5	3713557.1
<i>Uteodonaphanoecetes</i>	155.7	145.5	150.6	5.444741	278445.7	348140.7	208750.7
<i>Valdosaurus canaliculatus</i>	128.3	125	126.65	4.699502	50061.3	62591.6	37531
<i>Willinakaqe salitralensis</i>	76.6	69	72.8	5.966659	926101.4	1157904.6	694298.2
<i>Wulagasaurus dongi</i>	69	65.5	67.25	6.485248	3056665.9	3821749.4	2291582.4
<i>Xuwulong yueluni</i>	125	99.6	112.3	6.000508	1001170.3	1251763.2	750577.4
<i>Zalmoxes robustus</i>	70.6	65.5	68.05	5.092408	123711	154675.9	92746.1
<i>Zalmoxes shqiperorum</i>	70.6	69	69.8	5.082802	121004.5	151291.9	90717.1

Appendix 7. Node-age reconstructions for various time-scaled versions of the ornithopod tree. Ages are in millions of years. The standard time-calibrated tree (cal) represents the standard on which other time scaling methods can be compared.

Nodes	Time-Scaling Method					
	cal	equal.1	equal.10	aba	zbla	mbl
Ornithopoda	163.2	164.2	173.2	203.2	193.2	172.2
Thescelosauridae	130	152.8	158.8	169	160	133.3
	130	141.4	144.4	168	159	131
	99.6	120.5	122	136.6	128.6	100.6
	85.8	103.15	103.9	121.8	114.8	86.8
	128.3	146.675	151.175	166.3	158.3	131.3
	128.3	140.55	143.55	165.3	157.3	130.3
	68	98.15	98.15	104	97	69
	128.3	134.425	135.925	164.3	156.3	129.3
	106.4	120.4125	121.1625	141.4	134.4	107.4
	163.2	164.0889	172.0889	202.2	192.2	171.2
Iguanodontia	163.2	163.9778	170.9778	201.2	191.2	170.2
	163.2	163.8667	169.8667	200.2	190.2	169.2
	163.2	163.7556	168.7556	199.2	189.2	168.2
	163.2	163.6444	167.6444	198.2	188.2	167.2
	106.4	134.8	134.8	140.4	131.4	107.4
	85.8	122.55	122.55	118.8	110.8	88.8
	85.8	110.3	110.3	117.8	109.8	87.8
	70.6	78.2	78.2	101.6	94.6	71.6
	85.8	98.05	98.05	116.8	108.8	86.8
	163.2	163.5333	166.5333	197.2	187.2	166.2
	115	139.1	139.1	148	139	116
	163.2	163.4222	165.4222	196.2	186.2	165.2
	163.2	163.3111	164.3111	195.2	185.2	164.2
	155.7	159.5056	160.0056	186.7	177.7	157.7
	155.7	157.6028	157.8528	185.7	176.7	156.7
	128.3	147.8352	148.0019	157.3	149.3	130.3
	128.3	138.0676	138.1509	156.3	148.3	129.3
	155.7	159.5611	160.5611	187.7	178.7	157.7
	155.7	157.6306	158.1306	186.7	177.7	156.7
	140.2	151.8204	152.1537	170.2	162.2	142.4
	127	133.6	133.6	156	149	128
	140.2	146.0102	146.1769	169.2	161.2	141.4
	136.4	143.6076	143.7326	164.4	157.4	140
	136.4	141.2051	141.2884	163.4	156.4	139
Hadrosauroidea	136.4	138.8025	138.8442	162.4	155.4	138
	130	137.3355	137.3702	155	149	137
	130	135.8684	135.8961	154	148	136
	130	134.4013	134.4221	153	147	135

	130	132.9342	132.9481	152	146	134
	130	131.4671	131.474	151	145	131
	130	131.4671	131.474	151	145	133
	130	130.9781	130.9827	150	144	132
	130	130.489	130.4913	149	143	131
	112	126.2335	126.237	131	126	115
	112	121.489	121.4913	130	125	114
	112	116.7445	116.7457	129	124	113
	93.5	108.9963	108.9971	109.5	105.5	100.5
	93.5	101.2482	101.2486	108.5	104.5	99.5
	93.5	97.37409	97.37428	107.5	103.5	98.5
	87	92.18704	92.18714	100	97	97.5
Hadrosauridae	85.8	90.90963	90.90971	97.8	95.8	96.5
	85.8	89.63223	89.63228	96.8	94.8	95.5
Euhadrosauria	85.8	88.35482	88.35486	95.8	93.8	94.5
Hadrosaurinae	83.5	85.225	85.225	92.5	91.5	89.5
	83.5	84.65	84.65	91.5	90.5	86.5
	83.5	84.075	84.075	90.5	89.5	85.5
	83.5	83.7875	83.7875	89.5	88.5	84.5
	83.5	84.9375	84.9375	91.5	90.5	88.5
	83.5	84.65	84.65	90.5	89.5	87.5
	83.5	84.3625	84.3625	89.5	88.5	86.5
	83.5	84.075	84.075	88.5	87.5	85.5
	83.5	83.7875	83.7875	87.5	86.5	84.5
	76.6	80.3375	80.3375	80.6	80.6	77.6
	83.5	84.3625	84.3625	89.5	88.5	86.5
	76.5	80	80	81.5	81.5	78.5
	76.4	78.2	78.2	80.4	81.4	77.4
	83.5	84.075	84.075	88.5	87.5	85.5
	83.5	83.7875	83.7875	87.5	86.5	84.5
	72	77.89375	77.89375	75	75	73
Lambeosaurinae	85.8	87.07741	87.07743	94.8	92.8	93.5
	83.5	85.88494	85.88495	91.5	90.5	92.5
	83.5	84.69247	84.69248	90.5	89.5	84.5
	83.5	85.61995	85.61996	90.5	89.5	91.5
	83.5	85.35495	85.35496	89.5	88.5	90.5
	76.5	81.16667	81.16667	81.5	81.5	78.5
	76.5	78.83333	78.83333	80.5	80.5	77.5
	83.5	85.08996	85.08997	88.5	87.5	89.5
	69	76.25	76.25	73	73	70
	83.5	84.82497	84.82497	87.5	86.5	88.5
	83.5	84.55997	84.55998	86.5	85.5	87.5
	76.5	80	80	78.5	78.5	78.5
	76.5	78.25	78.25	77.5	77.5	77.5
	83.5	84.29498	84.29498	85.5	84.5	86.5

76.5	80	80	77.5	77.5	77.5
83.5	84.02999	84.02999	84.5	83.5	85.5
83.5	83.76499	83.76499	83.5	82.5	84.5

Appendix 8. Maximal body size data in ornithopods at three different bin sizes.

Bin	2 Ma Bins			5 Ma Bins			10 Ma Bins		
	N	Lower Bin Age (Ma)	Maximal Bin Size (\log_{10} g)	N	Lower Bin Age (Ma)	Maximal Bin Size (\log_{10} g)	N	Lower Bin Age (Ma)	Maximal Bin Size (\log_{10} g)
1	1	163.2	4.837	1	163.2	4.837	1	163.2	4.837
2	4	157.5	6.142	4	160.5	6.142	4	155.5	6.142
3	4	155.5	6.142	4	155.5	6.142	5	145.5	6.764
4	4	153.5	6.142	3	150.5	6.142	11	135.5	6.939
5	4	151.5	6.142	3	145.5	6.142	16	125.5	6.939
6	3	149.5	6.142	2	140.5	6.764	18	115.5	6.939
7	3	147.5	6.142	1	135.5	6.175	13	105.5	6.764
8	3	145.5	6.142	11	130.5	6.939	12	95.5	6.473
9	1	141.5	6.764	16	125.5	6.939	34	85.5	7.261
10	1	139.5	6.764	11	120.5	6.939	47	75.5	7.261
11	2	137.5	6.764	15	115.5	6.939			
12	1	135.5	6.175	11	110.5	6.764			
13	1	133.5	6.175	10	105.5	6.764			
14	6	131.5	6.939	13	100.5	6.764			
15	10	129.5	6.939	7	95.5	6.473			
16	11	127.5	6.939	9	90.5	6.275			
17	16	125.5	6.939	20	85.5	7.261			
18	12	123.5	6.939	26	80.5	7.261			
19	12	121.5	6.939	37	75.5	7.261			
20	11	119.5	6.939	26	70.5	7.209			
21	11	117.5	6.939						
22	13	115.5	6.939						
23	15	113.5	6.939						
24	8	111.5	6.473						
25	9	109.5	6.655						
26	10	107.5	6.764						
27	10	105.5	6.764						
28	10	103.5	6.764						
29	12	101.5	6.764						
30	5	99.5	6.764						
31	6	97.5	6.764						
32	4	95.5	6.473						
33	6	93.5	6.473						
34	4	91.5	6.275						
35	4	89.5	6.275						
36	8	87.5	6.275						
37	8	85.5	6.275						
38	20	83.5	7.261						
39	16	81.5	7.261						
40	12	79.5	7.261						
41	26	77.5	7.261						

42	28	75.5	7.261		
43	21	73.5	7.261		
44	29	71.5	7.261		
45	26	69.5	7.209		
46	15	67.5	6.978		

Copyright Acknowledgements

At the time of submission, chapters 2, 3, and 4 were not published in peer-review journals. However, chapter 1 was published in July 2012 in BMC Biology. Given the open access nature of the journal, no further copyright information is needed. To see the published version please refer to:

Campione, N. E., and D. C. Evans. 2012. A universal scaling relationship between body mass and proximal limb bone dimensions in quadrupedal terrestrial tetrapods. BMC Biology 10:60. <http://www.biomedcentral.com/1741-7007/10/60>